Single-Atom Porous Organic Polymer Catalysts for Asymmetric Catalysis

Yang, Faliu

Publication date:
2022

Document Version
Publisher's PDF, also known as Version of record

Single-Atom Porous Organic Polymer Catalysts for Asymmetric Catalysis

Ph.D. Thesis

Faliu Yang

Techinical University of Denmark

Supervisors:

Professor Søren Kegnæs

Associate Professor Søren Kramer

Kongens Lyngby, 2022

Preface

This dissertation details the research work of my Ph.D. that was conducted at Department of Chemistry at Technical University of Denmark (DTU). The work was carried out under the guidance of Professor Søren Kegnæs and Associate Professor Søren Kramer during the period September 2018 to April 2022. The PhD program comprised 33 ECTS of coursework and a minimum of 420 hours of work in knowledge diffusion, including teaching. China Scholarship Council (No. 201808410356) and DTU Chemistry provided financial support for the project.

This Ph.D. dissertation is divided into seven chapters, the first of which covers both catalysis and heterogenized homogeneous catalysts. The second chapter provides a brief introduction to heterogeneous single-atomic catalysis and the most common methods for fabricating porous organic polymers (POPs). The syntheses of nine kinds of POPs based on bipyridine (BPY), chiral ligands (*R*)-BINAP, and (*R*)-MeO-BIPHEP are described in Chapter 3. The borylation of arenes utilizing BPY-POP-1 is addressed in Chapter 4. The application of Ni-(*R*)-BINAP-POP-5 catalysis to the asymmetric α-arylation of ketones is discussed in Chapter 5. Chapter 6 covers the asymmetric hydrosilylation of ketones using the merger of Cu-(*R*)-BINAP-POP-6. Chapter 7, the conclusion, condenses all the projects.

Faliu Yang, Kgs. Lyngby, Denmark, April 2022

Acknowledgment

First and foremost, I would like to express a sincere gratitude to my main supervisor Professor Søren Kegnæs gave me the opportunity to be a member of his research group. He was supportive and helpful during my Ph.D. study and scientific research while also encouraging me to explore my own interests and ideas. Furthermore, I gratefully acknowledge my co-supervisor, Associate Professor Søren Kramer, for the laboratory support, sharing of chemistry expertise, guidance, and valuable advice. I will never stop appreciating the time and effort he has put into my research work. I wish him all the best in the future.

I would like to thank Søren Kegnæs group members for their camaraderie and assistance throughout the whole process. Thank you for our time together in the laboratory, Niklas R. Bennedsen, Mikkel B. Buendia, Balakrishna Bugga and Xuemeng Chen. I would like to convey my gratitude to my officemates Ping Zhu, Mahtab Madani, and GorGuy Kachaporn Saenluang for always being friendly and creating a pleasant working environment. Big thanks to those who helped me with instruments and specialized techniques: Dr. Farnoosh Goodarzi for performing scanning electron microscopy (SEM), Kai Gao for performing thermal gravimetric analysis (TGA), X-ray diffraction (XRD), and N_2-physisorption (BET). I would like to thank my colleagues at the Center for Catalysis and Sustainable Chemistry (CSC) and DTU Kemi.

I owe an enormous debt of appreciation to my friends Runtian Qie, Xinxin Xiao, and Ruwei Yao for their constant support and encouragement.

I would also like to give a thousand thanks to my family for their support and understanding.

My PhD study was additionally supported by the China Scholarship Council (No. 201808410356) and DTU Kemi.

Abstract

Catalysis reactions form the core of organic and industrial chemistry. Homogeneous catalysts exhibit excellent selectivity and high activity, but the difficulty of separation limits their exploitation. Alternatively, heterogeneous catalysts have a wide application in modern chemical industry owing to their durability and easy separation. However, when heterogeneous catalysts are used for formation of more complex compounds, they show low efficiency and selectivity owing to the low utilization rate of metal atoms and active compositions. The heterogenization of homogeneous catalysts combines the advantages of heterogeneous and homogeneous catalysts and offers a wide range of applications.

In this study, different strategies for synthesizing porous organic polymers (POPs) were developed. There are four types of POPs which are based on the bidentate chelating ligand-2,2′-bipyridine (BPY), and five types of chiral POP which are from (*R*)-BINAP and (*R*)-MeO-BIPHEP. Chiral POPs are used for asymmetric α-arylation of ketones and the borylation of arenes has been studied by BPY-POPs.

In the first project, the borylation of arenes was evaluated utilizing the Ir-BPY-POP combination. The in-situ catalytic system was composed with $[Ir(cod)Cl]_2$ and BPY-POP. The arenes could full borylate when B_2pin_2 was used for the transformation.

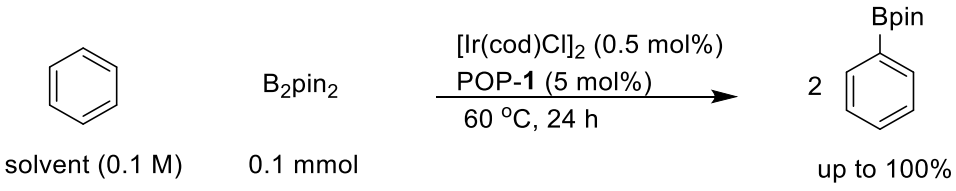

Scheme I Direct borylation of arenes using Ir-BPY-POP

The second project describes the asymmetric α-arylation of ketones using a nickel-BINAP-POP catalytic system. The combination of Ni-BINAP-POP displayed high catalytic activity and enantioselectivity, as well as good tolerance. The POP could be run three cycles without any enantioselectivity loss. The POP's activity can be maintained at the 40 % level after a run of three reactions.

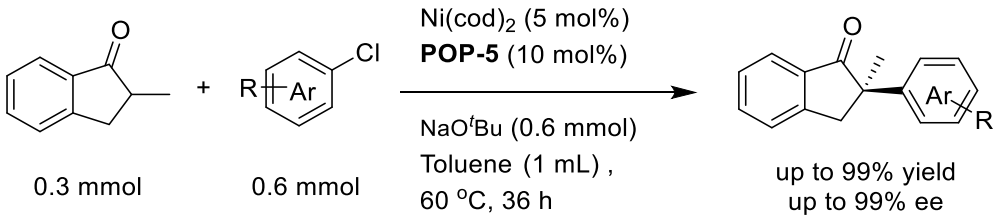

Scheme II Nickel-POP-catalyzed asymmetric α-arylation of ketones

The last project investigates the asymmetric hydrosilylation of ketones using the Cu-POP catalytic system. The Cu-POP catalyst exhibited excellent activity and high enantioselectivity, as well as good functional group tolerance. The POP could be recycled for three times while maintaining consistent enantioselectivity and high activity.

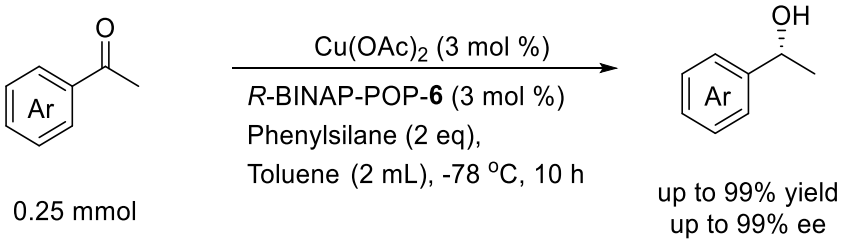

Scheme III Cu-POP-catalyzed asymmetric hydrosilylation of ketones

Resumé (Danish)

Katalyse reaktioner udgør kernen i organisk og industriel kemi. Homogene katalysatorer udviser fremragende selektivitet og høj aktivitet, men vanskeligheden ved separation begrænser deres udnyttelse. Alternativt har heterogene katalysatorer en bred anvendelse i moderne kemisk industri på grund af deres holdbarhed og nemme adskillelse. Når heterogene katalysatorer anvendes til dannelse af mere komplekse forbindelser, viser de imidlertid lav effektivitet og selektivitet på grund af den lave udnyttelsesgrad af metalatomer og aktive sammensætninger. Heterogenization af homogene katalysatorer kombinerer fordelene ved heterogene og homogene katalysatorer og tilbyder en bred vifte af anvendelser.

I dette arbejde blev der udviklet forskellige strategier til at syntetisere porøse organiske polymerer (POP'er). Der er fire typer POP'er, som er baseret på den bidentate chelaterende ligand-2,2'-bipyridin (BPY), og fem typer af chiral POP, som er fra (*R*)-BINAP og (*R*)-MeO-BIPHEP. Chirale POP'er bruges til asymmetrisk a-arylering af ketoner, og boryleringen af arener er blevet undersøgt af BPY-POP'er.

I det første projekt blev boryleringen af arener evalueret under anvendelse af Ir-BPY-POP-kombinationen. Det in-situ katalytiske system var sammensat med $[Ir(cod)Cl]_2$ og BPY-POP. Arenerne kunne borylere fuldt ud, når B_2pin_2 blev brugt til transformationen.

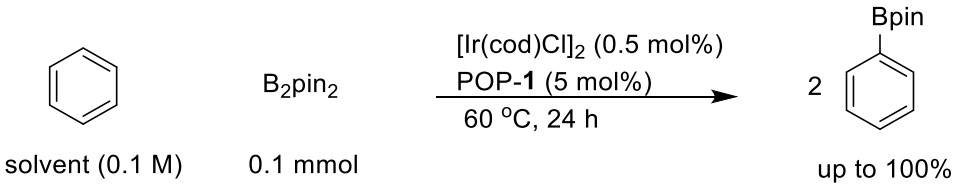

Skema I Direkte borylering af arener under anvendelse af Ir-BPY-POP

I det andet projekt beskriver den asymmetriske α-arylering af ketoner ved hjælp af et nikkel-BINAP-POP katalytisk system. Kombinationen af Ni-BINAP-POP viste høj katalytisk aktivitet og enantioselektivitet samt god tolerance. POP'en kunne køres tre cyklusser uden tab af enantioselektivitet. POP'ens aktivitet kan opretholdes på 40 %-niveauet efter en kørsel af tre reaktioner.

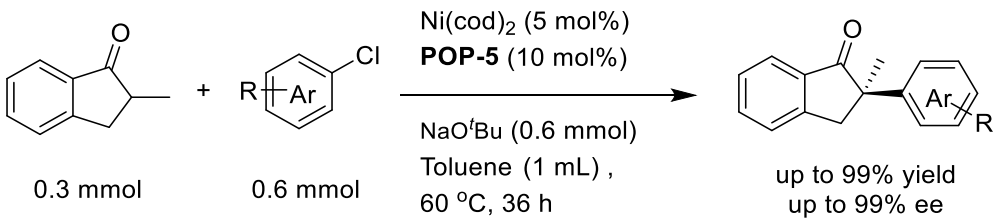

Skema II Nikkel-POP-katalyseret asymmetrisk α-arylering af ketoner

Det sidste projekt undersøger den asymmetriske hydrosilylering af ketoner ved hjælp af det Cu-POP katalytisk system. Cu-POP-katalysatoren udviste fremragende aktivitet og høj enantioselektivitet, såvel som god funktionel gruppetolerance. POP'en kunne genbruges tre gange, mens den bibeholdt ensartet enantioselektivitet og høj aktivitet.

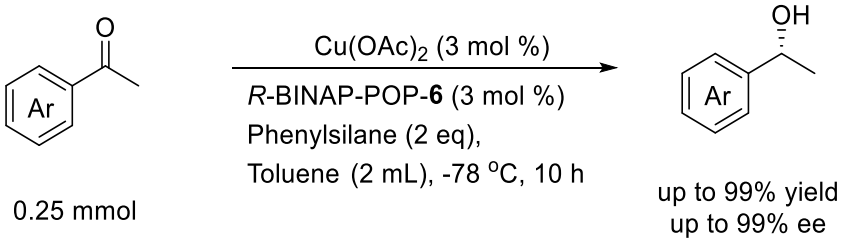

Skema III Cu-POP-katalyseret asymmetrisk hydrosilylering af ketoner

List of abbreviations

ΔG	Gibbs Free Energy
AIBN	Azo*bis*isobutyronitrile
BINAP	2,2′-bis(diphenylphosphino)-1,1′-binaphthyl
BINOL	1,1′-bi-2-naphthol
BPY	bipyridine
COD	1,5-cyclooctadiene
COF	Covalent Organic Framework
DCE	1,2-Dichloroethane
DEMS	Diethoxymethylsilane
DIOP	2,3-*O*-isopropylidene-2,3-dihydroxy-1,4-bis(diphenylphosphino)butane
DTA	Differential thermal analysis
DTBM-SEGPHOS	5,5′-Bis[di(3,5-di-*tert*-butyl-4-methoxyphenyl)phosphino]-4,4′-bi-1,3-benzodioxole
DVB	divinylbenzene
ee	enantiomeric excess
FID	Flame Ionization Detector
GC-MS	Gas Chromatography Mass Spectrometer
HPLC	High Performance Liquid Chromatography
LC-MS	Liquid Chromatography Mass Spectrometer
MOF	Metal Organic Framework
NMR	Nuclear Magnetic Resonance
pin	Pinacol
PMHS	polymethylhydrosiloxane
POP	Porous Organic Polymer
PS	Polystyrene
SACs	Single-Atom Catalysts
SEM	Scanning Electron Microscopy
^{t}Bu	*tert*-Butyl
TEM	Transmission Electron Microscopy
TGA	Thermal Gravimetric Analysis
TOF	Turn Over Frequency
TON	Turn Over Number

Table of Contents

1. Introduction to catalysis

1.1 Catalysis

Catalysis plays a significant role in a wide range of critical development and procedures of modern society, including producing crop protection, pharmaceuticals, fuels, and myriad commercial products. Food, petroleum, power, and chemicals are four of the most important sectors of the modern world economy that rely significantly on catalysis. [1] Haber-Bosch ammonia process, which is one of the most important industrial catalyzed processes for producing fertilizers in agriculture today, has an increasing impact on feeding half the world's population. [2]

In 1895, Friedrich Wilhelm Ostwald described the simplest, most concise definition of a catalyst: "*a catalyst accelerates a chemical reaction without affecting the position of the equilibrium*". [3] A catalyst can improve a chemical reaction's rate and selectivity without affecting the overall change in the Gibbs Free Energy of the whole reaction (Figure 1.1). Furthermore, it provides an alternative reaction process with a lower activation energy or reduces the energy barrier (red curve in Fig. 1.1). When a product is generated, the catalyst is not consumed because it returns to its original state. A catalytic cycle is the name given to the entire process, and the number of catalytic cycles for a particular quantity of catalyst is known as the "turnover number" (TON). Selectivity in catalysis is one of the most important criteria for the design of new catalysts because highly selective catalysts do not require expensive separation techniques, do not waste reactants, and generate fewer toxic pollutants. In asymmetric catalytic reactions, the enantiomeric excess (ee) is another important indicator, which is a measurement of product purity.

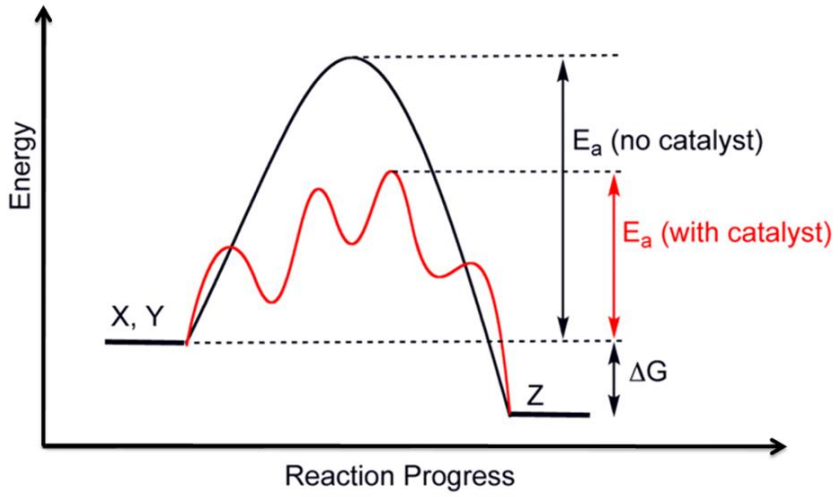

Figure 1.1 Potential energy diagram of a non-catalyzed (black) and a catalyzed (red) reaction. [4]

High selectivity and enantiomeric excess mean cheaper and greener catalytic reactions, which are the most critical goals in modern chemistry research. The idea of what aspects could develop green and sustainable synthetic processes was summarized in "The 12 Principles of Green Chemistry", published by Paul Anastas and John Warner (Figure 1.2). [5] Catalysis plays a key role in

implementing sustainable and green chemistry by reducing chemical waste, conserving energy, and using renewable feedstock.

The twelve Principles of Green Chemistry

1 Prevention. Preventing waste is better than treating or cleaning up waste after it is created.

2 Atom economy. Synthetic methods should try to maximize the incorporation of all materials used in the process into the final product. This means that less waste will be generated as a result.

3 Less hazardous chemical syntheses. Synthetic methods should avoid using or generating substances toxic to humans and/or the environment.

4 Designing safer chemicals. Chemical products should be designed to achieve their desired function while being as non-toxic as possible.

5 Safer solvents and auxiliaries. Auxiliary substances should be avoided wherever possible, and as non-hazardous as possible when they must be used.

6 Design for energy efficiency. Energy requirements should be minimized, and processes should be conducted at ambient temperature and pressure whenever possible.

7 Use of renewable feedstocks. Whenever it is practical to do so, renewable feedstocks or raw materials are preferable to non-renewable ones.

8 Reduce derivatives. Unnecessary generation of derivatives—such as the use of protecting groups—should be minimized or avoided if possible; such steps require additional reagents and may generate additional waste.

9 Catalysis. Catalytic reagents that can be used in small quantities to repeat a reaction are superior to stoichiometric reagents (ones that are consumed in a reaction).

10 Design for degradation. Chemical products should be designed so that they do not pollute the environment; when their function is complete, they should break down into non-harmful products.

11 Real-time analysis for pollution prevention. Analytical methodologies need to be further developed to permit real-time, in-process monitoring and control before hazardous substances form.

12 Inherently safer chemistry for accident prevention. Whenever possible, the substances in a process, and the forms of those substances, should be chosen to minimize risks such as explosions, fires, and accidental releases.

Figure 1.2 the 12 Principles of Green Chemistry [5]

1.2 Homogeneous and heterogeneous catalysis

According to the active phase of the catalyst, in chemistry catalysis is generally divided into homogeneous and heterogeneous catalysis. Homogeneous catalysis, in general, means that all the reactants, including substrates, catalysts, and products, are in the same phase throughout the reaction; this phase is often the liquid phase. Homogeneous catalytic systems have monodisperse atoms or molecules as active centers and low concentrations and have the advantage of a higher activity and selectivity because they have a higher degree of dispersion. Each individual catalyst center can be active. [6] However, the difficulty in separating catalysts and their recyclability are the two main drawbacks of homogeneous catalysis. Although the number of homogeneous catalytic reactions is greater than that of heterogeneous catalytic reactions, homogeneous catalysts account for just 10-15% of the market share. [7] The main advantage of heterogeneous catalysis, in

contrast, is the ease with which the catalyst can be separated and recycled. Heterogeneous catalysts are usually composed up of an active component that is stabilized on a support. Recycled catalyst could be reused after a simple post-processing step, such as filtration or centrifugation, without losing its initial activity or selectivity. Although heterogeneous catalysts have several active centers, these only exist on the surface of the solid support material. Thus, the concentration of active sites in this catalytic system is relatively low.

In addition to homogeneous and heterogeneous catalysts, other catalysts have been designed, such as biocatalysts and heterogenized homogeneous catalysts, as catalytic processes develop (Figure 1.3). [7]

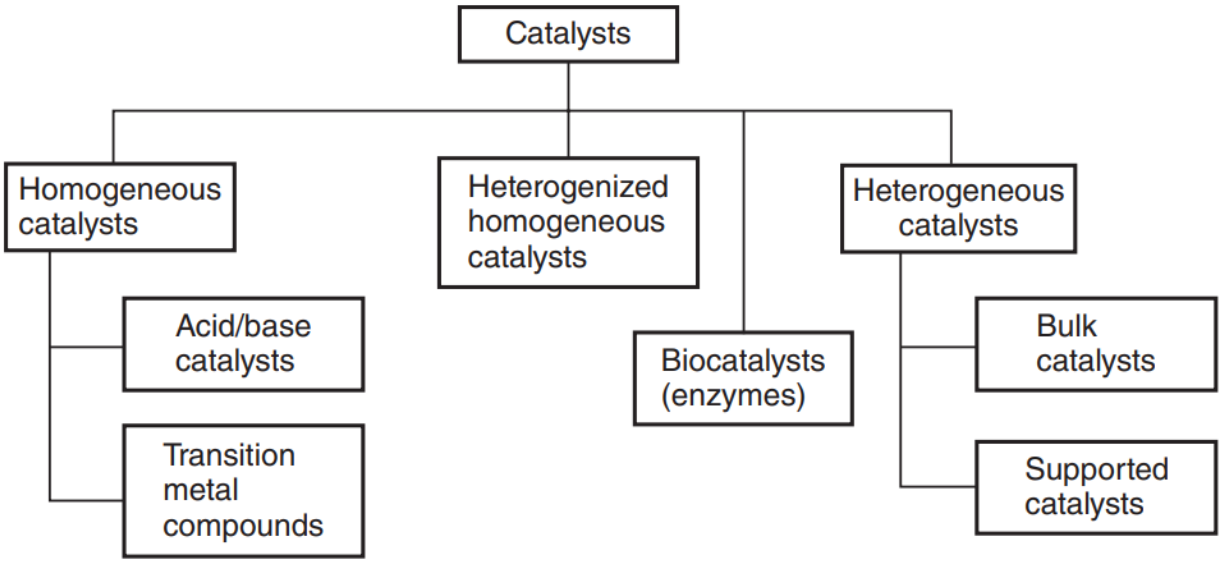

Figure 1.3 New classification of catalysts [7]

Many organic molecular activities can be performed under gentler reaction conditions owing to biocatalyst enzymes, and these biocatalysts exhibit excellent activity and selectivity in biocatalytic processes. [8] In most cases, enzymes are relatively difficult to acquire, and proteins require a specific pH and temperature, or the protein will be denatured within a short time. Although the cost of synthesizing enzymes is very high, the growth and demand for enzymes have increased in recent years owing to their high selectivity.

An interesting intermediate type of catalyst occurs between homogeneous and heterogeneous catalysts known as a heterogenized homogeneous catalyst. This type of catalyst has a large surface area, porous features, and multiple active sites (from heterogeneous catalysts). In the future, the catalysis can be performed in same phase with a high activity under mild conditions (from homogeneous catalysts). The heterogenized homogeneous catalysts combine the benefits of homogeneous and heterogeneous catalysts, displaying exceptional selectivity and efficiency, unique catalytic pathways, recyclability, sustainability, and separation simplicity.

1.3 Strategies for preparing heterogenized homogeneous catalysts

Plenty of strategies for the preparation of heterogeneous homogeneous catalysts have been developed over the last 20 years. Immobilized homogeneous catalysts on supporting materials are commonly used, such as metals on inorganic solid supporting materials and mesoporous silica or polymers. The second strategy involves the insertion of the homogeneous counterparts into supporting materials, such as metal organic frameworks (MOFs), covalent organic frameworks (COFs), and POPs. Below are a few examples from the literature where inorganic solids, mesoporous silica, polymers, MOFs, COFs, and POPs are used as heterogenized catalysts.

1.3.1 Metal on inorganic solid supporting material

A growing number of metal nanoparticles supported on solid supporting materials have been reported as immobilized heterogeneous catalysts. [9] Metal nanoparticle catalysts, such as Pd, Pt, and Au, have been used in many industrial reactions. [10] Gold nanoparticles on different solid supporting materials (zeolite, [11] carbon, [12] metal, [13] non-metal oxides, [14] and nanotubes [15]) are effective catalysts for the oxidation of alcohols and alkanes (Scheme 1.1 and 1.2).

Gold nanoparticles have been used in various alcohol oxidation processes, resulting in decreasing costs and hazardous wastes, ensuring the oxidation reaction is "greener." [16]

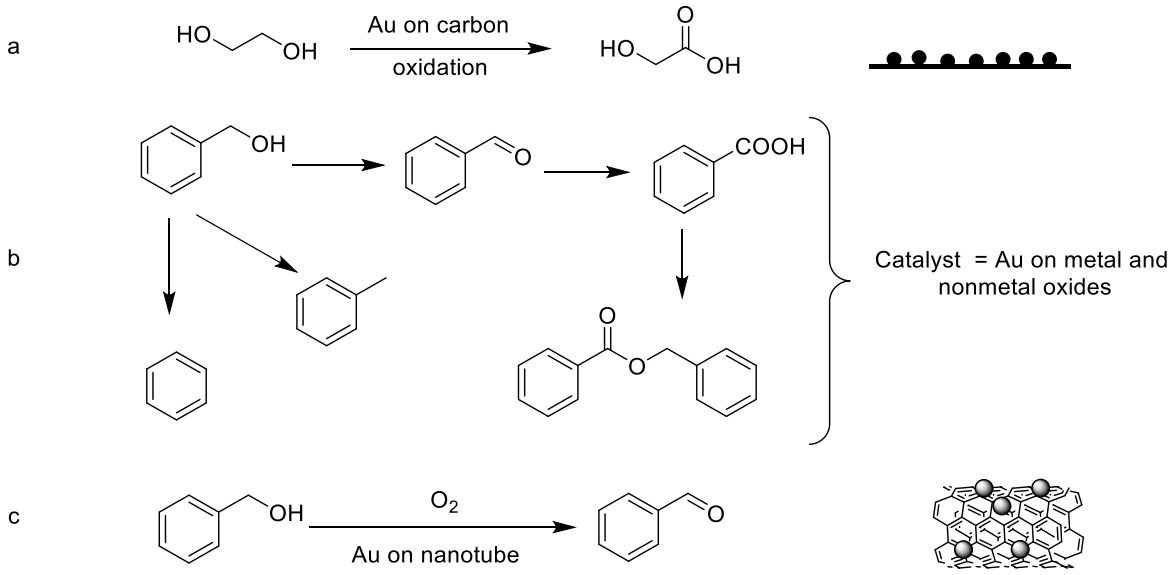

Scheme 1.1 Oxidation of alcohol by gold nanoparticles on supporting materials

Energy, gas, and oil are composed of various hydrocarbons. The transformation of C=O or C-O-H bonds from C-H bonds can generate more valuable products. In contrast, alkanes are very stable hydrocarbon molecules that are difficult to convert into oxygenated compounds. Therefore, researchers have investigated the oxidation of cyclohexane, methane, ethane, and propane using gold nanoparticles on zeolites. [17]

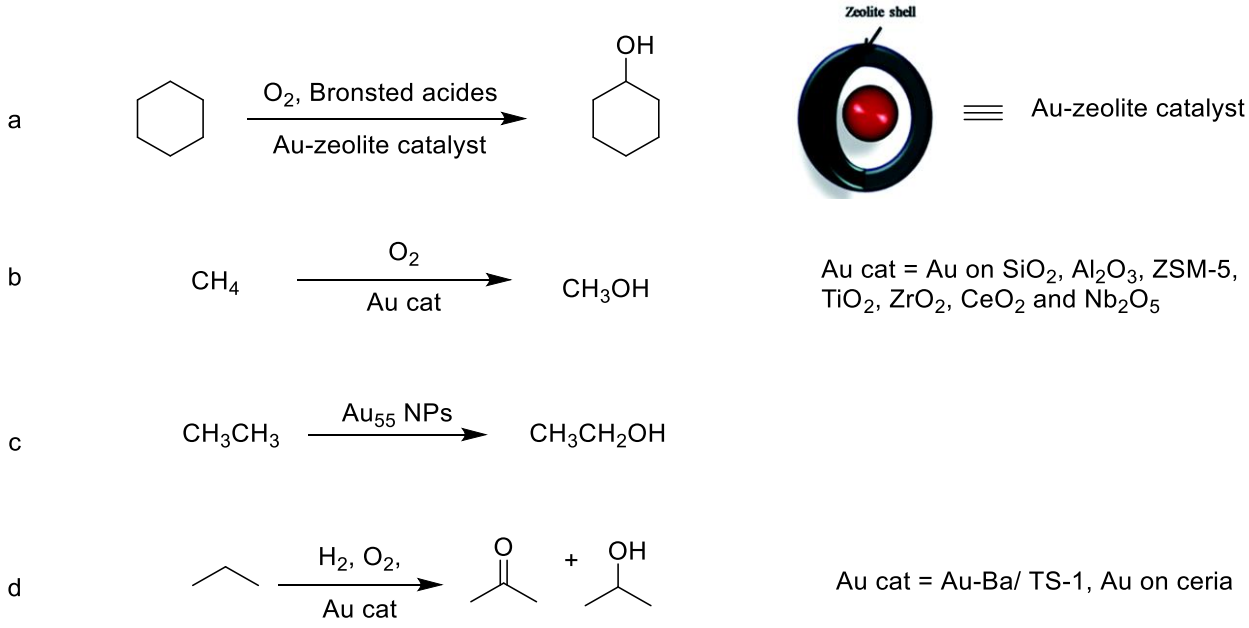

Scheme 1.2 Oxidation of alkane by Gold nanoparticles on supporting materials

1.3.2 Mesoporous silica as supporting material

Since Kinting's first example of stable silica as a supporting material for liquid phase hydrogenation in 1985, [18] other types of silica have received considerable attention. Mesoporous silica is a porous inorganic solid with a large interior surface area, which has enabled significant advances in medicine, [19] biosensors, [20] energy storage, [21] and water filtering. [22] In 2000, Thomas devised a heterogeneous catalyst supported by mesoporous silica, MCM-41, for the reduction of nicotinate to ethyl nicotinate (Scheme 1.3 a). [23] When the reduction reaction was performed, this mesoporous catalyst showed a high TON and 17 % ee. However, no enantiomeric selectivity was observed when an analogous homogeneous catalyst was employed in the reaction. Jones later reported hydrogenation of *E*-phenylcinnamic acid with two similar catalysts supported by the same mesoporous silica (Scheme 1.3 b). [24] On MCM-41, two types of homogeneous catalysts, Rh(cod) and Pd(allyl), were utilized to make heterogeneous catalysts. When compared to homogeneous catalysis reactions, the catalytic system showed better enantiomeric selectivity.

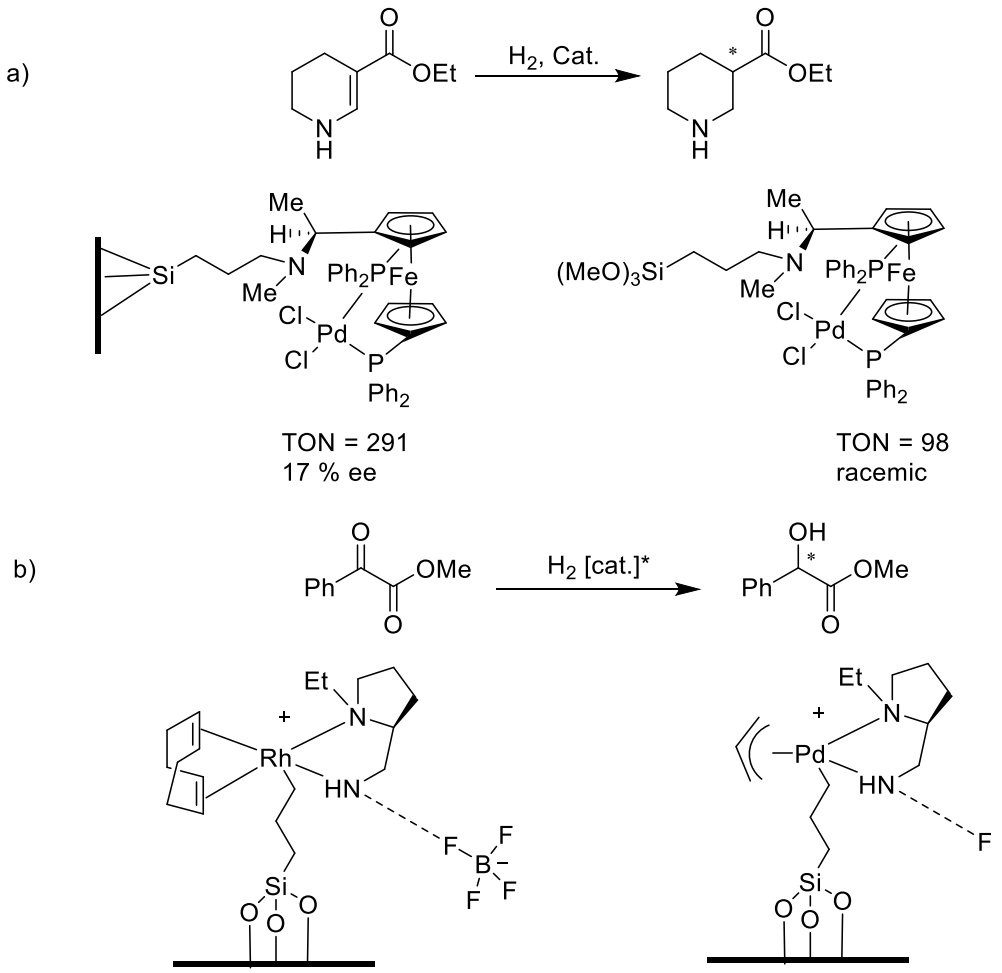

Scheme 1.3 Asymmeric catalysis using metal complexes on mesoporous silica

MCM-41 can support not just organic metal complexes, but also organocatalyst derived from proline, which can be immobilized on the same supporting material. By heterogenizing proline on the mesoporous material MCM-41, Alfonso accomplished direct asymmetric aldol condensation (Scheme 1.4). [25] The advantages of using the amino acid proline and functionalized pure silica mesoporous materials are combined in this catalysis system, such as no need of any metal, mild conditions, and recycle. [25] The obtained highest yield (90%) and highest ee values (99%) are comparable to homogenous proline counterparts. In addition, the catalyst was retrieved and recycled.

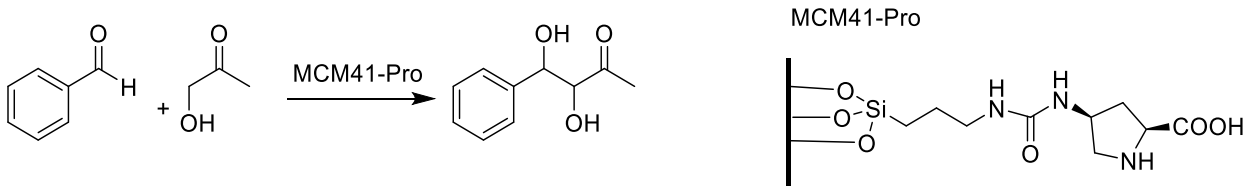

Scheme 1.4 Aldol condensation using proline on mesoporous silica [25]

Catalysts that are supported on other mesoporous silica materials have been developed for catalytic reactions during the determination of the application of mesoporous silica. MCM-48 has a 3 nm pore size and 15μm particle size, which are larger than those of MCM-41. MCM-48 has a cubic pore morphology. Liu et al. reported a chiral salen Mn (III) complex heterogeneous catalyst which is immobilized on MCM-48 mesoporous silica for asymmetric epoxidation (Scheme 1.5). [26] The chiral selectivity of the Mn heterogeneous catalysts was higher than that of the corresponding homogeneous catalysts. Owing to the three-dimensional cubic structure of MCM-48, the epoxidation of unfunctionalized olefins was completed in 2 h with a high efficiency (95%).

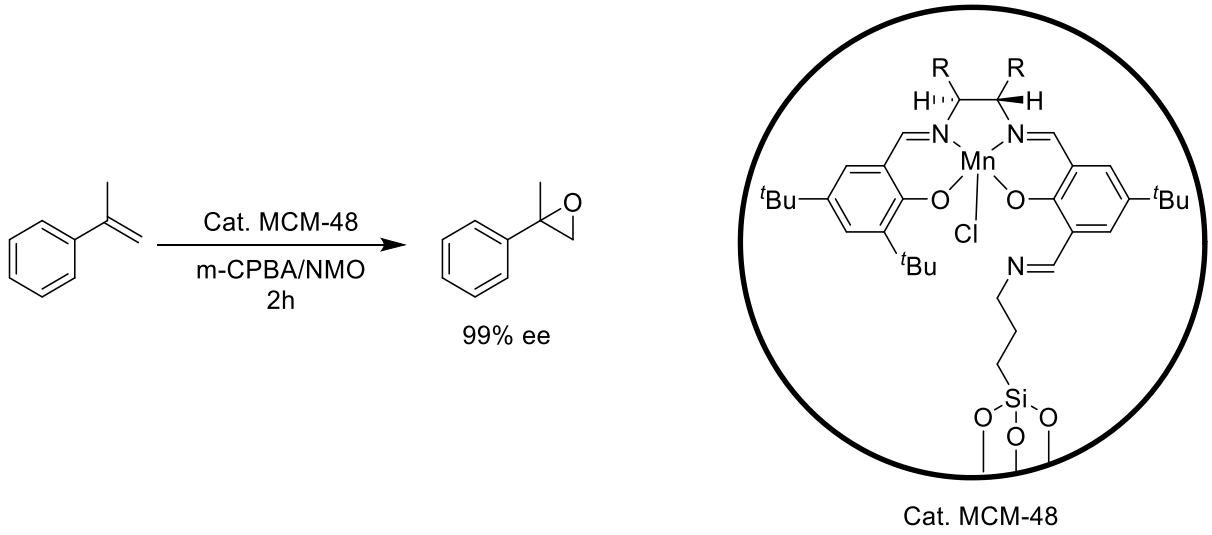

Scheme 1.5 Epoxidation of olefin using chiral Mn salen on mesoporous silica [26]

1.3.3 Polymers as supporting material

Since Merrifield's initial demonstration of employing solid-phase polymers in 1963, [27] polymers have been widely used to aid synthesis and catalyst immobilization using a variety of methods. Because of their heterogeneous nature, immobilized polymer catalysts can be easily separated and recycled. Many well-designed polymer-supported heterogeneous catalysts have been used for diverse catalytic reactions. [28] Several of the most used polymers are poly(ethylene glycol) (PEG), [29] dendrimers, [30] and JandaJels™. [31]

Tentagel™, which comprises PEG, is water-compatible and has been used as a heterogeneous support for catalysis under aqueous conditions. 1,3-Dibromobenzene with aryboronic acids' Suzuki-Miyaura cross-coupling reaction in water was reported by Uozumi who used an amphiphilic polystyrene-PEG resin-supported phosphine-palladium catalyst and obtained high yields (Scheme 1.6). [32] Later, Uozumi discovered that the same catalyst could be used for allylic aziridination reactions in water (Scheme 1.6). [32]

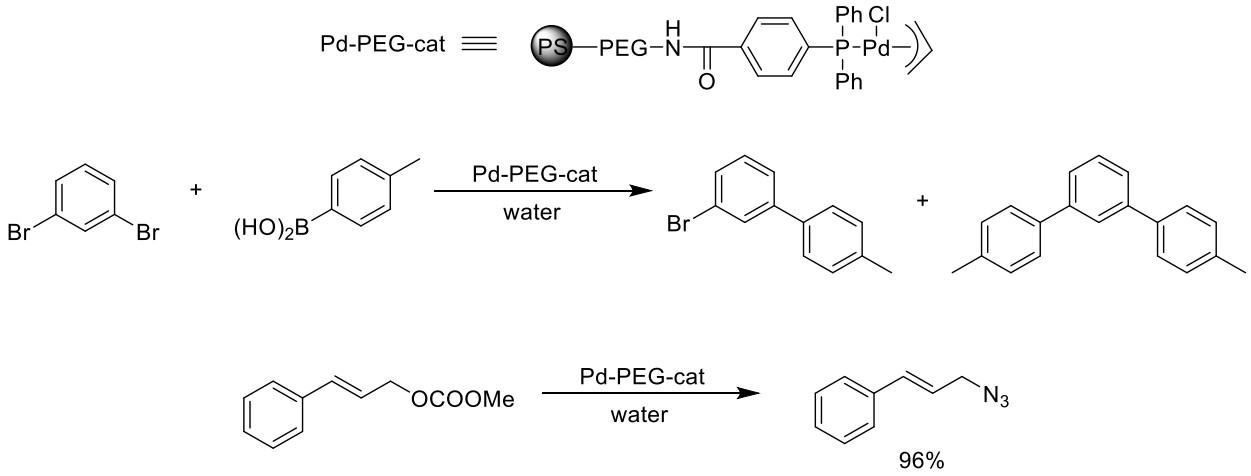

Scheme 1.6 Catalysis reactions using PEG-PS as supporting material [32]

Organocatalysts, in particular, the amino acid proline, are nontoxic, have low molecular weight, and are cost effective compared with transition metal-based catalysts. [33] It is preferable to immobilize proline, so that it can be recycled. Atsushi reported a novel poly side-chain heterogeneous catalyst carrying a proline moiety for direct asymmetric aldol reactions (Scheme 1.7). [34] However, the polystyrene catalyst did not have a chiral higher-order structure, resulting in a moderate yield and enantioselectivity.

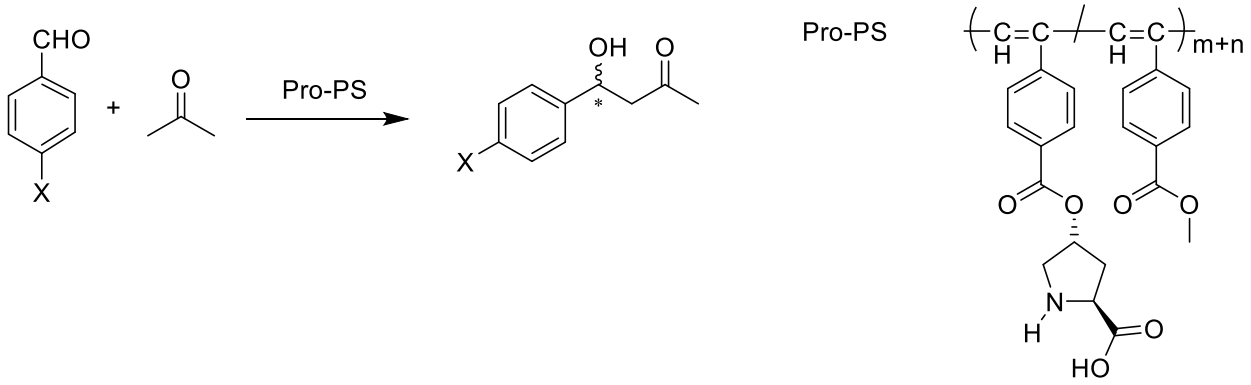

Scheme 1.7 Asymmetric reactions using proline immobilized on polystyrene

Dendrimers have a three-dimensional structure that resembles a tree and compact globular shape in solution. [35] Scheme 1.8 depicts typical dendrimer-supported catalytic reactions such as the Suzuki-Miyaura coupling reaction and asymmetric transfer hydrogenation. Tetsuaki synthesized a series of novel triarylphosphanes based on dendrimers for aryl chlorides' Suzuki-Miyaura coupling reaction. [36] The favorable dendritic effect of the dendrimer catalyst resulted in a high yield (93%). Noyori and Ikariya designed a core-functionalized dendritic ligand for the asymmetric hydrogenation of acetophenone. [36] The conversion of this dendrimer catalyst was high and the enantioselectivity was significant (95%).

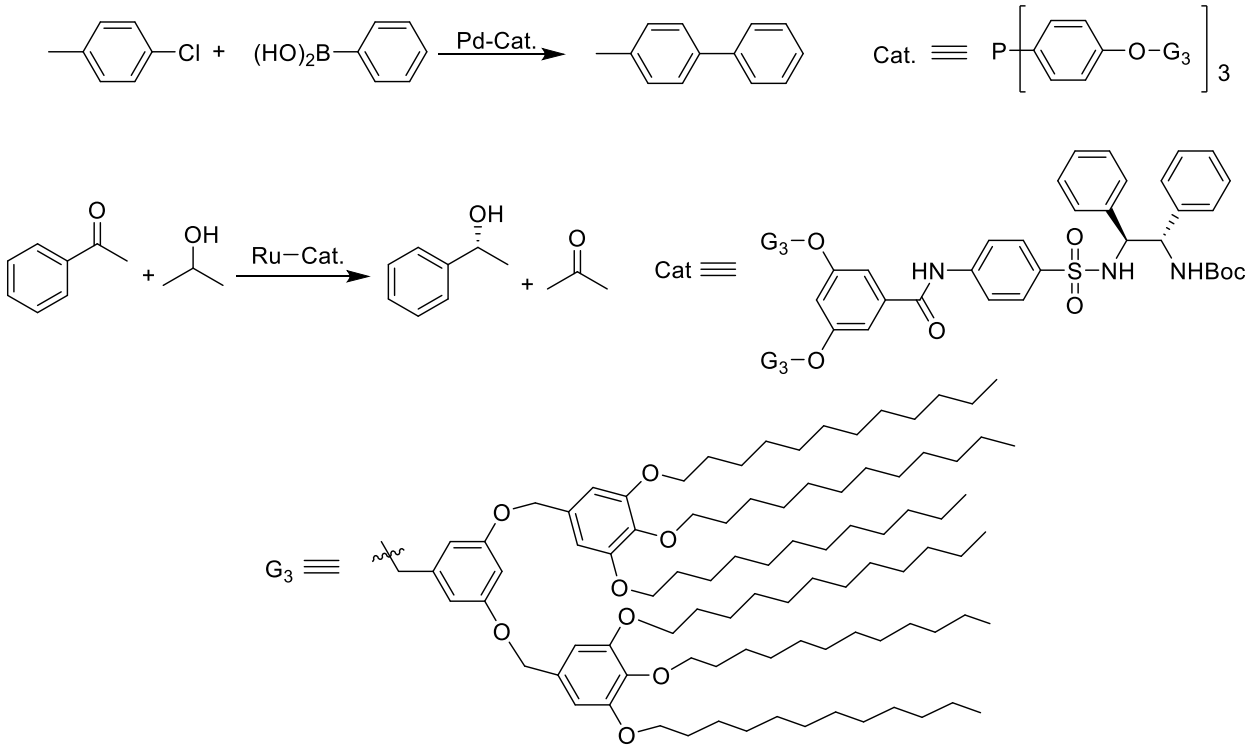

Scheme 1.8 Catalysis reactions using dendrimers as supporting material

JandaJels^{TM} is a polytetrahydrofuran-based crosslinker designed by Janda for broad organic synthesis. [37] The flexible crosslinker boosted the swelling and solvation characteristics of JandaJels^{TM} compared with those of polystyrene resins. [38] JandaJels^{TM} have been used for solid-supported organic synthesis (SPOS), [39] a wide variety of synthetic transformations, [40] and asymmetric catalysis. [41] Clapham used a JandaJel^{TM}-supported catalyst to perform the kinetic resolution of racemic secondary alcohols (Scheme 1.9). [42] Although the catalytic system had a lower activity, it had a comparable enantioselectivity (up to 97% ee), which was equivalent to that of homogeneous catalysis. In 2002, Song investigated JandaJel^{TM}-supported Trost-type bisphosphane catalysts for asymmetric allylic substitution reactions (Scheme 1.9). [43] This is the first time that asymmetric desymmetrization reaction was accomplished by a Trost-type heterogeneous catalyst, and it demonstrated high activity (98 % yield) and enantioselectivity (98 % ee).

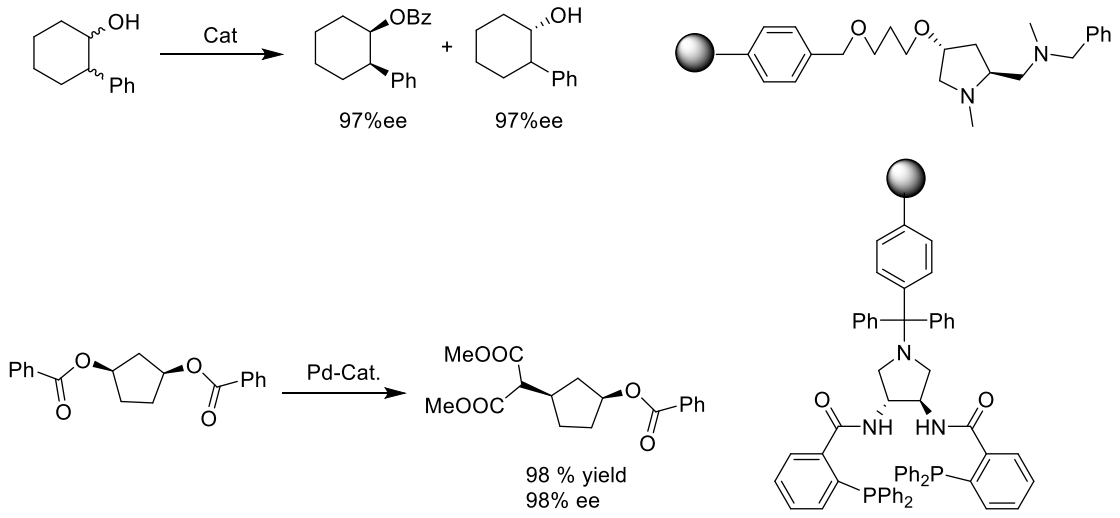

Scheme 1.9 Asymmetric catalysis reactions by JandaJel as supporting material

1.3.4 Metal Organic Frameworks (MOFs)

MOFs are porous crystalline materials with infinite lattices consisted of secondary building units, polydentate organic ligands (linkers), and metal or metal clusters (nodes) in one, two, or three dimensions (Figure 1.4). [44] Compared with the catalysts on the supporting materials mentioned above, MOFs have ultrahigh porosities and large internal surface areas. MOFs have a flexible structure and bridging organic and inorganic chemistry owing to the variation in the inherent nature of metal cations and organic linkers. MOFs meet the requirements for clean energy, [45] gas storage, [46] drug delivery, [47] chemical sensing, [48] various separations, [49] and are of great interest for potential catalytic reactions [50] because of these characteristics.

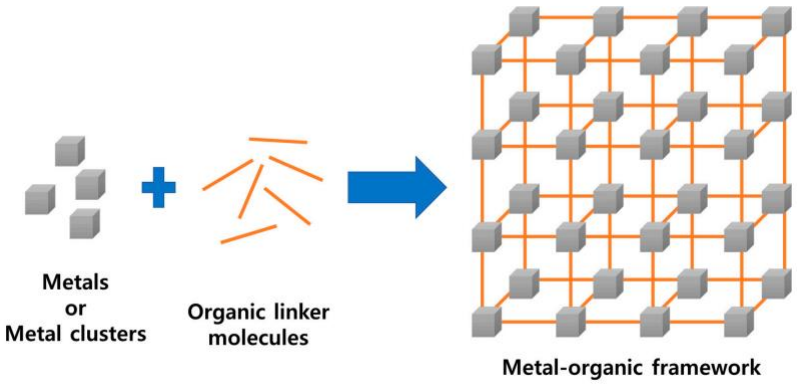

Figure 1.4 Schematic diagram for MOFs [44]

Because of their regular pore diameters and organized porous structure, MOFs are a relatively stable catalyst compared with the heterogeneous catalysts mentioned above. Furthermore, the pore shapes and sizes can be modified to accommodate the diffusion of substrates and products in catalytic reactions. The activity of heterogeneous catalysis decreases because of the insolubility of MOFs which makes easy separation and recycling of the catalyst. MOFs can be combined with

other nanostructures to improve swelling and conductivity, and have a wide range of catalytic applications, including reduction, oxidation, C-C bond forming reactions, electrocatalysis, and photocatalysis, as a result of continuous efforts to develop MOFs over the years. [51]

The reduction of alkenes and alkynes by hydrogenation is a challenge in the chemical industry and organic synthesis. [52] Zhang et al. developed a reversible dehydrogenation and hydrogenation of quinolone derivatives in water using a bimetallic Pd-Ni@MIL-100 (Fe) catalyst immobilized on MOFs (Figure 1.5). [53] Either dehydrogenation or hydrogenation could be achieved by changing the temperature and hydrogen pressure while using the same catalyst. The catalyst remained stable after six reaction cycles, with no notable loss in catalytic activity.

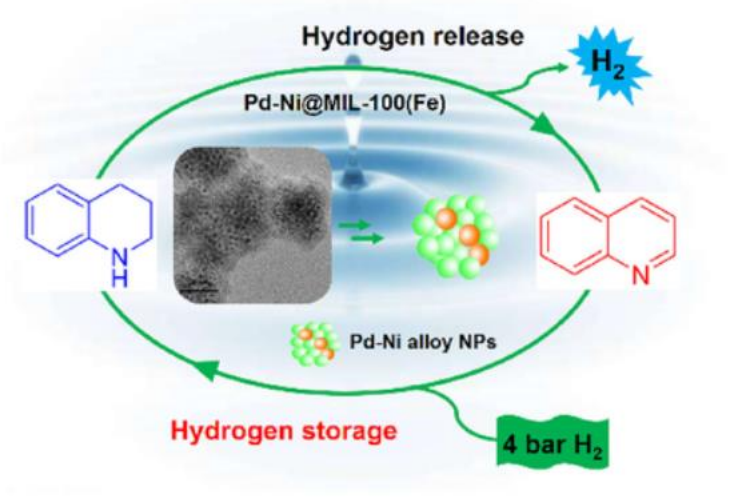

Figure 1.5 Dehydrogenation/hydrogenation of quinolone by bimetallic MOFs [52]

In addition to the hydrogenation of unsaturated hydrocarbons, other reductions, such as the reduction of nitroarenes, [54] hydrogenation of aldehydes [55] and carbon dioxide, [56] and transfer hydrogenation, [57] have been performed utilizing MOFs catalysts for heterogeneous catalysis.

Even if the mechanism of the selective oxidation of organic compounds is difficult to discern and the optimal techniques are difficult to establish, selective oxidation plays a more critical role in organic and industrial chemistry than reductions. Several MOF-based catalysts have been developed for high efficiency selective oxidation catalysis, such as the oxidation of unsaturated hydrocarbons, CO, and alcohols, [58] and these selective oxidations follow the "12 Principles of Green Chemistry."

The oxidation of olefins is critical in organic synthesis because functional groups can be introduced and modified toward synthesizing the target molecule. Bimetallic catalysts based on MOFs, such as Zn/Co, Au/Zn, and Cu/Fe, have been used for the oxidation of styrene, cyclohexene, and alkenes using different oxidants (TBHP, H_2O_2, and O_2) (Scheme 1.10). [59] These catalytic systems exhibit excellent selectivity and activity. Alcohols, CO, and sulfur compounds were successfully oxidized using MOF-based heterogeneous catalysts (Scheme 1.10). [60]

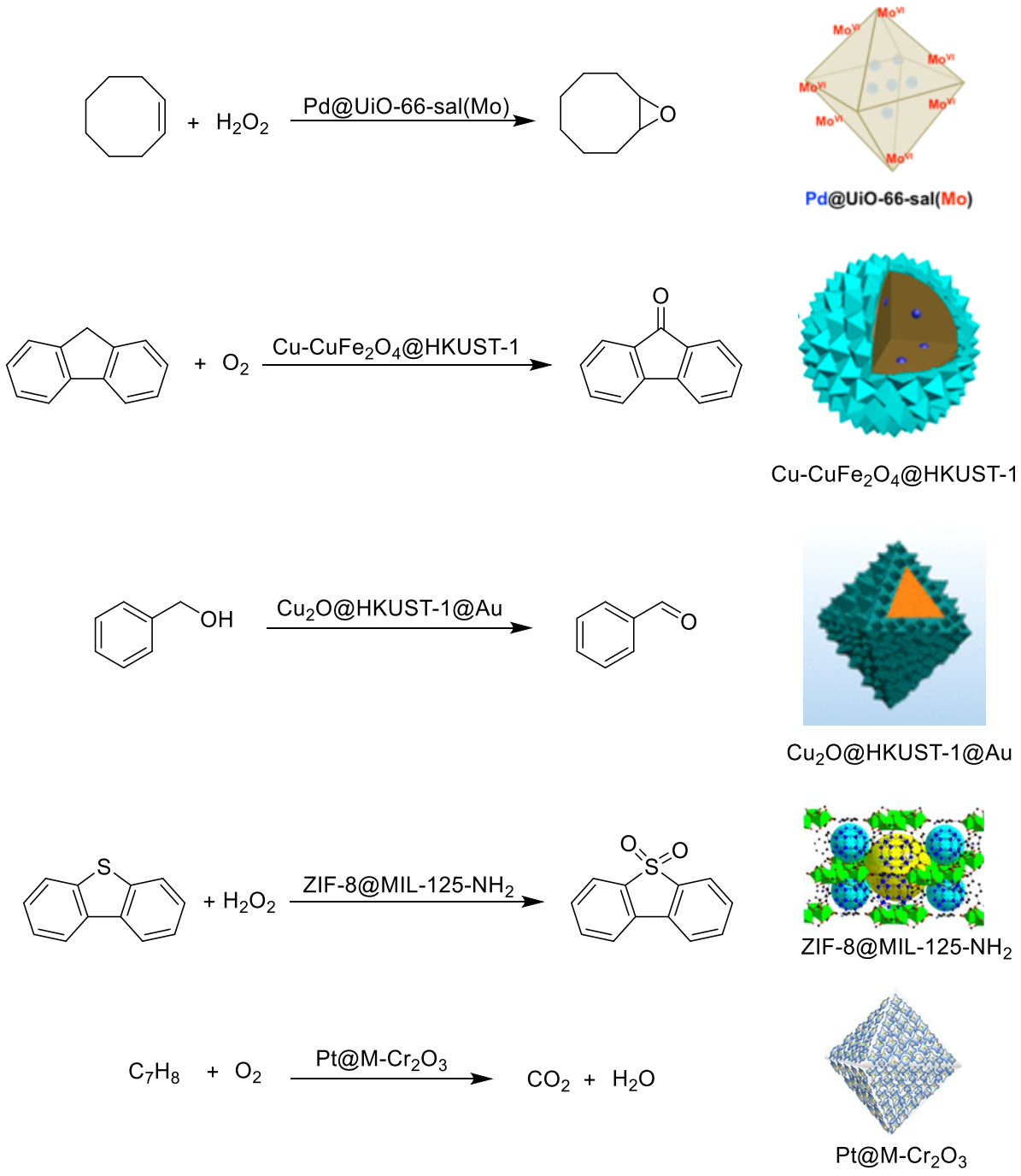

Scheme 1.10 Oxidations using MOFs-based catalysts [59-60]

The Diels-Alder, Michael, and Wittig reactions, the Suzuki-Miyaura coupling, Mizoroki-Heck reaction, Knoevenagel condensation, and A^3-coupling reactions are all examples of applied processes toward synthesizing medication and polymers.

An increasing number of MOFs catalysts have been investigated for various heterogeneous catalytic reactions of forming carbon-carbon bond. The following are some examples of studies performed thus far. Palani employed a $Ni(cod)_2$-immobilized UiO-66 MOF with good recyclable and reusable property for Suzuki-Miyaura Cross-Coupling at least seven cycles (Scheme 1.11). [61] Mohammed developed a hexagonal PdNPs@ZIF-8 MOF catalyst to achieve the Mizoroki-Heck reaction (Scheme 1.11). [62] Rodriguez and co-workers has reported that the Knoevenagel condensation can be used for carbon-carbon double bond by a nucleophilic addition of an active methylene compound with a carbonyl derivative. [63] Zhang reported the synthesis of RuNP/UiO-66 for catalyzing the Knoevenagel condensation (Scheme 1.11). [64] Meruyert designed an Ag-NHC-MOF efficient silver catalyst for A^3-coupling of paraformaldehyde, phenylacetylene, with diisopropylamine (Scheme 1.11). [65]

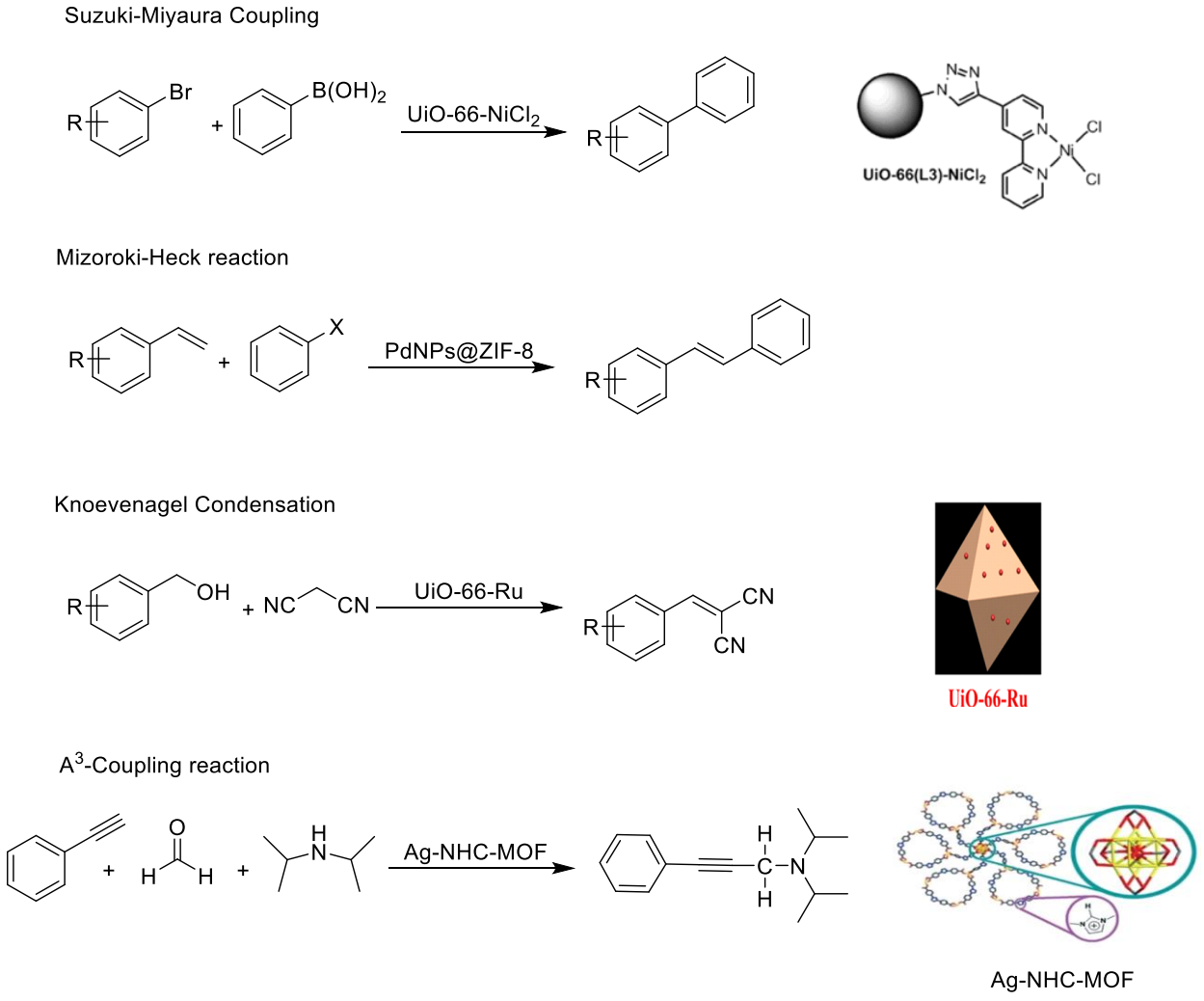

Scheme 1.11 C-C bond forming using MOFs-based catalysts [61-65]

Photocatalysis is an environmentally friendly and practical method that uses light energy to convert materials through a chemical reaction involving light and a catalyst. Photocatalytic reactions have

the potential to solve global energy and environmental problems, as the main photocatalytic reactions include hydrogen production, [66] carbon dioxide photoreduction, [67] and the degradation of organic contaminants. [68] Typical MOFs used for photocatalysis are UiO-66, [69] ZIF-8, [70] ZIF-9, [71] ZIF-67, [72] HKUST-1, [73] MIL-125, [74] MOF-74, [75] and Ni-MOL [76] (Figure 1.6).

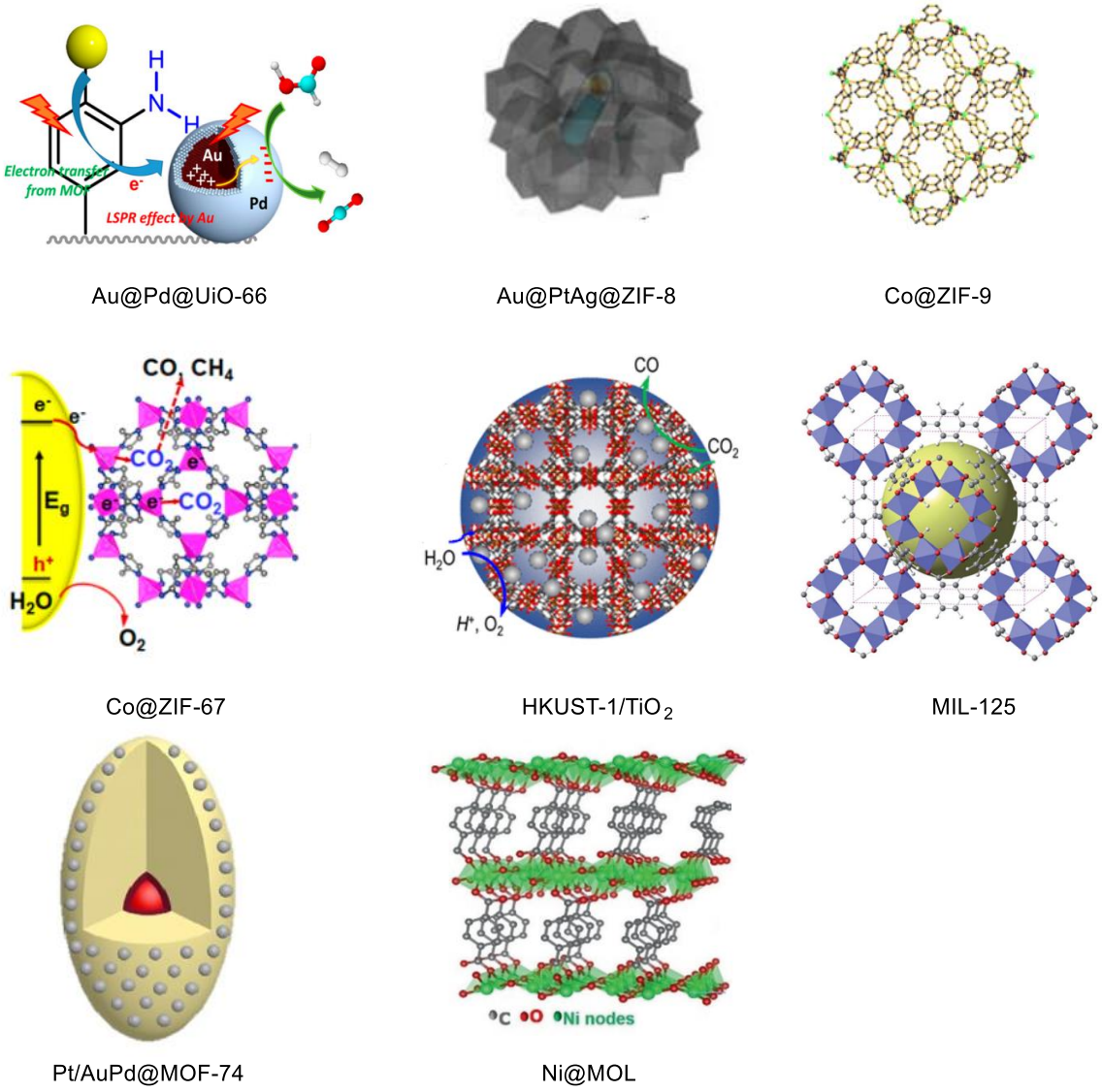

Figure 1.6 MOFs-based catalysts used for photocatalysis [66-76]

MOFs tools are being increasingly used in electrocatalysis for the hydrogen evolution reaction (HER), oxygen evolution reaction (OER), oxygen reduction reaction (ORR), and water splitting (HER+OER), in parallel with photocatalysis. [77] These four reactions can be performed using monometallic and bimetallic catalysts based on MOFs (Table 1.1). [78]

Table 1.1 Electrocatalysis using catalysts based on different MOFs [78]

	Monometallic catalysts	Bimetallic catalysts
Hydrogen evolution reaction	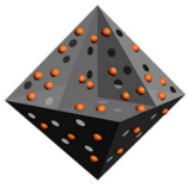 MoP@PC	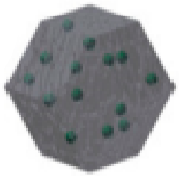 Co_9S_8/NC@MoS_2
Oxygen evolution reaction	 Co_9S_8/NSCNFs	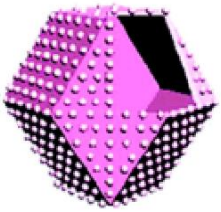 NiCoP/NC PHC
Oxygen reduction reaction	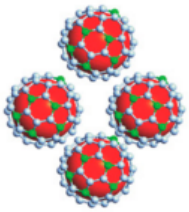 Co@NC	 ZnO/$ZnCo_2O_4$/C@rGO
Water splitting (HER+OER)	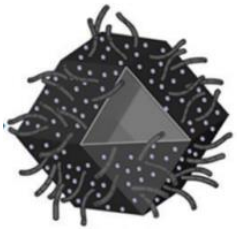 Co/CoP-HNC	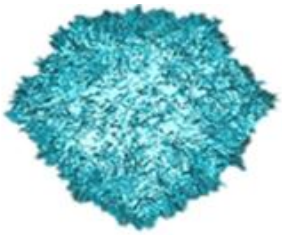 Co_3ZnC/Co-NCCP

Although MOFs are increasingly being used in catalytic processes, their reaction scope is still limited owing to low thermal and chemical stability. In addition, metal leaching decreases the catalytic activity and causes the collapse or distortion of the framework, an issue MOFs have in common with other solid-supported catalysts.

1.3.5 Covalent Organic Frameworks (COFs)

COFs are a new type of crystalline porous polymers developed in recent years. COFs are based on topology, and they have a stable structure because of the formation of irreversible covalent bonds. [79] Compared with MOFs, the COFs framework features a spatial network structure and is more thermally and chemically stable. The COFs framework consists of organic building blocks and light elements (e.g., C, H, O, N, B, and Si). COFs have the advantages of "designable" topology, regular structure, large specific surface area, adjustable pore size, unique pore channels, low-density, and easy modification, and functionalization. [80]

COFs have a wide range of organic building blocks of various sizes owing to the involvement of covalent bonds. [81] Having the flexibility of building blocks, the advantages of large porosities and stability, adjustable modification, and plentiful catalytic active sites ensure that COFs find application in many fields, including, gas storage, separation, optoelectronics, and most importantly, field catalysis. [82]

COFs are split into two major components based on their backbone: (a) an inherent covalent bonding backbone (left, Figure 1.7) and (b) modified functional groups (right, Figure 1.7). [83] Intrinsic COFs are composed of B-containing COFs, N-containing COFs, and Si-containing COFs. The normal methodologies for synthesizing COFs are the self-condensation and co-condensation of more organic building blocks.

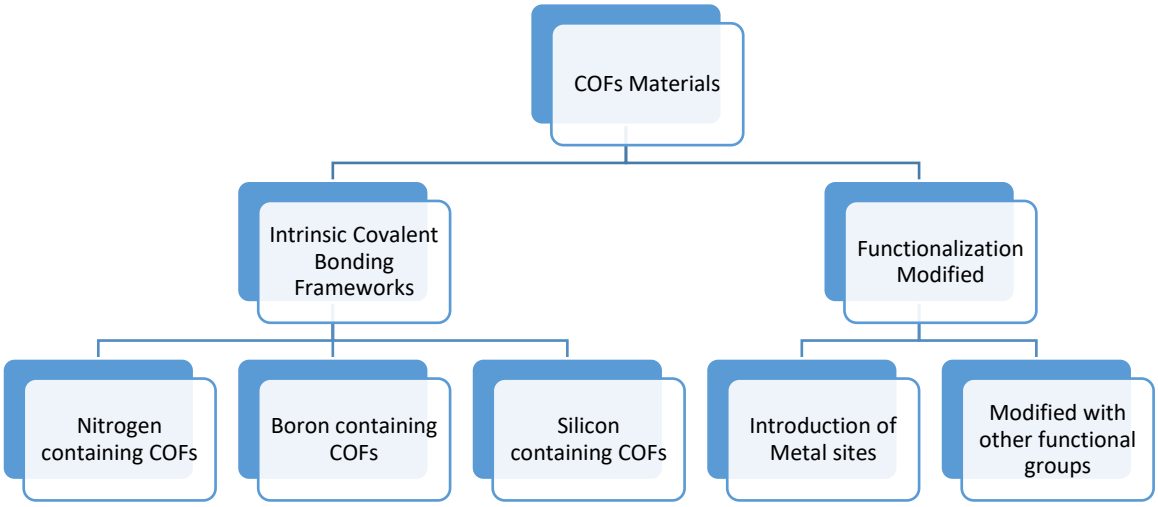

Figure 1.7 Classification of COFs [83]

COFs can be classified into intrinsic COFs catalysts and loaded COFs catalysts based on the type of catalyst. Intrinsic catalysts are designed by embedding catalytic active centers into the material backbone using a "bottom-up" approach; loaded catalysts are designed by loading metal particles or ions with COFs as heterogeneous catalysts. Intrinsic COFs catalysts are introduced by a

controlled number of uniformly dispersed active sites, and the regular and unique pore structure of COFs promotes the creation of heterogeneous catalysts and substrate transformation. The loaded COFs catalysts were post-modified to introduce a catalytic activity center, thus allowing good dispersion of the catalytic active sites and facilitating the binding of the substrate to the catalytically active site.

Since 2005 Yaghi et al. designed the first example of COF, the structural design, controlled synthesis, structure elucidation, and function discovery have all been investigated by researchers. [84] Because of their porous property, open pore structure, good stability, and ease of modification, COFs have demonstrated an increasing number of intriguing uses in catalysis, and the applications of COFs to photocatalytic reactions, electrocatalytic reactions, and organocatalysis has received widespread attention.

Stegbauer reported the first successful photocatalytic reaction, that is, hydrogen generation, utilizing COFs. [85] COFs are increasingly being developed for usage as photocatalysts and photosensitizers. Wang reported oxidative hydroxylation of arylboronic acids to phenols with a series of COFs (LZU-190, 191, and 192) under visible light. [86] LZU-190 exhibited excellent activity, a broad scope, and recyclability; the catalytic reaction was the first photocatalytic application using a metal-free benzoxazole-based COF (Scheme 1.12).

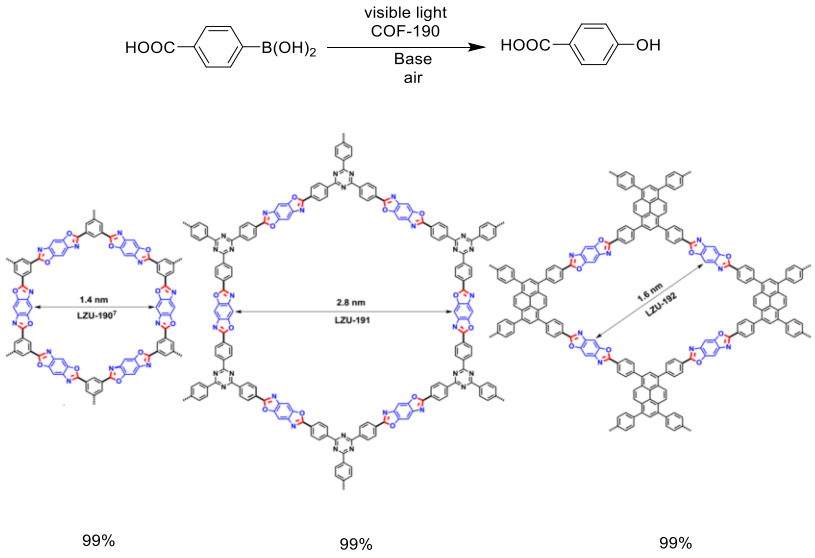

Scheme 1.12 Photocatalysis using catalysts based on COFs [86]

Electrocatalytic reactions including ORR, OER, and carbon dioxide reduction have been performed with a large number of COFs; COFs have also been used in photocatalytic reactions. [87] Ma published the first ORR using a cobalt-porphyrin-based COF as the catalyst in 2015. [88] The cobalt-porphyrin-based COF exhibited excellent catalytic activity and could replace commercial Pt catalysts. In the same year, Yaghi reported a series of 2D COFs using bimetallic centers (Co and Cu) with porphyrins to realize carbon dioxide reduction in water (Figure 1.8). [89] The 2D cobalt-copper COF achieved a high Faradaic efficiency of 90% and 29000 TON at an overpotential of -550 mV. In 2018, Yaghi developed a series of 2D COFs with porphyrin active

sites for reduction of carbon dioxide (Figure 1.8). [90] Yaghi's COF catalyst exhibited high selectivity at a low overpotential (550 mV) and a better efficiency performance than that of homogeneous catalysts at high current densities (65 mA/mg). The catalyst could operate for 12 h without any obvious deactivation.

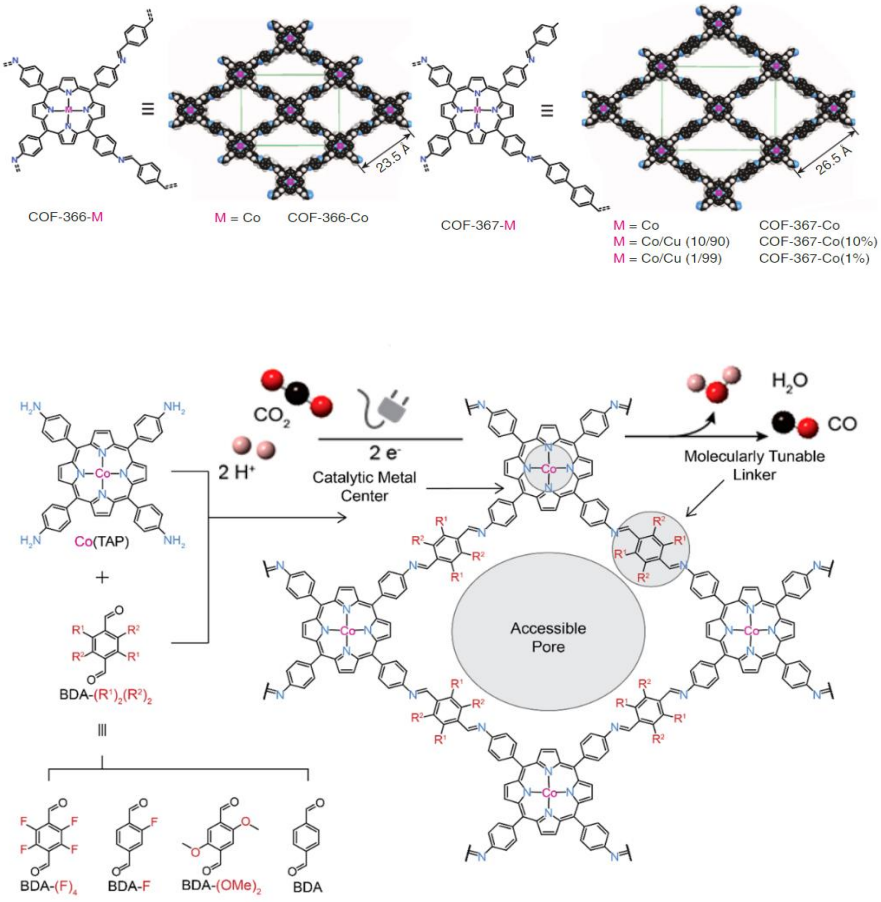

Figure 1.8 Electrocatalysis using catalysts based on COFs [89-90]

Except for photocatalysis and electrocatalysis, most multifunctional COFs are employed in organocatalysis, such as various coupling, oxidation and reduction, condensation, and addition reactions.

The Suzuki-Miyaura coupling reactions, and Sonogashira coupling reactions, are essential for forming new carbon-carbon bonds. Hou demonstrated the first COF (H_2P-Bph-COF), which was based on a nitrogen-rich porphyrin, for Suzuki-Miyaura coupling reaction of bromoarenes with phenylboronic acid under mild conditions (Scheme 1.13). [91]

The catalytic system Pd/H_2P-Bph-COF exhibited excellent catalytic performance (97.1%–98.5%) at the same level as that of homogeneous catalysis. Later, more coupling reactions were reported using heterogeneous COFs-based catalytic systems to produce C-C or C-N bonds, such as the Heck coupling, Chan-Evans-Lam coupling, among others (Scheme 1.13). [92]

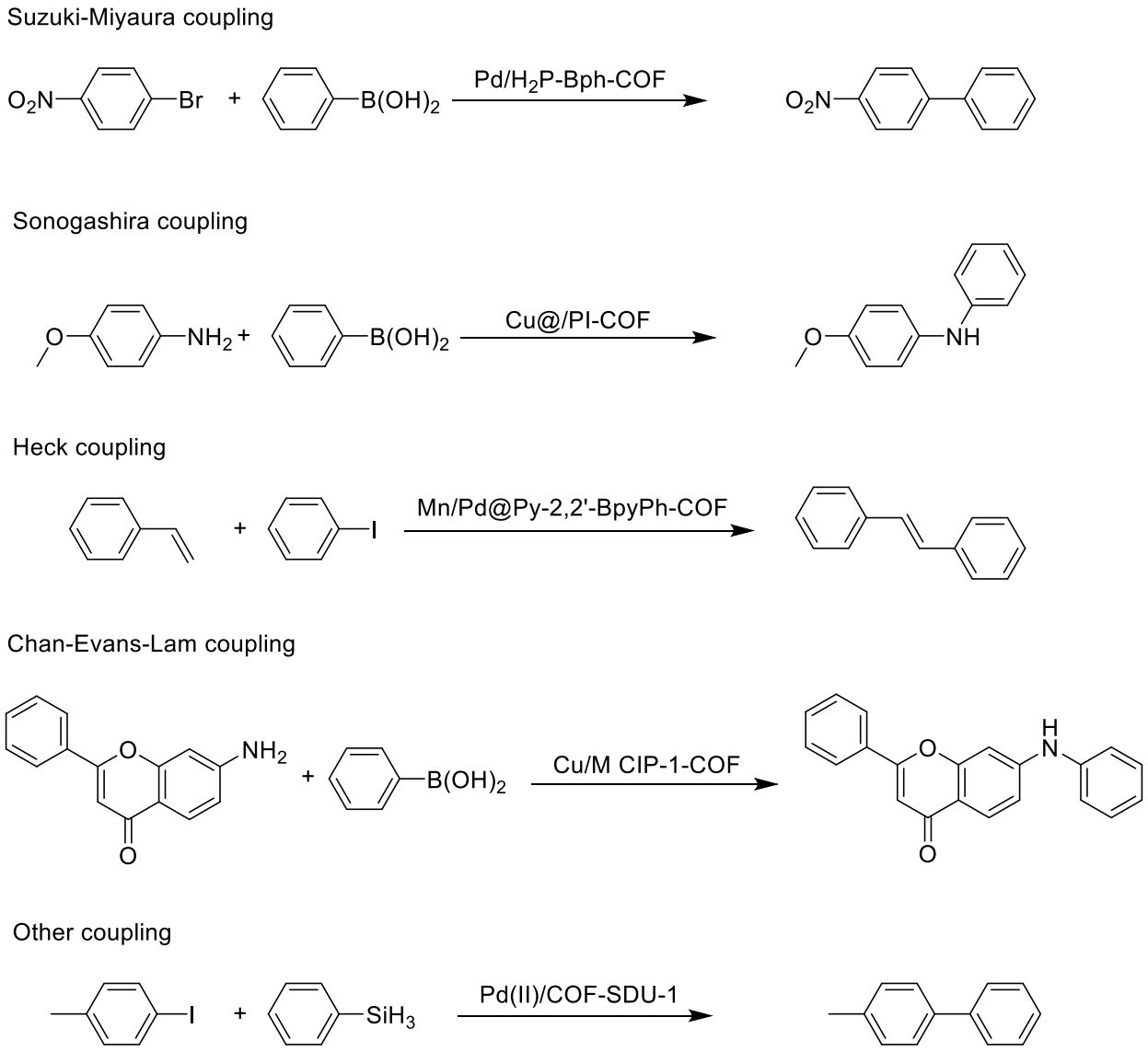

Scheme 1.13 Various coupling reactions using catalysts based on COFs [91-92]

Oxidation and reduction reactions are essential reactions in organic catalysis to synthesize organic compounds, natural products, and industrial chemicals. Fan designed two triazinyl-COFs with different pore sizes for the reduction of nitroarenes. (Scheme 1.14) [93] Compared with other homogeneous catalysts, the Pd@COF-BPh catalyst exhibited high activity (99%) and excellent stability in acidic and alkaline media.

Condensation is an alternative method for forming carbon-carbon bonds. The new porous materials-COFs exhibited high reaction activities (97%-99% yields) and good catalytic performances (good functional group tolerances) in general condensation reactions, such as Knoevenagel, Aldol and Mannich condensation (Scheme 1.14). [94]

In addition to the above-mentioned reactions, COFs catalysts are utilized for other addition reactions, for example the cycloaddition, Michael addition, and isomerization reactions. [95]

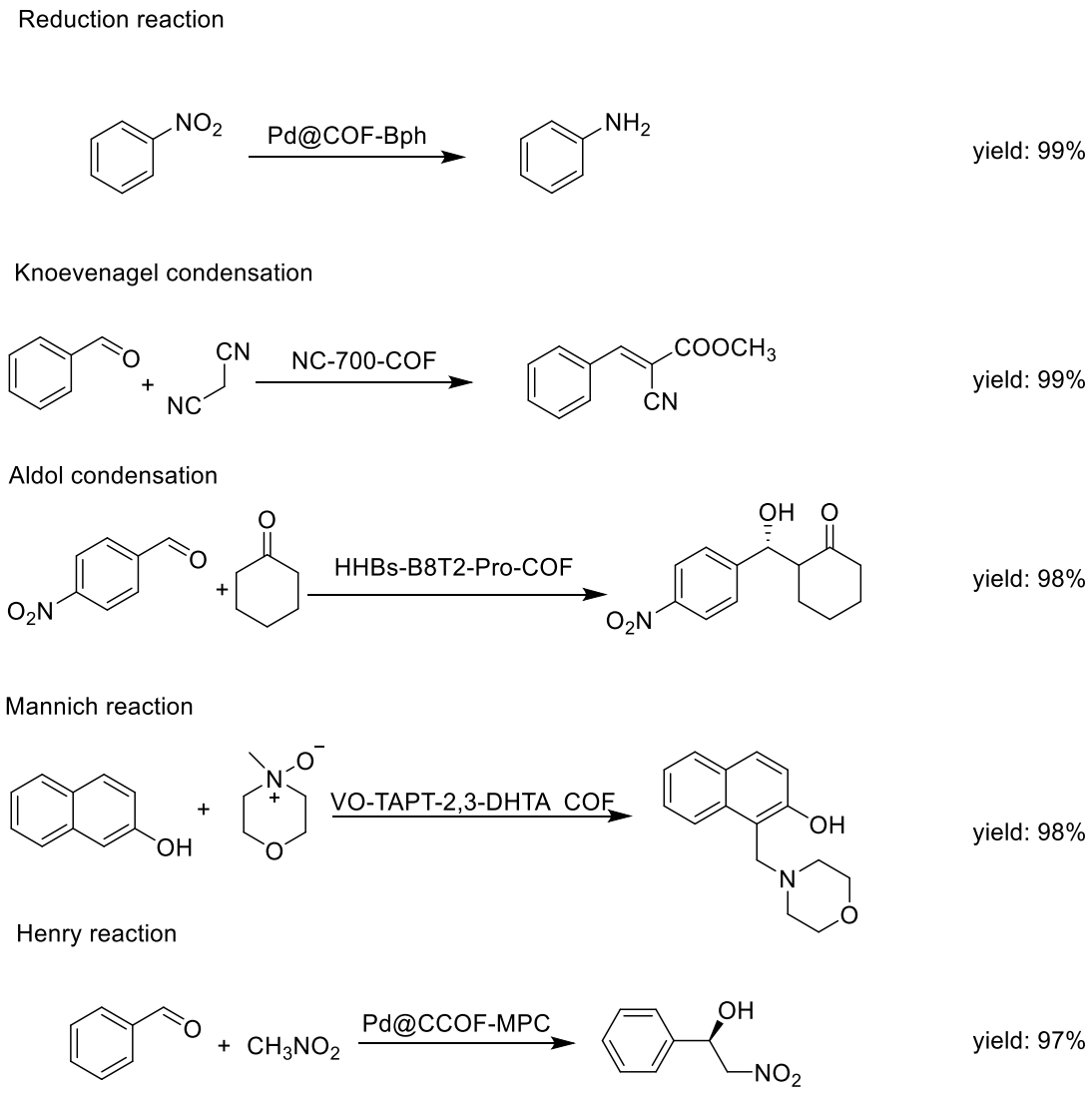

Scheme 1.14 Reduction and condensation reactions using catalysts based on COFs [93-94]

1.3.6 Porous Organic Polymers (POPs)

POPs are a vital type of multidimensional porous network materials, which are constructed from various organic building blocks with different topologies and geometries linked by strong irreversible covalent bonds. [96] This novel material has the advantages of high specific surface area, excellent stability, and good robustness in various solvents, which provide more active sites and are beneficial for mass transfer. [96] Permanent nanometer-scale holes can help expose the active areas for catalytic transformations. [97] In comparison to other porous materials, such as zeolites, MOFs, and silica, POPs can be easily designed and controlled by introduction of different specific functional organic building blocks. Xiao demonstrated that the swelling of POPs is beneficial for a high degree of flexibility and more accessible catalytic active sites to boost catalytic activity. [98] POPs have shown increasing potential for numerous applications, such as heterogeneous catalysis, gas storage/separation, chemical- and bio-sensing, photoelectric conversion, and energy storage and conversion. [99]

Amorphous and crystalline POPs are the two main types of POPs. Porous polymer networks (PPNs), conjugated microporous polymers (CMPs), polymers of intrinsic microporosity (PIMs), porous organic frameworks (POFs), hyper-cross-linked polymers (HCPs), polymeric organic networks, and porous aromatic frameworks are amorphous POPs, while the crystalline POPs are COFs (see the previous section) and crystalline triazine-based frameworks (Figure 1.9). [100] Crystallinity COFs has a uniform structure that is good for separation but can be detrimental to catalysis because of their insolubility. In the following, only the amorphous POPs are discussed.

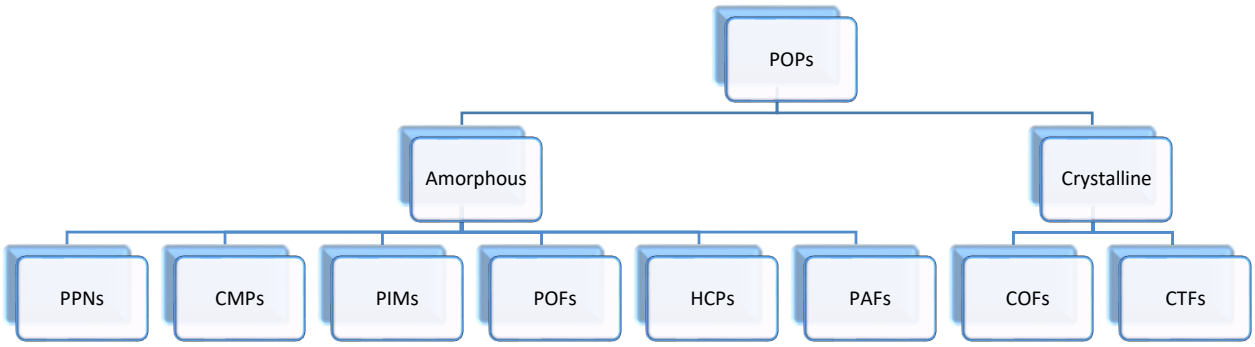

Figure 1.9 Classification of POPs [100]

The industrial use of solid-supported catalysts is limited because of their low efficiency. However, well-designed POPs catalysts can meet these academic and industrial demands, which are high activities and good catalytic performances. These tailored organic ligand groups bond via strong covalent bonds, which is the main advantage of POPs over other heterogeneous solid catalysts, such as zeolites, polymers, and MOFs.

POPs are rapidly evolving and have a broad spectrum of applications as metal-free organocatalysts or metal-POP catalysts. The reactions in which metal-free POP catalysts are used have been classified into four main categories: chiral catalysis, acid and base catalysis, and cycloaddition of carbon dioxide to epoxides. The reactions in which metal-POP catalysts are used include Lewis acid catalysis, oxidation, reduction, photocatalysis, and coupling reactions.

1.3.6.1 Metal-free POP Catalytic System

The first part of this section discusses how metal-free POP catalysts can be used. There are three types of acids used in acid catalysis: sulfonic acids, carbon-based acids, and hydrogen bond catalysts (as an alternative to Lewis acids). Xiao designed the first sulfonic acid functionalized POP-PDVB-x-SO_3H catalyst for the esterification of hexanoic acid with ethanol. [101] The activities of PDVB-x-SO_3H POP were higher than those of solid catalysts with counter parts, such as SBA-

15-Ar-SO_3H and Amberlyst 15. Bhaumik and co-workers synthesized a POP-COP-A with an acidic –COOH group for indole C3 functionalization using benzhydrols as electrophiles (Scheme 1.15). [102] The metal-free catalytic system had a high content of active sites and functioned under mild conditions (room temperature, 4 h). Kim discovered that melamine-POP was an efficient hydrogen-bonding catalyst (90-99% yields) for the acetalization of aldehyde and ketones with methanol (Scheme 1.15). [103] In terms of conversion and product selectivity, this catalytic system worked admirably. These three reactions do not require any harsh solvents and meet the requirements of the "12 Principles of Green Chemistry." [5]

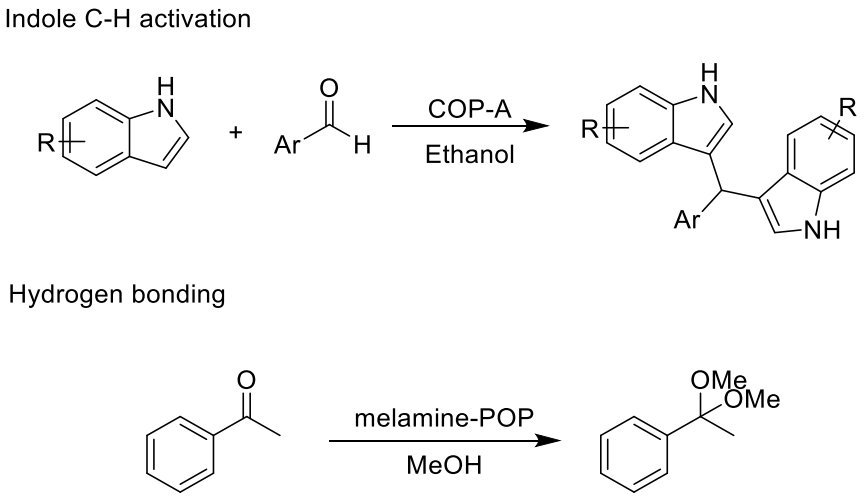

Scheme 1.15 Metal free-catalysis using acids on POPs [102-103]

The Knoevenagel condensation can be catalyzed by Tröger's base, forming a C-C bond. POP-PIM-Tb-Trip carrying triamino-triptycene was synthesized by Carta using the Knoevenagel condensation procedure (Scheme 1.16). [104] In Knoevenagel condensation of malononitrile with benzaldehyde, the metal-free POP enhanced activity more efficiently (100% in 2 h) than did Tröger's base (73% in 2 h).

The nucleophilic catalyst, DMAP (4-(*N*,*N*-dimethylamino)pyridine), is commonly utilized in a wide range of processes. [105] Wang et al. synthesized DMAP-NCP, which was used in a metal-free POP catalytic system for the acylation of alcohols (Scheme 1.16). [106] This POP can be utilized for continuous flow reactions because the nucleophilic DMAP-NCP does not degrade.

N-heterocyclic carbenes (NHCs) are POP catalysts that can be either nucleophilic or basic. The Kaskel group used NHC-POP as a nucleophilic catalyst to achieve conjugated umpolung reaction of trifluoroacetophenone with unsaturated cinnamaldehyde (Scheme 1.16). [107] NHCs POP catalytic system produced results comparable to those of homogeneous catalysis.

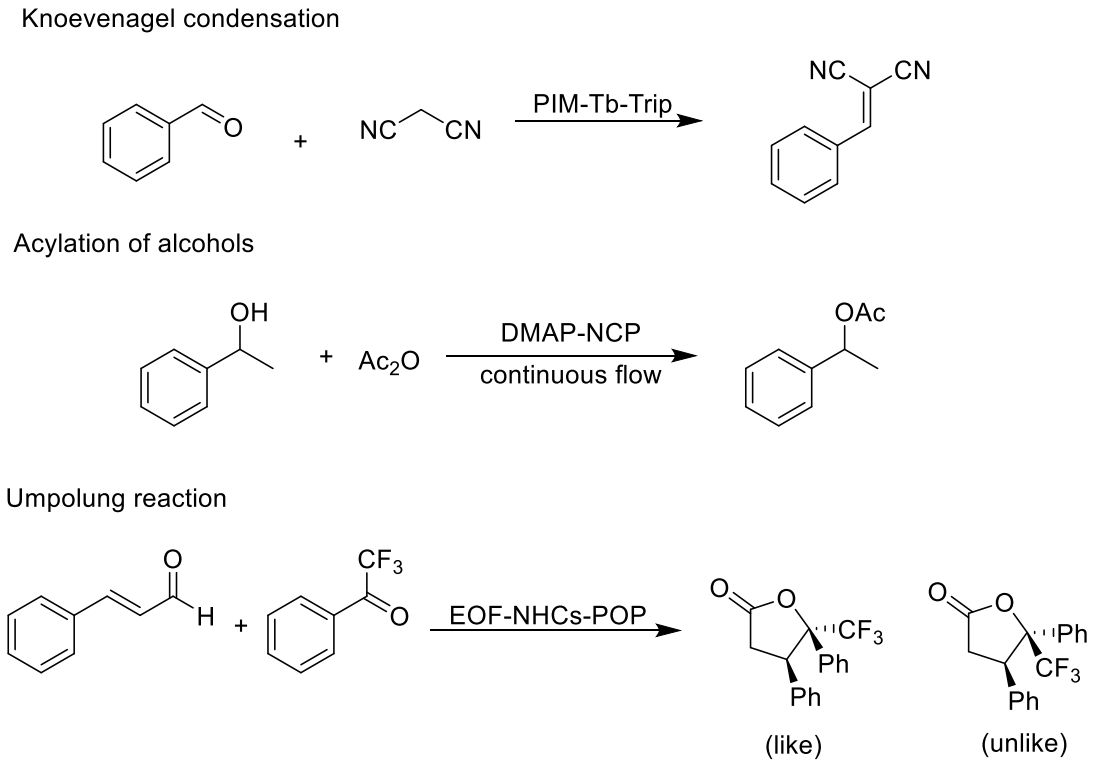

Scheme 1.16 Basic and nuclephilic catalysis using POPs [104, 105, 107]

Chiral catalysts are important in asymmetric catalysis and have sparked considerable interest in the pharmaceuticals, agricultural products, and industries. In recent years, using the immobilization of chiral catalytic moieties on POPs, as heterogeneous catalysts, has shown significant promise. The two basic methods for synthesizing chiral POPs are post-synthetic modification and a bottom-up method to immobilize chiral ligands on a POP. Chiral POPs have good mass transfer properties, therefore, the solubility of POP should be considered first when attempting to improve the catalytic activity of chiral POPs. Chiral POPs have been synthesized using various catalytic methods.

Chiral BINOL (1,1-bi-2-naphthol), is a homogeneous ligand widely used in organic chemistry. [108] The immobilization of chiral BINOL generated phosphonic acid on a polymer was initially described by Rueping et al. [109] Chiral POPs exhibit high enantioselectivity and yield when hydrogenating quinolones and benzoxazines. Thomas et al. later developed chiral POPs with the same chiral moiety for hydrogenation but excluded the metals (Scheme 1.17). [110] Six different types of chiral POPs share the same chiral moiety but were obtained using different ways, as shown in the Scheme 1.17 diagram. These chiral POPs have varied surface areas, pore diameters, and steric hindrances owing to different synthesis processes and monomers for polymers, and these differences cannot achieve the same level of outcomes.

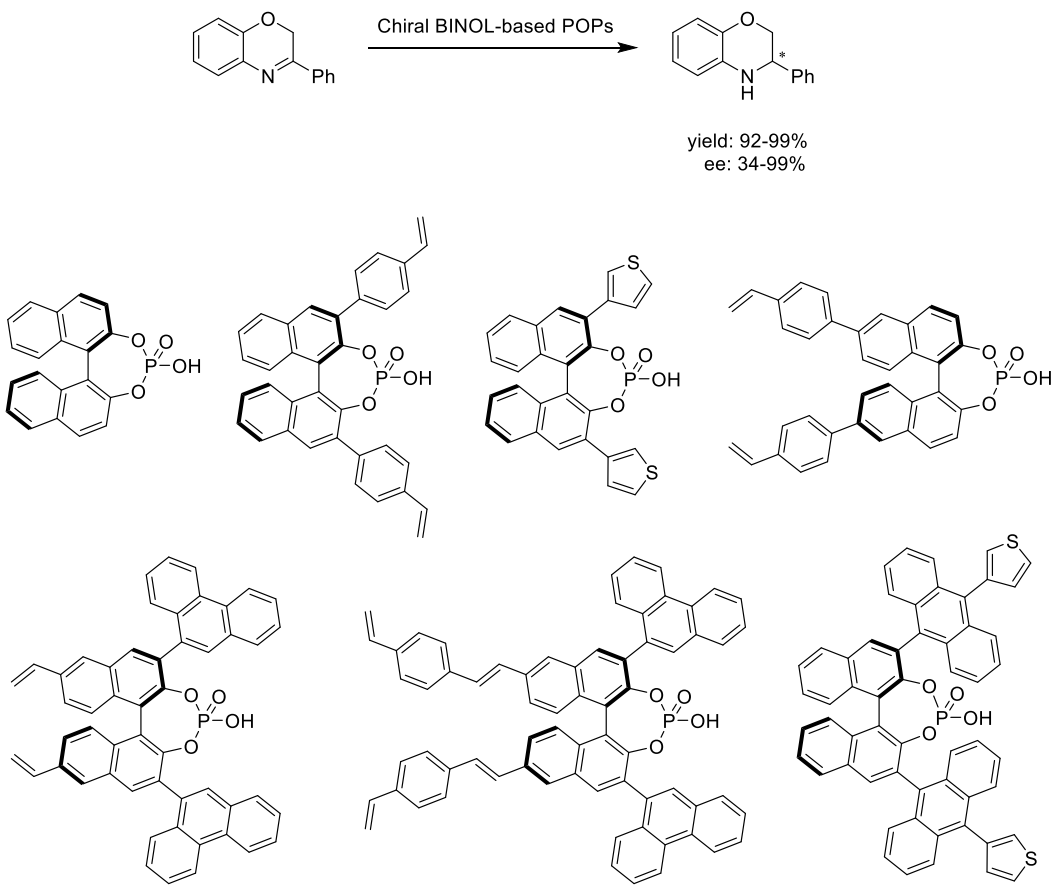

Scheme 1.17 Asymmetric hydrogenation and monomers used for chiral POPs [109-110]

List and MacMillan demonstrated that chiral amines play a significant role in asymmetric catalysis. [111] The use of chiral amines to reduce POPs has attracted significant interest. Wang's group developed a JH-CPP chiral POP with a diarylprolinol silyl ether catalyst for asymmetric Michael addition between aldehydes and nitrostyrenes in 2002. [112] In metal-free catalytic systems, a mixed solvent (ethanol and water) is considered a green solvent. Later, Wang et al. used a bottom-up strategy to create novel chiral POPs using a MacMillan catalyst to achieve an asymmetric Diels-Alder process (Scheme 1.18). [113] A MacMillan catalyst, namely, Mac-CPOP-2, has a high BET surface area, and the metal-free catalytic system shows good yields and enantioselectivities in a mixed methanol and water solvents (Scheme 1.18). In 2019, Lan et al. designed a chiral POP with a pyrrolidine moiety using the same bottom-up strategy, and the Py-CPP performed well in asymmetric Michael addition of nitroolefins with cyclohexanone in water (Scheme 1.18). [114]

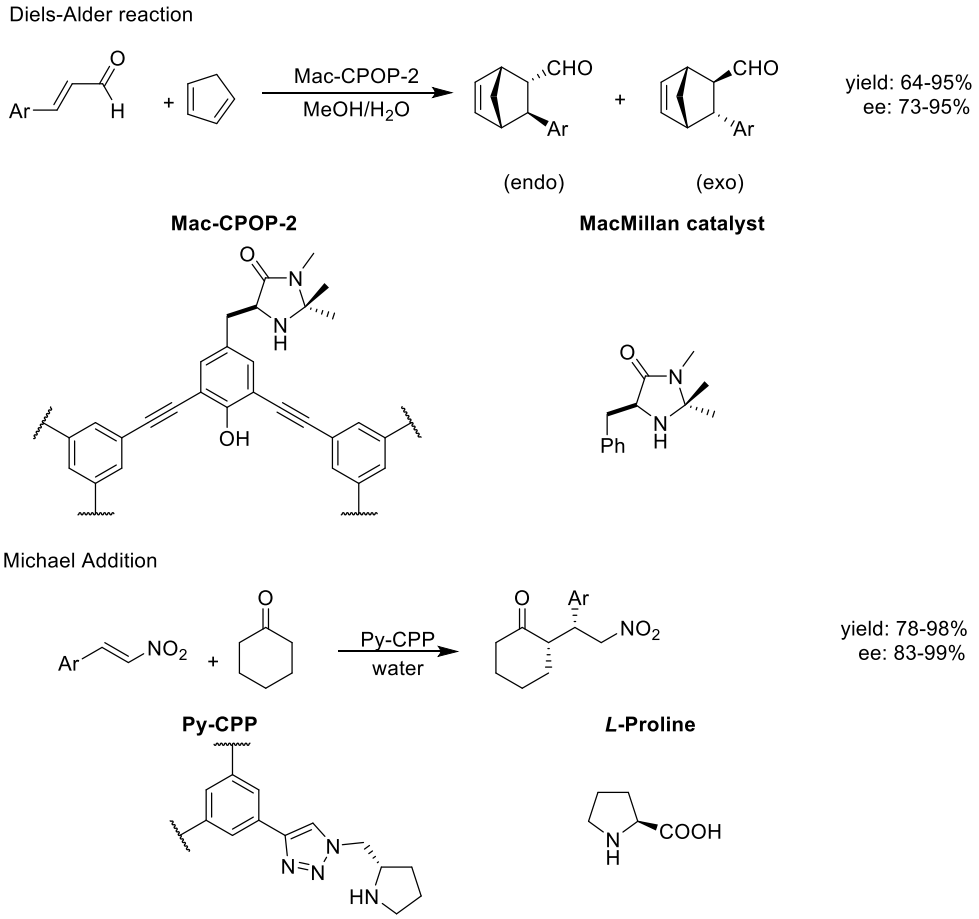

Scheme 1.18 Asymmetric catalysis using chiral amine POPs [113-114]

Metal-free POPs catalytic systems are also applied in photocatalysis, especially oxidation reactions. As Scheme 1.19 shows, the electrons are excited from valence bands (VB) to conduction bands (CB) when POPs obtain photons; the photons thereafter transfer to the surfaces of POPs for redox reaction. [115] It is speculated that two reactive species ($^1O_2$ and $O_2^{\cdot-}$) may have participated in the photocatalytic oxidation reactions. Both the reactive oxygen species can be generated during energy and charge transfer processes. One of the two main reactive species can operate as the principal oxidant. [116]

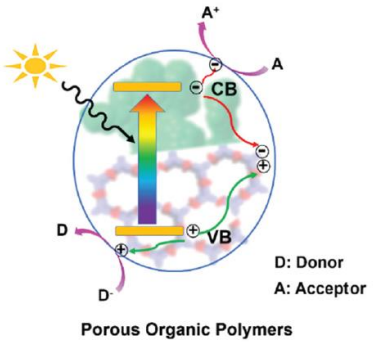

Scheme 1.19 General illustration for mechanism of photocatalysis using POPs [115]

When $^1O_2$ is used as the oxidant for photodriven oxidation, the POPs first absorb the photons and thereafter change into singlet excited state, shifting the energy to generate a singlet excited state $^1O_2$ on the triplet oxygen, while the electron undergoes the triplet excited state transformation. A series of porous conjugated polymers (CMPs) were synthesized by Zhang and co-workers for selective oxidation. [117] Under visible light irradiation, the metal-free CMPs catalytic system exhibited highly efficiency (yield up to 99%) for selective oxidation (Scheme 1.20). An example of using $O_2^{\cdot-}$ as an oxidant for photodriven oxidation, is the study by Kang who described a photoactive benzodifuran-containing microporous organic polymer for the oxidative conversion of amines to imines (Scheme 1.20). [118]

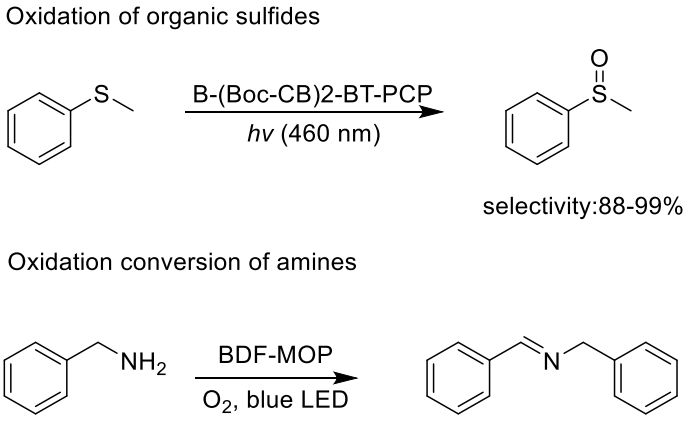

Scheme 1.20 Photocatalysis using metal free POPs [117-118]

1.3.6.2 Metal-POPs Catalytic System

Active catalysts play vital roles in various catalysis reactions. The incorporation of metals and POPs, which have modified ligand inside, can generate active catalyst sites. The metal-POP catalytic system is a single-atom-site catalyst and straddles the line between homogeneous and heterogeneous catalysis (Figure 1.10). [119] There are two approaches to incorporating metals into POPs. The first approach is a direct metalation by mixing POP with a metal precursor, and the second involves the polymerization of monomers or single-building blocks containing metal or metal complexes.

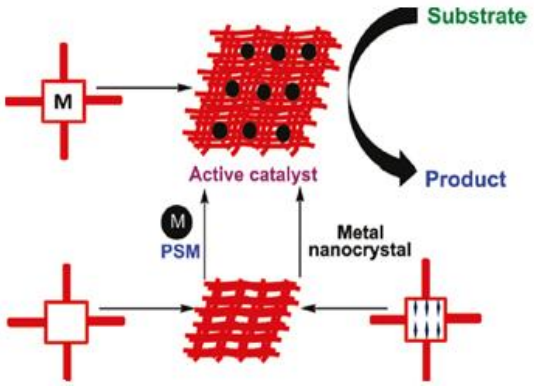

Figure 1.10 Illustration of metal-POP catalytic system [119]

The combination of metal-POPs has a wide variety of applications due to the rapid development of metal-POP catalytic systems; the reactions include Lewis acid catalysis, oxidation, reduction, photocatalysis, and coupling reactions.

Lewis acid organic catalysis is a reaction catalyzed by Lewis acids such as Al, Zn, Fe *etc.*; the Lewis acid offers an empty orbital for the nucleophile to increase the reactivity of the substrate. Many reactions catalyzed by a large range of metals (Zn, Al, Co, Fe, Mg, Mn, Cu, Ti, and Au) [120] have reported that metal-POP active sites have a big influence on Lewis acid organic catalysis. Consider the Ti-POP catalyst as a representative example; Lin designed a novel chiral POP based on chiral BINOL for Lewis acid catalysis (Figure 1.11). [120] The researcher used the metalation approach to generate a singlet active site for the asymmetric addition of aldehydes with diethylzinc. The method has high selectivity and conversion, and the catalyst can be reused up to ten times.

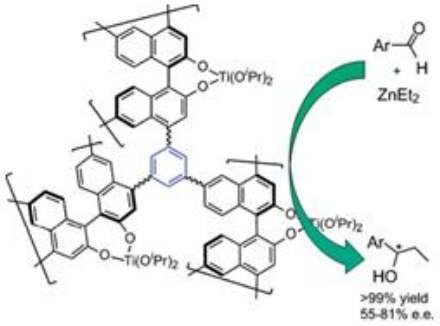

Figure 1.11 Illustration of diethylzinc addition to aldehydes catalyzed using Ti-POP [120]

The oxidation of organic compounds catalyzed using metal-POP has attracted remarkable interest, with the oxidation of alkenes being the most studied by researchers. Various metal-POP catalysts have been used for oxidation of alkenes, and Mn is the most commonly used metal. [121] In addition to alkenes, the oxidation of alcohols and arylalkanes can be catalyzed by a metal-POP active site system (Scheme 1.21). [122]

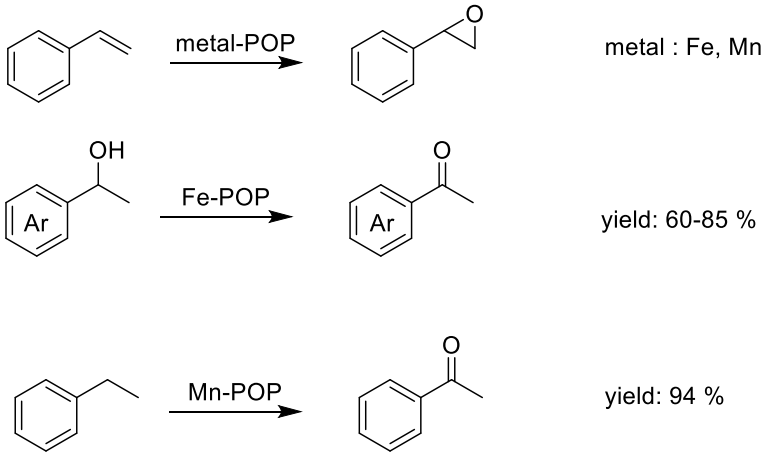

Scheme 1.21 Organic oxidations using metal-POP [121-122]

Metal-POP catalysts have also catalyzed several reduction reactions, for example, the hydrogenation of β-keto esters and quinolones, transfer hydrogenation, carbonyl hydrosilylation, and reductive amination (Scheme 1.22). [123] The corresponding products are β-hydroxy esters, amines, and chiral 1,2,3,4-tetrahydroquinoline derivatives, which are crucial building blocks for chiral biological medicines, natural products, [124] and silyl ethers, which are considered the synthetic equivalents of alcohols.

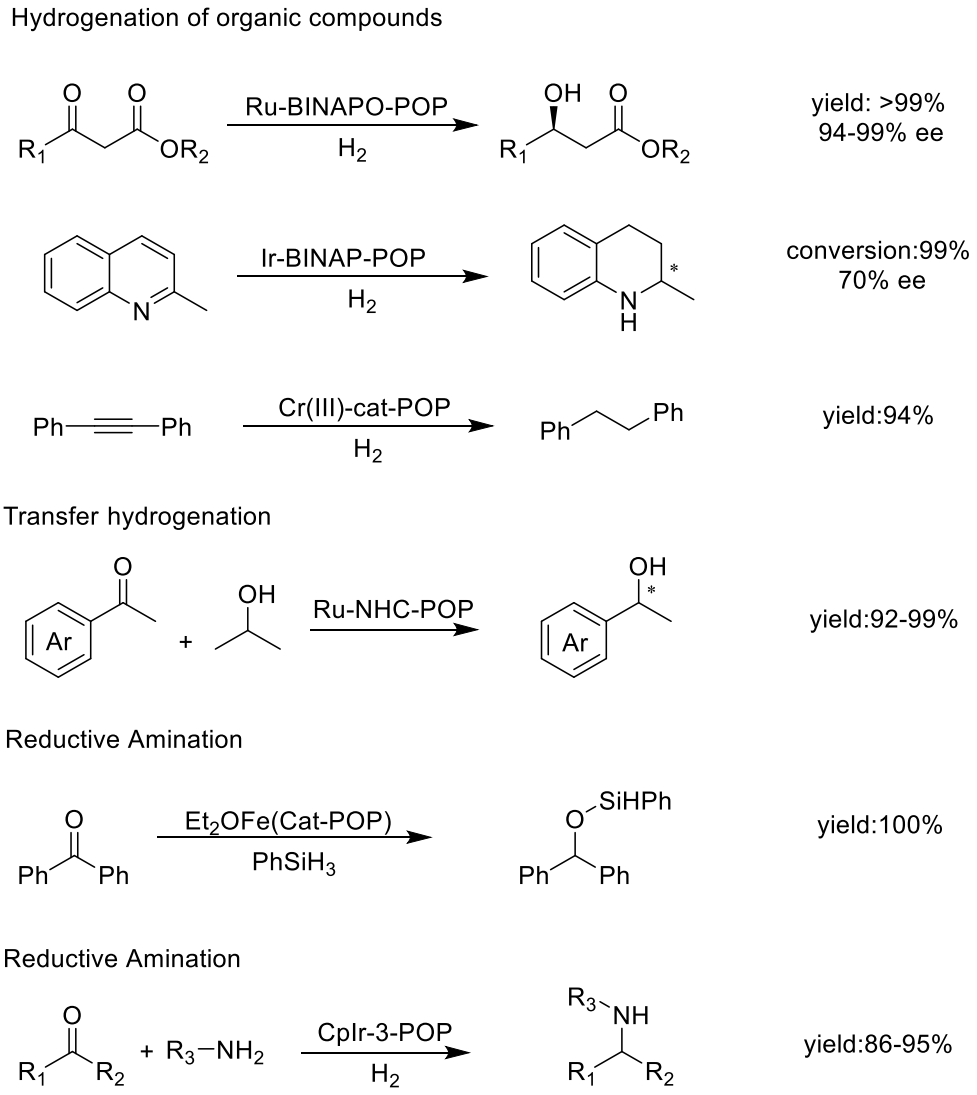

Scheme 1.22 Organic reductions using metal-POP [123]

Suzuki-Miyaura, Sonogashira, Heck, Ullmann, and oxidative coupling, which are general coupling reactions, have used metal-POP to generate C-C, C-N, and C-O bonds. [125] Sawamura, [125a] Mu, [125b] and Huang [125c] reported efficient Pd-POP catalysts for the Suzuki-Miyaura coupling (Scheme 1.23). The activities of the three Pd-POP catalysts were preserved for a longer duration by filtering the heterogeneous catalysts. Dong et al. reported the Sonogashira coupling reaction using *in-situ* Pd@PTC-POP as a phase transfer catalyst (Scheme 1.23). [125d] Pd@PTC-POP was synthesized using the second metalation method to avoid further Pd loading in the catalytic

reaction. The Pd-MsMOP-1-POP catalyst that was designed by Mu-catalyzed the Heck coupling reaction (Scheme 1.23). [125b] High catalytic efficiency was achieved in the Heck coupling reaction of diverse olefins and aryl halides. The catalytic activity (94%) was maintained after reusing five times. For the Ullmann coupling reaction, Xiao developed a Cu-incorporated Schiff base-modified POP, PDVB-SB-Cu-POP (Scheme 1.23). [125e] The high activity of PDVB-SB-Cu-POP is similar to that of the homogeneous catalyst. In comparison with other coupling reactions, this PDVB-SB-Cu-POP utilized the inexpensive metal Cu instead of the noble metal Pd to minimize the reaction costs. Oxidative coupling reactions are defined as the coupling of two nucleophiles via an oxidative reaction, with oxygen as the oxidant in most cases. Xiao, [125f] Shi, [125g] Yan, [125h] Wendt, [125i] and Yu. [125j] have reported different carbon substrates (C(sp), C(sp^2), C(sp^3)) for oxidative coupling reactions. Pd is the most used transition metal in these catalytic reactions. Xiao developed a similar Cu-POP catalyst to PDVB-SB-Cu-POP, namely, Cu-Phen-POP, to realize the oxidative coupling of phenylacetylene in the presence of oxygen (Scheme 1.23). [125f] The catalytic activity of Cu-Phen-POP is better than that of PDVB-SB-Cu-POP because it can be reused ten times with 97% yield.

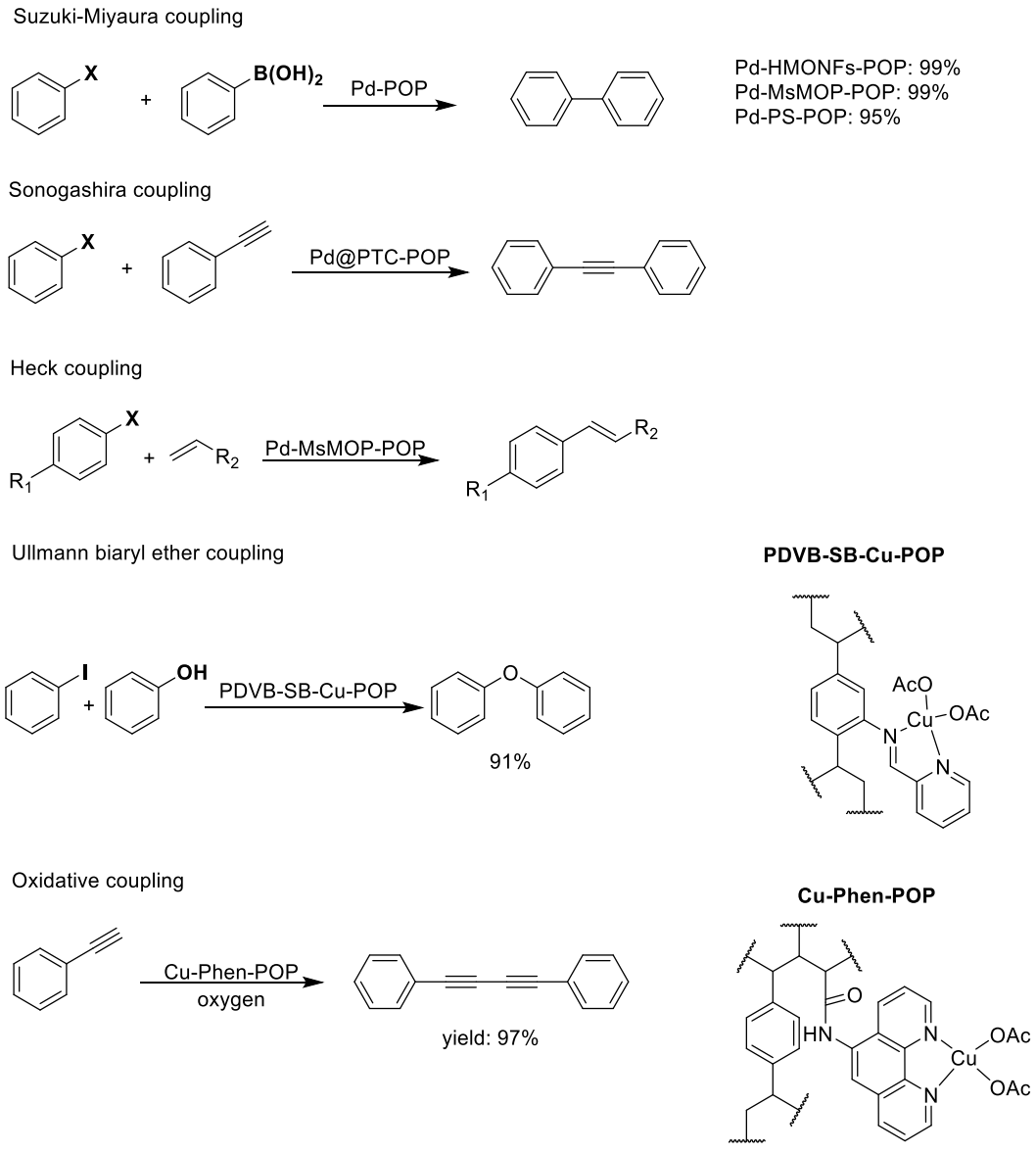

Scheme 1.23 Coupling reductions using metal-POP [125]

POP is a promising platform for highly efficient photocatalytic reactions with metal-free POP. The coupling of metal with POP to form a catalyst can also accomplish photocatalysis, such as the oxyamination of aldehyde, α-arylation of bromomalonate, and aza-Henry reaction. Lin reported two types of metal-POP catalysts that used different metals (Ir and Ru) for three photocatalytic reactions (Figure 1.12). [126] The POPs that contained bipyridyl Ir or Ru species were synthesized via $Co_2(CO)_8$-mediated trimerization. The Ir-bpy-POP and Ru-bpy-POP have high catalytic performance equivalent to those of homogeneous Ir and Ru complex photocatalysts in the oxyamination of aldehyde, α-arylation of bromomalonate, and aza-Henry reaction.

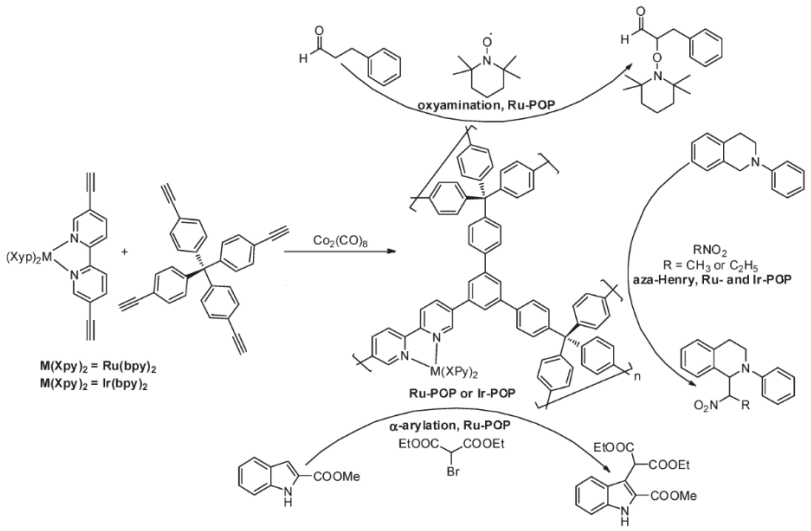

Figure 1.12 Illustration of synthesis of M-bpy-POPs and their applications in photocatalysis [119a, 126]

Kobayashi also synthesized a heterogeneous POP photocatalyst containing an Ir-based polypyridyl complex for the aza-Henry reaction between different P-based nucleophiles and tetrahydroisoquinolines (Scheme 1.24). [127] The Ir-ppy-POP catalyst could only be reused three recycles owing of Ir leaching.

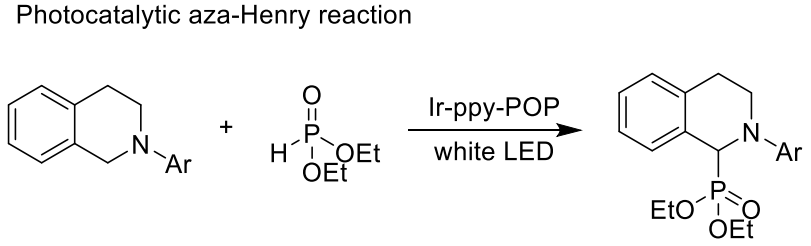

Scheme 1.24 Photocatalyzed aza-Henry reaction using Ir-ppy-POP [127]

1.4 References

[1] Calvin, B. H., Robert, J. F., *Fundamentals of Industrial Catalytic Processes, Second Edition*, John Wiley and Sons, Hoboken, NJ, **2006**.

[2] Erisman, J.W., Sutton, M.A., Galloway, J., Klimont, Z. and Winiwarter, W., *Nat. Geosci*. **2008**, *1*, 636-639.

[3] Ostwald, W., *Zeit. Phys. Chem*. **1894**, *15*, 705-706.

[4] Catalysis-Reaction progress, can be found under https://commons.wikimedia.org/wiki/File:Catalysis-_Reaction_progress.png (accessed 08/11/2021)

[5] Anastas, P. T., Warner, J. C., *Green Chemistry: Theory and Practice*, Oxford University Press: New York, **1998**.

[6] Falbe J., and Bahrmann, H., *Chem. Unserer Zeit*, 15, **1981**.

[7] Hagen, J., *Industrial Catalysis: Apractical Approach*, Wiley-VCH, **2015**.

[8] Fonds der Chemischen Industrie zur Förderung der Chemie und Biologischen Chemie, *Folienserie des Fonds der Chemischen Industrie*. **1999**.

[9] a) Prieto, G., Zečević, J., Friedrich, H., De Jong, K.P. and De Jongh, P.E, *Nature materials*, **2013**, *12*, 34-39. b) Zhu, J., Wang, T., Xu, X., Xiao, P. and Li, J., *Applied Catalysis B: Environmental* **2013**, *130*, 197-217. c) Schauermann, S., Nilius, N., Shaikhutdinov, S. and Freund, H.J., *Accounts of chemical research* **2013**, *46*, 1673-1681. d) Gallon, B.J., Kojima, R.W., Kaner, R.B. and Diaconescu, P.L., *Angewandte Chemie International Edition* **2007**, *46*, 7251-7254. e) Fan, Q.H., Wang, R. and Chan, A.S., *Bioorg. Med. Chem. Lett*. **2002**, *12*, 1867-71. f) Song, C. E.; Kim, D. H.; Choi, D. S., *Eur. J. Inorg. Chem*. **2006**, *15*, 2927–35. g) Song, C. E.; Park, I. S., *Advances in Organic Synthesis*. Bentham Publishers, **2005**. h) Li, C., *Catalysis Reviews– Science and Engineering*, **2004**, *46*, 419–92.

[10] a) Thompson, D. *Gold Bull*. **1998**, *31*, 111–118. b) Thompson, D. *Gold Bull*. **1999**, *32*, 12–19. c)Crampton, A.S., Rötzer, M.D., Schweinberger, F.F., Yoon, B., Landman, U. and Heiz, U., *Journal of Catalysis*, **2016**, *333*, 51-58.

[11] Saxena, S., Singh, R., Pala, R. G. S., and Sivakumar, S. *RSC Adv*. **2016**, *6*, 8015–8020.

[12] Chen, Z., Della Pina, C., Falletta, E., Faro, M.L., Pasta, M., Rossi, M. and Santo, N., *J. Catal*. **2008**, *259*, 1–4.

[13] a) Choudhary, V.R., Dhar, A., Jana, P., Jha, R. and Uphade, B.S., *Green Chem*. **2005**, *7*, 768–770. b) Choudhary, V.R. and Dumbre, D.K., *Catal. Commun*. **2009**, *10*, 1738–1742.

[14] Ferraz, C.P., Garcia, M.A.S., Teixeira-Neto, É. and Rossi, L.M., *RSC Adv*. **2016**, *6*, 25279–25285.

[15] Nepak, D., and Srinivas, D. *RSC Adv*. **2015**, *5*, 47740–47748.

[16] Tojo, G., and Fernández, M. *A Guide to Current Common Practice. New York, Springer*, **2006**.

[17] a) Carabineiro, S.A. and Thompson, D.T., *Nanocatalysis* **2007**, 377–489. b) Zhao, R., Ji, D., Lv, G., Qian, G., Yan, L., Wang, X. and Suo, J., *Chem. Commun*. **2004**, *904–905*. c) Hereijgers, B.P. and Weckhuysen, B.M., *Catal. Lett*. **2011**, *141*, 1429–1434. d) Staykov, A., Miwa, T., and Yoshizawa, K. *J.*

Catal. **2018**, *364*, 141–153. e) Bravo-Suárez, J.J., Bando, K.K., Akita, T., Fujitani, T., Fuhrer, T.J. and Oyama, S.T., *Chem. Commun*. **2008**, 3272–3274.

[18] Kinting, A., Krause, H. and Čapka, M., *Journal of Molecular Catalysis* **1985**, *33*, 215–223.

[19] Valenti, G., Rampazzo, E., Bonacchi, S., Petrizza, L., Marcaccio, M., Montalti, M., Prodi, L. and Paolucci, F., *J. Am. Chem. Soc*. **2006**, *138*, 15935–15942.

[20] Mitran, R.A., Berger, D., Munteanu, C. and Matei, C., *The Journal of Physical Chemistry C*. **2015**, *119*, 15177–15184.

[21] Glasing, J., Champagne, P. and Cunningham, M.F., *Current Opinion in Green and Sustainable Chemistry*. **2016**.

[22] Nandiyanto, A.B.D., Iskandar, F. and Okuyama, K., *Chemistry Letters*. **2008**, *37*, 1040–1041.

[23] Raynor, S.A., Thomas, J.M., Raja, R., Johnson, B.F., Bell, R.G. and Mantle, M.D., *Chem. Commun*. **2000**, 1925–1926.

[24] Jones, M.D., Raja, R., Thomas, J.M., Johnson, B.F., Lewis, D.W., Rouzaud, J. and Harris, K.D., *Angew. Chem., Int. Ed*. **2003**, *42*, 4326–4331.

[25] Calderón, F., Fernández, R., Sánchez, F. and Fernández-Mayoralas, A., *Advanced Synthesis & Catalysis* **2005**, *347*, 1395-1403.

[26] Yu, K., Lou, L.L., Lai, C., Wang, S., Ding, F. and Liu, S., *Catalysis Communications* **2006**, *7*, 1057–1060.

[27] Merrifield, R.B., *J. Am. Chem. Soc*. **1963**, *85*, 2149-2154.

[28] a) McNamara, C.A., Dixon, M.J. and Bradley, M., *Chem. Rev*. **2002**, *102*, 3275–3300. b) Itsuno, S., Arakawa, Y. and Haraguchi, N., *Journal of the Society of the Rubber Industry of Japan* **2006**, *79*, 448–454. c) de Miguel, Y.R., Brulé, E. and Margue, R.G., *Journal of the Chemical Society–Perkin Transactions* **2001**, *1*, 3085–3094. d) Clapham, B., Reger, T.S. and Janda, K.D., *Tetrahedron: Asymmetry* **2001**, *57*, 4637–4662. e) El-Shehawy, A.A., Itsuno, S., *Current Topics in Polymer Research.* New York, **2005**. f) Itsuno, S., Haraguchi, N., Arakawa, Y., *Recent Research Developments in Organic Chemistry* **2005**, *9*, 27–47.

[29] a) Anyanwu, U. K., Venkataraman, D., *Tetrahedron Letters* **2003**, *44*, 6445–6448. b) Wang, X., Yin, L., Yang, T., Wang, Y., *Tetrahedron: Asymmetry* **2007**, *18*, 108–114.

[30] a) Astruc, D., Lu, F. and Aranzaes, J.R., *Angew Chem* **2005**, 117, 8062–8083. b) Wu, L., Li, Z.W., Zhang, F., He, Y.M. and Fan, Q.H., *Adv Synth Catal* **2008**, *350*, 846–862. c) Janssen, M.C.C., Vogt, D. and Müller, C., *Adv Synth Cat* **2009**, *351*, 313–318.

[31] a) Degni, S., Wilén, C.E. and Leino, R., *Org. Lett*. **2001**, *3*, 2551–2554. b) Degni, S., Wilén, C.E. and Leino, R., *Tetrahedron: Asymmetry* **2004**, *15*, 231–237.

[32] a) Nakai, Y. and Uozumi, Y., *Org. Lett*. **2005**, *7*, 291-293. b) Nakai, Y., Kimura, T. and Uozumi, Y., *Synlett* **2006**, 3065-3068.

[33] a) List, B., Lerner, R.A. and Barbas, C.F., *J. Am. Chem. Soc*. **2000**, *122*, 2395 – 2396. b) Notz, W. and List, B., *J. Am. Chem. Soc*. **2000**, *122*, 7386 – 7387. c) Sakthivel, K., Notz, W., Bui, T. and Barbas, C.F., *J. Am. Chem. Soc*. **2001**, *123*, 5260 – 5267. d) Gröger, H. and Wilken, J., *Angew. Chem. Int. Ed*. **2001**, *40*,

529 – 532. e) Bøgevig, A., Kumaragurubaran, N. and Jørgensen, K.A., *Chem. Commun*. **2002**, 620 – 621. f) Pidathala, C., Hoang, L., Vignola, N. and List, B., *Angew. Chem. Int. Ed*. **2003**, *42*, 2785 – 2788. g) Northrup, A.B., Mangion, I.K., Hettche, F. and MacMillan, D.W., *Angew. Chem. Int. Ed*. **2004**, *43*, 2152 – 2154. h) Northrup, A.B. and MacMillan, D.W., *Science*. **2004**, 1752 – 1755.

[34] Ikeda, A., Terada, K., Shiotsuki, M. and Sanda, F., *Journal of Polymer Science Part A: Polymer Chemistry* **2011**, *17*, 3783-3796.

[35] Bosman, D.A., Janssen, H.M. and Meijer, E.W., *Chem Rev* **1999**, *99*, 1665–1688.

[36] a) Fujihara, T., Yoshida, S., Ohta, H. and Tsuji, Y., *Angew. Chem. Int. Ed*. **2008**, *47*, 8310–8314. b) Hashiguchi, S., Fujii, A., Takehara, J., Ikariya, T. and Noyori, R., *J. Am. Chem. Soc.* **1995**, *117*, 7562–7563. c) Haack, K.J., Hashiguchi, S., Fujii, A., Ikariya, T. and Noyori, R., *Angewandte Chemie*, **1997**, *109*, 297–300.

[37] a) Toy, P.H. and Janda, K.D., *Tetrahedron Lett*. **1999**, *40*, 6329-6332. b) Garibay, P., Toy, P.H., Hoeg-Jensen, T. and Janda, K.D., *Synlett* **1999**, *09*, 1438-1440. c) Toy, P.H., Reger, T.S., Garibay, P., Garno, J.C., Malikayil, J.A., Liu, G.Y. and Janda, K.D., *J. Comb. Chem*. **2001**, *3*, 117-124.

[38] Vaino A.R. and Janda, K.D., *J. Comb. Chem*. **2000**, *6*, 579-596.

[39] a) Tois, J. and Koskinen, A., *Tetrahedron Letters*. **2003**, *44*, 2093-2095. b) Brümmer, O., Clapham, B. and Janda, K.D., *Tetrahedron Letters*. **2001**, *42*, 2257-2259.

[40] a) Chung, C.W.Y. and Toy, P.H., *Tetrahedron*. **2005**, *61*, 709-715. b) Choi, M.K.W. and Toy, P.H., *Tetrahedron*. **2004**, *60*, 2875-2879.

[41] a) Takamura, M., Funabashi, K., Kanai, M. and Shibasaki, M., *J. Am. Chem. Soc*., **2001**, 123, 6801-6808. b) Selkälä, S.A., Tois, J., Pihko, P.M. and Koskinen, A.M., *Adv. Syn. Cat*. **2002**, *344*, 941-945.

[42] Clapham, B., Cho, C.W. and Janda, K.D., *J. Org. Chem*. **2001**, *66*, 868-873.

[43] Song, C.E., Yang, J.W., Roh, E.J., Lee, S.G., Ahn, J.H. and Han, H., *Angew. Chem., Int. Ed.* **2002**, *41*, 3852-3854.

[44] a) Furukawa, H., Cordova, K.E., O'Keeffe, M. and Yaghi, O.M., *Science* **2013**, *341*, 1230444. b) Kitagawa, S., Kitaura, R. and Noro, S.I., *Angew. Chem., Int. Ed*. **2004**, *43*, 2334−2375. c) Kim, C.R., Uemura, T., Kitagawa, S., *Chem. Soc. Rev*. **2016**, *45*, 3828−3845. d) Dang, S., Zhu, Q.L. and Xu, Q., *Nat. Rev. Mater*. **2018**, *3*, 1-14. e) Heo, D.Y., Do, H.H., Ahn, S.H. and Kim, S.Y., *Polymers*, **2020**, *12*, 2061.

[45] Xu, Q. *EnergyChem*. **2019**, *1*, 100007.

[46] Li, H., Li, L., Lin, R.B., Zhou, W., Zhang, Z., Xiang, S. and Chen, B., *EnergyChem*. **2019**, *1*, 100006.

[47] Lázaro, I.A. and Forgan, R.S., *Coord. Chem. Rev.*, **2019**, *380*, 230–259.

[48] Zhang, Y., Yuan, S., Day, G., Wang, X., Yang, X. and Zhou, H.C., *Coord. Chem. Rev.*, **2018**, *354*, 28–45.

[49] Li, H., Wang, K., Sun, Y., Lollar, C.T., Li, J. and Zhou, H.C., *Mater. Today*, **2018**, *21*, 108–121.

[50] a) Dhakshinamoorthy, A., Li, Z. and Garcia, H., *Chem. Soc. Rev.*, **2018**, *47*, 8134–8172. b) Wasson, M.C., Buru, C.T., Chen, Z., Islamoglu, T. and Farha, O.K., *Appl. Catal., A*, **2019**, *586*, 117214.

[51] Wang, Q., and Didier A., *Chemical reviews*., **2019**, *120*, 1438-1511.

[52] Chirik, P.J., *Acc. Chem. Res*. **2015**, *48*, 1687−1695.

[53] Zhang, J.W., Li, D.D., Lu, G.P., Deng, T., Cai, C., *ChemCatChem* **2018**, *10*, 4966−4972.

[54] a) Yang, S., Zhang, Z.H., Chen, Q., He, M.Y., Wang, L., *Appl. Organomet. Chem*. **2018**, *32*, e4132. b) Sun, X., Olivos-Suarez, A.I., Oar-Arteta, L., Rozhko, E., Osadchii, D., Bavykina, A., Kapteijn, F. and Gascon, J., *ChemCatChem* **2017**, *9*, 1854−1862. c) Neeli, C.K.P., Puthiaraj, P., Lee, Y.R., Chung, Y.M., Baeck, S.H. and Ahn, W.S., *Catal. Today* **2018**, *303*, 227−234.

[55] a) Yuan, K., Song, T., Wang, D., Zhang, X., Gao, X., Zou, Y., Dong, H., Tang, Z., Hu, W., *Angew. Chem., Int. Ed*. **2018**, *57*, 5708−5713. b) Chen, L., Zhan, W., Fang, H., Cao, Z., Yuan, C., Xie, Z., Kuang, Q., Zheng, L., *Chem. -Eur. J*. **2017**, *23*, 11397−11403. c) Chen, Y.Z., Cai, G., Wang, Y., Xu, Q., Yua, S.H., Jiang, H.L., *Green Chem*. **2016**, *18*, 1212−1217.

[56] a) Li, Y., Cai, X., Chen, S., Zhang, H., Zhang, K.H., Hong, J., Chen, B., Kuo, D.H. and Wang, W., *ChemSusChem* **2018**, *11*, 1040−1047. b) Zhang, J., An, B., Hong, Y., Meng, Y., Hu, X., Wang, C., Lin, J., Lin, W. and Wang, Y., *Mater. Chem. Front*. **2017**, *1*, 2405−2409. c) Zhen, W., Gao, F., Tian, B., Ding, P., Deng, Y., Li, Z., Gao, H. and Lu, G., *J. Catal*. **2017**, *348*, 200−211.

[57] a) Kuwahara, Y., Kango, H., Yamashita, H., *ACS Sustainable Chem. Eng*. **2017**, *5*, 1141−1152. b) Chen, J., Zhang, Z., Bao, Z., Su, Y., Xing, H., Yang, Q., Ren, Q., *ACS Appl. Mater. Interfaces* **2017**, *9*, 9772−9777. c) Jagadeesh, R.V., Murugesan, K., Alshammari, A.S., Neumann, H., Pohl, M.M., Radnik, J., Beller, M., *Science* **2017**, *358*, 326−332.

[58] a) Kirillov, A.M., Shul'pin, G.B., *Coord. Chem. Rev*. **2013**, *257*, 732−754. b) Bryliakov, K.P., *Chem. Rev*. **2017**, *117*, 11406−11459. c) Guo, Z., Liu, B., Zhang, Q., Deng, W., Wang, Y., Yang, Y., *Chem. Soc. Rev*. **2014**, *43*, 3480−3524. d) Nodzewska, A., Wadolowska, A., Watkinson, M., *Coord. Chem. Rev*. **2019**, *382*, 181−216.

[59] a) Cancino, P., Paredes-García, V., Torres, J., Martínez, S., Kremerd, C., Spodine, E., *Catal. Sci. Technol*. **2017**, *7*, 4929−4933. b) Limvorapitux, R., Chou, L.Y., Young, A.P., Tsung, C.K., Nguyen, S.T., *ACS Catal*. **2017**, *7*, 6691−6698. c) Fan, S., Dong, W., Huang, X., Gao, H., Wang, J., Jin, Z., Tang, J., Wang, G., *ACS Catal*. **2017**, *7*, 243−249.

[60] a) Fu, Y., Guo, Y., Guo, Y., Wang, Y., Wang, L., Zhan, W., Lu, G., *Catal. Sci. Technol*. **2017**, *7*, 4136−4144. b) Guo, P., Froese, C., Fu, Q., Chen, Y.T., Peng, B., Kleist, W., Fischer, R.A., Muhler, M., Wang, Y., *J. Phys. Chem. C* **2018**, *122*, 21433−21440.

[61] Elumalai, P., Mamlouk, H., Yiming, W., Feng, L., Yuan, S., Zhou, H.C., Madrahimov, S.T., *ACS Appl. Mater. Interfaces* **2018**, *10*, 41431−41438.

[62] Shaikh, M.N., Aziz, M.A., Helal, A., Kalanthoden, A.N., Yamani, Z.H., *ChemSelect* **2017**, *2*, 9052−9057.

[63] Simon, C., Constantieux, T., Rodriguez, J., *Eur. J. Org. Chem*. **2004**, *2004*, 4957−4980.

[64] Yang, Q., Zhang, H.Y., Wang, L., Zhang, Y., Zhao, J., *ACS Omega* **2018**, *3*, 4199−4212.

[65] Kassymova, M., de Mahieu, A., Chaemchuen, S., Demeyere, P., Mousavi, B., Zhuiykov, S., Yusubov, M.S. and Verpoort, F., *Catal. Sci. Technol*. **2018**, *8*, 4129−4140.

[66] Qiu, J., Zhang, X., Feng, Y., Zhang, X., Wang, H., Yao, J., *Appl. Catal., B* **2018**, *231*, 317−342.

[67] Zhang, T., Jin, Y., Shi, Y., Li, M., Li, J., Duan, C., *Coord. Chem. Rev*. **2019**, *380*, 201−229.

[68] Yuan, S., Qin, J.S., Xu, H.Q., Su, J., Rossi, D., Chen, Y., Zhang, L., Lollar, C., Wang, Q., Jiang, H.L., Son, D.H., Xu, H., Huang, Z., Zou, X., Zhou, H.C., *ACS Cent. Sci*. **2018**, *4*, 105−111.

[69] Su, Y., Zhang, Z., Liu, H., Wang, Y., *Appl. Catal., B* **2017**, *200*, 448−457.

[70] Maina, J.W., Schütz, J.A., Grundy, L., Des Ligneris, E., Yi, Z., Kong, L., Pozo-Gonzalo, C., Ionescu, M., Dumee, L.F., *ACS Appl. Mater. Interfaces* **2017**, *9*, 35010−35017.

[71] Chen, M., Han, L., Zhou, J., Sun, C., Hu, C., Wang, X., Su, Z., *Nanotechnology* **2018**, *29*, 284003.

[72] Chen, W., Han, B., Tian, C., Liu, X., Liang, S., Deng, H., Lin, Z., *Appl. Catal., B* **2019**, *244*, 996−1003.

[73] He, X., Gan, Z., Fisenko, S., Wang, D., El-Kaderi, H.M., Wang, W.N., *ACS Appl. Mater. Interfaces* **2017**, *9*, 9688−9698.

[74] Li, Y., Fu, Y., Ni, B., Ding, K., Chen, W., Wu, K., Huang, X., Zhang, Y., *AIP Adv*. **2018**, *8*, No. 035012.

[75] Zhao, H., Wang, X., Feng, J., Chen, Y., Yang, X., Gao, S. and Cao, R., *Catal. Sci. Technol*. **2018**, *8*, 1288−1295.

[76] Han, B., Ou, X., Deng, Z., Song, Y., Tian, C., Deng, H., Xu, Y.J. and Lin, Z., *Angew. Chem., Int. Ed*. **2018**, *57*, 16811−16815.

[77] a) Han, S.S., Mendoza-Cortés, J.L. and Goddard Iii, W.A., *Chem. Soc. Rev*. **2009**, *38*, 1460−1476. b) Hong, D.Y., Hwang, Y.K., Serre, C., Ferey, G. and Chang, J.S., *Adv. Funct. Mater*. **2009**, *19*, 1537−1552.

[78] a) Li, J.S., Zhang, S., Sha, J.Q., Wang, H., Liu, M.Z., Kong, L.X. and Liu, G.D., *ACS Appl. Mater. Interfaces* **2018**, *10*, 17140−17146. b) Li, H., Qian, X., Xu, C., Huang, S., Zhu, C., Jiang, X., Shao, L. and Hou, L., *ACS Appl. Mater. Interfaces* **2017**, *9*, 28394−28405. c) Wu, L.L., Wang, Q.S., Li, J., Long, Y., Liu, Y., Song, S.Y. and Zhang, H.J., *Small* **2018**, *14*, 1704035. d) Zhang, X., Huang, L., Wang, Q. and Dong, S., *J. Mater. Chem. A* **2017**, *5*, 18839−18844. e) Peera, S.G., Balamurugan, J., Kim, N.H. and Lee, J.H., *Small* **2018**, *14*, 1800441. f) Liu, Y., Jiang, H., Hao, J., Liu, Y., Shen, H., Li, W. and Li, J., *ACS Appl. Mater. Interfaces* **2017**, *9*, 31841−31852. g) Hao, Y., Xu, Y., Liu, W. and Sun, X., *Mater. Horiz.* **2018**, *5*, 108−115. h) Yu, Z., Bai, Y., Zhang, S., Liu, Y., Zhang, N., Wang, G., Wei, J., Wu, Q. and Sun, K., *ACS Appl. Mater. Interfaces* **2018**, *10*, 6245−6252.

[79] a) Jiang, J., Zhao, Y. and Yaghi, O.M., *J. Am. Chem. Soc.*, **2016**, *138*, 3255−3265. b) Dogru, M. and Bein, T., *Chem. Commun*. **2014**, *50*, 5531−5546. c) Bisbey, R.P. and Dichtel, W.R., ACS *Cent. Sci.*, **2017**, *3*, 533−543.

[80] Diercks, C.S. and Yaghi, O.M., *Science*, **2017**, *355*, 6328.

[81] Waller, P.J., Gándara, F. and Yaghi, O.M., *Acc. Chem. Res.*, **2015**, *48*, 3053−3063.

[82] a) Hu. H., Yan Q.Q., Ge R.L. and Gao Y.N., *Chin. J. Catal*. **2018**, *39*, 1167–1179. b) El-Kaderi, H.M., Hunt, J.R., Mendoza-Cortés, J.L., Côté, A.P., Taylor, R.E., O'Keeffe, M. and Yaghi, O.M., *Science* **2007**, *316*, 268– 272. c) Trandafir, M.M., Pop, L., Hădade, N.D., Florea, M., Neațu, F., Teodorescu, C.M., Duraki, B., van Bokhoven, J.A., Grosu, I., Pârvulescu, V.I. and Garcia, H., *Catal. Sci. Technol*. **2016**, *6*, 8344 – 8354.

[83] Liu, J., Wang, N. and Ma, L., *Chemistry–An Asian Journal*, **2020**, *15*, 338-351.

[84] Cote, A.P., Benin, A.I., Ockwig, N.W., O'Keeffe, M., Matzger, A.J. and Yaghi, O.M., *Science* **2005**, *310*, 1166 – 1170.

[85] Stegbauer, L., Schwinghammer, K. and Lotsch, B.V., *Chem. Sci*. **2014**, *5*, 2789-2793.

[86] Wei, P.F., Qi, M.Z., Wang, Z.P., Ding, S.Y., Yu, W., Liu, Q., Wang, L.K., Wang, H.Z., An, W.K. and Wang, W., *J. Am. Chem. Soc*. **2018**, *140*, 4623-4631.

[87] a) Yan, Y., He, T., Zhao, B., Qi, K., Liu, H. and Xia, B.Y., *J. Mater. Chem. A* **2018**, *6*, 15905-15926. b) Lin, C.Y., Zhang, D., Zhao, Z. and Xia, Z., *Adv. Mater*. **2018**, *30*, 1703646-1703662.

[88] Ma, W., Yu, P., Ohsaka, T. and Mao, L., *Electrochem. Commun*. **2015**, *52*, 53–57.

[89] Lin, S., Diercks, C.S., Zhang, Y.B., Kornienko, N., Nichols, E.M., Zhao, Y., Paris, A.R., Kim, D., Yang, P., Yaghi, O.M. and Chang, C.J., *Science*, **2015**, *349*, 1208–1213.

[90] Diercks, C.S., Lin, S., Kornienko, N., Kapustin, E.A., Nichols, E.M., Zhu, C., Zhao, Y., Chang, C.J. and Yaghi, O.M., *J. Am. Chem. Soc*. **2018**, *140*, 1116–1122.

[91] Hou, Y., Zhang, X., Sun, J., Lin, S., Qi, D., Hong, R., Li, D., Xiao, X. and Jiang, J., *Microporous Mesoporous Mater*. **2015**, *214*, 108-114.

[92] a) Han, Y., Zhang, M., Zhang, Y.Q. and Zhang, Z.H., *Green Chem*. **2018**, *20*, 4891-4900. b) Leng, W., Ge, R., Dong, B., Wang, C. and Gao, Y., *RSC Adv*. **2016**, *6*, 37403-37406. c) Puthiaraj, P. and Pitchumani, K., *Chem. Eur. J*. **2014**, *20*, 8761–8770. d) Lin, S., Hou, Y.X., Deng, X., Wang, H.L., Sun, S.Z. and Zhang, X.M., *RSC Adv*. **2015**, *5*, 41017-41024.

[93] Fan, M., Wang, W.D., Zhu, Y., Sun, X., Zhang, F. and Dong, Z., *Appl. Catal. B* **2019**, *257*, 117942.

[94] a) Hu, X., Long, Y., Fan, M., Yuan, M., Zhao, H., Ma, J. and Dong, *Appl. Catal. B* **2019**, *244*, 25 –35. b) An, Z., Guo, Y., Zhao, L., Li, Z. and He, J., *ACS Catal*. **2014**, *4*, 2566 – 2576. c) Vardhan, H., Hou, L., Yee, E., Nafady, A., Al-Abdrabalnabi, M.A., Al-Enizi, A.M., Pan, Y., Yang, Z. and Ma, S., *ACS Sustainable Chem. Eng*. **2019**, *7*, 4878– 4888. d) Ma, H.C., Kan, J.L., Chen, G.J., Chen, C.X. and Dong, Y.B., *Chem. Mater*. **2017**, *29*, 6518 – 6524.

[95] a) Xu, H., Gao, J. and Jiang, D., *Nat. Chem*. **2015**, *7*, 905 – 913. b) Dou, Z., Xu, L., Zhi, Y., Zhang, Y., Xia, H., Mu, Y. and Liu, X., *Chem. Eur. J*. **2016**, *22*, 9919 – 9922. c) Bhadra, M., Kandambeth, S., Sahoo, M.K., Addicoat, M., Balaraman, E. and Banerjee, R., *J. Am. Chem. Soc*. **2019**, *141*, 6152– 6156.

[96] Zhang, T., Xing, G., Chen, W. and Chen, L. *Materials Chemistry Frontiers*, **2020**, *4*, 332-353.

[97] Zhang, Y. and Riduan, S.N., *Chem. Soc. Rev*. **2012**, *41*, 2083–2094.

[98] Sun, Q., Dai, Z., Liu, X., Sheng, N., Deng, F., Meng, X. and Xiao, F.S., *J. Am. Chem. Soc*. **2015**, *137*, 5204−5209.

[99] a) Doonan, C.J., Tranchemontagne, D.J., Glover, T.G., Hunt, J.R. and Yaghi, O.M., *Nat. Chem*., **2010**, *2*, 235–238. b) Li, B., Zhang, Y., Krishna, R., Yao, K., Han, Y., Wu, Z., Ma, D., Shi, Z., Pham, T., Space, B. and Liu, J., *J. Am. Chem. Soc*., **2014**, *136*, 8654–8660. c) Lin, S., Diercks, C.S., Zhang, Y.B., Kornienko, N., Nichols, E.M., Zhao, Y., Paris, A.R., Kim, D., Yang, P., Yaghi, O.M. and Chang, C.J., *Science*, **2015**, *349*, 1208–1213. d) Ding, S.Y., Gao, J., Wang, Q., Zhang, Y., Song, W.G., Su, C.Y. and Wang, W. *J. Am. Chem. Soc*., **2011**, *133*, 19816–19822. e) Dalapati, S., Jin, S., Gao, J., Xu, Y., Nagai, A. and Jiang, D., *J.*

Am. Chem. Soc., **2013**, *135*, 17310–17313. f) Ding, S.Y., Dong, M., Wang, Y.W., Chen, Y.T., Wang, H.Z., Su, C.Y. and Wang, W., *J. Am. Chem. Soc.*, **2016**, *138*, 3031–3037. g) Wan, S., Guo, J., Kim, J., Ihee, H. and Jiang, D., *Angew. Chem., Int. Ed.*, **2008**, *47*, 8826–8830. h) Jin, S., Ding, X., Feng, X., Supur, M., Furukawa, K., Takahashi, S., Addicoat, M., El-Khouly, M.E., Nakamura, T., Irle, S. and Fukuzumi, S., *Angew. Chem., Int. Ed.*, **2013**, *52*, 2017–2021. i) DeBlase, C.R., Silberstein, K.E., Truong, T.T., Abruña, H.D. and Dichtel, W.R., *J. Am. Chem. Soc.*, **2013**, *135*, 16821–16824.

[100] Wang, W., Zhou, M. and Yuan, D. *Journal of Materials Chemistry A*, **2017**, *5*, 1334-1347.

[101] Liu, F., Meng, X., Zhang, Y., Ren, L., Nawaz, F. and Xiao, F.S., *J. Catal.*, 2010, *271*, 52–58.

[102] Modak, A., Mondal, J. and Bhaumik, A., *ChemCatChem*, **2013**, *5*, 1749–1753.

[103] Kim, J.J., Lim, C.R., Reddy, B.M. and Park, S.E., *Mol. Catal.*, **2018**, *451*, 43–50.

[104] Carta, M., Croad, M., Bugler, K., Msayib, K.J. and McKeown, N.B., *Polym. Chem.*, **2014**, *5*, 5262–5266.

[105] Hassner, A., *Encyclopedia of Reagents for Organic Synthesis*, **2001**, *2*, 3–4.

[106] Zhang, Y., Zhang, Y., Sun, Y.L., Du, X., Shi, J.Y., Wang, W.D. and Wang, W., *Chem. – Eur. J.*, **2012**, *18*, 6328–6334.

[107] Rose, M., Notzon, A., Heitbaum, M., Nickerl, G., Paasch, S., Brunner, E., Glorius, F. and Kaskel, S., *Chem. Commun.*, **2011**, *47*, 4814–4816.

[108] Merad, J., Lalli, C., Bernadat, G., Maury, J. and Masson, G., *Chem. – Eur. J.*, **2018**, *24*, 3925–3943.

[109] Rueping, M., Sugiono, E., Steck, A. and Theissmann, T., *Adv. Synth. Catal.*, **2010**, *352*, 281–287.

[110] a) Bleschke, C., Schmidt, J., Kundu, D.S., Blechert, S. and Thomas, A., *Adv. Synth. Catal.*, **2011**, *353*, 3101–3106. b) Kundu, D.S., Schmidt, J., Bleschke, C., Thomas, A. and Blechert, S., *Angew. Chem., Int. Ed.*, **2012**, *51*, 5456–5459. c) Schmidt, J., Kundu, D.S., Blechert, S. and Thomas, A., *Chem. Commun.*, **2014**, *50*, 3347–3349. d) Huangfu, Y., Sun, Q., Pan, S., Meng, X. and Xiao, F.S., *ACS Catal.*, **2015**, *5*, 1556–1559.

[111] a) List, B., Lerner, R.A. and Barbas, C.F., *J. Am. Chem. Soc.*, **2000**, *122*, 2395–2396. b) Ahrendt, K.A., Borths, C.J. and MacMillan, D.W., *J. Am. Chem. Soc.*, **2000**, *122*, 4243–4244.

[112] C. A. Wang, Z. K. Zhang, T. Yue, Y. L. Sun, L. Wang, W. D. Wang, Y. Zhang, C. Liu and W. Wang, *Chem. – Eur. J.*, **2012**, *18*, 6718–6723.

[113] Wang, C.A., Zhang, Z.K., Yue, T., Sun, Y.L., Wang, L., Wang, W.D., Zhang, Y., Liu, C. and Wang, W., *Polym. Chem.*, **2017**, *8*, 5561–5569.

[114] Lan, Y., Yang, C., Zhang, Y., An, W., Xue, H., Ding, S., Zhou, P. and Wang, W., *Polym. Chem.*, **2019**, *10*, 3298–3305.

[115] a) Peng, Y.K. and Tsang, S.E., *Nano Today*, **2018**, *18*, 15; b) Xiao, M., Luo, B., Wang, S. and Wang, L., J. *Energy Chem.*, **2018**, *27*, 1111-1123.

[116] DeRosa, M.C. and Crutchley, R.J., *Coord. Chem. Rev.*, **2002**, *233*, 351-371.

[117] Wang, Z.J., Ghasimi, S., Landfester, K. and Zhang, K.A.,*Chem. Commun.*, **2014**, *50*, 8177-8180.

[118] Kang, N., Park, J.H., Ko, K.C., Chun, J., Kim, E., Shin, H.W., Lee, S.M., Kim, H.J., Ahn, T.K., Lee, J.Y. and Son, S.U., *Angew. Chem., Int. Ed*., **2013**, *52*, 6228-6232.

[119] a) Kaur, P., Hupp, J.T. and Nguyen, S.T., *ACS Catal*. **2011**, *1*, 819−835. b) Kramer, S., Bennedsen, N.R. and Kegnæs, S., *ACS Catal* **2018**, *8*, 6961–6982.

[120] a) Li, C., Wang, W., Yan, L., Wang, Y., Jiang, M. and Ding, Y., *J. Mater. Chem. A* **2016**, *4*, 16017−16027. b) Dai, Z., Sun, Q., Liu, X., Bian, C., Wu, Q., Pan, S., Wang, L., Meng, X., Deng, F. and Xiao, F.S., *J. Catal*. **2016**, *338*, 202−209. c) Wang, S., Song, K., Zhang, C., Shu, Y., Li, T. and Tan, B., *J. Mater. Chem. A* **2017**, *5*, 1509−1515. d) Chen, Y., Luo, R., Xu, Q., Zhang, W., Zhou, X. and Ji, H., *ChemCatChem* **2017**, *9*, 767−773. e) Dou, Z., Xu, L., Zhi, Y., Zhang, Y., Xia, H., Mu, Y. and Liu, X., *Chem. - Eur. J.* **2016**, *22*, 9919−9922. f) Dai, Z., Sun, Q., Liu, X., Guo, L., Li, J., Pan, S., Bian, C., Wang, L., Hu, X., Meng, X. and Zhao, L., *ChemSusChem* **2017**, *10*, 1186−1192. g) Oveisi, A.R., Zhang, K., Khorramabadi-Zad, A., Farha, O.K. and Hupp, J.T., *Sci. Rep*. **2015**, *5*, 10621. h) Ma, L., Wanderley, M.M. and Lin, W., *ACS Catal*. **2011**, *1*, 691−697. i) Cai, R., Ye, X., Sun, Q., He, Q., He, Y., Ma, S. and Shi, X., *ACS Catal*. **2017**, *7*, 1087−1092.

[121] a) Shultz, A.M., Farha, O.K., Hupp, J.T. and Nguyen, S.T., *Chem. Sci*. **2011**, *2*, 686-689. b) Zhang, K., Farha, O.K., Hupp, J.T. and Nguyen, S.T., *ACS Catal*. **2015**, *5*, 4859−4866. c) Ding, Z.D., Zhu, W., Li, T., Shen, R., Li, Y., Li, Z., Ren, X. and Gu, Z.G., *Dalt. Trans*. **2017**, *46*, 11372−11379. d) Liu, T.T., Lin, Z.J., Shi, P.C., Ma, T., Huang, Y.B. and Cao, R., *ChemCatChem* **2015**, *7*, 2340−2345.

[122] Modak, A., Mondal, J. and Bhaumik, A., *Appl. Catal., A* **2013**, *459*, 41−51.

[123] a) Tanabe, K.K., Siladke, N.A., Broderick, E.M., Kobayashi, T., Goldston, J.F., Weston, M.H., Farha, O.K., Hupp, J.T., Pruski, M., Mader, E.A. and Johnson, M.J., *Chem. Sci*. **2013**, *4*, 2483−2489. b) Wang, X., Lu, S., Li, J., Liu, Y. and Li, C., *Catal. Sci. Technol*. **2015**, *5*, 2585−2589. c) Wang, T., Lyu, Y., Xiong, K., Wang, W., Zhang, H., Zhan, Z., Jiang, Z. and Ding, Y., *Cuihua Xuebao/Chin. J. Catal*. **2017**, *38*, 890−898. d) Tanabe, K.K., Ferrandon, M.S., Siladke, N.A., Kraft, S.J., Zhang, G., Niklas, J., Poluektov, O.G., Lopykinski, S.J., Bunel, E.E., Krause, T.R. and Miller, J.T., *Angew. Chem. Int. Ed*. **2014**, *53*, 12055−12058. e) Camacho-Bunquin, J., Siladke, N.A., Zhang, G., Niklas, J., Poluektov, O.G., Nguyen, S.T., Miller, J.T. and Hock, A.S., *Organometallics* **2015**, *34*, 947−952. f) Kraft, S.J., Sánchez, R.H. and Hock, A.S., *ACS Catal*. **2013**, *3*, 826−830. g) Rangel-Rangel, E., Verde-Sesto, E., Rasero-Almansa, A.M., Iglesias, M. and Sánchez, F., *Catal. Sci.Technol*. **2016**, *6*, 6037−6045. h) Kraft, S.J., Zhang, G., Childers, D., Dogan, F., Miller, J.T., Nguyen, S.T. and Hock, A.S., *Organometallics* **2014**, *33*, 2517−2522. i) Jiang, J.X., Wang, C., Laybourn, A., Hasell, T., Clowes, R., Khimyak, Y.Z., Xiao, J., Higgins, S.J., Adams, D.J. and Cooper, A.I., *Angew. Chem., Int. Ed*. **2011**, *50*, 1072−1075. j) Sun, Q., Meng, X., Liu, X., Zhang, X., Yang, Y., Yang, Q. and Xiao, F.S., *Chem. Commun*. **2012**, *48*, 10505−10507.

[124] a) Andrushko, N. and Andrushko, V., **Stereoselective Synthesis of Drugs and Natural Products**, *Wiley*, **2013**, 909–959. b) De Kimpe, N. and Keppens, M., *Tetrahedron* **1996**, *52*, 3705−3718.

[125] a) Li, H., Xu, B., Liu, X., Sigen, A., He, C., Xia, H. and Mu, Y., *J. Mater. Chem. A* **2013**, *1*, 14108−14114. b) Xu, Y., Wang, T., He, Z., Zhou, M., Yu, W., Shi, B. and Huang, K., *Appl. Catal., A* **2017**, *541*, 112−119. c) Iwai, T., Harada, T., Hara, K. and Sawamura, M., *Angew. Chem., Int. Ed*. **2013**, *52*, 12322−12326. d) Dong, Y., Chen, Y.Q., Jv, J.J., Li, Y., Li, W.H. and Dong, Y.B., *RSC advances*, **2019**, *9*, 21671-21678. e) Wang, L., Zhang, J., Sun, J., Zhu, L., Zhang, H., Liu, F., Zheng, D., Meng, X., Shi, X. and Xiao, F. S. *ChemCatChem* **2013**, *5*, 1606−1613. f) Sun, Q., Lv, Z., Du, Y., Wu, Q., Wang, L., Zhu, L., Meng, X., Chen, W. and Xiao, F. S. *Chem. - Asian J*. **2013**, *8*, 2822−2827. g) Cai, R., Ye, X., Sun, Q., He, Q., He, Y., Ma, S. and Shi, X., *ACS Catal*. **2017**, 7, 1087−1092. h) Liu, Y., Zhou, Y., Li, J., Wang, Q., Qin,

Q., Zhang, W., Asakura, H., Yan, N. and Wang, J., *Appl. Catal., B* **2017**, *209*, 679−688. i) Majeed, M.H., Shayesteh, P., Wallenberg, L.R., Persson, A.R., Johansson, N., Ye, L., Schnadt, J. and Wendt, O.F., *Chem. -Eur. J.* **2017**, *23*, 8457−8465. j) Lee, L.C., He, J., Yu, J.Q. and Jones, C.W., *ACS Catal*. **2016**, *6*, 5245−5250.

[126] a) Xie, Z., Wang, C., de Krafft, K.E.and Lin, W., *J. Am. Chem. Soc*. **2011**, *133*, 2056–2059. b) Yoo, W.J. and Kobayashi, S., *Green Chem*. **2014**, *16*, 2438−2442.

2. Synthesis of POP catalysts

POPs have attracted the attention of researchers because POPs may be used in catalytic reactions as a good catalysis platform. Usually, a supporting material is required to avoid strong interactions between solid supports and the catalysis complex. However, the amorphous structure of POPs, the drawback of solid-supported heterogeneous catalysts, can be overcome by the metalation of metal complexes with POPs.

In this chapter, heterogeneous single-atom catalysts (SACs) are introduced, and different synthesis methods for POPs are presented.

2.1 Heterogeneous single atomic catalysis

Catalysis is important in the modern chemical industry, and catalysts are the core of the catalytic process. Homogeneous catalysts exhibit high activities and selectivities owing to their unique and isolated active sites existing in the same phase. However, the difficulty in separation limits the application of homogeneous catalysts in today chemical products. Few homogeneous catalysts have been commercialized. [1] Owing to the low utilization rate of metal atoms and active compositions, heterogeneous catalysts are relatively less efficient and selective. Nevertheless, most large-scale industrial catalytic procedures are primarily based on heterogeneous catalysts because of their sturdiness and convenient separation. [2] Table 2.1 shows the comparison of homogeneous and heterogeneous catalysts. [3] The combination of the benefits of heterogeneous and homogeneous catalysts has attracted significant attention; these benefits may be combined by the heterogenization of homogeneous catalysts by attaching a homogeneous catalyst onto insoluble supporting materials [4] as mentioned in the first chapter.

In 2011, Zhang et al. proposed the ‘single-atom catalysis’ concept. [5] Single-atom catalysis refers to the reaction catalyzed by a ‘single-atom catalysts’ (SACs), which contains isolated single atoms distributed on a supporting material in the catalytic process. [6] This new strategy provides an alternative for the heterogenization of homogeneous catalysts and has attracted significant attention from researchers in recent years as a topical research subject and is considered a novel approach in catalysis. [7] Single-atom catalysts have the advantages of steady and are sepatated from the reaction mixture as conveniently as heterogeneous catalysts. Furthermore, SACs have isolated active sites that are spread across the supporting materials, similar to homogeneous catalysis. This crucial property can boost the atomic efficiency of the metal and provide more consistent, well-defined active sites. [8] It is acknowledged that SACs combine the benefits of heterogeneous and homogeneous catalysts. The properties of SACs are listed in Table 2.1.

Table 2.1 Comparison of homogeneous and heterogeneous catalysts, and SACs [3, 5]

Property	Homogeneous catalysts	Heterogeneous catalysts	SACs
Catalyst recovery	difficult and expensive	easy and cheap	easy and cheap
Thermal stability	poor	good	good
Selectivity	excellent/good	good/poor	excellent/good/poor
Catalytic performance tenability	good	poor	poor
Active sites	isolated atoms or clusters, often containing ligand	multiple active sites	isolated atoms, often with neighboring atoms from supporting materials
Uniformity of active sites	uniform	non-uniform	relatively uniform
Metal electronic state	depends on ligand, commonly positive	commonly metallic	depends on supporting material, commonly positive
Atomic efficiency	high	relatively low	high

SACs are heterogeneous catalysts containing isolated active sites. By tuning the combination of metals and supporting materials, the design and development of suitable SACs can merge homogeneous catalysis' high activity and selectivity with heterogeneous catalysis' high stability and ease of separation, thus providing a novel method for the heterogenization of homogeneous catalysts and demonstrating that SACs can be a bridge between heterogeneous and homogeneous catalysis. MOFs, COFs, and POPs are the primary examples of SACs. This chapter only deals with amorphous POPs, so only SACs based on POPs will be discussed.

2.2 Synthesis of POPs

POPs are a promising platform for catalysis, and many applications have been reported utilizing POPs. Our group has also used POPs for asymmetric C(sp^2)-H functionalization and the Michael addition of malonates to aliphatic nitroalkenes. [9]

In general, six main polymerization techniques are used to synthesize POPs (Figure 2.1). [10] The most essential qualities of POPs are the surface area, porosity, and swelling because these properties affect the catalytic performance. Therefore, the method for obtaining POPs must consider these properties. The six main types of polymerization methods are radical

polymerization, Friedel-Crafts reactions, alkyne trimerization, Sonogashira coupling, nitrile trimerization, and miscellaneous reactions (Figure 2.1).

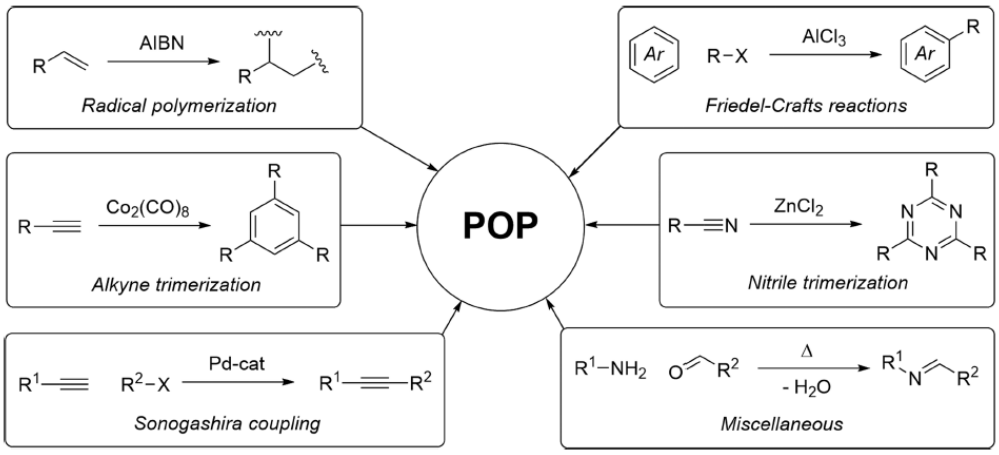

Figure 2.1 Six different polymerization techniques for synthesis POPs [10]

2.2.1 Radical polymerization

Radical polymerization is the most common strategy for the polymerization of alkene groups on the ligand. The first step involves inserting alkene groups on the original ligand or directly using the ligand with alkene groups; this step is followed by the polymerization of the ligands with alkene groups using radical initiators such as azo*bis*(isobutyronitrile) (AIBN). Divinylbenzene and styrene are often used as organic co-building blocks to provide a high surface area and porosity, because they also contain alkene groups, which are used for polymerization.

Radical polymerization is a relatively simple method to synthesize POPs because there are no metal complexes that participate in the reaction. Therefore, it is not possible to generate other metal-POP species in the radical polymerization step. After metalation with the corresponding metal complex, there is only one type of metal-POP in the catalytic reactions. The radical polymerization step is performed in the absence of oxygen because the oxidation and cross-coupling of benzylic C-H groups occur easily in the presence of oxygen.

Bennedsen reported synthesizing a POP using radical polymerization based on a phosphoramidite ligand bearing vinyl groups for asymmetric C(sp^2)–H functionalization (Scheme 2.1). [9a] The first step is to insert the alkene into BINOL, and the second step is radical polymerization with divinylbenzene and styrene using AIBN.

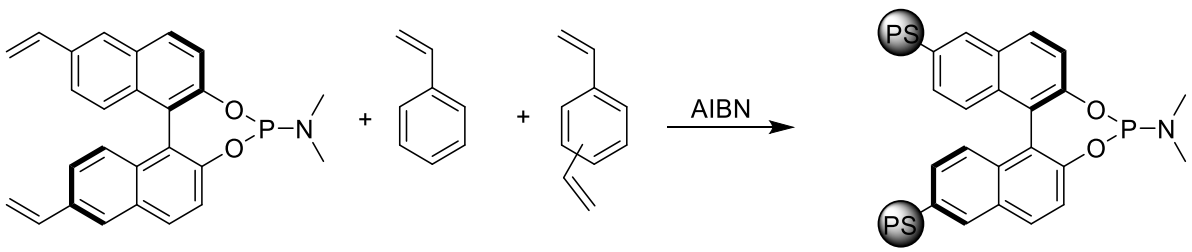

Scheme 2.1 Radical polymerization for synthesis of POPs [9a]

2.2.2 Friedel-Crafts reactions

Polymerization using the Friedel-Crafts acylation/alkylation is the second strategy for producing POP. Friedel-Crafts reaction polymerizations require stoichiometric or excess quantities of iron(III) chloride or aluminum chloride. However, the ligand already has a metal center in the monomer, and iron(III) chloride or aluminum chloride cannot easily replace the metal center in the monomer. The majority of monomers have metalloporphyrin molecular structures, and the aryl parts of the metalloporphyrin undergo the Friedel-Crafts reactions; thus, the obtained M-POPs have flexible active centers similar to homogeneous catalysts. A metalloporphyrin-based POP, which was synthesized by Liu and co-workers via typical Friedel-Crafts alkylation polymerization, could be applied for hetero-Diels-Alder reactions between dienes with aldehydes (Scheme 2.2). [11]

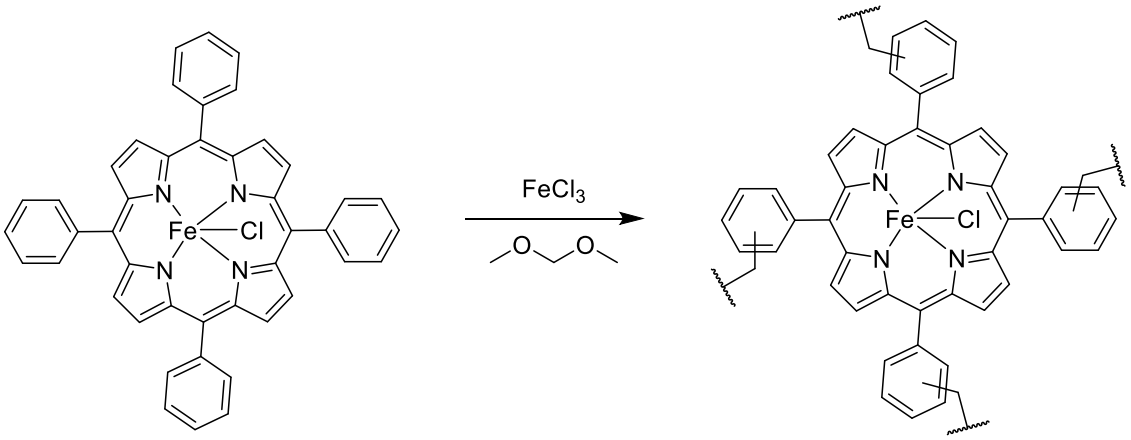

Scheme 2.2 Friedel-Crafts reaction polymerization for synthesis of POPs [11]

2.2.3 Alkyne Trimerization

Alkyne trimerization is another common method used to synthesize POPs. [12] Three alkyne groups can form a benzene ring by connecting building blocks bearing alkyne groups. Thus, the ratio of the building blocks can be modified, and the surface area and porosity can be controlled. Nguyen et al. synthesized catechol-functionalized POPs using a Co-catalyzed acetylene trimerization strategy (Figure 2.2). [13] Alkyne trimerization is different when using radical polymerization because the metal-catalysis is necessary. However, before the second step that requires the metalation with other metals, the removal of the catalyst metal is essential. The metal-free POPs are usually generated by washing with concentrated acids.

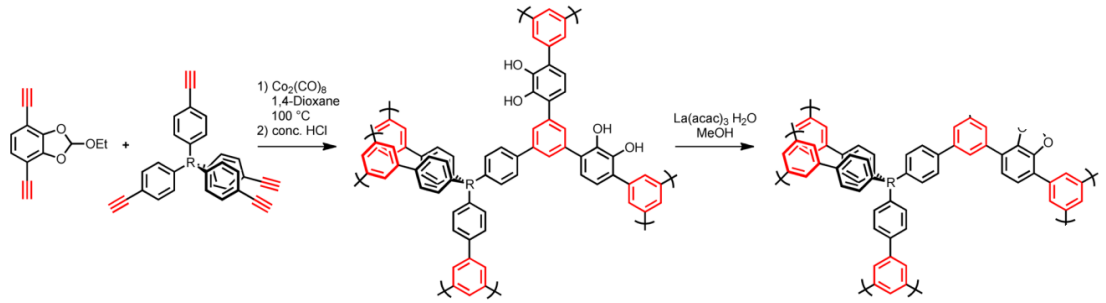

Figure 2.2 Alkyne Trimerization polymerization for synthesis of POPs [13]

2.2.4 Nitrile Trimerization

Nitrile trimerization, which uses a nitrile group to form triazines by linking different building blocks, is a technique similar to alkyne trimerization. [14] A triazine moiety requires three nitrile groups, which can originate from the same monomer or from different building blocks, similarly to how three alkyne groups can form one benzene linker. In comparison to alkyne trimerization, nitrile trimerization produces POPs with a higher nitrogen content and more binding sites, allowing for the incorporation of more metals. Wang and co-workers synthesized a series of POPs based on tetrakis (4-cyanatophenyl) structures via nitrile trimerization (Figure 2.3). [15] The POPs with the highest value for the BET surface area was the porous cyanate resin, which had a BET surface area of 960 m^2g^{-1} at that time.

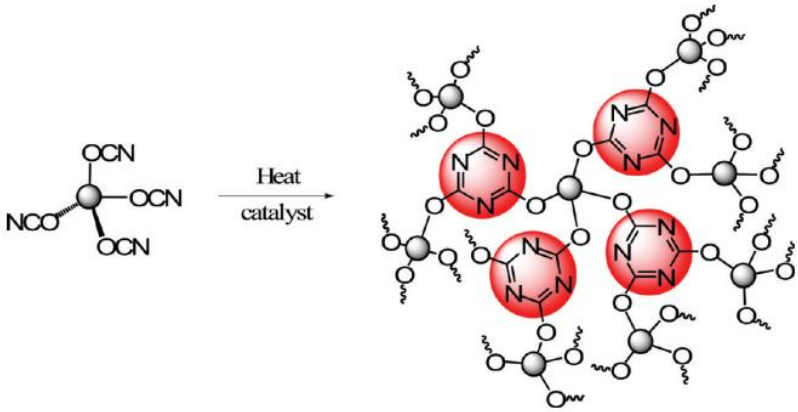

Figure 2.3 Alkyne Trimerization polymerization for synthesis of POPs [15]

2.2.5 Sonogashira Coupling

The Sonogashira cross-coupling reaction can also be utilized to synthesize POPs as a polymerization technique. [16] Sonogashira coupling reactions require two substrates: an aryl halide monomer and another monomer or building blocks containing terminal alkynes. The reaction is catalyzed by a Pd/Cu bimetallic catalytic system, and it is necessary to remove the two metals after the completion of the reaction. Sánchez reported a novel (dipyrrin)(bipyridine)Ru(II) (CMPBDP-Ru) POP *via* a Sonogashira cross-coupling reaction in three steps (Figure 2.4). [17] The first step,

step a, is the Sonogashira coupling reaction catalyzed by $Pd(PPh)_4$/CuI with Et_3N; step b is the deprotection of the dipyrrin moieties using BBr_3, followed by hydrolysis in a water/acetone mixture; step c is metalation with $Ru(bpy)_2Cl_2$, after which the metal-POP SACs is obtained. During this procedure, the Pd/Cu bimetal is removed before steps b and c to avoid the formation of undesired Pd-POP or Cu-POP catalysts, respectively.

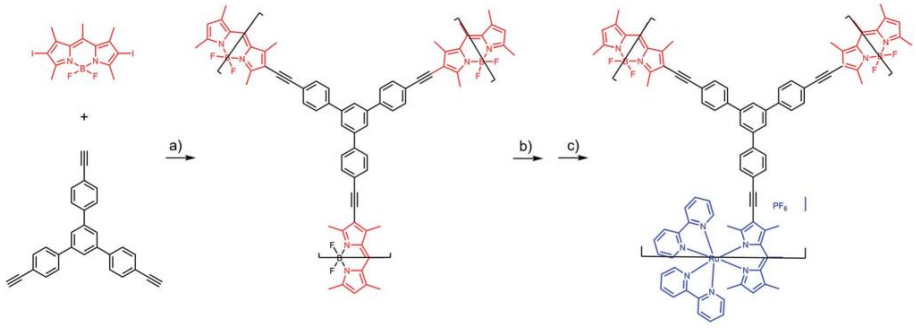

Figure 2.4 Sonogashira coupling polymerization for synthesis of POPs [17]

2.2.6 Other Miscellaneous methods

In addition to the five methods, condensation and oxidative coupling are two other methods for synthesizing POPs. Gu et al. developed a metalloporphyrin-based POP (Mn-PPOP-1) for the oxidation of arylalkanes and olefins. [18] Gu reported the condensation of Mn-porphyrin tetraamines (TBPP) and 1,3,5-triformylphloroglucinol (TP) could synthesize Mn-PPOP-1 by releasing water as a driving force (Figure 2.5). [18] Mn-PPOP-1 has a high surface area and porosity, exhibits excellent catalytic performance in oxidation of olefins and arylalkanes and is more stable than the homogeneous manganese porphyrins. The oxidative coupling reaction was also utilized for synthesizing two types of POPs, CPOP-20, and CPOP-21. [19] CPOP-20 and CPOP-21 have large BET surface areas (up to 480 m^2g^{-1}). Han et al. used two Ir-POPs catalytic systems to achieve a photocatalytic aza-Henry reaction at room temperature with high catalytic activity.

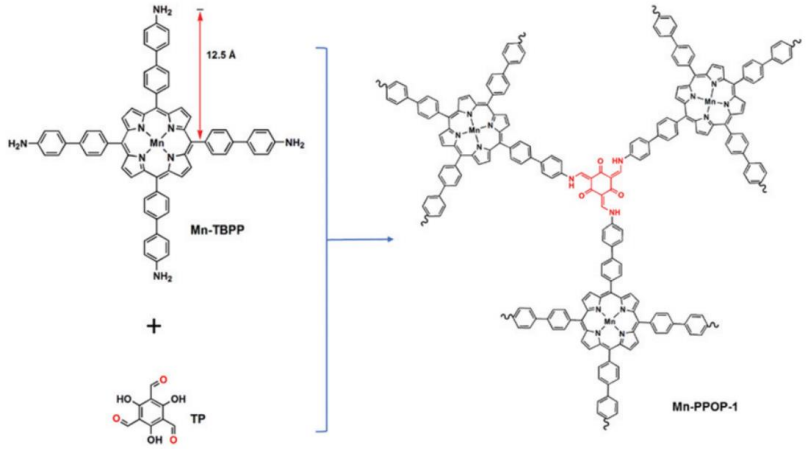

Figure 2.5 Condensation polymerization for synthesis of POPs [18]

2.3 Metalation

When POPs are metal-free catalysts, POPs are directly applied in catalytic reactions. However, most catalytic reactions require both active metals and ligands. Therefore, metalation is crucial; in particular, a SACs is required for the catalytic reaction. There are two different methods for metalating POPs. The first method involves metalation by mixing a metal complex with POP, which is obtained via the polymerization of a polymer monomer, and the second method involves polymerization of the metal-monomer group (Figure 2.6). In the first method, the ratio of metal complexes to monomers is controlled by the addition of the metal precursors or POP. In the second metalation method, the metal-POP catalytic system has a highly dispersed single-atom site in the solution because the metal has already been incorporated into the monomer. Nevertheless, the second method could be affected by the polymerization step because the metal catalyst could replace the metal in the metal-monomer group.

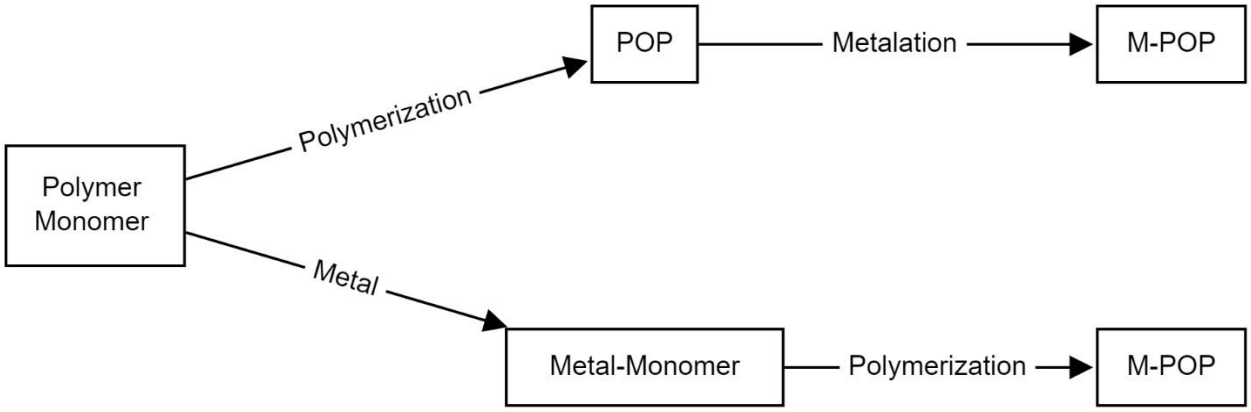

Figure 2.6 Illustration of two different methods of metalation of POPs

There are two examples of using the above two metalation methods for asymmetric catalytic reactions (Scheme 2.3). Bennedsen reported asymmetric C(sp^3)–H functionalization using the first method of metalation. [9a] Buendia accomplished the asymmetric Michael addition via the second method of metalation. [9b]

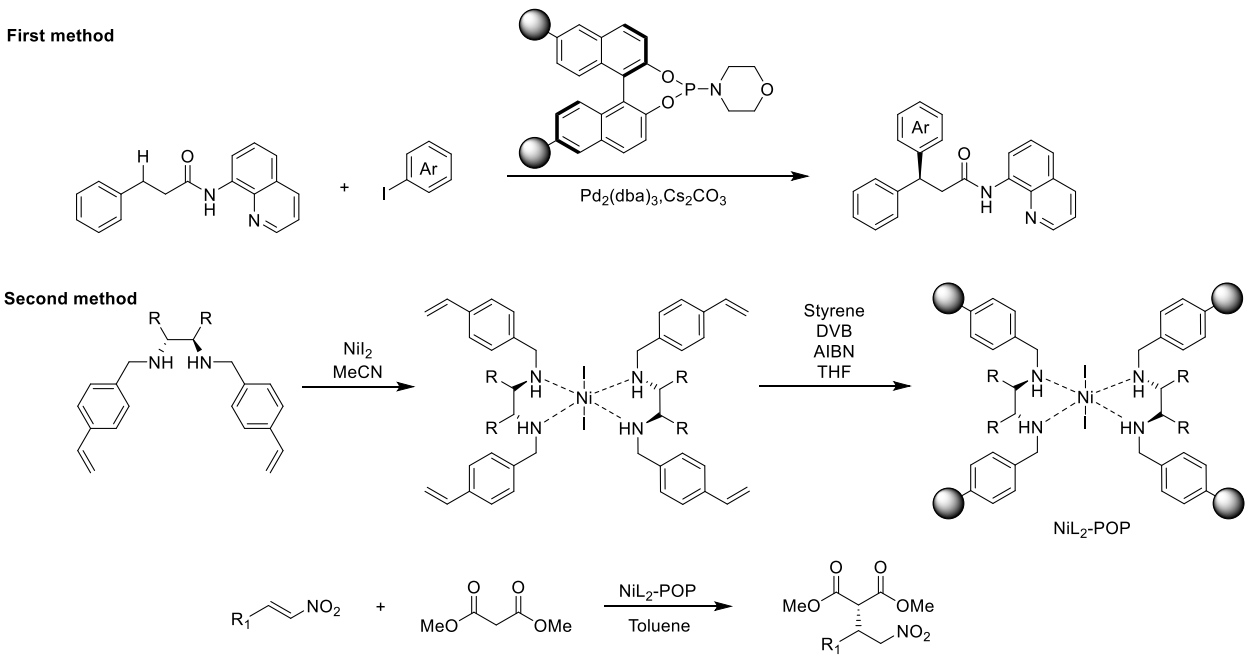

Scheme 2.3 Examples of two different methods of metalation of POPs [9]

2.4 References

[1] Bhaduri, S. and Mukesh, D., *Homogeneous Catalysis: Mechanisms and Industrial Applications*, John Wiley & Sons, **2014**.

[2] Deutschmann, O., Knözinger, H., Kochloefl, K. and Turek, T., *Ullmann's encyclopedia of industrial chemistry*. Wiley‐VCH, **2000**.

[3] Farnetti, E., Monte, R.D. and Kašpar, J., *Inorganic and Bio‐Inorganic Chemistry*.

[4] Kemball, C., Dowden, D.A. and Scurrell, M.S., *Heterogenized Homoge‐neous Catalysts in: Catalysis*, **1978**, 215–242.

[5] Qiao, B., Wang, A., Yang, X., Allard, L.F., Jiang, Z., Cui, Y., Liu, J., Li, J. and Zhang, T., *Nat. Chem.*, **2011**, *3*, 634–641.

[6] Liu, J.Y., *ACS Catal.*, **2017**, *7*, 34–59.

[7] a) Yang, X.F., Wang, A., Qiao, B., Li, J., Liu, J. and Zhang, T., *Acc. Chem. Res.*, **2013**, *46*, 1740–1748. b) Flytzani-Stephanopoulos, M. and Gates, B.C., *Annual Rev. Chem. Biomol. Eng.*, **2012**, *3*, 545–574. c) Wang, L., Huang, L., Liang, F., Liu, S., Wang, Y. and Zhang, H., *Chin. J. Catal.*, **2017**, *38*, 1528–1539. d) Zhou, H., Yang, X., Wang, A., Miao, S., Liu, X., Pan, X., Su, Y., Li, L., Tan, Y. and Zhang, T., *Chin. J. Catal.*, **2016**, *37*, 692–699.

[8] Li, J., Liu, J.J. and Zhang, T., *Chin. J. Catal.*, **2017**, *38*, 1431.

[9] a) Buendia, M.B., Kegnæs, S. and Kramer, S., *Adv. Synth. Catal*. **2020**, *362*, 5506-5512. b) Bennedsen, N.R., Kramer, S. and Kegnæs, S., *Catalysis Science & Technology* **2020**, *10*, 7697-7705.

[10] Kramer, S., Bennedsen, N.R. and Kegnæs, S., ACS Catal 2018, 8, 6961–6982.

[11] Dou, Z., Xu, L., Zhi, Y., Zhang, Y., Xia, H., Mu, Y. and Liu, X., *Chem. - Eur. J.* **2016**, *22*, 9919−9922.

[12] a) Camacho-Bunquin, J., Siladke, N.A., Zhang, G., Niklas, J., Poluektov, O.G., Nguyen, S.T., Miller, J.T. and Hock, A.S., *Organometallics* **2015**, *34*, 947−952. b) Tanabe, K.K., Ferrandon, M.S., Siladke, N.A., Kraft, S.J., Zhang, G., Niklas, J., Poluektov, O.G., Lopykinski, S.J., Bunel, E.E., Krause, T.R. and Miller, J.T., *Angew. Chem., Int. Ed*. **2014**, *53*, 12055−12058. c) Camacho-Bunquin, J., Ferrandon, M., Das, U., Dogan, F., Liu, C., Larsen, C., Platero-Prats, A.E., Curtiss, L.A., Hock, A.S., Miller, J.T. and Nguyen, S.T., *ACS Catal*. **2017**, *7*, 689−694.

[13] Totten, R.K., Weston, M.H., Park, J.K., Farha, O.K., Hupp, J.T. and Nguyen, S.T., *ACS Catal*. **2013**, *3*, 1454−1459.

[14] a) Gunasekar, G.H., Park, K., Ganesan, V., Lee, K., Kim, N.K., Jung, K.D. and Yoon, S.,*Chem. Mater*. **2017**, *29*, 6740−6748. b) Kuhn, P., Antonietti, M. and Thomas, A., *Angew. Chem., Int. Ed*. **2008**, *47*, 3450−3453. c) Gomes, R., Bhanja, P. and Bhaumik, A., *Chem. Commun*. **2015**, *51*, 10050−10053.

[15] Yu, H., Shen, C., Tian, M., Qu, J. and Wang, Z., *Macromolecules* **2012**, *45*, 5140−5150.

[16] a) Broicher, C., Foit, S.R., Rose, M., Hausoul, P.J.C. and Palkovits, R., *ACS Catal*. **2017**, *7*, 8413−8419. b) Wang, W., Zheng, A., Zhao, P., Xia, C. and Li, F., *ACS Catal*. **2014**, *4*, 321−327. c) Liu, T.T., Lin, Z.J., Shi, P.C., Ma, T., Huang, Y.B. and Cao, R., *ChemCatChem* **2015**, *7*, 2340−2345.

[17] Liras, M., Pintado-Sierra, M., Iglesias, M. and Sánchez, F., *J. Mater. Chem. A* **2016**, *4*, 17274−17278.

[18] Ding, Z.D., Zhu, W., Li, T., Shen, R., Li, Y., Li, Z., Ren, X. and Gu, Z.G., *Dalt. Trans*. **2017**, *46*, 11372−11379.

[19] Pan, L., Xu, M.Y., Feng, L.J., Chen, Q., He, Y.J. and Han, B.H., *Polym. Chem*. **2016**, *7*, 2299−2307.

3. Design and synthesis of POPs

Having introduced SACs and described the synthesis methods for POPs in Chapters 1 and 2, the following chapter will describe strategies for producing several POPs that may be used as SACs catalysts.

3.1 General strategy for synthesizing POPs

For most polymer synthesis processes, ligands containing C=C or C≡C bonds play an essential role in radical polymerization. The C=C or C≡C bonds on the ligands will open, and interact with the supporting structure material to form polymers. One of the challenges was how to add the C=C or C≡C bonds to the ligands in a suitable manner; this was resolved by using the Suzuki-Miyauru cross-coupling of halogenated ligands to convert halogen atoms into C=C bonds, and POPs can be produced by the radical polymerization of well-modified monomers.

Based on previous research by our group, there are three steps for synthesizing POPs from normal ligands using a general strategy (Figure 3.1). The first step is bromination using bromine on the correct positon of the ligands. For C=C bond substitution reactions, it is easy for the vinyl group to replace the bromo atoms, which are the leaving groups on the ligands. Vinylation is the second step in the insertion of the C=C group or styryl group on the ligand. The last step is radical polymerization, which is a simple method that does not involve metal complex pollution. Several POPs were synthesized according to this general strategy.

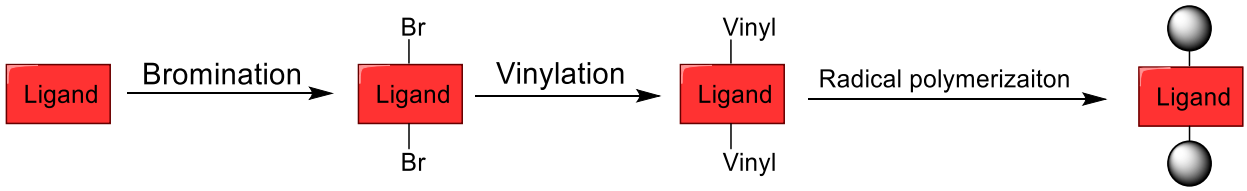

Figure 3.1 General strategy for synthesizing POPs

3.2 Bipyridine-POPs

In coordination chemistry, bipyridine is the most extensively utilized ligand to provide the most explored chelate system. [1] The asymmetrical and symmetrical isomers of bipyridine are 2,2′-, 3,3′-, 4,4′-, 2,3′-, 2,4′-, and 3,4′-bipyridine. The most widespread bipyridine is 2,2′-bipyridine (bpy) (Figure 3.2), which can chelate a variety of metal ions to form complexes, such as $Mo(CO)_4(bpy)$, $RuCl_2(bpy)_2$, $[Ru(bpy)_3]Cl_2$, and $[Fe(bpy)_3]^{2+}$. The combination of transition metals with bpy can also achieve catalytic reactions, such as C-H borylation by Ir-bpy, cycloaddition reactions by Co-bpy, and CO_2 photoreduction by [Ir(tpy)(bpy)]Cl. [2]

From the structure of 2,2′-bipyridine, the C=C bond could be introduced in a symmetrical position, 4,4′ and 5,5′. If the 3,3′ position introduces C=C bond the flexible structure of POPs may be affected, if the 6,6′ position introduces C=C bond there is a decrease in the chelation of N atoms with the metal.

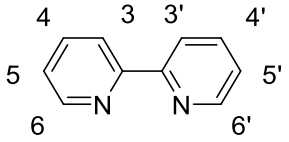

Figure 3.2 The structure of 2,2'-bipyridine (bpy)

4,4'- and 5,5'-Dibromo-2,2'-dipyridyl are commercially available, therefore, there was no need for the bromination step. The Suzuki cross-coupling reaction was used to synthesize symmetrical vinyl-substituted bipyridine in high yields (87% and 75%), according to Zhong and co-workers. [3] Two types of divinyl-bpy were obtained using commercial dibromo-bpy, based on the general strategy for synthesizing POPs (Scheme 3.1). [3]

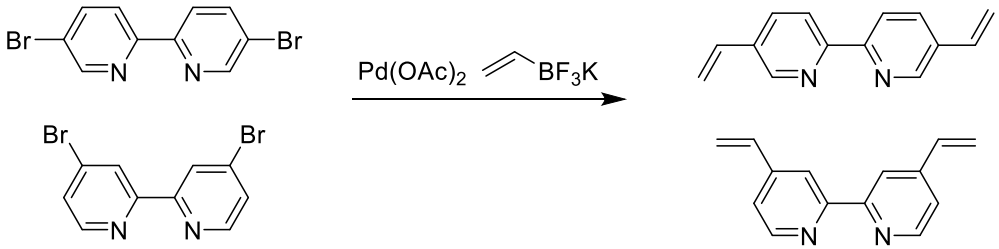

Scheme 3.1 Illustration of synthesis for 4,4'-divinyl-2,2'-bipyridine and 5,5'- divinyl-2,2'-bipyridine [3]

In the last step of the polymerization, bpy-POP 1-4 was synthesized using radical polymerization with bpy, styrene, divinylbenzene, and azo*bis*(isobutyronitrile) (AIBN) as radical initiators (Scheme 3.2).

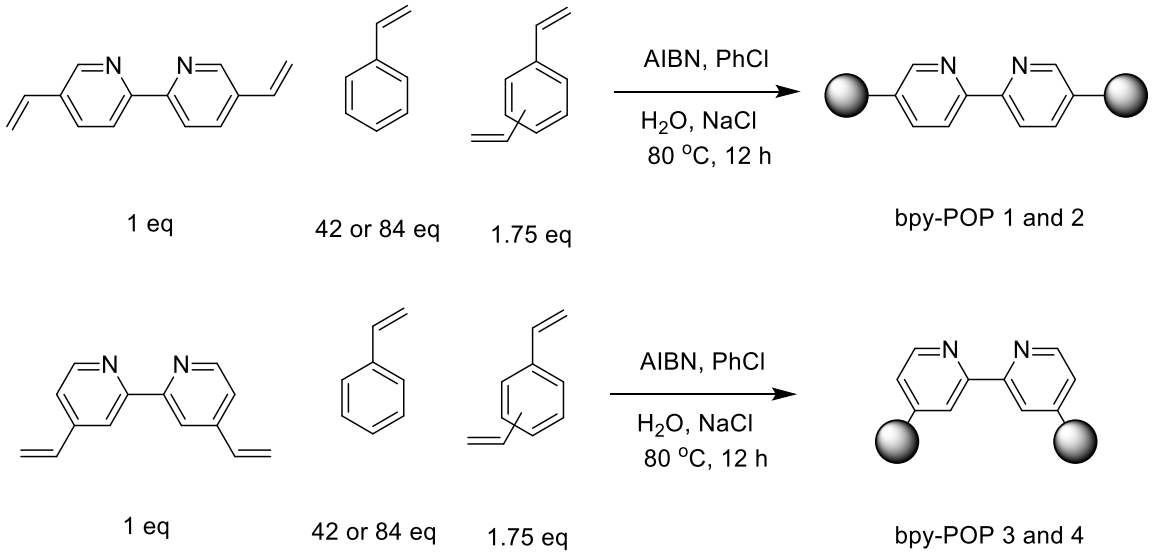

Scheme 3.2 Radical polymerization for synthesizing bpy-POP-1to 4

3.3 BINAP-POPs

BINAP [1,1-binaphthalene]-2,2-diyl*bis*[diphenylphosphine] was discovered by Noyori in 1980,

and it has been the most used chiral ligand since metal complexes were introduced as catalysts in organic asymmetric catalysis; BINAP exhibits a very high ee and turnover. [4] Normally there are four methods to produce BINAP in industry. The methods are the Noyori/Takasago, Merck Inc., Monsanto, and Merck Gmbh methods. BINAP is commercially available; therefore, the introduction of a C=C bond on BINAP is a facile manner in which to obtain POPs. However, it should be considered that the C=C bond's electronic effect are less sensitive to the large conjugated naphthyl rings than to the phosphorus moiety, and steric hindrance on the phosphorus moiety can decrease the coordination of the metal with phosphorus atoms. Thus, the naphthyl rings must be modified (Figure 3.3).

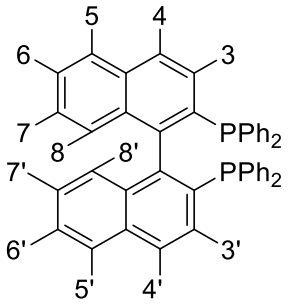

Figure 3.3 the structure of BINAP

Considering the structure of BINAP, 3–8 positions can be substituted. However, the dihedral angle will change if positions 7 or 8 have substituted groups, and the modified properties of BINAP can also change. Substitution at the 3 and 3' positions of BINAP would incur a large steric hindrance owing of the phosphine groups' strong *ortho*-directing effect, and the radical polymerization step would be affected by the close proximity between the phosphine and vinyl groups. There are no methods to achieve the 6 and 6' positions of BINAP using direct electrophilic substitution from commercial BINAP. The 6 and 6' positions of BINOL are more reactive than those of BINAP, and there are some synthetic routes to produce BINAP from BINOL. Nevertheless, the cost is high because these synthetic routes require many steps and produce low yields. The modification of the 4,4'- and 5,5'-positions of BINAP is a good alternative. According the previous research, substitution at the 4,4'-position of BINAP has been accomplished. [5a] The 5,5'-position of BINAP is similar to the 4,4'-position. The 5,5′-position of BINAP is farther away from the phosphine group, and vinylation of the 5,5′-positions will have less impact on BINAP. Commercial BINAP will be utilized as an initial materials, and it should be protected in the formation of BINAP oxide to protect phosphine groups because phosphine groups are sensitive to oxidation by oxygen and Br_2. Inspired by the work of Ding and Marc [5] and the general strategy, (*R*)-5,5'-divinyl-BINAP was synthesized from (*R*)-BINAP (Scheme 3.3). The first step was oxidation, with a high yield (99%). Bromination of 5, 5'-position of (*R*)-BINAPO (BINAP oxide) was the second step to form (*R*)-dibromo-BINAPO (90% yield), and it is necessary to introduce C=C bonds on chiral BINAP. Subsequently, utilizing the Suzuki cross-coupling reaction in the third step can produce chiral (*R*)-5,5'-divinyl-BINAPO (77% yield). Before (*R*)-5,5'-divinyl-BINAP forms a polymer, it is usually reduced from (*R*)-5,5'-divinyl-BINAPO. However, the POP from (*R*)-5,5'-divinyl-BINAP was oxidized again in the polymerization step. Therefore, the radical polymerization of chiral (*R*)-5,5'-

divinyl-BINAPO is a simple and general step. The last step is the reduction of the POP oxidation state.

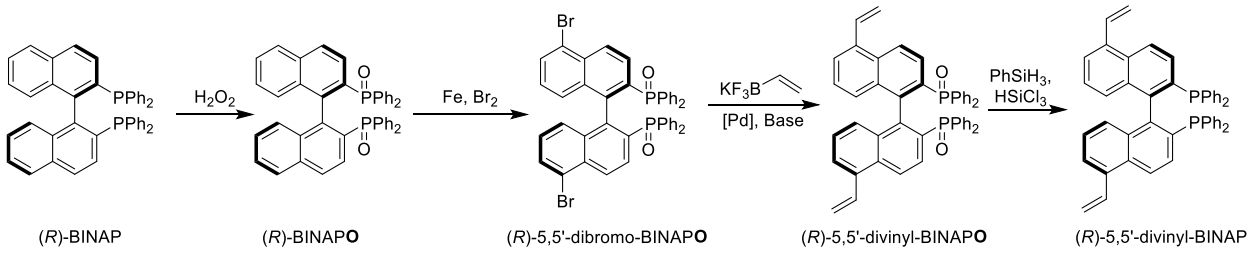

Scheme 3.3 Synthesis route for (*R*)-Divinyl-BINAP

Two types of *R*-BINAPO-gum-POP were synthesized, based on different ratios of chiral (*R*)-5,5'-divinyl-BINAPO, in the polymerization step occurring in warm water, with styrene, divinylbenzene, acacia gum, and AIBN as radical initiators. *R*-BINAP-POP-7 was formed in THF in the absence of acacia gum. After the reduction of POP, three types of chiral BINAP-POP-**5**,-**6**, and -**7** were obtained. Because the polymerization step was considered 100% conversion, the total yields of each chiral-BINAP-POP was 68.6% from (*R*)-BINAP (Scheme 3.4).

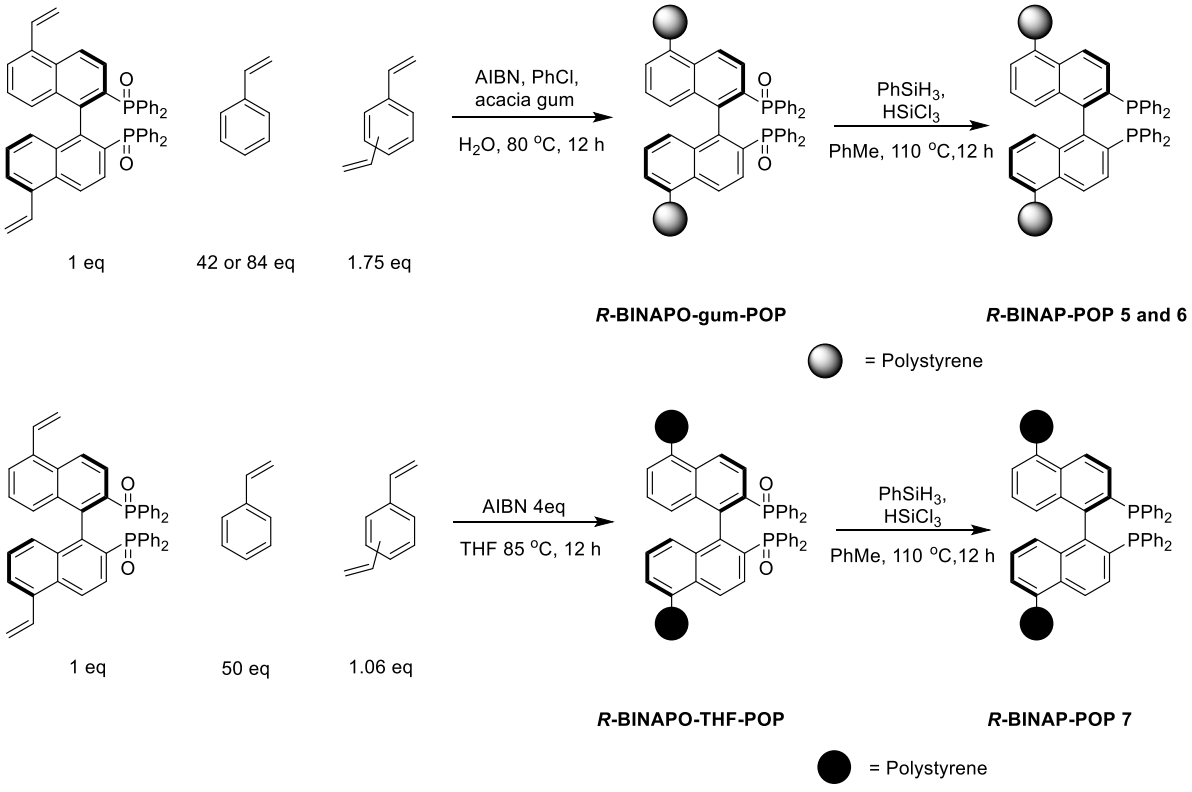

Scheme 3.4 Illustration of synthesis method for (*R*)-BINAP-POP-**5**, -**6** and -**7**

3.4 Vinylbenzyl-O-BIPHEP-POPs

(R)-MeO-BIPHEP, (R)-[6,6′-dimethoxybiphenyl-2,2′-diyl)*bis*(diphenylphosphine)], is another Noyori ligand that is similar to BINAP and its analogs. MeO-BIPHEP was synthesized by Schmid

in 1991 and developed by Roche. [6] MeO-BIPFEP has a wide performance profile for asymmetric catalytic applications because it can offer adequate stiffness to boost the stability of the biphenyl skeleton and markedly improve catalytic activity. MeO-BIPHEP is commercially available; therefore, the modification of MeO-BIPHEP does not occur on the phosphine group like that in BINAP. The vinyl group or C=C bonds can be introduced into the biphenyl skeleton at three positions (Figure 3.4). However, after experimenting with a variety of bromination procedures on MeO-BIPHEP, no plausible approach for bromo substitution at the 3–5 positions has emerged.

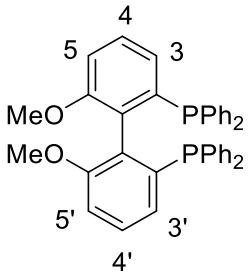

Figure 3.4 the structure of MeO-BIPHEP

The methoxy group is far from the phosphine group, which strongly influences the catalytic performance for the coordination of metal complexes with phosphorus atoms. In addition, modification of the methoxy group did not decrease the stability of the biphenyl skeleton. Thus, it is a good choice to introduce vinyl groups or C=C bonds on the methoxy group. According to Zhang's work, [7] the demethylated product, HO-BIPHEP is obtained in high yield (84%). Similar to the general strategy used for BINAP-POP, the synthetic route for (*R*)-vinylbenzyl-O-BIPHEP-POP-**8** was designed as follows (Scheme 3.5):

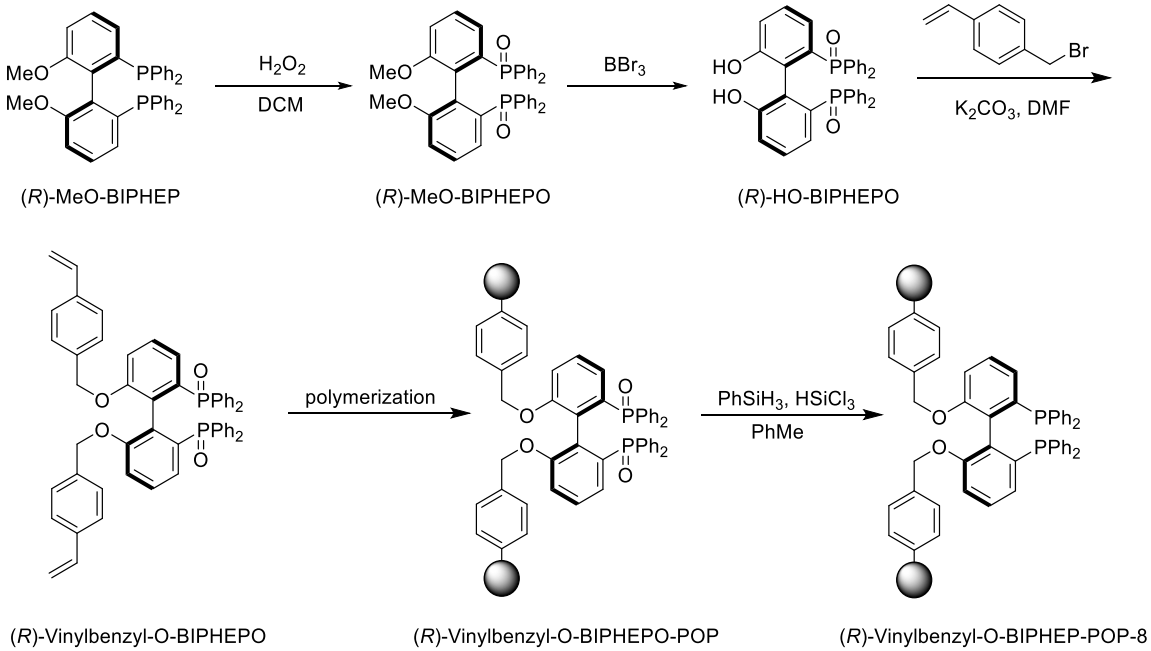

Scheme 3.5 Illustration of synthetic route for Vinylbenzyl-O-BIPHEP-POP-**8**

The entire procedure is similar to the general strategy used for BINAP-POP; however, the introduction of the vinyl group utilized a different method. To decrease the effect of changing the dihedral angle and biphenyl skeleton after the vinylbenzyl group is connected to HO-BIPHEP, there is an alternative method that uses 1-(4-bromobutyl)-4-vinylbenzene to replace 4-vinylbenzyl chloride. Currently, there is a longer chain (*R*)-Vinylbenzyl-O-BIPHEP-POP-**9** synthetic route to (*R*)-HO-BIPHEP (Scheme 3.6).

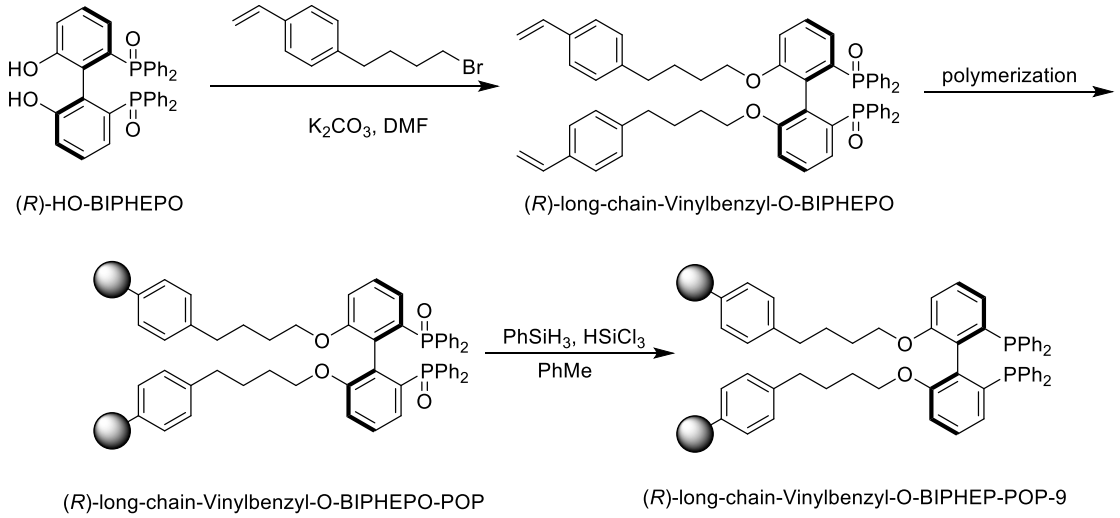

Scheme 3.6 Illustration of synthetic route for (*R*)-long-chain-Vinylbenzyl-O-BIPHEP-POP-**9**

3.5 Summary

Nine types of POP were synthesized based on the general strategy for producing POP.

POP 1–4 were obtained from 4,4'-dibromo-2,2'-bipyridine or 5,5'-dibromo-2,2'-bipyridine via vinylation and polymerization. The procedures to synthesize these four POPs are simple because the two types of dibromo-bpy are commercially available, and the first bromination step is not required. POP 1–4 were applied for the borylation of the arenes.

POP 5–7 were from the widely used chiral ligand (*R*)-BINAP. (*R*)-5,5'-Divinyl-BINAPO was the monomer of these three POPs and was synthesized by modifying the 5,5'-position of BINAP. Two polymerization methods were used to prepare POP 5–7.

POP 8–9 used MeO-BIPHEPO derivatives as monomers. The procedure to synthesize POP-8 and POP-9 were different from the general strategy. Polymerization was achieved by the introduction of different vinyl groups.

Chiral POP 5–9 will be used for the asymmetric α-arylation of ketones, asymmetric hydrosilylation of ketones, and other asymmetric catalysis reactions.

The synthetic POPs 1–9 are illustrated in Figure 3.5.

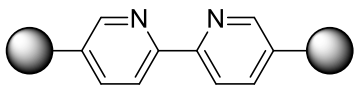

bpy-POP 1

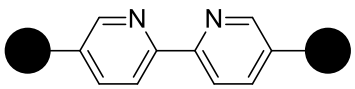

bpy-POP 2

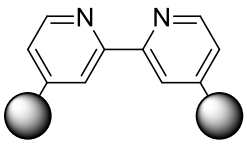

bpy-POP 3

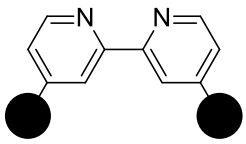

bpy-POP 4

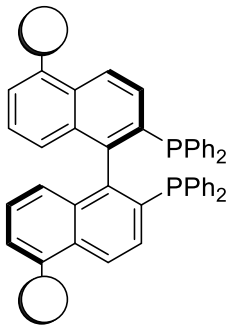

R-BINAP-POP 5

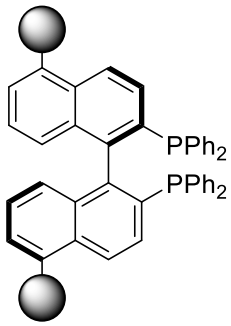

R-BINAP-POP 6

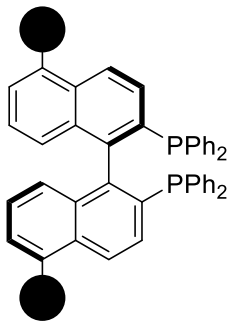

R-BINAP-POP 7

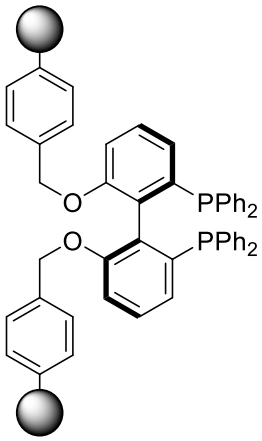

R-BIPHEP-POP 8

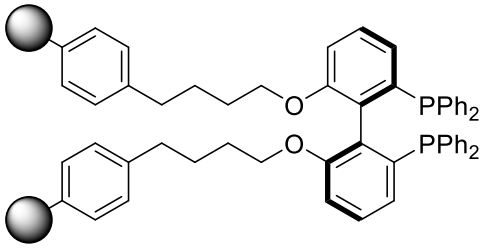

R-BIPHEP-POP 9

= polystyrenes

Figure 3.5 Structures of all synthetic POPs

3.6 Experimental

Chemicals

All commercially available chemicals were used as received.

R-BINAP [(*R*)-(+)-2,2′-Bis(diphenylphosphino)-1,1′-binaphthalene], 4,4'- and 5,5'-dibromo-2,2'-bipyridine, bromine, chlorobenzene, tetrakis(triphenylphosphine)palladium(0), phenylsilane, [1,1'-Bis(diphenylphosphino)ferrocene] dichloropalladium(II), palladium acetate, sodium chloride, (*R*)-MeO-BIPHEP [(*R*)-(+)-(6,6′-Dimethoxybiphenyl-2,2′-diyl)bis(diphenylphosphine)], K_2CO_3, hydrogen peroxide, iron powder, trichlorosilane, boron tribromide, 4-vinylbenzyl chloride, potassium vinyltrifluoroborate, , Et_3N, styrene, divinylbenzne, AIBN, are acquired from Sigma Aldrich.

Equipments

Anhydrous solvents were from Puresolv MD-7 (a solvent purification system). ^{1}H-NMR, ^{13}C-NMR, and ^{31}P-NMR spectra were measured on a Bruker Ascend 400 (400 MHz) spectrometer. The deuterated solvents were $CDCl_3$ and d_8-Toluene. Silica gel 60 was used for column chromatography. MS was carried out on either GC-MS/FID analysis on an Agilent 7890A GC equipped with an HP-5 column and a 5975C VLMSD with triple-axis detector (EI) or Waters AQUITY UPLC system equipped with PDA and SQD2 electrospray (ESI) MS detector.

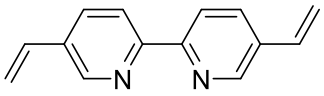

5,5'-divinyl-2,2'-bipyridine

In a 15 mL high-pressure tube with a dry stir bar, 5,5'-dibromo-2,2'-bipyridine (100 mg, 0.32 mmol), $Pd(OAc)_2$ (1.4 mg, 0.0064 mmol), PPh_3 (5 mg, 0.02 mmol), Cs_2CO_3 (311 mg, 0.096 mmol) and potassium vinyltrifluoroborate (4 eq., 1.27 mmol, 169 mg) were weighed and put in the high-pressure tube. The tube was connected with the Schlenk line, after three cycles of evacuation and back-filling with nitrogen, and 5 mL of mixture solvent (THF: H_2O = 24:1) was added by syringe. The tube was stirred in an oil bath at 85 ˚C for 48 h. The suspension was cooled down to room temperature and diluted with 5 mL of water, then extracted with DCM three times (10 mLx3). Organic layers were gathered, dried over $MgSO_4$, and concentrated by rotation. The crude product was purified by column chromatography and a white solid was obtained (50 mg, 75 %).

^{1}H NMR (400 MHz, Chloroform-d) δ 8.59 (d, *J* = 2.3 Hz, 2H), 8.30 (d, *J* = 8.3 Hz, 2H), 7.78 (dd, *J* = 8.3, 2.3 Hz, 2H), 6.69 (dd, *J* = 17.6, 10.9 Hz, 2H), 5.82 (d, *J* = 17.6 Hz, 2H), 5.34 (d, *J* = 10.9 Hz, 2H). ^{13}C NMR (101 MHz, Chloroform-d) δ 155.0, 147.8, 133.5, 133.3, 133.0, 120.8, 116.3. NMR data are in accordance with literature values. [3]

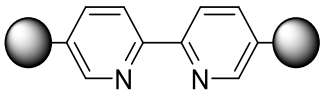

BPY-POP-1

NaCl (6.468 g), acacia gum (10.348 g), and water (250 mL) were put into a 500 mL round bottom flask with a magnetic stir bar. The flask was purged with nitrogen and put the mixture on a stirring plate to get a clear solution. Meanwhile 5,5'-divinyl-2,2'-bipyridine (0.77 mmol, 160 mg), styrene (84 eq, 64.68 mmol, 7.39 mL), divinylbenzene (2.695 mmol, 373 μL), chlorobenzene (13 mL) and a stir bar were mixed together in a 50 mL round bottom flask. The suspension was purged with nitrogen for 15 min, then AIBN (0.2 M in toluene) was added dropwise. The organic content was added dropwise to the aqueous solution in the 500 mL flask by a syringe. The mixture was stirred for half-hour and heated to 80 ˚C and left to start the polymerization. After stirring for 15 hours, the mixture was cooled down to room temperature. The **BPY-POP-1** was collected by a glass funnel and washed with water (100 mL x 3), methanol (100 mL x 3), THF (100 mL x 3), and toluene (100 mL x 3). Then **BPY-POP-1** was dried in a vacuum oven overnight and white beads were obtained (5.282 g, 0.77 mmol, 0.01457 mmol/100 mg).

The **POP-2** was prepared in the same procedure and changed the ratio of 5,5'-divinyl-2,2'-bipyridine with styrene.

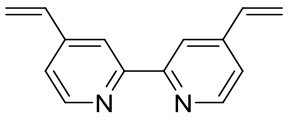

4,4'-divinyl-2,2'-bipyridine

The title compound was prepared according to 5,5'-divinyl-2,2'-bipyridine from 4,4'-dibromo-2,2'-bipyridine (87 %).

^{1}H NMR (400 MHz, Chloroform-d) δ 8.62 (dd, *J* = 5.2, 1.5 Hz, 2H), 8.40 (s, 2H), 7.33 – 7.27 (m, 2H), 6.76 (ddd, *J* = 17.6, 10.8, 1.6 Hz, 2H), 6.08 (dd, *J* = 17.6, 1.6 Hz, 2H), 5.52 (dd, *J* = 10.9, 1.6 Hz, 2H). ^{13}C NMR (101 MHz, Chloroform-d) δ 156.4, 149.4, 145.8, 134.9, 120.7, 118.9, 118.5. NMR data are in accordance with literature values. [3]

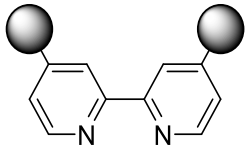

BPY-POP-3 and **4**

The POP-**3** and **4** were prepared with the similar POP-1 procedure with 4,4'-divinyl-2,2'-bipyridine as starting material and changed the ratio of 4,4'-divinyl-2,2'-bipyridine with styrene. (**BPY-POP-3** used 42 eq. styrene and **BPY-POP-4** used 84 eq. styrene)

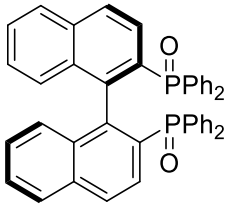

(*R*)-BINAPO

In a 50 mL round-bottomed flask, (*R*)-BINAP (1 mmol, 623mg) was dissolved in dichloromethane (DCM, 20 mL). The mixture was cooled to 0 ˚C (ice water bath) and 2 mL of hydrogen peroxide (35%) was added dropwise. After stirring for 3 h at room temperature, 20 mL of water was added. Aqueous phases were extracted with 20 mL of DCM. The organic phases were washed with 30 mL aqueous sodium hydrogen sulfite solution and dried over $MgSO_4$. The solvent was removed under vacuum and (*R*)-BINAPO was obtained as a white solid (655 mg, 99%).

^{1}H NMR (400 MHz, Chloroform-d) δ 7.88–7.77 (m, 4H), 7.75–7.63 (m, 4H), 7.49–7.30 (m, 12H), 7.30–7.18 (m, 9H), 6.85–6.75 (m, 4H). ^{31}P (162 MHz, $CDCl_3$): 28.68. NMR data are in accordance with literature values. [5]

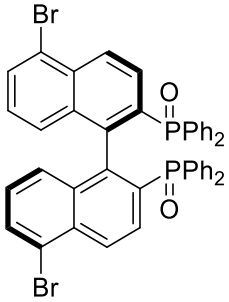

(*R*)-5,5′-DibromoBINAPO

A solution of (*R*)-BINAPO (655 mg, 1 mmol) in 1,2-dichloroethane (DCE, 10 mL) was added dropwise to a stirred refluxing solution of DCE (10 mL), Br_2(1 mL, 20 mmol, 20 equiv) and iron powder (84 mg, 1.5 mmol, 1.5 equiv). After refluxing for 12 h, the solution was cooled to room temperature and filtered to remove any iron. The organic layer was washed with H_2O, 10% $NaHSO_3$ aqueous solution, saturated brine, and saturated sodium hydrogen sulfite solution, dried over $MgSO_4$. The mixture was concentrated and purified by silica gel chromatography affording the product as a white solid (731 mg, 90% yield).

^{1}H NMR (400 MHz, Chloroform-d) δ 8.33 (dd, *J* = 8.9, 1.7 Hz, 2H), 7.77–7.64 (m, 6H), 7.57 (dd, *J* = 11.5, 8.9 Hz, 2H), 7.45–7.38 (m, 8H), 7.34–7.25 (m, 8H), 6.74 (d, *J* = 8.5 Hz, 2H), 6.64 (t, 2H). ^{31}P (162 MHz, $CDCl_3$): 28.23. NMR data are in accordance with literature values. [5]

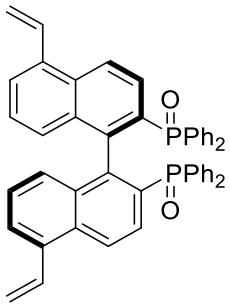

(*R*)-5,5′-DivinylBINAPO

(*R*)-5,5′-DibromoBINAPO(731 mg, 0.9 mmol), potassium vinyltrifluoroborate (288 mg, 2.16 mmol, 4eq.) and $PdCl_2(dppf)CH_2Cl_2$ (52 mg, 0.072 mmol) were weighed off in a three-necked flask and a stir bar was added. The setup was connected to a reflux condenser and made inert by 3 vacuum/N_2 cycles with Schlenk techniques. 1-PrOH (10 mL) and Et_3N (1.8 mmol, 250 μL) were added to the flask. After refluxing for 12 h, the solvent was removed under a vacuum. The precipitate was passed through a silica gel column and dried under vacuum to produce a white solid (490 mg, 77% yield).

^{1}H NMR (400 MHz, Chloroform-d) δ 8.13 (dd, *J* = 8.9, 2.4 Hz, 2H), 7.72–7.66 (m, 4H), 7.51–7.33 (m, 15H), 7.30–7.20 (m, 9H), 6.78 (d, *J* = 4.6 Hz, 2H), 5.75 (dd, *J* = 17.3, 1.6 Hz, 2H), 5.48 (dd, *J* = 10.9, 1.6 Hz, 2H). ^{31}P (162 MHz, $CDCl_3$): 28.43. NMR data are in accordance with literature values. [5]

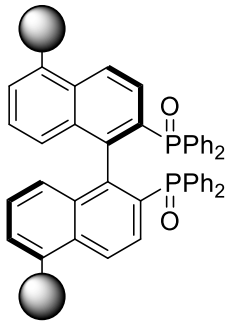

(*R*)-5,5′-DivinylBINAPO-gum-1-POP

A 250 mL round-bottomed flask was charged with H_2O (120 mL), NaCl (2.856 g), acacia gum (4.57 g), and a magnetic stir bar. Next, the solution was purged with nitrogen for 15 minutes. At the same time, (*R*)-5,5′-DivinylBINAPO (480 mg, 0.68 mmol), styrene (3.28 mL, 28.56 mmol), AIBN (0.2 M in toluene, 2.86 mL, 0.57 mmol), divinylbenzene (212 μL, 1.19 mmol) and chlorobenzene (6 mL) were measured and added in a 25 mL of dry round-bottomed flask. The mixture was purged with nitrogen for 15 minutes. Then, the organic solution was added *via* a syringe to the aqueous solution at one time. The mixed solution was heated to 80 °C and stirred overnight. After cooling to room temperature, (*R*)-5,5′-DivinylBINAPO-gum-1-POP was collected on a glass sintered funnel and washed with H_2O (100 mL x 3 times), MeOH (100 mL x3

times), THF (100 mL x 3 times) and toluene (100 mL x 3 times) and dried in a vacuum oven (60 °C) overnight to yield transparent beads (3 g).

^{31}P (162 MHz, $CDCl_3$): 26.59.

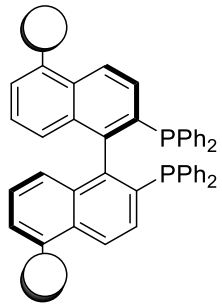

(*R*)-5,5′-DivinylBINAP-POP-5

In a 100 mL round-bottomed flask under a nitrogen atmosphere fitted with a reflux condenser was placed, (*R*)-5,5′-DivinylBINAPO-gum-1-POP (0.68 mmol, 3 g), phenylsilane (340 μL, 2.72 mmol, 4equiv) and 40 mL of toluene was added. The solution was stirring for 10 minutes, and trichlorosilane (3.4 mL, 27.2 mmol, 40 equiv) was added dropwise. Then the mixture was heated to 110 °C overnight. After cooling to 0 °C (ice bath), saturated sodium hydroxide solution (10 mL) was added dropwise to the flask and stirred for 2 h. Then the mixed solution was filtered through a glass sintered funnel and washed with H_2O (100 mL), MeOH (100 mL), THF (100 mL), and toluene (100 mL). After drying in a vacuum oven (60 °C) overnight, (*R*)-5,5′-DivinylBINAP-POP-**5** was obtained as transparent beads (2.9 g, 0.68 mmol, 0.0234 mmol/100 mg polymer).

^{31}P (162 MHz, $CDCl_3$): -15.52.

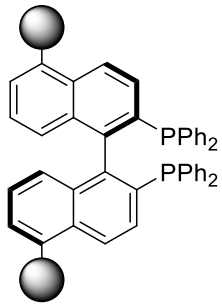

(*R*)-5,5′-DivinylBINAP-POP-6

The (*R*)-5,5′-DivinylBINAP-POP-6 was prepared according to the (*R*)-5,5′-DivinylBINAP-POP-5 procedure and changed the ratio of (R)-BINAP with styrene (3715 mg, 0.5 mmol, 0,01329 mmol/100 mg polymer).

^{31}P (162 MHz, $CDCl_3$): -15.75.

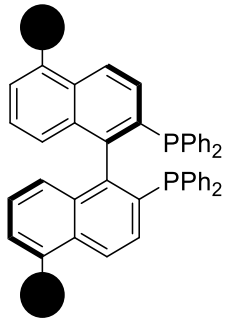

(*R*)-5,5′-DivinylBINAP-POP-7

The (*R*)-5,5′-DivinylBINAP-POP-7 was prepared according to POP-5 procedure and changed the ratio of (R)-BINAP and styrene without acacia gum in THF.

^{31}P (162 MHz, $CDCl_3$): -15.86.

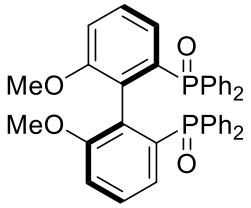

(*R*)-MeO-BIPHEPO

In a 25 mL round-bottomed flask, (*R*)-MeO-BIPHEP (0.17 mmol, 100mg) was dissolved in dichloromethane (DCM, 10 mL). The mixture was cooled to 0 ˚C (ice water bath) and 0.5 mL of hydrogen peroxide (35%) was added dropwise. After stirring for 3 h at room temperature, 10 mL of water was added. Aqueous phases were extracted with 10 mL of DCM. The organic phases were washed with 30 mL aqueous sodium hydrogen sulfite solution and dried over $MgSO_4$. The solvent was removed under vacuum and (*R*)-MeO-BIPHEPO was obtained as a white solid (106 mg, 99%).

^{1}H NMR (400 MHz, Chloroform-d) δ 7.59 (ddd, *J* = 23.7, 12.0, 7.5 Hz, 8H), 7.46–7.29 (m, 12H), 7.20 (td, *J* = 8.0, 3.5 Hz, 2H), 6.86 (dd, *J* = 13.4, 7.7 Hz, 2H), 6.74 (d, *J* = 8.2 Hz, 2H), 3.11 (s, 6H). ^{31}P NMR (162 MHz, Chloroform-d) δ 31.23. NMR data are in accordance with literature values. [7]

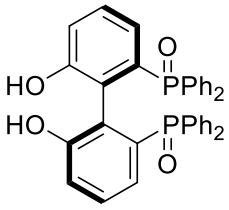

(*R*)-HO-BIPHEPO

A solution of (*R*)-MeO-BIPHEPO (0.17 mmol, 106 mg) in DCM (10 mL) was cooled to -78 ˚C and bubbled with nitrogen for 15 min. To this solution was added BBr_3 (0.85 mmol, 82 μL, 5 eq) via a syringe over 10 min. The mixture solution was stirred at -78 ˚C for 1 h, and then slowly warmed to room temperature and stirred overnight. After the mixture was cooled to 0 ˚C (in an ice bath), degassed water (10 mL) was added slowly and the aqueous layer was removed. The organic phase was washed subsequently with water and brine and dried over $MgSO_4$. The mixture was concentrated and purified by silica gel chromatography affording the product as a white solid (56 mg).

^{1}H NMR (400 MHz, Chlorofzorm-d) δ 7.36 – 7.25 (m, 9H), 7.20 (dq, *J* = 7.3, 3.8, 3.4 Hz, 2H), 6.87 (d, *J* = 8.1 Hz, 1H), 6.83 (d, *J* = 6.9 Hz, 1H), 4.27 (bs, 1H). ^{31}P NMR (162 MHz, Chloroform-d) δ 30.67. NMR data are in accordance with literature values. [7]

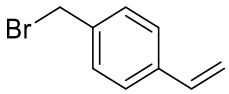

1-(bromomethyl)-4-vinylbenzene

The title compound was prepared by Paul's method [8] from 4-vinylbenzyl chloride.

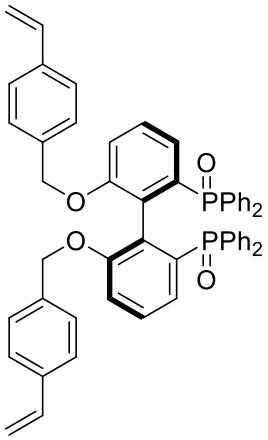

(*R*)-Vinylbenzyl-O-BIPHEPO

(*R*)-HO-BIPHEPO (85.7 mg, 0.146 mmol), K_2CO_3 (100mg, 0.73 mmol, 5 eq), 1-(bromomethyl)-4-vinylbenzene (120 mg, 0.614 mmol, 4.2 eq) were weighed off in a round-bottomed flask and a stir bar was added. The setup was made inert by 3 vacuum/nitrogen cycles and bubbled with nitrogen for 15 min with Schlenk techniques. The mixture was heated to 60 ˚C for 48 h. After removal of the solvent, the residue was extracted with ether, washed with water and brine, and dried over $MgSO_4$. The white solid after evaporation of solvents was purified by a silica gel column with DCM-MeOH as the eluent (65 mg).

^{1}H NMR (400 MHz, Chloroform-*d*) δ 8.65 (dd, *J* = 12.1, 7.6 Hz, 2H), 8.53 (dd, *J* = 11.7, 7.6 Hz, 2H), 8.39 (t, *J* = 7.5 Hz, 1H), 8.34–8.27 (m, 3H), 8.23–8.13 (m, 3H), 8.10 (d, *J* = 7.9 Hz, 2H), 7.83 (t, *J* = 8.4 Hz, 4H), 7.60 (dd, *J* = 17.6, 10.9 Hz, 1H), 6.63 (d, *J* = 17.6 Hz, 1H), 6.17 (d, *J* = 10.9 Hz, 1H), 5.70 (d, *J* = 13.3 Hz, 1H), 5.42 (d, *J* = 13.2 Hz, 1H). ^{13}C NMR (101 MHz, Chloroform-

d) δ 156.4, 136.9, 136.5, 136.3, 132.6, 132.5, 132.3, 132.2, 131.1, 130.8, 128.1, 127.9, 127.7, 127.6, 126.0, 125.6, 125.5, 114.3, 113.5, 68.6, 29.3. ^{31}P (162 MHz, $CDCl_3$): 29.35. MS (EI) m/z ($M^{\cdot+}$) calcd for $C_{54}H_{44}O_4P_2$: 818, found 818.

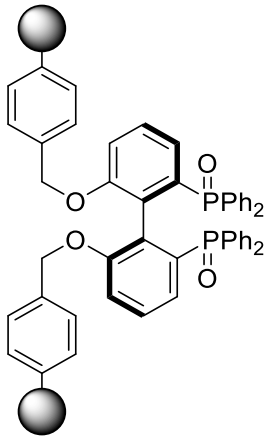

(*R*)-Vinylbenzyl-O-BIPHEPO-POP

A 50 mL round-bottomed flask was charged with H_2O (7 mL), NaCl (168 mg), acacia gum (269 mg), and a magnetic stir bar. Next, the solution was purged with nitrogen for 15 minutes. At the same time, (*R*)-Vinylbenzyl-O-BIPHEPO (32.8 mg, 0.04 mmol), styrene (192 μL, 1.68 mmol), AIBN (0.2 M in toluene, 168 μL, 0.033 mmol), divinylbenzene (9.7 μL, 0.07 mmol) and chlorobenzene (0.35 mL) were measured and added in a 5 mL of the dry round-bottomed flask. The mixture was purged with nitrogen for 15 minutes. Then, the organic solution was added *via* a syringe to the aqueous solution at one time. The mixed solution was heated to 80 °C and stirred overnight. After cooling to room temperature, (*R*)-Vinylbenzyl-O-BIPHEPO-POP was collected on a glass sintered funnel and washed with H_2O (20 mL x 3 times), MeOH (20 mL x 3 times), THF (20 mL x 3 times) and toluene (20 mL x 3 times) and dried in a vacuum oven (60 °C) overnight to yield transparent beads (50.4 mg).

^{31}P (162 MHz, $CDCl_3$): 29.92.

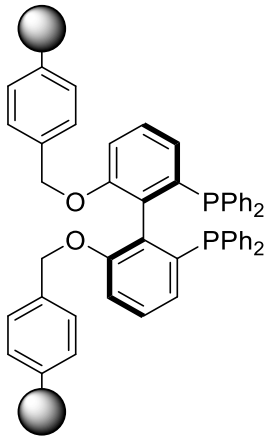

(*R*)-Vinylbenzyl-O-BIPHEPO-POP-8

In a 25 mL round-bottomed flask under a nitrogen atmosphere fitted with a reflux condenser was placed, (*R*)-Vinylbenzyl-O-BIPHEPO-POP (0.04 mmol, 50.4 mg), phenylsilane (20 μL, 0.16 mmol, 4 equiv) and 10 mL of toluene were added. The solution was stirring for 10 minutes; trichlorosilane (0.2 mL, 1.6 mmol, 40 equiv) was added dropwise. Then the mixture was heated to 110 °C overnight. After cooling to 0 °C (ice bath), saturated sodium hydroxide solution (1 mL) was added dropwise to the flask and stirred for 2 h. Then the mixed solution was filtered through a glass sintered funnel and washed with H_2O (25 mL), MeOH (25 mL), THF (25 mL), and toluene (25 mL). After drying in a vacuum oven (60 °C) overnight, (*R*)-Vinylbenzyl-BIPHEP POP-8 was obtained as transparent beads (40.6 mg, 0.04 mmol, 0.0985 mmol/100 mg polymer).

^{31}P NMR (162 MHz, Toluene-d_8) δ -5.11.

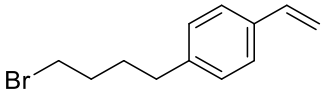

1-(4-bromobutyl)-4-vinylbenzene

The title compound was prepared by Masatoshi's method [9] from 1-(bromomethyl)-4-vinylbenzene.

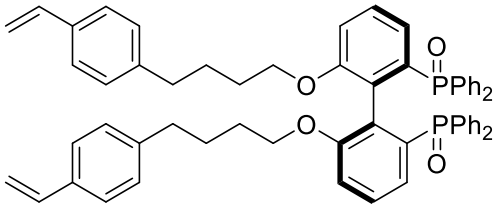

(*R*)-long-chain-Vinylbenzyl-O-BIPHEPO

(*R*)-HO-BIPHEPO (52 mg, 0.0887 mmol), K_2CO_3 (61 mg, 0.45 mmol, 5 eq), 1-(4-bromobutyl)-4-vinylbenzene (88 mg, 0.37 mmol, 4.2 eq) were weighed off in a round-bottomed flask and a stir bar was added. The setup was made inert by 3 vacuum/nitrogen cycles and bubbled with nitrogen for 15 min with Schlenk techniques. The mixture was heated to 60 °C for 48 h. After removal of the solvent, the residue was extracted with ether, washed with water and brine, and dried over $MgSO_4$. The white solid after evaporation of solvents was purified by a silica gel column with DCM-MeOH as the eluent (39.4 mg, 49 %).

^{1}H NMR (400 MHz, Chloroform-d) δ 7.55 (ddd, *J* = 24.9, 12.0, 7.8 Hz, 8H), 7.33 – 7.06 (m, 20H), 6.83 (d, *J* = 7.8 Hz, 4H), 6.75 (dd, *J* = 13.2, 7.8 Hz, 2H), 6.60 (d, *J* = 6.7 Hz, 2H), 5.60 (dd, *J* = 17.6, 0.9 Hz, 2H), 5.11 (d, *J* = 10.9 Hz, 2H), 3.28 (ddt, *J* = 24.4, 8.9, 5.5 Hz, 4H), 2.31 – 2.16 (m, 4H), 1.16 – 0.89 (m, 8H).

^{13}C NMR (101 MHz, Chloroform-d) δ 136.6, 132.6, 132.3, 132.2, 128.5, 127.9, 127.8, 127.6, 127.5, 126.0, 112.9, 69.5, 67.2, 53.9, 35.0, 31.7, 29.7, 29.3, 28.2, 27.3.

^{31}P (162 MHz, $CDCl_3$): 28.56. MS (EI) m/z ($M^{\cdot+}$) calcd for $C_{60}H_{56}O_4P_2$: 902, found 902.

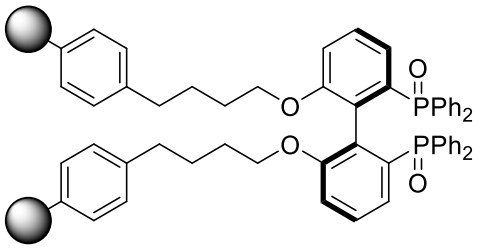

(*R*)-long-chain-Vinylbenzyl-O-BIPHEPO-POP

A 50 mL round-bottomed flask was charged with H_2O (14 mL), NaCl (357 mg), acacia gum (570 mg), and a magnetic stir bar. Next, the solution was purged with nitrogen for 15 minutes. At the same time, (*R*)-long-chain-Vinylbenzyl-O-BIPHEPO (76 mg, 0.084 mmol), styrene (405 μL, 3.54 mmol), AIBN (0.2 M in toluene, 363 μL, 0.0708 mmol), divinylbenzene (21.4 μL, 0.147 mmol) and chlorobenzene (0.7 mL) were measured and added in a 5 mL of dry round-bottomed flask. The mixture was purged with nitrogen for 15 minutes. Then, the organic solution was added *via* a syringe to the aqueous solution at one time. The mixed solution was heated to 80 ˚C and stirred overnight. After cooling to room temperature, (*R*)-long-chain-Vinylbenzyl-O-BIPHEPO-POP was collected on a glass sintered funnel and washed with H_2O (20 mL x 3 times), MeOH (20 mL x 3 times), THF (20 mL x 3 times) and toluene (20 mL x 3 times) and dried in a vacuum oven (60 ˚C) overnight to yield transparent beads (290 mg).

^{31}P (162 MHz, $CDCl_3$): 26.76.

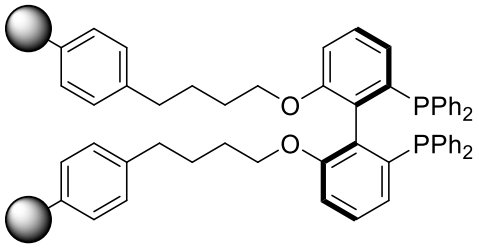

(*R*)-long-chain-Vinylbenzyl-O-BIPHEP-POP-9

In a 25 mL round-bottomed flask under a nitrogen atmosphere fitted with a reflux condenser was placed, (*R*)-long-chain-Vinylbenzyl-O-BIPHEPO-POP (0.084 mmol, 290 mg), phenylsilane (42 μL, 0.336 mmol, 4 equiv) and 15 mL of toluene was added. The solution was stirring for 10 minutes, and trichlorosilane (0.344 mL, 3.36 mmol, 40 equiv) was added dropwise. Then the mixture was heated to 110 ˚C overnight. After cooling to 0 ˚C (ice bath), saturated sodium hydroxide solution (2 mL) was added dropwise to the flask and stirred for 2 h. Then the mixed solution was filtered through a glass sintered funnel and washed with H_2O (25 mL), MeOH (25 mL), THF (25 mL), and toluene (25 mL). After drying in a vacuum oven (60 ˚C) overnight, (*R*)-long-chain-Vinylbenzyl-O-BIPHEP-POP-9 was obtained as white beads (274 mg, 0.084 mmol, 0.0306 mmol/100 mg polymer).

^{31}P NMR (162 MHz, Toluene-d_8) δ -11.6.

3.7 References

[1] Kaes, C., Katz, A. and Hosseini, M.W., *Chemical reviews*, **2000**, *100*, 3553-3590.

[2] a) Ishiyama, T., Takagi, J., Hartwig, J.F. and Miyaura, N., *Angew. Chem., Int. Ed*, **2002**, *41*, 3056-3058. b) Gutnov, A., Heller, B., Fischer, C., Drexler, H.J., Spannenberg, A., Sundermann, B. and Sundermann, C., *Angew. Chem., Int. Ed*, **2004**, *43*, 3795-3797. c) Sato, S. and Morikawa, T., *ChemPhotoChem*, **2018**, *2*, 207-212.

[3] Nie, H.J., Yao, J. and Zhong, Y.W., *J. Org. Chem*. **2011**, *76*, 4771-4775.

[4] Berthod, M., Mignani, G., Woodward, G. and Lemaire, M., *Chemical reviews*, **2005**, *105*, 1801-1836.

[5] a) Wang, T., Wang, W., Lyu, Y., Xiong, K., Li, C., Zhang, H., Zhan, Z., Jiang, Z. and Ding, Y., *Chinese, J. Catal*. **2017**, *38*, 691-698. b) Berthod, M., Mignani, G. and Lemaire, M., *Tetrahedron: Asymmetry*, **2004**, *15*, 1121-1126.

[6] Schmid R., Foricher J., Cereghetti M. and Schonholzer P., *Helv. Chim. Acta*. **1991**, *74*, 370-381.

[7] Zhang, Z., Qian, H., Longmire, J. and Zhang, X., *J. Org. Chem.*, **2000**, *65*, 6223-6226.

[8] Hisey, B., Buddingh, J.V., Gillies, E.R. and Ragogna, P.J., *Langmuir*, **2017**, *33*, 14738-14747.

[9] Seki, A., Ishiwata, F., Takizawa, Y. and Asami, M., *Tetrahedron*, **2002**, *60*, 5001-5011.

4. Borylation of arenes by Ir-BPY-POP

4.1 Introduction to borylation of arenes

Arylboronic acids and their derivatives are important intermediates in the chemical industry and organic synthesis. [1] They are used in a wide range of transformations, including Suzuki-Miyaura coupling [2] and conjugate additions to carbonyl compounds, [3] and C-N and C-O coupling reactions [4] in organic chemistry. The direct C-H arylborylation catalyzed by homogeneous catalytic system has become a topical research topic in modern synthetic chemistry. Significant efforts have been expended to design and synthesize efficient homogeneous catalysts, such as Re, [5] Rh, [6] Pd, [7] Ir, [8] Co, [9] Cu, [10] Ni, [11] and Fe [12]. The regiocontrol and selectivity of aryl compounds have attracted significant attention for C-H activation via various interactions. [13]

Considering future practical applications and cost reduction, [14] the heterogenization of homogeneous catalysts on supporting materials is important for catalysts' recovery and recycling. [15] One of these new strategies, SACs, facilitates the understanding of the nature of the active sites, which can help optimize efficient reaction conditions and perform mechanistic studies through the fine-tuning of spatial or electronic effects in the transition state.

Recently, SACs have been used for C-H arylborylation using various supporting materials, such as ionic liquids, [16] organosilica, [17] nanotubes, [18] MOFs, [19] COF [20] and polymers [21] (Scheme 4.1). Most of these materials have a bipyridine structure, which implies that the bipyridine in these supporting materials has potential for the heterogenization of the catalyst without loss of activity. However, with the consecutive reuse of heterogeneous catalysts, the reaction activity and selectivity progressively decrease owing to the decomposition of the supporting materials. Thus, the development of new support materials containing bipyridine remains a challenge for practical applications. Based on the research on POPs, the developing a single-atom heterogeneous catalyst based on bipyridine structure can catalyze the direct C-H arylborylation.

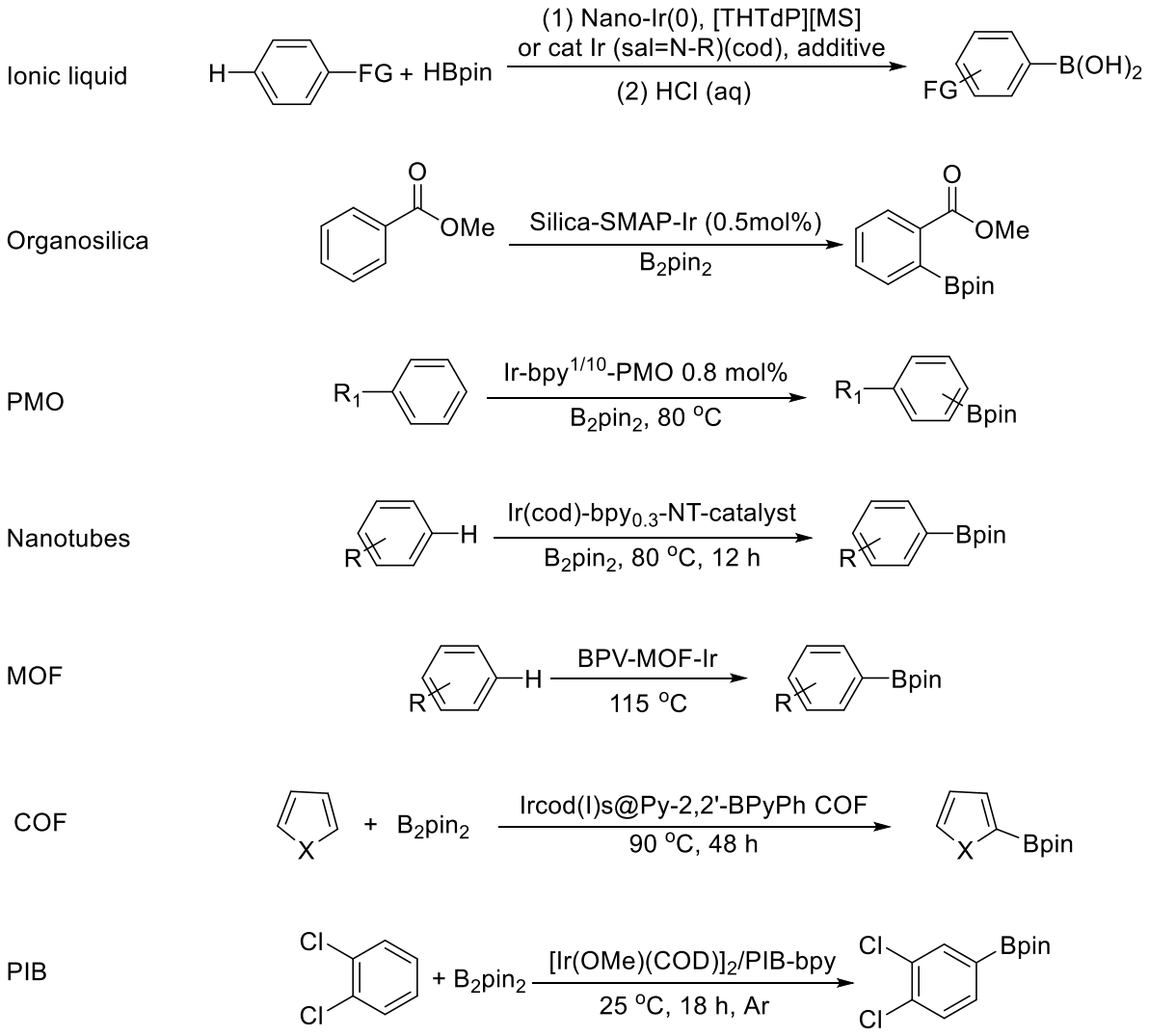

Scheme 4.1 Heterogeneous catalysts for Borylation of Arenes [16-21]

4.2 Optimization of the reaction conditions

Bpy-POP-**1** was synthesized as described in Chapter 3 and evaluated for the borylation of benzene in the presence of an Ir complex. To produce a highly dispersed active single-atom site in solution, the Ir complex must be incorporated with bpy-POP before reacting with the boron source. Table 4.1 shows an overview of the different parameters studied to optimize the reaction conditions. B_2pin_2 was consumed, and single borylated benzene was obtained in a 100% yield when excess benzene was used as the substrate and solvent (Table 4.1, entry 1). Reducing the reaction time (from 6 h to 4 h) still provided a quantitative product (Table 4.1, entry 2). As the benzene concentration increased, the yield decreased marginally to 90% (Table 4.1, entry 3). When the $[Ir(cod)Cl]_2$ was replaced with $[Ir(cod)OMe]_2$, the yield decreased to 95% (Table 4.1, entry 4). A lower quantity (2.5 mol%) of bpy-POP-1 decreased the yield to 61% (Table 4.1, entry 5). There was no product formed in the catalytic borylation reaction when 1.5 mol% of bpy-POP-1 was used (Table 4.1, entry 6). $[Ir(cod)Cl]_2$ could not catalyze the reaction without the presence of bpy-POP-

1 (Table 4.1, entry 7). Changing benzene to toluene as the substrate and solvent under the same reaction conditions decreased the yield to 33%. However, prolonging the reaction time to 24 h increased the yield to 100% (Table 4.1, entries 8–9). When toluene was used as the substrate, the optimum reaction condition for direct C-H borylation of arenes utilizing the Ir-bpy-POP catalyst was $[Ir(cod)Cl]_2$ (0.5 mol%), bpy-POP-1 (5 mol%), arenes (0.1 M) and B_2pin_2 (0.1 mmol) at 60 °C for 24 h.

Table 4.1 Optimization of reaction conditions for borylation of arenes

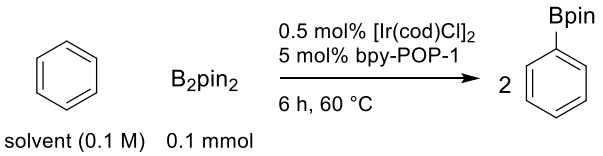

Entry[a]	Modification	Yield[b]
1	-	100%
2	4 h	100%
3	0.2 M	90%
4	$[Ir(cod)MeO]_2$	95%
5	2.5 mol%	61%
6	1.5 mol%	0%
7	no POP	0%
8[c]	toluene	33%
9[c]	toluene, 24 h	100%

[a] Iridium and POP are premixed for 10 min in the solvent before the addition of B_2pin_2.
[b] Yields are quantified by NMR using 1,3,5-trimethoxybenzene as standard.
[c] Regioselectivity = *para:meta:ortho* 1:2:0.

4.3 Substrate scope

Having optimized the conditions for the Ir-bpy-POP catalytic system, substrate scopes of the borylation reaction were investigated (Table 4.2). The use of toluene as the substrate provided products in quantitative yields with a steady distribution (*para*-: *meta*- = 1:2) (Table 4.2, entry 1). There was a steady distribution (2:1) between the *meta*- and *para*- substitution borylated toluene products and no *ortho*-substitution borylated toluene was produced when toluene was the substrate and solvent on a large scale (2.0 mmol, Scheme 4.2). When anisole was used as the substrate, the catalytic system produced an excellent yield (96%); however, the ratio of the two products changed to 1:3.6 (*para*-: *meta*-) and no *ortho*-product was produced (Table 4.2, entry 2). Three products (*para*-: *meta*-: *ortho*- =1:2.7:1.8) were produced and the yield was still high (92%) when fluorobenzene was evaluated in the catalytic reaction (Table 4.2, entry 3). Chlorobenzene afforded a high yield (98%) and the proportion of the *para*-product increased in comparison with that of toluene (Table 4.2, entry 4). Iodobenzene furnished a moderate yield (61%) and the ratio of the *para*- and *meta*-functionalized products became 1:1.4 (Table 4.2, entry 5). *m*-Xylene was a challenging substrate, with a yield of 9%, and produced only one product under the same conditions; however, the yield improved to 50% when the temperature increased to 100 °C (Table

4.2, entry 6). It is evident from entries 1–6, that the different substituent groups on arenes produced different ratios of products.

Table 4.2 Substrate scope

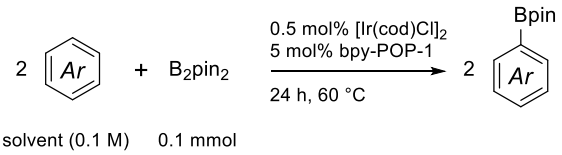

Entry[a]	Substrates	Products	Yield[b]	Product distribution *para:meta:ortho*
1	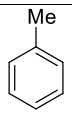	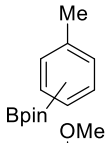	100%	1:2.0:0
2	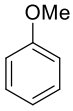	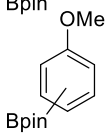	96%	1:3.6:0
3	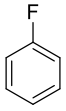	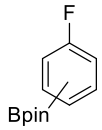	92%	1:2.7:1.8
4	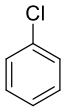	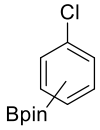	98%	1:2.2:0
5	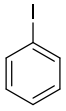	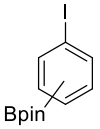	61%	1:1.4:0
6	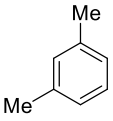	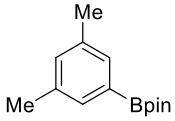	9% (50%)[c]	

[a] The $[Ir(cod)Cl]_2$ and POP are premixed for 10 min in the solvent before the addition of B_2pin_2.
[b] Yields are quantified by NMR using 1,3,5-trimethoxybenzene as standard.
[c] Reaction done at 100 °C with the yield shown in parentheses.

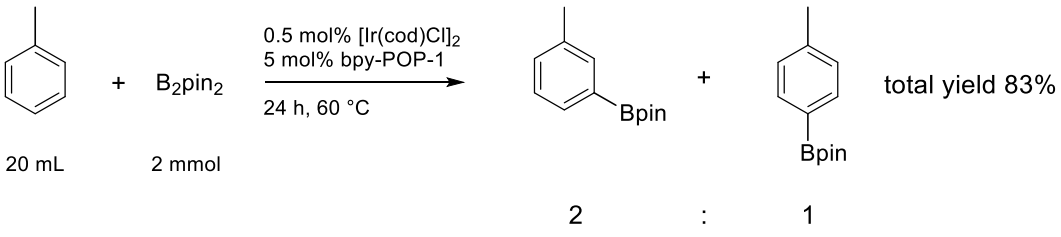

Scheme 4.2 Steady distribution of *meta*- and *para*- product on a large scale (2.0 mmol).

In this Ir-bpy-POP catalytic system, the boron source-B_2pin_2 was consumed and produced twice the quantity of product. This catalytic reaction meets the requirements for green chemistry. The following reaction was performed to detect whether the two remaining protons, which were replaced by Bpin groups, could form hydrogen gas. The headspace gas was collected and analyzed using GC-FID/MS, and it was verified that hydrogen gas was generated. The bpy-POP did not undergo any change after the catalytic reaction. The same result was obtained for the homogeneous catalysis reaction using 2,2′-bipyridine, and hydrogen was also present in the gas. This indicates that bpy-POP was not a hydrogen acceptor.

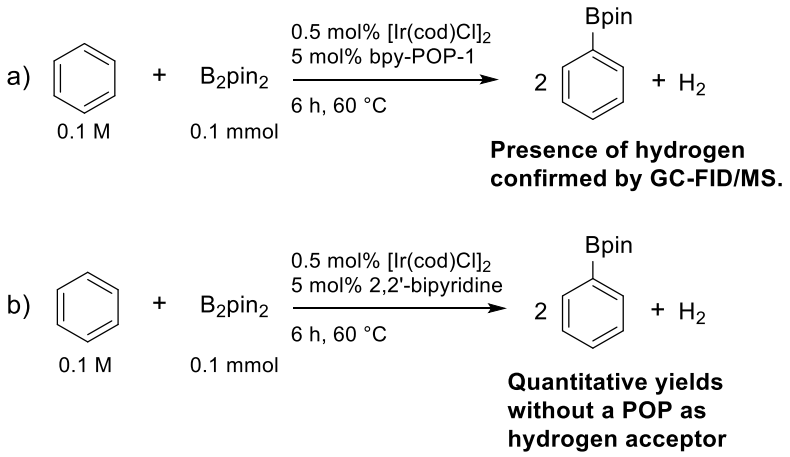

Scheme 4.3 GC-FID/MS to determine release of hydrogen using bpy-POP (a) and 2,2′-bipyridine (b)

4.4 Recycling

After the first run, the Ir-bpy-POP solids were easily recovered by extraction and washing with hexane in air. However, the second run reaction did not occur when these recovered solids were used. This indicated that the recovered catalyst might decompose in air.

When the Ir-bpy-POP were recovered in the glovebox, the second run reaction started by adding a new stock benzene solution of B_2pin_2 (0.1 M). After being sealed, the reaction could occur for the first recycle with a 100 % yield. Repeating the recycling procedure, the Ir-bpy-POP produced a 100 % yield for the second recycle. However, the yield decreased markedly to 2% after the third recycle, and the recovered solids could not produce any product after the fourth recycle. Although the recycling procedure was conducted in a glovebox, the heating time was performed outside the glovebox, and air might have caused the decomposition of the Ir-bpy-POP catalyst.

Table 4.3 Recycling experiments

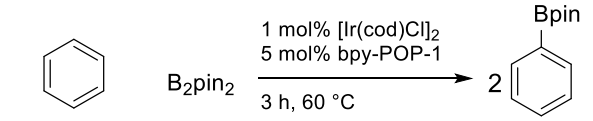

solvent (0.1 M) 0.1 mmol

Entry[a]	Recycles	Yield[b]
1	0	100%
2	1	100%
3	2	100%
4	3	2%
5	4	0%

[a] The $[Ir(cod)Cl]_2$ and POP are premixed for 10 min in the solvent before the addition of B_2pin_2.
[b] Yields are quantified by NMR using 1,3,5-trimethoxybenzene as standard.

4.5 Summary

In summary, an *in-situ* Ir-bpy-POP catalytic system was developed for direct C(sp^2)-H borylation of arenes. The optimized reaction conditions exhibited excellent activity and good tolerance in catalytic reactions. The combination of the Ir complex and bpy-POP is capable of borylating twice per molecule, in accordance with the "12 Principles of Green Chemistry", and hydrogen gas can be collected. The catalyst could be recovered simply and can be recycled three times without any obvious loss in yield.

4.6 Experimental

Chemicals

All commercially available chemicals were used as received.

Dibenzyl ether, 1,3,5-trimethoxybenzene, B_2pin_2, $[Ir(cod)Cl]_2$, $[Ir(cod)OMe]_2$, HBpin, anisole, fluorobenzene, chlorobenzene, iodobenzene, 1,3-dimethylbenzene, d_6-benzene were purchased from Sigma.

Benzene was obtained TCI.

Equipments

Anhydrous solvents were from Puresolv MD-7 (a solvent purification system). Micrometrics 3Flex instrument measured the BET and surface area and pore volume of POPs. ^{1}H-NMR spectra was measured on a Bruker Ascend 400 (400 MHz) spectrometer. The deuterated solvent was $CDCl_3$ (7.26 ppm). Silica gel 60 was used for column chromatography. MS was carried out on either GC-MS/FID analysis on an Agilent 7890A GC equipped with an HP-5 column and a 5975C VLMSD with triple-axis detector (EI) or Waters AQUITY UPLC system equipped with PDA and SQD2 electrospray (ESI) MS detector.

General borylation procedure in a small scale (0.1 mmol)

A stock solution of $[Ir(cod)Cl]_2$ or $[Ir(cod)OMe]_2$ was prepared in arene or heterocycle in the glovebox. bpy-POP-1 was weighed into a 4 mL vial and a tiny magnetic stir bar was added before mixing in 1 mL of the Ir-stock solution. The resulting mixture was premixed for 10 minutes before adding B_2pin_2 and sealing the vial was sealed with a PTFE-lined screw cap. The vial was placed outside the glovebox in an aluminum heating block at either 60 or 100 °C for the specified time. After the prescribed time, the reaction mixture was cooled to rt before an NMR internal standard of 1,3,5-trimethoxybenzene or dibenzyl ether in DCM was added. Following that, 1 mL hexane was added to the reaction, which was properly mixed before about 0.4 mL was filtered through a syringe filter and concentrated in a vacuum. Using $CDCl_3$ as a solvent, the resulting mixture was evaluated by NMR.

General borylation procedure in a big scale (2.0 mmol)

$[Ir(cod)Cl]_2$ (0.01 mmol, 6.69 mg) and bpy-POP-1 (0.1 mmol) were weighed off in a 50 mL round-bottomed flask. A stir bar was added and the flask was sealed with a rubber septum. The flask was connected to the Schlenk line and made inert by 3 vacuum/N_2 cycles. Toluene (15 mL) was added to the flask and the resulting mixture was premixed for 10 min before a solution of B_2pin_2 (508 mg, 2.0 mmol) in toluene (5 mL) was added to the mixture. The round-bottomed flask was put into

an oil bath and heated to 60 °C for 24 h. After allowing the mixture to cool to room temperature, 20 mL of hexane was added to the flask. The solid catalysts were collected in a glass funnel and washed with hexane and 20% EtOAc (200 mL). The solid catalysts were dried in a vacuum oven before being recycled. The mixed solution was concentrated, yielding clear oil of borylated toluene.

Recycling experiment

In the glovebox, a stock solution of $[Ir(cod)Cl]_2$ (1.2 mg, 0.0017 mmol) was prepared in benzene (3.5 mL). A 4 mL vial with bpy-POP-1 (0.005 mmol) and a magnetic stir bar was charged. The vial was filled with 1 mL of stock solution. The resultant liquid was premixed for 10 minutes before adding B_2pin_2 (25.4 mg, 0.1 mmol). A PTFE-lined screw cap was used to close the 4 mL vial. The vial was heated in an aluminum heating block at 60 °C for 3 hours before being cooled to room temperature. Excess benzene was removed from the mixture in the glovebox. Hexane was used to wash the solids and the organic phase was combined. A solution of B_2pin_2 in benzene (1 mL) was added to the remaining solids, and the vial was sealed. To repeat the operation, the vial was removed and placed on the heating block. 0.1 mmol of 1,3,5-trimethoxybenzene (16.8 mg) was added to the mixed organic phase, which was then condensed under reduced pressure and examined by NMR using $CDCl_3$.

4.7 References

[1] (a) Hartwig, J. F. *Acc. Chem. Res*. **2012**, *45*, 864−873. b) Liu, T., Shao, X., Wu, Y. and Shen, Q., *Angew. Chem., Int. Ed*. **2012**, *51*, 540−543. c) Liskey, C.W., Liao, X. and Hartwig, J.F., *J. Am. Chem. Soc.* **2010**, *132*, 11389−11391. d) Murphy, J.M., Liao, X. and Hartwig, J.F., *J. Am. Chem. Soc*. **2007**, *129*, 15434−15435. e) Partridge, B.M. and Hartwig, J.F., *Org. Lett*. **2013**, *15*, 140−143.

[2] Miyaura N. and Suzuki A., *Chem. Rev*. **1995**, *95*, 2457-2483.

[3] a) Sibi M.P., Tatamidani H. and Patil K., *Org. Lett*. **2005**, *7*, 2571-2573. b) Chen G., Tokunaga N. and Hayashi T., *Org. Lett*. **2005**, *7*, 2881-2884. c) Schlüter A.D., *J. Polym. Sci. A* **2001**, *39*, 1533-1556.

[4] Chan D.M.T., Monaco K.L., Li R., Bonne D., Clarke C.G. and Lam P.Y.S., *Tetrahedron Lett*. **2003**, *44*, 3863-3865.

[5] Chen H. and Hartwig J.F., *Angew. Chem. Int. Ed*. **1999**, *38*, 3391-3393.

[6] Chen H., Schlecht S., Semple T.C. and Hartwig J.F., *Science* **2000**, *287*, 1995-1997.

[7] Dai H. and Yu J., *J. Am. Chem.Soc*. **2012**, *134*, 134−137.

[8] a) Ishiyama, T., Takagi, J., Ishida, K., Miyaura, N., Anastasi, N.R. and Hartwig, J. F. *J. Am. Chem. Soc*. **2002**, *124*, 390-391. b) Ishiyama, T., Takagi, J., Hartwig, J.F. and Miyaura, N., *Angew. Chem., Int. Ed.* **2002**, *41*, 3056-3058. c) Harrison, P., Morris, J., Marder, T.B. and Steel, P.G., *Org. Lett*. ***2009***, *11*, 3586–3589. d) Iwadate, N. and Suginome M., *J. Organomet. Chem.* ***2009***, *694*, 1713–1717. e) Jo, T.S., Kim, S.H., Shin, J. and Bae, C. *J. Am. Chem. Soc*. ***2009***, *131*, 1656–1657. f) Finke, A.D. and Moore, J.S., *Org. Lett*. ***2008***, *10*, 4851–4854. g) Boebel, T.A. and Hartwig, J.F., *J. Am. Chem. Soc*. ***2008***, *130*, 7534–7535. h) Shin, J., Jensen, S.M., Ju, J., Lee, S., Xue, Z., Noh, S.K. and Bae, C. *Macromolecules* ***2007***, *40*, 8600–8608. i) Paul, S., Chotana, G.A., Holmes, D., Reichle, R.C., Maleczka, R.E., Jr. and Smith, M.R., III *J. Am. Chem. Soc*. ***2006***, *128*, 15552–15553. j) Iverson, C.N. and Smith, M.R., III. *J. Am. Chem. Soc*. **1999**, *121*, 7696−7697.

[9] a) Obligacion J., Semproni S., Pappas I. and Chirik P., *J. Am. Chem. Soc.* **2016**, *138*, 10645−10653. b) Obligacion J., Semproni S. and Chirik P., *J. Am. Chem. Soc.* **2014**, *136*, 4133−4136.

[10] Yu H., Islam S. and Mankad N., *ACS Catal*. **2020**, *10*, 3670−3675.

[11] Das A., Hota P. and Mandal S., *Organometallics* **2019**, *38*, 3286-3293.

[12] Dombray T., Werncke C., Jiang S., Grellier M., Vendier L., Bontemps S., Sortais J., Sabo S. and Darcel C., *J. Am. Chem. Soc*., ***2015***, *137*, 4062–4065.

[13] a) Ishiyama T., Isoua H., Kikuchia T. and Miyaura N. *Chem. Commun*., **2010**, *46*, 159-161. b) Chattopadhyay B., Dannatt J. E., Sanctis I. L., Gore K. A., Maleczka R., Singleton D. and Smith M., *J. Am. Chem. Soc*. ***2017***, *139*, 7864−7871. c) Roosen P., Maleczka R., Singleton D. and Smith M., *J. Am. Chem. Soc*. ***2012***, *134*, 11350−11353. d) Li H., Kanai M. and Kuninobu Y., *Org. Lett*. ***2017***, *19*, 5944−5947. e) Li H., Kanai M. and Kuninobu Y., *Angew. Chem*. ***2017***, *129*, 1517 –1521. f) Yang L., Uemura N. and Nakao Y., *J. Am. Chem. Soc*. ***2019***, *141*, 7972−7979. g) Kuninobu Y., Ida H., Nishi M. and Kanai M., *Nature Chemistry* ***2015***, *7*, 712-717. h) Davis H., Mihai M. and Phipps R., *J. Am. Chem. Soc*. **2016**, *138*, 12759−12762. i) Davis H., Genov G. and Phipps R., *Angew. Chem. Int. Ed*. **2017**, *56*, 13351 –13355. j) Bastidas J., Oleskey T., Miller S., Smith M. and Maleczka R., *J. Am. Chem. Soc*. **2019**, *141*, 15483−15487. k) Saito Y., Segawa Y. and Itami K., *J. Am. Chem. Soc*. ***2015***, *137*, 5193−5198. l) Haines, B., Saito, Y.,

Segawa, Y., Itami, K. and Musaev, D.G., *ACS Catal*. **2016**, *6*, 7536-7546. m) Yang, L., Semba, K., Nakao, Y., *Angew. Chem., Int. Ed*. **2017**, *56*, 4853-4857. n) Hoque M.E., Bisht R., Haldar C., and Chattopadhyay B., *J. Am. Chem. Soc*. ***2017***, *139*, 7745−7748.

[14] a) Gong, J., Yue, H., Zhao, Y., Zhao, S., Zhao, L., Lv, J., Wang, S. and Ma, X., *J. Am. Chem. Soc*., **2012**, *134*, 13922–13925. b) Yue, H., Zhao, Y., Zhao, S., Wang, B., Ma, X. and Gong, J., *Nat. Commun*., **2013**, *4*, 2339–2345. c) Zhang, C., Zhu, W., Li, S., Wu, G., Ma, X., Wang, X. and Gong, J., *Chem. Commun*., **2013**, *49*, 9383–9385.

[15] a) Coperet, C., Estes, D.P., Larmier, K. and Searles, K., *Chem. Rev*., **2016**, *116*, 8463–8505. b) Comito, R.J., Fritzsching, K.J., Sundell, B.J., Schmidt-Rohr, K. and Dincă, M., *J. Am. Chem. Soc*., **2016**, *138*, 10232–10237. c) Pelletier, J.D. and Basset, J.M., *Acc. Chem. Res*., **2016**, *49*, 664–677. d) Burgess, S.A., Kassie, A., Baranowski, S.A., Fritzsching, K.J., Schmidt-Rohr, K., Brown, C.M. and Wade, C.R., *J. Am. Chem. Soc*., **2016**, *138*, 1780–1783. e) Conley, M.P., Coperet, C. and Thieuleux, C., *ACS Catal*., **2014**, *4*, 1458–1469. f) Li, B., Li, F., Bai, S., Wang, Z., Sun, L., Yang, Q. and Li, C., *Energy Environ. Sci*., **2012**, *5*, 8229–8233. g) Wu, F., Feng, Y. and Jones, C.W., *ACS Catal*., **2014**, *4*, 1365–1375. h) Copéret, C. and Basset, J.M., *Adv. Synth. Catal*., **2007**, *349*, 78–92.

[16] a) Yinghuai, Z., Yan, K.C., Jizhong, L., Hwei, C.S., Hon, Y.C., Emi, A., Zhenshun, S., Winata, M., Hosmane, N.S. and Maguire, J.A., *J. Organomet. Chem*. ***2007***, *692*, 4244−4250. b) Yinghuai, Z., Chenyan, K., Peng, A.T., Emi, A., Monalisa, W., Kui-Jin Louis, L., Hosmane, N.S. and Maguire, J.A., *Inorg. Chem*. ***2008***, *47*, 5756−5761.

[17] a) Kawamorita, S., Ohmiya, H., Hara, K., Fukuoka, A. and Sawamura, M. *J. Am. Chem. Soc*. **2009**, *131*, 5058−5059. b) Yamazaki K., Kawamorita S., Ohmiya H. and Sawamura, M. *Org. Lett*. **2010**, *13*, 3978−3981. c) Wu F., Feng Y. and Jones C. W., *ACS Catalysis*, **2014**, *4*, 1365-1375. d) Waki M., Fukuoka A. and Inagaki S., *J. Am. Chem. Soc*. **2014**, *136*, 4003−4011. e) Maegawa Y. and Inagaki S., Dalton Trans., **2015**, *44*, 13007−13016. f) Gruning W., Siddiqi G., Safonova O. and Coperet C., *Adv. Synth. Catal*. **2014**, *356*, 673 – 679.

[18] Zhang S., Wang H., Li M., Liu X. and Gong J., *Chem. Sci*., **2017**, *8*, 4489–4496.

[19] a) Manna K., Zhang T. and Lin W., *J. Am. Chem. Soc*. **2014**, *136*, 6566−6569. b) Manna K., Zhang T., Greene F. and Lin W., *J. Am. Chem. Soc*. **2015**, *137*, 2665−2673.

[20] Vardhan H., Pan Y. and Ma S., *APL Materials* **2019**, *7*, 101111.

[21] Mamlouk H., Suriboot J., Manyam P., AlYazidi A., Bergbreiter D. and Madrahimov S., *Catal. Sci. Technol*., **2018**, *8*, 124–127.

5. Nickel-catalyzed asymmetric α-arylation of ketones by POP

5.1 Introduction

C-H functionalization is a reaction that directly converts the C-H bond into a C-R bond (R is C, O, N, etc., excluding H). Over the past few decades, direct C-H functionalization has become a topical research topic and an "external theme" in the field of organic chemistry. [1] In this respect, the asymmetric α-arylation of carbonyl derivatives has also received increasing attention. This is because a new $C(sp^3)$–$C(sp^2)$ bond can be constructed, which is an important structural feature of bioactive natural products, drug intermediates, and functionalized substrates. [2] The wide range of natural products and drugs, which have this scaffold, shows that this catalytic asymmetric strategy remains in high demand (Figure 5.1). For example, the antidepressant (*S*)-nafenodone (**1**) [3] and the natural product (+) pauciflorol F (**2**). [4] Some anti-inflammatory and immunosuppressive agents can be further synthesized from α-aryl carbonyl molecules, such as acetylcholinesterase inhibitors (+)-corynoline (**3**), [5] (+)-DeN-corynoline (**4**), [6] and corynoloxine (**5**). [7] Oxindole derivative (**6**) [8] can be used as antiproliferative agent for the treatment of cancer.

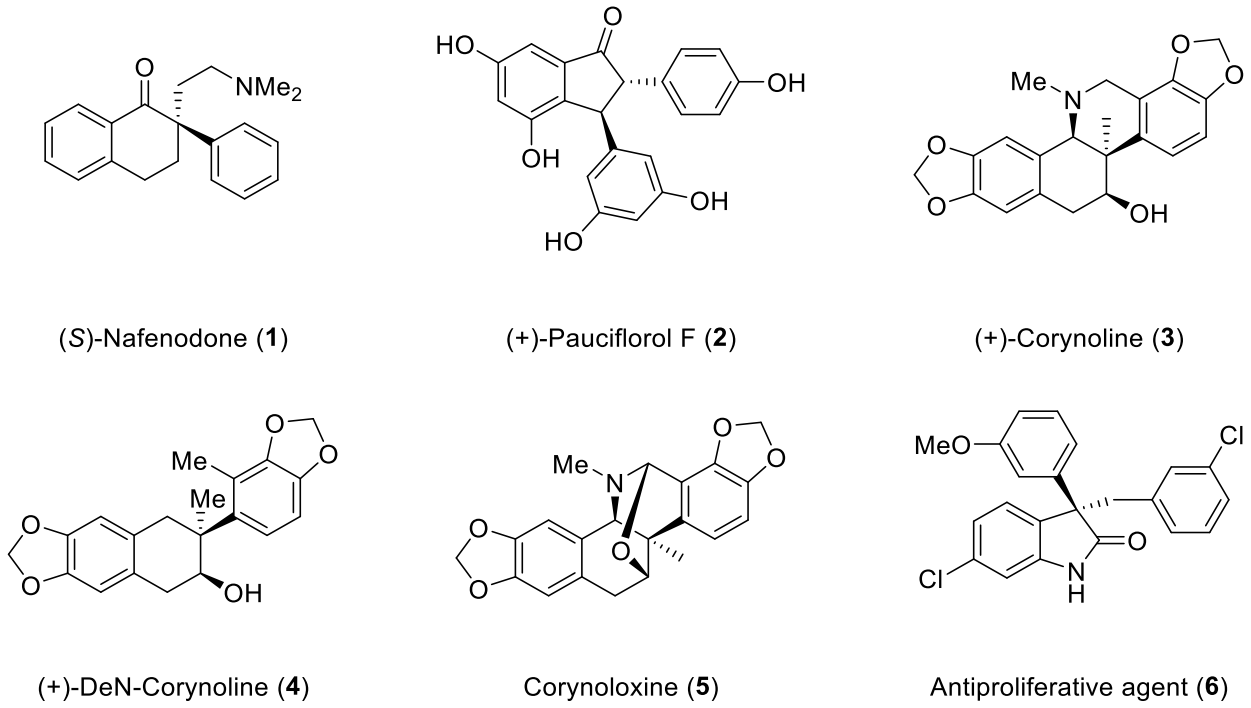

Figure 5.1 Cyclic natural products and bioactive molecules containing an α-aryl carbonyl moiety.

In 1997, Buchwald and co-workers used cyclohexanone and bromoarene to accomplish the first example of intermolecular catalytic α-arylation. [9] The catalytic system, which was composed with chiral ligand Tol-BINAP and $Pd_2(dba)_3$ produced the α-aryl compound with a yield of 83% (Scheme 5.1a). Buchwald proposed that the key step in the catalytic system was the generation of an active enol-Pd(II)-aryl complex. Subsequently, this theory was demonstrated using other enol substrates. [10]

In 1998, Buchwald and co-workers replaced Tol-BINAP with (*S*)-BINAP using $Pd_2(dba)_3$ or $Pd(OAc)_2$ to realize the asymmetric α-arylation of aryl bromides with ketones. (Scheme 5.1b). [11] Ketones were the first time as substrates in the asymmetric α-arylation with good ee value (61-98%). However, this catalytic system requires a high catalyst loading (up to 20 mol%) and has a narrow substrate scope (nine examples). Later, Buchwald continued to develop a similar catalytic system and discovered that a combination of $Pd_2(dba)_3$ (1 mol%) with chiral monophosphine ligand (2.5 mol%), realizing efficient enantioselective α-arylation of ketones. [12] This catalytic system needs to synthesize the bulky chiral ligand and has a narrower scope (six examples). In 2006, Chan group discovered an asymmetric α-arylation of ketone enolates catalyzed by $Ni(cod)_2$ with an atropisomeric dipyridydiphosphine (P-Phos). [13] This catalytic system established better control of the α-methyl-1-tetralone substrates but had poor control of the α-methyl-1-indanone and α-methyl benzocyloheptanone substrates.

In 2008, Hartwig et al. reported the first asymmetric α-arylation using aryl triflates, catalyzed by the difluorophore complexes of $Pd_2(dba)_3$ and $Ni(cod)_2$ (Scheme 5.1c). [14] However, under the standard catalytic conditions, α-methyl-1-indanone had a low ee value (78%). Later in 2011, Hartwig and co-workers developed a simple catalytic system that used a low catalyst loading and that had a large substrate scope, including heterocyclic ketones and heteroaryl chlorides. [15] The combination of $Ni(cod)_2$ and (*R*)-BINAP showed high yields and enantioselectivities in α-arylation of indanone and tetralone.

Glorius et al. merged $Pd(dba)_2$ with chiral quinine to accomplish the asymmetric α-arylation of indanones or tetralones with aryl halides (Scheme 5.1d). [16] In this catalytic system, chiral quinine was the unmodified *Cinchona* alkaloids and it was the first example of asymmetric cross-coupling with transition metal complex. The palladium-*Cinchona* alkaloid catalytic system exhibited the same level of selectivity and yield, or even better than those of the Pd-BINAP catalyst with specific substrates.

In 2015, Martin accomplished the asymmetric α-arylation of ketones through C-O cleavage of aryl esters (Scheme 5.1e). [17] The chiral α-arylation products was obtained with a high yield (up to 91%) and high ee values (up to 98%) by the catalytic system, which was composed with NaO^tBu, $Ni(cod)_2$, and (*S*)-Tol-BINAP. C-O cleavage was a good choice in the formation of C-C bond.

Three years later, Tang and co-workers reported the asymmetric α-arylation of sterically hindered substrates using $Pd(OAc)_2$ and bulky chiral phosphorus ligand (*R*)-BI-DIME as the catalyst (Scheme 5.1f). [18] This catalytic system is highly efficient for synthesizing α-arylation products and has a broad substrate scope. In addition, several bioactive chiral natural drugs have been synthesized using this system, such as (-)-DeN-corynoline, (-)-corynoline, and the antidepressant (*S*)-nafenodone.

The homogeneous asymmetric α-arylation of ketones has a big potential for the efficient and straightforward preparation of active natural products and drugs, and significant progresses have been achieved in this regard in organic synthesis.

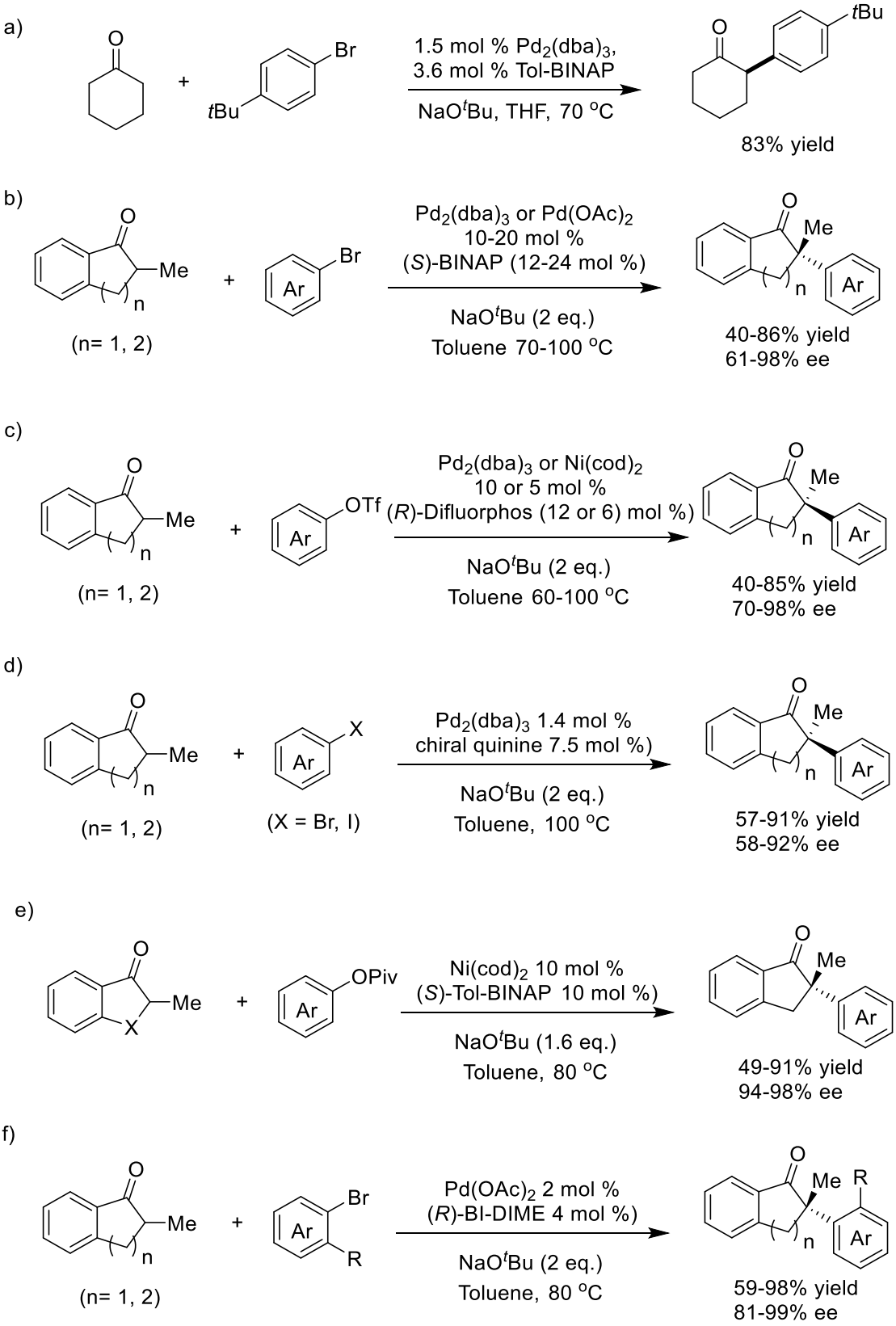

Scheme 5.1 Previous works on asymmetric α-arylation of ketones in homogeneous catalysis

Homogeneous asymmetric α-arylation of ketones is limited to achieving green transformation to the point at which it accomplishes the challenge of the "12 Principles of Green Chemistry" despite the remarkable progress, because of the use of expensive chiral ligands (single use) and heavy metals. [19]

Compared with homogeneous catalysis, heterogeneous catalysts (nanoparticles, POPs, MOFs, and COFs) have significant advantages, such as recyclability, sustainability, and robustness. [20] Therefore, utilizing a heterogeneous catalyst for asymmetric α-arylation of ketones could be widely explored in the future.

In 2010, Glorius et al. developed a chiral heterogeneous Pd catalyst from Fe_3O_4/Pd nanoparticles and enantiomerically pure NHCs for the asymmetric α-arylation of ketones (Scheme 5.2). [21] The nanoparticles (NPs) Pd catalyst could be removed easily and could be recycled five runs without significant loss of selectivity and activity. However, there is space for improvement in the moderate yield (56–91%) and ee value (33–85%).

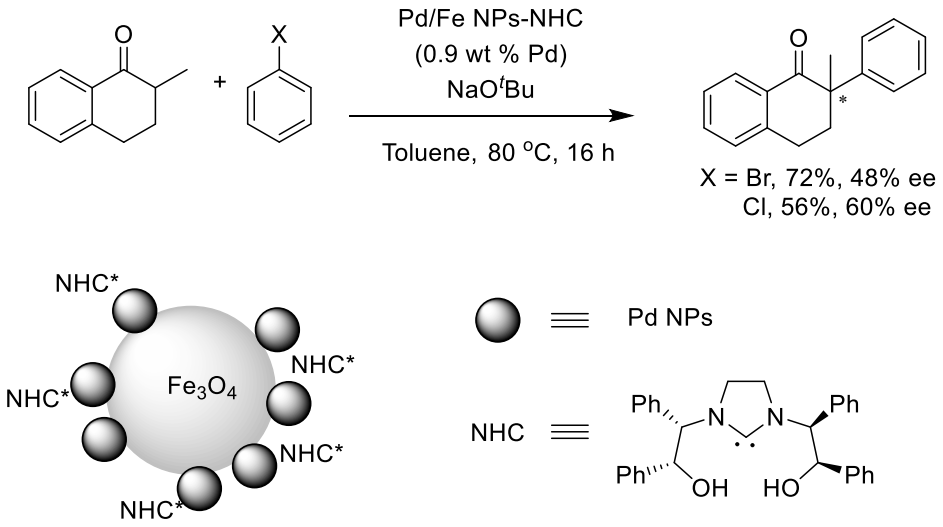

Scheme 5.2 Previous work on asymmetric α-arylation of ketones in heterogeneous catalysis

Although there are many cases of the asymmetric α-arylation of ketones in homogeneous catalysis, few cases of asymmetric α-arylation of ketones by heterogeneous catalysts have been investigated. To our knowledge, the successful examples of POP for the asymmetric α-arylation of ketones have not yet been reported.

According to a literature research and previous work in our lab, [22] we chose Ni (0)-BINAP as the standard catalytic system and introduced a vinyl group on BINAP to synthesize BINAP-POP for asymmetric α-arylation of cyclic ketones.

5.2 Optimization of the reaction conditions

Initially, POP-5 and POP-6 were evaluated for the asymmetric α-arylation of cyclic ketones (Table 5.1). POP-5 exhibited the better conversion, yield and ee value than POP-6. Compared with homogeneous catalysis, this is not in the same level with yield; however, the ee value (98.9%) is better. POP-5 was chosen for the remainder of the optimization step.

Table 5.1 Catalytic performances of POP-5 and POP-6 in asymmetric α-arylation of cyclic ketones.

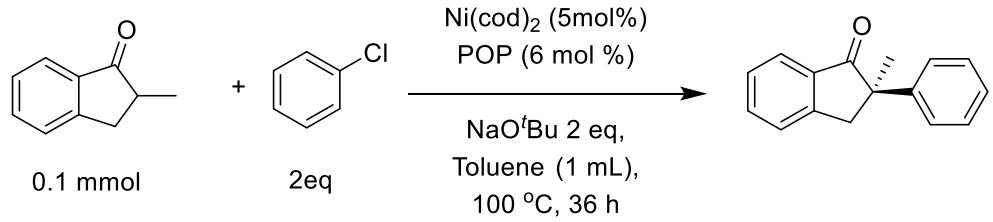

Entry	POP	Conv.[a]	Yield[a]	ee[b]
1	POP-5	54%	39%	98.9%
2	POP-6	50%	23%	97.7%

[a] Conversion and yield quantified by ^{1}H-NMR using 1,3,5-trimethoxybenzene as standard.
[b] Enantiomeric excess determined by chiral-HPLC.

Thereafter, the effects of the base were evaluated (Table 5.2). Considering the alkaline strength of the catalytic system, three types of strong organic bases were used in the catalytic reactions. NaO^{t}Bu exhibited the best results.

Table 5.2 Effects of base

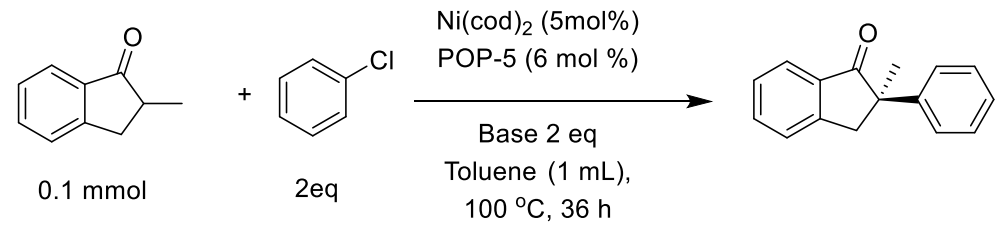

Entry	Base	Conv.[a]	Yield[a]	ee[b]
1	NaO^{t}Bu	54%	39%	98.9%
2	KO^{t}Bu	12%	1%	-
3	LiO^{t}Bu	0	0	-

[a] Conversion and yield quantified by ^{1}H-NMR using 1,3,5-trimethoxybenzene as standard.
[b] Enantiomeric excess determined by chiral-HPLC.

The temperature and POP-5 loading were evaluated simultaneously (Table 5.3). High temperature decreased the ee value (entries 1–5), and higher POP-5 loading increased the yield (entries 1, 6, and 7).

Table 5.3 Effects of temperature and POP-5 loading

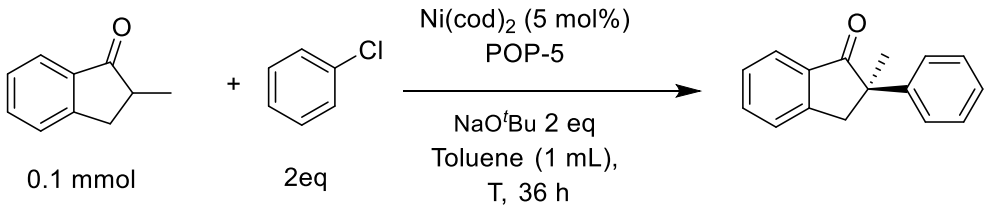

Entry	Temperature(°C)	POP-1 loading (%)	Yield(%)[a]	ee(%)[b]
1	60	6	25.3	>99
2	80	6	34.3	99
3	100	6	39	98.9
4	110	6	8	97
5	120	6	1	-
6	60	8	31	>99
7	60	10	44.6	>99

[a] Yield quantified by ^{1}H-NMR using 1,3,5-trimethoxybenzene as standard.

[b] Enantiomeric excess determined by chiral-HPLC.

The concentrations and reaction times were evaluated simultaneously (Table 5.4). With increasing substrate concentration, the yields improved (entries 1–4, 9, and 10). When the reaction time was increased from 12 h to 36 h, yields improved linearly (entries 8–9, 10–12).

Toluene was the best solvent in which POP-5 exhibited good swelling.

The optimum reaction condition for the asymmetric α-arylation of cyclic ketones were, 0.3 mmol cyclic ketone, 0.6 mmol chlorobenzene, 5 mmol% $Ni(cod)_2$, 10 mmol% POP-5, 0.6 mmol NaO^tBu, and 1 mL toluene at 60 °C for 36 h.

Table 5.4 Effects of concentration and reaction time

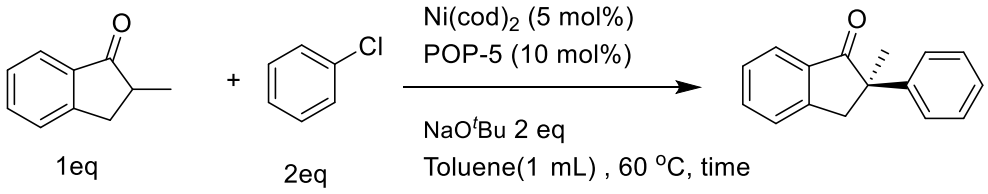

Entry	Ketone (mmol)	Time (h)	Yield(%)[a]	ee(%)[b]
1	0.1	36	44.6	>99
2	0.15	36	45	>99
3	0.2	36	65	>99
4[c]	0.2	36	29	>99
5[d]	0.2	36	50	>99
6[e]	0.2	36	49	>99
7[f]	0.2	36	23	96.2
8	0.25	24	62	>99
9	0.25	36	94	>99
10	**0.3**	**36**	**95**	**>99**
11	0.3	12	59	>99
12	0.3	24	79	>99

[a] Yield quantified by ^{1}H-NMR using 1,3,5-trimethoxybenzene as standard.

[b] Enantiomeric excess determined by chiral-HPLC.

[c] Toluene (2 mL).

[d] 1.5 eq chlorobenzene.

[e] 3 eq chlorobenzene.

[f] Bromobenzene.

5.3 Substrate scope

Using the optimum reaction conditions, the scope and generality of the asymmetric α-arylation of ketones were investigated. As shown in Table 5.5, 2-methyl-1-indanone reacted with chlorobenzene, and furnished the corresponding coupled product in 95% yield with 99% ee (entry 1), whereas bromobenzene and iodobenzene afforded the same product with slightly reduced yields and lower ee values (entries 2–3). A range of electron-deficient, electron-neutral, and electron-rich *meta*-and *para*-substituted chloroarenes produced very good yields (92%-99%) and high enantiomeric excess from (93%-99%) (entries 4-13). These *meta*-and *para*-substituted corresponding product yields were better than those obtained in previous homogeneous catalysis reactions, and their enantioselectivities were the same or better than those reported previously. [13-17] The catalytic system was applicable when chloroheteroarenes such as pyridine, naphthalene, biphenyl, and thiophene were evaluated, providing moderate to high yields (55–96%) and excellent enantioselectivities (92–98%) (entries 14, 16, 18, 20 and 21). Compared with chloroheteroarenes, bromoheteroarenes could offer similar yields; however, the enantiomeric excess values fell in the range from marginal to severe (entries 15, 17, 19). Especially for the bulky

substrate, the ee value of 2-chloronaphthalene was twice that of 2-bromonaphthalene (92% vs. 46%).

Table 5.5 Scope of aryl halides

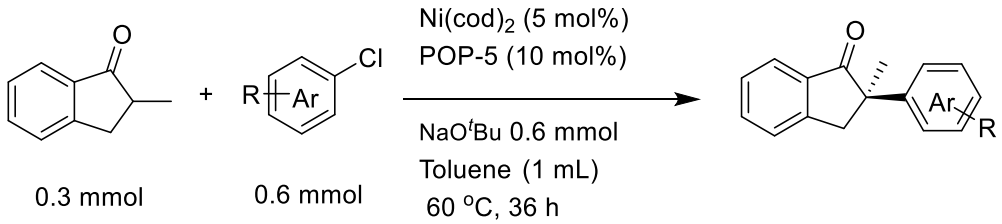

0.3 mmol 0.6 mmol

Entry	Aryl halides	Yield [%][a]	ee [%][b]
1	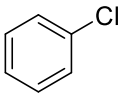	95	99
2	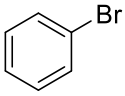	82	93
3	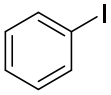	75	63
4	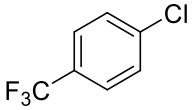	99	99
5	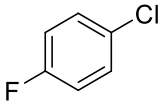	97	99
6	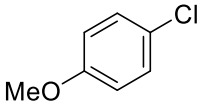	96	96
7	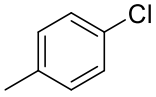	97	99
8	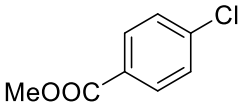	93	99
9	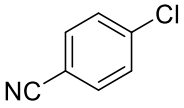	92	97

Table 5.5 (Continued)

Entry	Aryl halides	Yield [%][a]	ee [%][b]
10	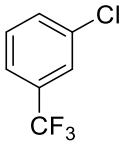	95	99
11	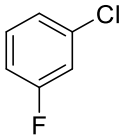	99	99
12	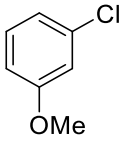	99	99
13	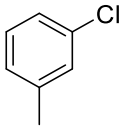	94	99
14	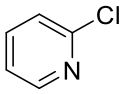	55	93
15	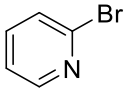	59	89
16	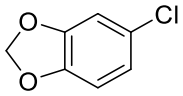	85	98
17	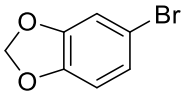	63	63
18	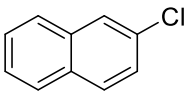	73	92
19	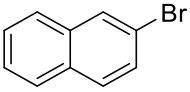	57	46
20	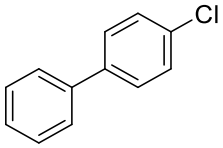	96	97
21	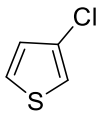	69	99

[a] Yield quantified by ^{1}H-NMR using an internal standard.

[b] ee value determined by chiral-HPLC.

Other ketone counterparts were investigated to determine the robustness of the Ni-POP-5 catalytic enantioselective system (Table 5.6). For indanones, when the number of substitution groups of the cyclic ketone increased, the yields decreased from 95% for the methyl group to 52% for the ethyl group, and to 60% for the benzyl group. However, the enantioselectivities of the corresponding products increased from 99% to 99.9% (entries 1–3). Using 2-methyl-tetralone (six-membered ring) to replace 2-methyl-1-indanone (five-membered ring) significantly hampered the reaction activity (from 95% to 65%) and enantioselectivity (from 99% to 82%) (entry 4). Particularly noteworthy was the observation that the enantiomeric excess improved more than 15% when the benzyl group was substituted on the ketone ring of tetralone (entry 5).

Table 5.6 Scope of ketone counterparts

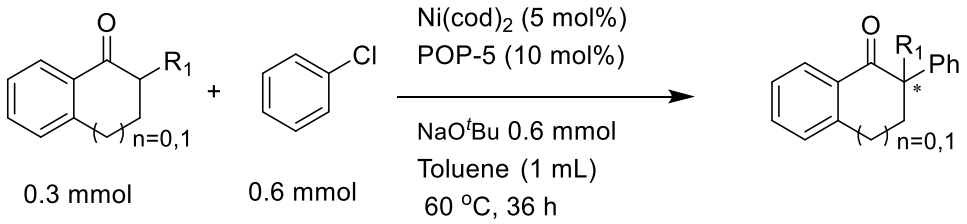

0.3 mmol 0.6 mmol

Entry	ketones	Yield [%][a]	ee [%][b]
1	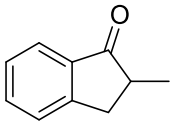	95	99%
2	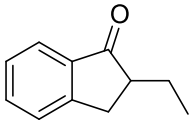	52	99%
3	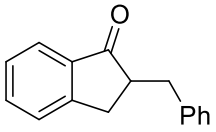	60	99%
4	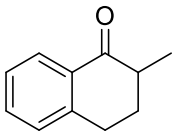	65	82%
5	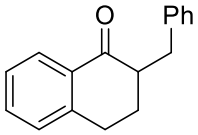	17	98%

[a] Yield quantified by ^{1}H-NMR using an internal standard.

[b] ee value determined by chiral-HPLC.

5.4 Recycling

The recyclability of POP is an excellent property. Owing to the insolubility of the polymer, BINAP-POP was washed thrice with water (to remove excess NaO^{t}Bu) and ether (for other substrates and products on the surface of POP) after the reaction to check its recyclability. BINAP-POP may be used after drying for the same reaction, however, the second run did not work without adding new Ni(cod)$_2$ (Table 5.7, entries 1–2), and it was clear that the combination of Ni-BINAP-POP decomposed during the washing time. Ni(cod)$_2$ is sensitive to air; therefore, the catalytic system could be recycled by adding new Ni(cod)$_2$ to recover POP. Interestingly, reusing POP did not diminish its enantioselectivity (Table 5.7, entries 3–6). Unfortunately, the yield was reduced by 50% after the second run (Table 5.7, entry 4). The third and fourth runs had small decreases in yield, 9% and 20%, respectively (Table 5.7, entries 5–6). This result clearly demonstrated the recyclability of POP without any loss in enantioselectivity. Although the yield decreased after four reaction runs, the easy separation and high enantioselectivity show the potential of BINAP-POP for organic and industrial applications in the future.

Table 5.7 Recycling experiments

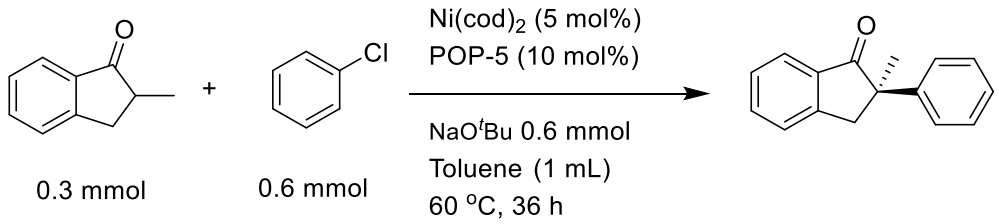

Entry	Run times	Modifications	Yield [%][a]	ee [%][b]
1	1	-	95	99
2	2	-	-	-
3	1	-	95	99
4	2	new Ni(cod)$_2$	52	99
5	3	new Ni(cod)$_2$	41	99
6	4	new Ni(cod)$_2$	21	99

[a] Yield quantified by ^{1}H-NMR using an internal standard.

[b] ee value determined by chiral-HPLC.

5.5 Gram-scale synthesis

In order to evaluate the potential for the Ni-BINAP-POP catalytic system, a gram-scale reaction was performed using 2-methyl-1-indanone and 4-chlorobenzotrifluoride to afford the corresponding product with an isolated yield of 97% and 99% ee (Scheme 5.3). This appealing result indicated the high efficiency and excellent enantioselectivity of this Ni-BINAP-POP catalytic system in a big scale, as well as this procedure could be a practical and efficient method to produce chiral products in the future.

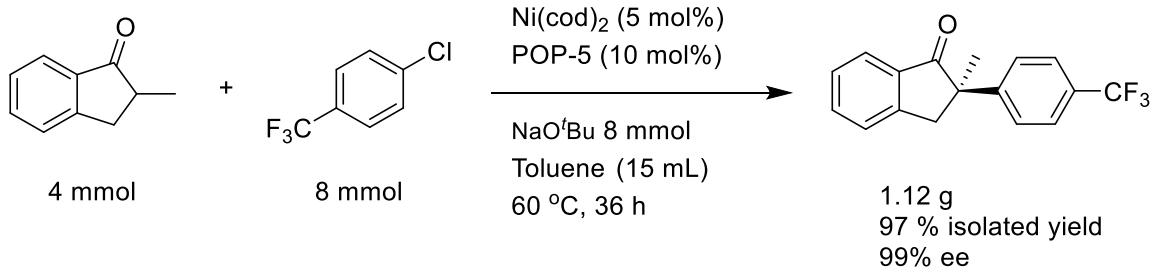

Scheme 5.3 Gram-scale synthesis

5.6 Summary

In this study, the first chiral BINAP-POP was investigated for asymmetric α-arylation of ketones with chloroarenes. The combination of Ni-BINAP-POP displayed excellent activity and high enantioselectivity. Notably, yields of most of the *meta*- and *para*-substituted chloroarenes were higher than that obtained from the homogenous catalysis, and the enantioselectivity was the same as that of homogeneous catalysis. Chloroheteroarenes exhibited moderate to good reactivity and high ee values. However, bromoarenes produced lower yields and enantioselectivities than chloroarenes. This catalytic system is also applicable to other cyclic ketones. The larger the substitution groups of the cyclic ketones, the lower the yields. Nevertheless, the enantioselectivity was still excellent. POP is easy to recover and can be reused three recycles without any noticeable loss in enantioselectivity. The gram-scale reaction demonstrated the high efficiency and promising application of this Ni-BINAP-POP catalytic system. Furthermore, with excellent enantioselectivity and good recyclability, chiral BINAP-POP will have a big potential in industrial production and pharmaceutical chemistry.

5.7 Characterization of chiral (*R*)-BINAP-POP-5

5.7.1 Thermal Gravimetric Analysis (TGA)

The melting and boiling points of Arabic acacia gum are 100 °C and 250 °C, respectively. There is no weight loss of POP-5 from 0 °C to 100 °C, which implies that POP-5 is stable at temperatures below 100 °C. A 10% weight loss was recorded by TGA accompanied by an endothermic DTA peak in a temperature range of 100-250 °C. The weight loss represents the transition of acacia gum from the molten state to the gaseous state. This is followed by an 80% weight loss of POP-5 in the

temperature range of 300-400 °C, which is the gasification process of acacia gum. The weight decrease from 20% to 10% at 400 °C indicates the decomposition of the organic block polymer with an exothermic DTA peak. In this project, the optimum temperature was 60 °C; thus, POP-5 was stable during the catalytic reactions. There was no loss of weight of POP-5 after the recycling reactions.

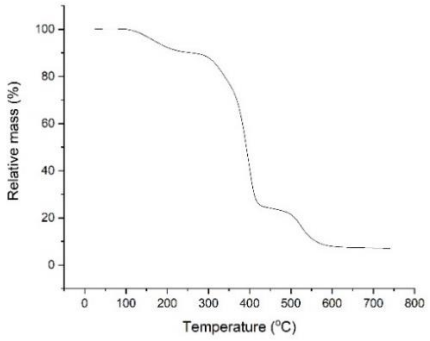

Figure 5.2 TGA of **POP-5**

5.7.2 Scanning Electron Microscopy (SEM)

The following SEM image showed that the diameter of POP-5 was greater than 200 μm, and the surface of POP-5 was irregular. Some tiny holes are embedded in the structure from the surface to the interior. This special structure allows it to combine with metal ions, and the substrate passes through its structure.

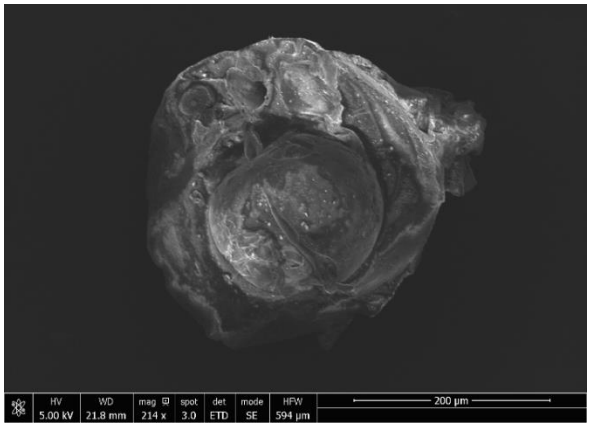

Figure 5.3 SEM image of **POP-5**

5.7.3 N_2-physisorption

POP-5 exhibited a lower surface area and pore volume (53.8268 m^2/g and 0.071535 cm^3/g, respectively) than **POP-6** (102.3192 m^2/g and 0.187223 cm^3/g, respectively) because acacia gum occupied the material space. Compared with the co-monomers divinylbenzene and styrene, which are rigid bulky blocks, acacia gum has longer carbon chains with a long linear structure.

5.8 Experimental

Chemicals

All commercially available chemicals were used as received.

Bis(1,5-cyclooctadiene)nickel(0), sodium *tert*-butoxide, lithium *tert*-butoxide, potassium *tert*-butoxide, 1,3,5-trimethoxybenzene, 2-methyl-1-indanone, 2-ethyl-1-indanone, chlorobenzene, 4-chlorobenzotrifluoride, 1-chloro-4-fluorobenzene, 1-chloro-3-fluorobenzene, methyl 4-chlorobenzoate, 1-chloro-4-methoxybenzene, 1-chloro-3-methoxybenzene, bromobenzene, iodobenzene, 4-chlorotoluene, 3-chlorotoluene, and 4-chloro-1,1′-biphenyl were obtained from Sigma Aldrich.

5-chloro-1,3-benzodioxole, 3-chlorothiophene, 2-chloronaphthalene, 3-chlorobenzotrifluoride, were acquired from Combi-Blocks.

Equipments

Anhydrous solvents were from Puresolv MD-7 (a solvent purification system). Quanta 200 ESEM FEG microscope (FEI) was used for SEM images. Micrometrics 3Flex instrument measured the BET and surface area and pore volume of POPs. Mettler Toledo TGA/DSC 1 STARe System tests the TGA of POPs. ^{1}H-NMR, ^{13}C-NMR, and ^{31}P-NMR spectra were measured on a Bruker Ascend 400 (400 MHz) spectrometer. The deuterated solvents were $CDCl_3$ and d_8-Toluene. Silica gel 60 was used for column chromatography. MS was carried out on either GC-MS/FID analysis on an Agilent 7890A GC equipped with an HP-5 column and a 5975C VLMSD with triple-axis detector (EI) or Waters AQUITY UPLC system equipped with PDA and SQD2 electrospray (ESI) MS detector. The enantiomeric excess was measured by a chiral HPLC with stationary phases.

Substrates synthesis

The following two substrates were prepared by the previously published method. [24]

2-benzyl-2,3-dihydro-1*H*-inden-1-one

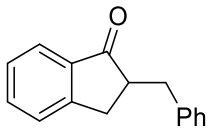

A 20-mL screw-capped vial was charged with LiO^tBu (6 mmol, 480 mg), 1-Indanone (3 mmol, 396 mg), and a magnetic stirring bar, and the vial was sealed with a cap containing a PTFE septum. The vial was made inert by 3 vacuum/ N_2 cycles with Schlenk techniques. Benzyl alcohol (4.5 mmol, 1.5 eq.) and toluene (10 mL) were added by syringe. The vial was stirred in an oil bath at 110 ˚C for 12 h. The reaction mixture was then allowed to cool to room temperature, quenched by the addition of a saturated NH_4Cl solution (5 mL), and extracted with diethyl ether twice. Organic

layers were gathered, dried over $MgSO_4$, filtered, and concentrated via rotation. The crude product was purified by column chromatography on silica gel using the eluent (2% ethyl acetate in hexane) and a yellowish-tan oil was obtained (70 % yield).

^{1}H NMR (400 MHz, Chloroform-*d*) δ 7.81 (d, *J* = 7.7 Hz, 1H), 7.60 (td, *J* = 7.5, 1.3 Hz, 1H), 7.45 – 7.37 (m, 2H), 7.35 – 7.30 (m, 2H), 7.28 – 7.22 (m, 2H), 3.43 (dd, *J* = 13.9, 4.3 Hz, 1H), 3.24 – 3.16 (m, 1H), 3.03 (ddt, *J* = 10.4, 8.0, 4.2 Hz, 1H), 2.89 (dd, *J* = 17.2, 4.0 Hz, 1H), 2.70 (dd, *J* = 14.0, 10.4 Hz, 1H).

^{13}C NMR (101 MHz, Chloroform-*d*) δ 207.8, 153.6, 139.7, 136.6, 134.8, 128.9, 128.5, 127.4, 126.6, 126.4, 124.0, 48.9, 37.0, 32.2.

NMR data are in accordance with literature values. [24]

2-benzyl-3,4-dihydronaphthalen-1(2*H*)-one

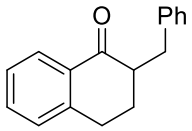

A 4-mL screw-capped vial was charged with LiO^tBu (2 mmol, 160 mg), α-Tetralone (1 mmol, 146 mg), and a magnetic stirring bar, and the vial was sealed with a cap containing a PTFE septum. The vial was made inert by 3 vacuum/ N_2 cycles with Schlenk techniques. Benzyl alcohol (1.5 mmol, 1.5 eq.) and toluene (2 mL) were added by syringe. The vial was stirred in an aluminum heating block at 110 °C for 12 h. The reaction mixture was then allowed to cool to room temperature, quenched by the addition of a saturated NH_4Cl solution (1 mL), and extracted with diethyl ether twice. Organic layers were gathered, dried over $MgSO_4$, filtered, and concentrated via rotation. The crude product was purified by column chromatography on silica gel using the eluent (2 % ethyl acetate in hexane) and the product white solid was obtained (211 mg, 90% yield).

^{1}H NMR (400 MHz, Chloroform-d) δ 8.11 (dd, *J* = 7.8, 1.4 Hz, 1H), 7.50 (td, *J* = 7.5, 1.5 Hz, 1H), 7.37 – 7.32 (m, 3H), 7.26 (t, *J* = 7.3 Hz, 4H), 3.54 (dd, *J* = 13.6, 3.9 Hz, 1H), 3.00 – 2.93 (m, 2H), 2.83 – 2.75 (m, 1H), 2.68 (dd, *J* = 13.6, 9.6 Hz, 1H), 2.19 – 2.10 (m, 1H), 1.88 – 1.76 (m, 1H).

^{13}C NMR (101 MHz, Chloroform-d) δ 199.4, 144.0, 140.1, 133.3, 132.5, 129.3, 128.7, 128.4, 127.6, 126.6, 126.2, 49.5, 35.7, 28.6, 27.7.

NMR data are in accordance with literature values. [24]

Standard Catalytic Reaction

A 4-mL screw-capped vial was charged with NaO^tBu (57.6 mg, 0.6 mmol), POP-5 (0.03 mmol, 10 mol%), and a magnetic stirring bar, and the vial was sealed with a cap containing a PTFE septum. The 4-mL vial was made inert by 3 vacuum/N_2 cycles with Schlenk techniques. The $Ni(cod)_2$ standard solution (4.2 mg in 1 mL toluene) was added into the vial *via* a 1-mL syringe. The phenyl coupling partner (0.6 mmol, 2 eq.), 2-methyl-1-indanone (43.8 mg, 0.3 mmol) were

injected into the vial by a Hamilton syringe. The vial was stirred in an aluminum heating block at 60 °C for 36 h and then cooled to room temperature. The mixture was quenched with a saturated aqueous NH_4Cl solution (1 mL) and extracted with Et_2O (10 mL, 3 times). The combined extract was dried over $MgSO_4$, filtered, and concentrated under reduced pressure. 1,3,5-trimethoxybenzene or dibenzyl ether was added to the mixture. The conversion and yield were analyzed by NMR. The enantiomeric excess was checked by chiral HPLC after purification of the crude mixture by silica gel chromatography (1-10 % EtOAc in hexane).

Recycling Experiment

An experiment was started as a Standard Catalytic Reaction with 2-methyl-1-indanone (43.8 mg, 0.3 mmol) and chlorobenzene (62.7 μL, 0.6 mmol). After 36 h, the vial was cooled to room temperature. The mixture was quenched with 1 mL saturated aqueous NH_4Cl solution. The POP was collected by a glass funnel, and washed with Et_2O (10 mL x3) and water (10 mL x3). Then POP was dried in a vacuum oven overnight for next time use. The crude mixture was extracted by ether, dried over $MgSO_4$, and concentrated by rotation. NMR analyzed the yield and the enantiomeric excess was quantified by chiral HPLC. Thereafter, the recycling experiment was repeated as Standard Catalytic Reaction with the addition of NaO^tBu (57.6 mg, 0.6 mmol), $Ni(cod)_2$ standard solution (4.2 mg in 1 mL toluene), 2-methyl-1-indanone (43.8 mg, 0.3 mmol), chlorobenzene (62.7 μL, 0.6 mmol).

Gram-scale reaction

NaO^tBu (8 mmol), and POP-5 (0.4 mmol) were weighed in a 50 ml round-bottomed flask and a stir bar was added. The flask was sealed and connected to the Schlenk line. After 3 vacuum/N_2 cycles, $Ni(cod)_2$ (0.2 mmol) was added to the flask in the glovebox. Toluene (15 mL), 2-methyl-1-indanone (4 mmol), and 4-chlorobenzotrifluoride (8 mmol) were added to the flask via syringes under nitrogen outside of the glovebox. The resulting solution was put into an oil bath and heated to 60 °C for 36 h. The mixture was cooled down to room temperature then 15 mL saturated aqueous NH_4Cl solution was added to the flask to quench the reaction. The organic layer was extracted with Et_2O (30 mL, 3 times). The combined extract was dried over $MgSO_4$, filtered, and concentrated under reduced pressure. The crude product was purified by silica gel chromatography affording the corresponding product as a colorless oil in 97% isolated yield (99% ee).

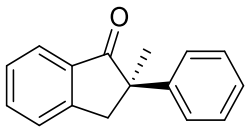

(*R*)-2-methyl-2-phenyl-2,3-dihydro-1*H*-inden-1-one

The title compound was prepared according to Standard Catalytic Reaction from chlorobenzene.

The crude product was purified by silica gel chromatography (2% EtOAc in hexane) affording (*R*)-2-methyl-2-phenyl-2,3-dihydro-1*H*-inden-1-one as a colorless oil in 95% (99% ee). The enantiomeric excess was determined by Chiralpack AD-H column with hexane/ isopropanol = 95:5, 1.00 mL/min; retention times = 9.45 min for major isomer and 10.57 min for minor isomer.

The title compound was prepared according to Standard Catalytic Reaction from bromobenzene in 59% yield (93% ee).

The title compound was prepared according to Standard Catalytic Reaction from iodobenzene in 75% yield (63% ee).

^{1}H NMR (400 MHz, Chloroform-d) δ 7.85 (d, *J* = 7.6 Hz, 1H), 7.67 (t, *J* = 7.4 Hz, 1H), 7.52 (d, *J* = 7.6 Hz, 1H), 7.45 (t, *J* = 8.0 Hz, 1H), 7.37 – 7.29 (m, 4H), 7.27 – 7.20 (m, 1H), 3.63 (d, *J* = 16.8 Hz, 1H), 3.34 (d, *J* = 17.4 Hz, 1H), 1.69 (s, 3H).

^{13}C NMR (101 MHz, Chloroform-d) δ 208.6, 152.5, 143.9, 135.6, 135.1, 128.6, 127.7, 126.6, 126.4, 126.1, 124.9, 53.1, 44.9, 24.5. MS (EI) m/z ($M^{\cdot+}$) calcd for $C_{16}H_{14}O$: 222, found 222. NMR data are in accordance with literature values. [15]

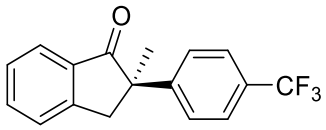

(*R*)-2-methyl-2-(4-(trifluoromethyl)phenyl)-2,3-dihydro-1*H*-inden-1-one

The title compound was prepared according to Standard Catalytic Reaction from 1-chloro-4-(trifluoromethyl)benzene. The crude product was purified by silica gel chromatography (1% EtOAc in hexane) affording (*R*)-2-methyl-2-(4-(trifluoromethyl)phenyl)-2,3-dihydro-1*H*-inden-1-one as a colorless oil in 99% (99% ee). The enantiomeric excess was determined by Chiralpack AD-H column with hexane/ isopropanol = 95:5, 1.00 mL/min; retention times = 7.90 min for major isomer and 9.25 min for minor isomer.

^{1}H NMR (400 MHz, Chloroform-d) δ 7.83 (dd, *J* = 7.7, 0.5 Hz, 1H), 7.67 (td, *J* = 7.5, 1.2 Hz, 1H), 7.55 (d, *J* = 8.2 Hz, 2H), 7.51 (dt, *J* = 7.7, 0.9 Hz, 1H), 7.48 – 7.41 (m, 3H), 3.58 (d, *J* = 17.4 Hz, 1H), 3.35 (d, *J* = 17.7 Hz, 1H), 1.68 (s, 3H).

^{13}C NMR (101 MHz, Chloroform-d) δ 207.8, 152.2, 147.9, 135.4, 135.3, 128.0, 126.6, 126.4, 125.6, 125.5, 125.5, 125.1, 53.1, 44.6, 24.6. MS (EI) m/z ($M^{\cdot+}$) calcd for $C_{17}H_{13}F_3O$: 290, found 290. NMR data are in accordance with literature values. [15]

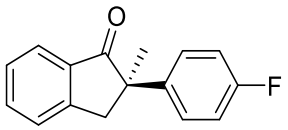

(*R*)-2-(4-fluorophenyl)-2-methyl-2,3-dihydro-1*H*-inden-1-one

The title compound was prepared according to Standard Catalytic Reaction from 1-chloro-4-fluorobenzene. The crude product was purified by silica gel chromatography (2% EtOAc in hexane)

affording (*R*)-2-(4-fluorophenyl)-2-methyl-2,3-dihydro-1*H*-inden-1-one as a colorless oil in 97% (99% ee). The enantiomeric excess was determined by Chiralpack AD-H column with hexane/ isopropanol = 95:5, 1.00 mL/min; retention times = 8.95 min for major isomer and 10.13 min for minor isomer.

^{1}H NMR (400 MHz, Chloroform-d) δ 7.84 (dd, *J* = 7.7, 0.6 Hz, 1H), 7.68 (td, *J* = 7.4, 1.2 Hz, 1H), 7.52 (dt, *J* = 7.7, 1.0 Hz, 1H), 7.45 (td, *J* = 7.5, 0.9 Hz, 1H), 7.33 – 7.28 (m, 2H), 7.03 – 6.96 (m, 2H), 3.58 (d, *J* = 17.3 Hz, 1H), 3.34 (d, *J* = 17.4 Hz, 1H), 1.66 (s, 3H).

^{13}C NMR (101 MHz, Chloroform-d) δ 208.4, 162.8, 160.3, 152.3, 139.6, 139.5, 135.4, 135.3, 127.9, 127.8, 127.7, 126.4, 125.0, 115.4, 115.2, 52.6, 44.8, 24.8. MS (EI) m/z ($M^{\cdot+}$) calcd for $C_{16}H_{13}FO$: 240, found 240. NMR data are in accordance with literature values. [15]

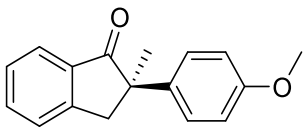

(*R*)-2-(4-methoxyphenyl)-2-methyl-2,3-dihydro-1*H*-inden-1-one

The title compound was prepared according to Standard Catalytic Reaction from 1-chloro-4-methoxybenzene. The crude product was purified by silica gel chromatography (1% EtOAc in hexane) affording (*R*)-2-(4-methoxyphenyl)-2-methyl-2,3-dihydro-1*H*-inden-1-one as a colorless oil in 96 % (95.5 % ee). The enantiomeric excess was determined by Chiralpack AD-H column with hexane/ isopropanol = 95:5, 1.00 mL/min; retention times = 16.62 min for major isomer and 20.42 min for minor isomer.

^{1}H NMR (400 MHz, Chloroform-d) δ 7.83 – 7.79 (m, 1H), 7.64 (td, *J* = 7.4, 1.2 Hz, 1H), 7.49 (dt, *J* = 7.6, 0.9 Hz, 1H), 7.41 (td, *J* = 7.4, 1.0 Hz, 1H), 7.25 – 7.21 (m, 2H), 6.85 – 6.81 (m, 2H), 3.77 (s, 3H), 3.57 (d, *J* = 17.2 Hz, 1H), 3.29 (d, *J* = 17.6 Hz, 1H), 1.64 (s, 3H).

^{13}C NMR (101 MHz, Chloroform-d) δ 208.8, 158.2, 152.5, 135.8, 135.6, 135.1, 127.7, 127.2, 126.4, 124.9, 113.9, 55.3, 52.5, 44.8, 24.6. MS (EI) m/z ($M^{\cdot+}$) calcd for $C_{17}H_{16}O_2$: 252, found 252. NMR data are in accordance with literature values. [15]

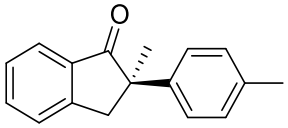

(*R*)-2-methyl-2-(*p*-tolyl)-2,3-dihydro-1*H*-inden-1-one

The title compound was prepared according to Standard Catalytic Reaction from 4-chlorotoluene. The crude product was purified by silica gel chromatography (2% EtOAc in hexane) affording (*R*)-2-methyl-2-(*p*-tolyl)-2,3-dihydro-1*H*-inden-1-one as a colorless oil in 97% (99% ee). The enantiomeric excess was determined by Chiralpack AD-H column with hexane/ isopropanol = 95:5, 1.00 mL/min; retention times = 9.73 min for major isomer and 10.97 min for minor isomer.

^{1}H NMR (400 MHz, Chloroform-d) δ 7.84 (dd, *J* = 7.6, 1.1 Hz, 1H), 7.66 (td, *J* = 7.5, 1.2 Hz, 1H), 7.51 (dd, *J* = 7.7, 0.9 Hz, 1H), 7.44 (t, *J* = 7.4 Hz, 1H), 7.23 (d, *J* = 8.0 Hz, 2H), 7.13 (d, *J* = 8.0 Hz, 2H), 3.61 (d, *J* = 17.3 Hz, 1H), 3.32 (d, *J* = 17.3 Hz, 1H), 2.33 (s, 3H), 1.67 (s, 3H).

^{13}C NMR (101 MHz, Chloroform-d) δ 208.8, 152.6, 140.8, 136.2, 135.6, 135.0, 129.3, 127.7, 126.4, 126.0, 124.9, 52.8, 44.8, 24.5, 20.9. MS (EI) m/z ($M^{\cdot+}$) calcd for $C_{17}H_{16}O$: 236, found 236. NMR data are in accordance with literature values. [16]

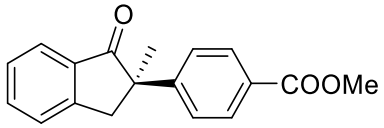

(*R*)-Methyl 4-(2-methyl-1-oxo-2,3-dihydro-1*H*-inden-2-yl)benzoate

The title compound was prepared according to Standard Catalytic Reaction from methyl 4-chlorobenzoate. The crude product was purified by silica gel chromatography (1% EtOAc in hexane) affording (*R*)-methyl 4-(2-methyl-1-oxo-2,3-dihydro-1*H*-inden-2-yl)benzoate as a colorless oil in 93 % (99.5% ee). The enantiomeric excess was determined by Chiralpack AD-H column with hexane/ isopropanol = 90:10, 1.00 mL/min; retention times = 18.38 min for major isomer and 20.17 min for minor isomer.

^{1}H NMR (400 MHz, Chloroform-d) δ 7.96 (dt, *J* = 8.0, 2.0 Hz, 2H), 7.83 (dd, *J* = 7.7, 0.6 Hz, 1H), 7.66 (td, *J* = 7.5, 1.2 Hz, 1H), 7.50 (dt, *J* = 7.7, 0.9 Hz, 1H), 7.44 (td, *J* = 7.4, 0.9 Hz, 1H), 7.39 (dt, *J* = 12.0, 2.0 Hz, 2H), 3.89 (s, 3H), 3.58 (d, *J* = 17.4 Hz, 1H), 3.33 (dd, *J* = 20.0, 2.0 Hz, 1H), 1.67 (s, 3H).

^{13}C NMR (101 MHz, Chloroform-d) δ 207.9, 166.8, 152.3, 149.1, 135.4, 129.9, 128.5, 127.9, 126.4, 126.2, 125.0, 53.3, 52.1, 44.6, 24.5. MS (EI) m/z ($M^{\cdot+}$) calcd for $C_{18}H_{16}O_3$: 280, found 280. NMR data are in accordance with literature values. [15]

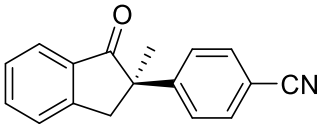

(*R*)-4-(2-methyl-1-oxo-2,3-dihydro-1*H*-inden-2-yl)benzonitrile

The title compound was prepared according to Standard Catalytic Reaction from 4-chlorobenzonitrile. The crude product was purified by silica gel chromatography (1% EtOAc in hexane) affording (*R*)-4-(2-methyl-1-oxo-2,3-dihydro-1*H*-inden-2-yl)benzonitrile as a colorless oil in 78 % (97 % ee). The enantiomeric excess was determined by Chiralpack AD-H column with hexane/ isopropanol = 95:5, 1.00 mL/min; retention times = 25.92 min for major isomer and 33.36 min for minor isomer.

^{1}H NMR (400 MHz, Chloroform-d) δ 7.82 (d, *J* = 7.7 Hz, 1H), 7.68 (td, *J* = 7.5, 1.3 Hz, 1H), 7.61 – 7.59 (m, 1H), 7.58 (d, *J* = 2.0 Hz, 1H), 7.51 (dt, *J* = 7.7, 1.0 Hz, 1H), 7.47 – 7.41 (m, 3H), 3.56 (d, *J* = 17.4 Hz, 1H), 3.35 (d, *J* = 17.4 Hz, 1H), 1.66 (s, 3H).

^{13}C NMR (101 MHz, Chloroform-d) δ 207.3, 152.0, 149.3, 135.6, 135.1, 132.4, 128.1, 127.1, 126.5, 125.1, 118.7, 110.6, 53.3, 44.4, 24.6. MS (EI) m/z ($M^{\cdot+}$) calcd for $C_{17}H_{13}NO$: 247, found 247. NMR data are in accordance with literature values. [15]

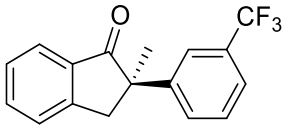

(*R*)-2-methyl-2-(3-(trifluoromethyl)phenyl)-2,3-dihydro-1*H*-inden-1-one

The title compound was prepared according to Standard Catalytic Reaction from 1-chloro-3-(trifluoromethyl)benzene. The crude product was purified by silica gel chromatography (1% EtOAc in hexane) affording (*R*)-2-methyl-2-(3-(trifluoromethyl)phenyl)-2,3-dihydro-1*H*-inden-1-one as a colorless oil in 95 % (99.3% ee). The enantiomeric excess was determined by Chiralpack OJ-H column with hexane/ isopropanol = 98:2, 0.50 mL/min; retention times = 15.13 min for major isomer and 16.20 min for minor isomer.

^{1}H NMR (400 MHz, Chloroform-d) δ 7.84 (dd, *J* = 7.7, 0.6 Hz, 1H), 7.67 (td, *J* = 7.4, 1.2 Hz, 1H), 7.60 (s, 1H), 7.53 – 7.47 (m, 3H), 7.47 – 7.38 (m, 2H), 3.58 (d, *J* = 17.3 Hz, 1H), 3.36 (d, *J* = 17.3 Hz, 1H), 1.68 (s, 3H).

^{13}C NMR (101 MHz, Chloroform-d) δ 207.8, 152.1, 144.9, 135.4, 135.2, 131.0, 130.7, 129.8, 129.0, 128.0, 126.5, 125.5, 125.1, 123.6, 123.6, 123.6, 123.5, 123.0, 122.9, 122.9, 53.0, 44.6, 24.9. MS (EI) m/z ($M^{\cdot+}$) calcd for $C_{17}H_{13}F_3O$: 290, found 290. NMR data are in accordance with literature values. [15]

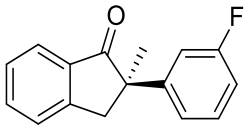

(*R*)-2-(3-fluorophenyl)-2-methyl-2,3-dihydro-1*H*-inden-1-one

The title compound was prepared according to Standard Catalytic Reaction from 1-chloro-3-fluorobenzene. The crude product was purified by silica gel chromatography (1% EtOAc in hexane) affording (*R*)-2-(3-fluorophenyl)-2-methyl-2,3-dihydro-1*H*-inden-1-one as a colorless oil in 99 % (99 % ee). The enantiomeric excess was determined by Chiralpack AD-H column with hexane/ isopropanol = 99:1, 1.00 mL/min; retention times = 13.78 min for major isomer and 14.73 min for minor isomer.

^{1}H NMR (400 MHz, Chloroform-d) δ 7.82 (dd, *J* = 7.7, 0.6 Hz, 1H), 7.66 (td, *J* = 7.5, 1.2 Hz, 1H), 7.50 (dt, *J* = 7.7, 1.0 Hz, 1H), 7.43 (td, *J* = 7.4, 0.9 Hz, 1H), 7.29 – 7.22 (m, 1H), 7.09 – 7.02 (m, 2H), 6.91 (tdd, *J* = 8.3, 2.5, 1.0 Hz, 1H), 3.57 (d, *J* = 17.4 Hz, 1H), 3.31 (dd, *J* = 17.4, 0.6 Hz, 1H), 1.65 (s, 3H).

^{13}C NMR (101 MHz, Chloroform-d) δ 207.9, 164.1, 161.7, 152.3, 146.5, 146.4, 135.3, 135.3, 130.0, 130.0, 127.9, 126.4, 125.0, 121.8, 121.8, 113.7, 113.6, 113.5, 113.3, 52.9, 52.9, 44.7, 24.5. MS

(EI) m/z ($M^{\cdot+}$) calcd for $C_{16}H_{13}FO$: 240, found 240. NMR data are in accordance with literature values. [15]

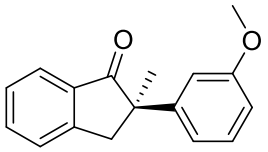

(*R*)-2-(3-methoxyphenyl)-2-methyl-2,3-dihydro-1*H*-inden-1-one

The title compound was prepared according to Standard Catalytic Reaction from 1-chloro-3-methoxybenzene. The crude product was purified by silica gel chromatography (1% EtOAc in hexane) affording (*R*)-2-(3-methoxyphenyl)-2-methyl-2,3-dihydro-1*H*-inden-1-one as a colorless oil in 99 % (99 % ee). The enantiomeric excess was determined by Chiralpack AD-H column with hexane/ isopropanol = 95:5, 1.00 mL/min; retention times = 13.02 min for major isomer and 14.10 min for minor isomer.

^{1}H NMR (400 MHz, Chloroform-d) δ 7.82 (dd, *J* = 7.6, 0.6 Hz, 1H), 7.64 (td, *J* = 7.4, 1.2 Hz, 1H), 7.48 (dt, *J* = 7.7, 0.9 Hz, 1H), 7.42 (ddd, *J* = 8.0, 7.2, 0.9 Hz, 1H), 7.24 – 7.19 (m, 1H), 6.89 – 6.85 (m, 2H), 6.78 – 6.74 (m, 1H), 3.77 (s, 3H), 3.59 (d, *J* = 17.4 Hz, 1H), 3.29 (dd, *J* = 17.4, 0.6 Hz, 1H), 1.65 (s, 3H).

^{13}C NMR (101 MHz, Chloroform-d) δ 208.4, 159.7, 152.6, 145.5, 135.6, 135.1, 129.5, 127.7, 126.4, 124.9, 118.5, 112.7, 111.4, 55.2, 53.1, 44.9, 24.4. MS (EI) m/z ($M+H^{+}$) calcd for $C_{17}H_{16}O_2$: 253, found 253. NMR data are in accordance with literature values. [15]

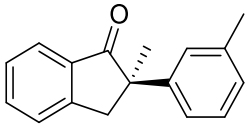

(*R*)-2-methyl-2-(*m*-tolyl)-2,3-dihydro-1*H*-inden-1-one

The title compound was prepared according to Standard Catalytic Reaction from 3-chlorotoluene. The crude product was purified by silica gel chromatography (1% EtOAc in hexane) affording (*R*)-2-methyl-2-(*m*-tolyl)-2,3-dihydro-1*H*-inden-1-one as a colorless oil in 94% (99% ee). The enantiomeric excess was determined by Chiralpack AD-H column with hexane/ isopropanol = 95:5, 1.00 mL/min; retention times = 7.13 min for major isomer and 8.50 min for minor isomer.

^{1}H NMR (400 MHz, Chloroform-d) δ 7.86 (d, *J* = 7.7 Hz, 1H), 7.67 (td, *J* = 7.5, 1.2 Hz, 1H), 7.52 (dd, *J* = 7.7, 0.9 Hz, 1H), 7.45 (t, *J* = 7.4 Hz, 1H), 7.22 (t, *J* = 7.6 Hz, 1H), 7.13 (d, *J* = 10.2 Hz, 2H), 7.06 (d, *J* = 7.0 Hz, 1H), 3.62 (d, *J* = 17.4 Hz, 1H), 3.32 (d, *J* = 17.4 Hz, 1H), 2.34 (s, 3H), 1.68 (s, 3H).

^{13}C NMR (101 MHz, Chloroform-d) δ 208.9, 152.6, 143.8, 138.1, 135.7, 135.1, 128.5, 127.7, 127.4, 126.9, 126.4, 124.9, 123.2, 53.0, 45.0, 24.5, 21.6. MS (EI) m/z ($M^{\cdot+}$) calcd for $C_{17}H_{16}O$: 236, found 236. NMR data are in accordance with literature values. [25]

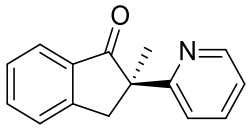

(*R*)-2-methyl-2-(pyridin-2-yl)-2,3-dihydro-1*H*-inden-1-one

The title compound was prepared according to Standard Catalytic Reaction from 2-chloropyridine. The crude product was purified by silica gel chromatography (1% EtOAc in hexane) affording (*R*)-2-methyl-2-(pyridin-2-yl)-2,3-dihydro-1*H*-inden-1-one as a colorless oil in 55 % (93 % ee). The enantiomeric excess was determined by Chiralpack AD-H column with hexane/ isopropanol = 95:5, 1.00 mL/min; retention times = 10.23 min for major isomer and 13.40 min for minor isomer.

The title compound was prepared according to Standard Catalytic Reaction from 2-bromopyridine in 59 % (89 % ee). The enantiomeric excess was determined by Chiralpack AD-H column with hexane/ isopropanol = 95:5, 1.00 mL/min; retention times = 10.22 min for major isomer and 13.35 min for minor isomer.

^{1}H NMR (400 MHz, Chloroform-d) δ 7.83 – 7.79 (m, 1H), 7.64 (td, *J* = 7.5, 1.2 Hz, 1H), 7.48 (dt, *J* = 7.7, 0.9 Hz, 1H), 7.41 (td, *J* = 7.4, 0.9 Hz, 1H), 6.80 – 6.71 (m, 3H), 5.90 (s, 2H), 3.53 (d, *J* = 17.4 Hz, 1H), 3.28 (dd, *J* = 17.4, 0.7 Hz, 1H), 1.61 (s, 3H).

^{13}C NMR (101 MHz, Chloroform-d) δ 208.5, 152.4, 147.8, 146.2, 137.7, 135.5, 135.1, 127.8, 126.4, 125.0, 119.2, 108.1, 107.0, 101.0, 52.8, 45.0, 24.6. MS (EI) m/z ($M^{\cdot+}$) calcd for $C_{15}H_{13}NO$: 223, found 223. NMR data are in accordance with literature values. [15]

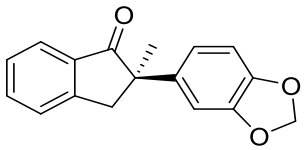

(*R*)-2-(benzo[d][1,3]dioxol-5-yl)-2-methyl-2,3-dihydro-1*H*-inden-1-one

The title compound was prepared according to Standard Catalytic Reaction from 5-chlorobenzo[d][1,3]dioxole. The crude product was purified by silica gel chromatography (1% EtOAc in hexane) affording (*R*)-2-(benzo[d][1,3]dioxol-5-yl)-2-methyl-2,3-dihydro-1*H*-inden-1-one as a colorless oil in 85 % (98 % ee). The enantiomeric excess was determined by Chiralpack AD-H column with hexane/ isopropanol = 95:5, 1.00 mL/min; retention times = 29.27 min for major isomer and 32.08 min for minor isomer.

The title compound was prepared according to Standard Catalytic Reaction from 5-bromobenzo[d][1,3]dioxole in 63 % (91 % ee). The enantiomeric excess was determined by Chiralpack AD-H column with hexane/ isopropanol = 95:5, 1.00 mL/min; retention times = 28.82 min for major isomer and 31.73 min for minor isomer.

^{1}H NMR (400 MHz, Chloroform-d) δ 7.83 (dd, *J* = 7.7, 0.6 Hz, 1H), 7.66 (td, *J* = 7.5, 1.2 Hz, 1H), 7.50 (dt, *J* = 7.7, 0.9 Hz, 1H), 7.44 (td, *J* = 7.4, 0.9 Hz, 1H), 6.83 – 6.72 (m, 3H), 5.93 (s, 2H), 3.56 (d, *J* = 17.4 Hz, 1H), 3.30 (dd, *J* = 17.3, 0.7 Hz, 1H), 1.63 (s, 3H).

^{13}C NMR (101 MHz, Chloroform-d) δ 208.5, 152.4, 147.8, 146.2, 137.7, 135.5, 135.2, 127.8, 126.4, 125.0, 119.2, 108.1, 107.0, 101.0, 52.8, 45.0, 24.6. MS (EI) m/z ($M+H^+$) calcd for $C_{17}H_{14}O_3$: 267, found 267. NMR data are in accordance with literature values. [15]

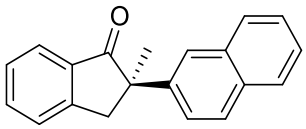

(*R*)-2-methyl-2-(naphthalen-2-yl)-2,3-dihydro-1*H*-inden-1-one

The title compound was prepared according to Standard Catalytic Reaction from 2-chloronaphthalene. The crude product was purified by silica gel chromatography (1% EtOAc in hexane) affording (*R*)-2-methyl-2-(naphthalen-2-yl)-2,3-dihydro-1*H*-inden-1-one as a colorless oil in 73% (92% ee). The enantiomeric excess was determined by Chiralpack OD-H column with hexane/ isopropanol = 95:5, 1.00 mL/min; retention times = 7.43 min for major isomer and 8.90 min for minor isomer.

The title compound was prepared according to Standard Catalytic Reaction from 2-bromonaphthalene in 57 % (46% ee). The enantiomeric excess was determined by Chiralpack OD-H column with hexane/ isopropanol = 95:5, 1.00 mL/min; retention times = 7.45 min for major isomer and 8.92 min for minor isomer.

^{1}H NMR (400 MHz, Chloroform-d) δ 7.87 (dd, *J* = 7.7, 0.5 Hz, 1H), 7.84 – 7.75 (m, 4H), 7.67 (td, *J* = 7.5, 1.2 Hz, 1H), 7.52 (dt, *J* = 7.7, 0.9 Hz, 1H), 7.48 – 7.42 (m, 3H), 7.34 (dd, *J* = 8.7, 2.0 Hz, 1H), 3.69 (d, *J* = 17.4 Hz, 1H), 3.38 (dd, *J* = 17.3, 0.7 Hz, 1H), 1.77 (s, 3H).

^{13}C NMR (101 MHz, Chloroform-d) δ 208.7, 152.6, 141.2, 135.7, 135.2, 133.3, 132.2, 128.4, 128.0, 127.8, 127.4, 126.5, 126.1, 125.8, 125.0, 124.7, 124.7, 53.3, 44.8, 24.5. MS (EI) m/z ($M+H^+$) calcd for $C_{20}H_{16}O$: 273, found 273. NMR data are in accordance with literature values. [17]

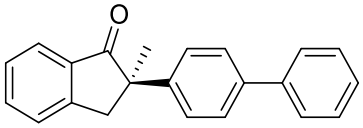

(*R*)-2-([1,1'-biphenyl]-4-yl)-2-methyl-2,3-dihydro-1*H*-inden-1-one

The title compound was prepared according to Standard Catalytic Reaction from 4-chloro-1,1'-biphenyl. The crude product was purified by silica gel chromatography (1% EtOAc in hexane) affording (*R*)-2-([1,1'-biphenyl]-4-yl)-2-methyl-2,3-dihydro-1*H*-inden-1-one as a colorless oil in 96 % (97 % ee). The enantiomeric excess was determined by Chiralpack AD-H column with hexane/ isopropanol = 95:5, 1.00 mL/min; retention times = 15.57 min for major isomer and 18.97 min for minor isomer.

^{1}H NMR (400 MHz, Chloroform-d) δ 7.85 (dd, *J* = 7.7, 0.5 Hz, 1H), 7.66 (td, *J* = 7.5, 1.2 Hz, 1H), 7.57 – 7.50 (m, 5H), 7.46 – 7.37 (m, 5H), 7.35 – 7.30 (m, 1H), 3.65 (d, *J* = 17.4 Hz, 1H), 3.38 – 3.31 (m, 1H), 1.71 (s, 3H).

^{13}C NMR (101 MHz, Chloroform-d) δ 208.6, 152.6, 142.9, 140.7, 139.6, 135.6, 135.2, 128.7, 127.8, 127.3, 127.2, 127.1, 126.6, 126.4, 125.0, 53.0, 44.8, 24.5. MS (EI) m/z ($M+H^+$) calcd for $C_{22}H_{18}O$: 299, found 299. NMR data are in accordance with literature values. [17]

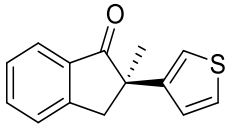

(*R*)-2-methyl-2-(thiophen-2-yl)-2,3-dihydro-1*H*-inden-1-one

The title compound was prepared according to Standard Catalytic Reaction from 3-chlorothiophene. The crude product was purified by silica gel chromatography (1% EtOAc in hexane) affording (*R*)-2-methyl-2-(thiophen-2-yl)-2,3-dihydro-1*H*-inden-1-one as a colorless oil in 69 % (99.3 % ee). The enantiomeric excess was determined by Chiralpack AD-H column with hexane/ isopropanol = 95:5, 1.00 mL/min; retention times = 10.08 min for major isomer and 10.93 min for minor isomer.

^{1}H NMR (400 MHz, Chloroform-d) δ 7.82 (dd, *J* = 7.7, 0.6 Hz, 1H), 7.65 (td, *J* = 7.5, 1.2 Hz, 1H), 7.50 (dt, *J* = 7.7, 0.9 Hz, 1H), 7.43 (td, *J* = 7.4, 0.9 Hz, 1H), 7.28 – 7.26 (m, 1H), 7.17 (dd, *J* = 3.0, 1.4 Hz, 1H), 6.99 (dd, *J* = 5.0, 1.4 Hz, 1H), 3.60 (d, *J* = 17.2 Hz, 1H), 3.30 (dd, *J* = 17.1, 0.6 Hz, 1H), 1.66 (s, 3H).

^{13}C NMR (101 MHz, Chloroform-d) δ 207.6, 152.1, 144.4, 135.2, 135.2, 127.8, 126.4, 126.2, 126.0, 125.0, 120.3, 51.1, 43.7, 25.2. MS (EI) m/z ($M+H^+$) calcd for $C_{14}H_{12}OS$: 229, found 229. NMR data are in accordance with literature values. [15]

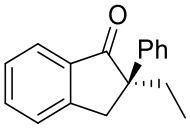

(*R*)-2-ethyl-2-phenyl-2,3-dihydro-1*H*-inden-1-one

The title compound was prepared according to Standard Catalytic Reaction from chlorobenzene with 2-Ethyl-1-indanone. The crude product was purified by silica gel chromatography (1% EtOAc in hexane) affording (*R*)-2-ethyl-2-phenyl-2,3-dihydro-1*H*-inden-1-one as a white solid in 61% (99.8 % ee). The enantiomeric excess was determined by Chiralpack AD-H column with hexane/ isopropanol = 95:5, 1.00 mL/min; retention times = 9.78 min for major isomer and 10.58 min for minor isomer.

^{1}H NMR (400 MHz, Chloroform-d) δ 7.78 (d, *J* = 7.6 Hz, 1H), 7.62 (td, *J* = 7.4, 1.2 Hz, 1H), 7.50 (dt, *J* = 7.7, 1.0 Hz, 1H), 7.42 – 7.36 (m, 3H), 7.32 – 7.27 (m, 2H), 7.23 – 7.17 (m, 1H), 3.59 (d, *J* = 17.4 Hz, 1H), 3.38 (d, *J* = 17.4 Hz, 1H), 2.23 – 2.14 (m, 1H), 2.11 – 2.00 (m, 1H), 0.84 (t, *J* = 7.4 Hz, 3H).

^{13}C NMR (101 MHz, Chloroform-d) δ 208.1, 152.7, 142.2, 136.5, 135.0, 128.5, 127.6, 126.6, 126.5, 126.1, 124.5, 57.5, 40.5, 31.2, 9.2. MS (EI) m/z ($M^{\cdot+}$) calcd for $C_{17}H_{16}O$: 236, found 236. NMR data are in accordance with literature values. [15]

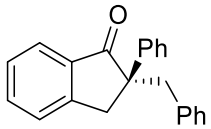

(*R*)-2-benzyl-2-phenyl-2,3-dihydro-1*H*-inden-1-one

The title compound was prepare according to Standard Catalytic Reaction from chlorobenzene with 2-benzyl-2,3-dihydro-1*H*-inden-1-one. The crude product was purified by silica gel chromatography (1% EtOAc in hexane) affording (*R*)-2-benzyl-2-phenyl-2,3-dihydro-1*H*-inden-1-one as a white solid in 60% (99 % ee). The enantiomeric excess was determined by Chiralpack AD-H column with hexane/ isopropanol = 95:5, 1.00 mL/min; retention times = 11.0 min for major isomer and 11.58 min for minor isomer.

^{1}H NMR (400 MHz, Chloroform-d) δ 7.73 (dt, *J* = 7.8, 1.0 Hz, 1H), 7.51 (td, *J* = 7.5, 1.3 Hz, 1H), 7.47 – 7.43 (m, 2H), 7.36 (dt, *J* = 7.7, 1.0 Hz, 1H), 7.34 – 7.27 (m, 3H), 7.24 – 7.19 (m, 1H), 7.15 – 7.09 (m, 3H), 7.02 – 6.98 (m, 2H), 3.57 – 3.49 (m, 3H), 3.32 (d, *J* = 13.6 Hz, 1H).

^{13}C NMR (101 MHz, Chloroform-d) δ 207.3, 152.5, 142.1, 137.3, 136.1, 134.9, 130.3, 128.5, 128.0, 127.5, 126.9, 126.8, 126.5, 126.0, 124.5, 58.3, 44.1, 38.7, 29.7. MS (EI) m/z ($M+H^+$) calcd for $C_{22}H_{18}O$: 299, found 299. NMR data are in accordance with literature values. [15]

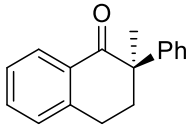

(*R*)-2-methyl-2-phenyl-3,4-dihydronaphthalen-1(2*H*)-one

The title compound was prepare according to Standard Catalytic Reaction from 2-methyl-3,4-dihydronaphthalen-1(2*H*)-one. The crude product was purified by silica gel chromatography (1% EtOAc in hexane) affording (*R*)-2-methyl-2-phenyl-3,4-dihydronaphthalen-1(2H)-one as a colorless oil in 65 % (82 % ee). The enantiomeric excess was determined by Chiralpack AD-H column with hexane/ isopropanol = 98:2, 1.00 mL/min; retention times = 8.78 min for major isomer and 7.50 min for minor isomer.

^{1}H NMR (400 MHz, Chloroform-d) δ 8.16 (dd, J = 7.9, 1.5 Hz, 1H), 7.42 (td, J = 7.5, 1.5 Hz, 1H), 7.33 – 7.26 (m, 3H), 7.24 – 7.17 (m, 3H), 7.12 (dd, J = 7.6, 0.7 Hz, 1H), 2.86 – 2.81 (m, 2H), 2.63 (dt, J = 14.0, 4.0 Hz, 1H), 2.27 (ddd, J = 14.0, 10.1, 6.3 Hz, 1H), 1.54 (s, 3H).

^{13}C NMR (101 MHz, Chloroform-d) δ 201.3, 143.6, 142.1, 133.1, 132.7, 128.7, 128.6, 128.0, 126.7, 126.6, 126.4, 50.5, 36.2, 27.1, 26.1. MS (EI) m/z ($M+H^+$) calcd for $C_{17}H_{16}O$: 237, found 237. NMR data are in accordance with literature values. [16]

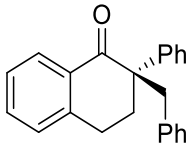

(*R*)-2-benzyl-2-phenyl-3,4-dihydronaphthalen-1(2*H*)-one

The title compound was prepare according to Standard Catalytic Reaction from 2-benzyl-3,4-dihydronaphthalen-1(2*H*)-one. The crude product was purified by silica gel chromatography (1% EtOAc in hexane) affording (*R*)-2-benzyl-2-phenyl-3,4-dihydronaphthalen-1(2*H*)-one as a colorless oil in 17 % (98 % ee). The enantiomeric excess was determined by Chiralpack AD-H column with hexane/ isopropanol = 98:2, 1.00 mL/min; retention times = 10.78 min for major isomer and 8.05 min for minor isomer.

^{1}H NMR (400 MHz, Chloroform-*d*) δ 8.17 (dd, *J* = 7.9, 1.5 Hz, 1H), 7.36 (td, *J* = 7.4, 1.5 Hz, 1H), 7.28 – 7.20 (m, 4H), 7.19 – 7.12 (m, 5H), 7.04 (d, *J* = 7.6 Hz, 1H), 6.94 – 6.88 (m, 2H), 3.39 (d, *J* = 13.5 Hz, 1H), 3.15 (d, *J* = 13.5 Hz, 1H), 2.95 – 2.84 (m, 1H), 2.77 (ddd, *J* = 17.3, 4.8, 2.6 Hz, 1H), 2.58 (ddd, *J* = 14.3, 4.3, 2.7 Hz, 1H), 2.21 (ddd, *J* = 14.3, 12.8, 3.3 Hz, 1H).

^{13}C NMR (101 MHz, Chloroform-*d*) δ 199.4, 143.3, 138.4, 137.5, 133.1, 132.8, 131.1, 128.5, 128.4, 128.2, 127.6, 127.3, 127.0, 126.4, 126.2, 54.6, 46.3, 30.9, 25.7. MS (EI) m/z ($M+H^+$) calcd for $C_{23}H_{20}O$: 313, found 313. NMR data are in accordance with literature values. [15]

5.9 References

[1] a) Godula, K. and Sames, D., *Science*, **2006**, *312*, 67–72. b) He, J., Wasa, M., Chan, K.S., Shao, Q. and Yu, J.Q., *Chem. Rev*., **2017**, *117*, 8754–8786.

[2] a) Culkin D.A. and Hartwig, J.F., *Acc. Chem. Res.*, **2003**, *36*, 234-245. b) Fuji, K., *Chem. Rev*., **1993**, *93*, 2037-2066. c) Bolm, C., Hildebrand, J.P., Muñiz, K. and Hermanns, N., *Angew. Chem., Int. Ed*., **2001**, *40*, 3284-3308. d) Rodrigalvarez, J., Nappi, M., Azuma, H., Floden, N.J., Burns, M.E. and Gaunt, M.J., *Nat. Chem.*, **2020**, *12*, 76–81; e) Zhao, J. and Nanjo, T., *Nat. Chem.* , **2019**, *11*, 213–221.

[3] a) Pérez-Vizcaíno, F., Carrón, R., Delpón, E., Duarte, J. and Tamargo, J., *Eur. J. Pharmacol*., **1993**, *232*, 105-111. b) Seitz, W., Michel, A., Teschendorf, H.J., Kreiskott, H., Hofmann, J.P. and Traut M., *DE3243518A1*, **1982**.

[4] a) Liu, F., Dong, Z., Wang, J. and Dong, G., *Angew. Chem., Int. Ed*. **2019**, *58*, 2144−2148. b) Ito, T., Tanaka, T., Iinuma, M., Nakaya, K., Takahashi, Y., Sawa, R., Murata, J. and Darnaedi, D., *J. Nat. Prod*., **2004**, *67*, 932−937.

[5] a) Ninomiya, I., Yamamoto, O. and Naito, T., *J. Chem. Soc. Chem. Commun*., **1976**, *12*, 437-437. b) Ninomiya, I., Yamamoto, O. and Naito, T., *J. Chem. Soc. Perkin Trans.1,* **1980**, 212-216. c) Cushman, M. Abbaspour, A. and Gupta, Y. P. *J. Am. Chem. Soc*. **1983**, *105*, 2873-2879. d) Cushman, M. and Chen, J.K., *J. Org. Chem*. **1987**, *52*, 1517-1521. e) Petrone, D.A., Yoon, H., Weinstabl, H. and Lautens, M., *Angew. Chem.* **2014**, *126*, 8042-8046.

[6] Takao, N., Kamigauchi, M. and Iwasa, K., *Tetrahedron* **1979**, *35*, 1977-1979.

[7] Takao, N., Bersch, H. and Takao, S., *Chem. Pharm. Bull.*, **1971**, *19*, 259-262.

[8] a) Luk, K.C., So, S.S., Zhang, J., Zhang, Z.F., Roche AG, *PCT Int. Appl. WO2006136606*, **2006**, *121*, 34−40. b) Katayev, D. and Kündig, E.P., *Helv. Chim. Acta* **2012**, *95*, 2287−2295.

[9] Palucki, M. and Buchwald, S.L., *J. Am. Chem. Soc*. **1997**, *119*, 11108–11109.

[10] a) Svennebring, A., Garg, N., Nilsson, P., Hallberg, A. and Larhed, M., *J. Org. Chem*. **2005**, *70*, 4720–4725. b) Storgaard, M., Dörwald, F.Z., Peschke, B. and Tanner, D., *J. Org. Chem.* **2009**, *74*, 5032–5040. c) Belanger, E., Cantin, K., Messe, O., Tremblay, M. and Paquin, J.F., *J. Am. Chem. Soc*. **2007**, *129*, 1034–1035. d) Solé, D., Vallverdú, L., Solans, X., Font-Bardía, M. and Bonjoch, J., *J. Am. Chem. Soc*. **2003**, *125*, 1587–1594. e) Huang, Z., Chen, Z., Lim, L.H., Quang, G.C.P., Hirao, H. and Zhou, J., *Angew. Chem. Int. Ed*. **2013**, *52*, 5807–5812.

[11] Åhman, J., Wolfe, J.P., Troutman, M.W., Palucki, M. and Buchwald, S.L., *J. Am. Chem. Soc.* **1998**, *120*, 1918−1919.

[12] Hamada, T., Chieffi, A., Åhman, J. and Buchwald, S.L., *J. Am. Chem. Soc*. **2002**, *124*, 1261−1268.

[13] Chen, G., Kwong, F.Y., Chan, H.O., Yu, W.Y. and Chan, A.S.C., *Chem. Commun*. **2006**, *13*, 1413−1415.

[14] Liao, X., Weng, Z. and Hartwig, J.F., *J. Am. Chem. Soc*. **2008**, *130*, 195−200.

[15] Ge, S. and Hartwig, J.F., *J. Am. Chem. Soc*. **2011**, *133*, 16330−16333.

[16] Richter, C., Ranganath, K.V.S. and Glorius, F., *Adv. Synth. Catal*., **2012**, *354*, 377−382.

[17] Cornella, J., Jackson, E.P. and Martin, R., *Angew. Chem., Int. Ed*. **2015**, *54*, 4075−4078.

[18] Rao, X., Li, N., Bai, H., Dai, C., Wang, Z. and Tang, W., *Angew. Chem., Int. Ed*. **2018**, *57*, 12328−12332.

[19] Anastas, P.T. and Warner, J.C., *Green Chemistry: Theory and Practice*; Oxford University Press, New York, **1988.**

[20] Kramer, S., Bennedsen, N.R. and Kegnæs, S., *ACS Catal* **2018**, *8*, 6961–6982.

[21] Ranganath, K.V., Kloesges, J., Schäfer, A.H. and Glorius, F., *Angew. Chem*. **2010**, *122*, 7952–7956.

[22] a) Bennedsen, N. R.; Kramer, S.; Kegnæs, S. *Catal. Sci. Technol*. **2020**, *10*, 7697−7705; b) M. B. Buendia, S. Kegnæs and S. Kramer, *Adv. Synth. Catal.*, **2020**, *362*, 5506–5512.

[23] a) Wang, T., Wang, W., Lyu, Y., Xiong, K., Li, C., Zhang, H., Zhan, Z., Jiang, Z. and Ding, Y., *Chinese, J. Catal*. **2017**, *38*, 691-698. b) Berthod, M., Mignani, G. and Lemaire, M., *Tetrahedron: Asymmetry*, **2004**, *15*, 1121-1126.

[24] Liang, Y.F., Zhou, X.F., Tang, S.Y., Huang, Y.B., Feng, Y.S. and Xu, H.J., *RSC advances*, **2013**, *21*, 7739-7742.

[25] Janssen-Müller, D., Schedler, M., Fleige, M., Daniliuc, C.G. and Glorius, F., *Angewandte Chemie International Edition*, **2015**, *54*, 12492-12496.

6. Asymmetric hydrosilylation of ketones by Cu-POP

6.1 Introduction

Optically pure chiral alcohols play a critical role in the formation of diverse bioactive molecules and building blocks in fragrance, agrochemicals, and pharmaceuticals, including compounds such as antidepressants (*S*-duloxetine and *R*-Fluoxetine), lung-anticancer medication (Crizotinib), neurokinin-1 receptor antagonists (Aprepitant for preventing nausea and vomiting), attention deficit hyperactivity disorder medication (Atomoxetine), muscle relaxer (e.g., Orphenadrine as the racemate) and others (Figure 6.1). [1] Asymmetric hydrogenation [2] and transfer hydrogenation [3] are two of the most often utilized methods for producing target chiral secondary alcohols. However, the cost of asymmetric hydrogenations is expensive because it relies on high hydrogen pressure, elevated temperatures and special equipment (such as autoclaves). Furthermore, transfer hydrogenation, also known as the Meerwein-Ponnodorf-Verley reduction, requires excess isopropanol and produces equal amount of byproduct-acetone. The third method is the asymmetric hydrosilylation (AHS) of prochiral ketones that only needs two steps to obtain the chiral secondary alcohols; the first step is formed silyl ethers and the second step is the hydrolysis of silyl ether. AHS is a promising alternative approach owing to its mild reaction conditions, economic efficiency and operational simplicity. [4]

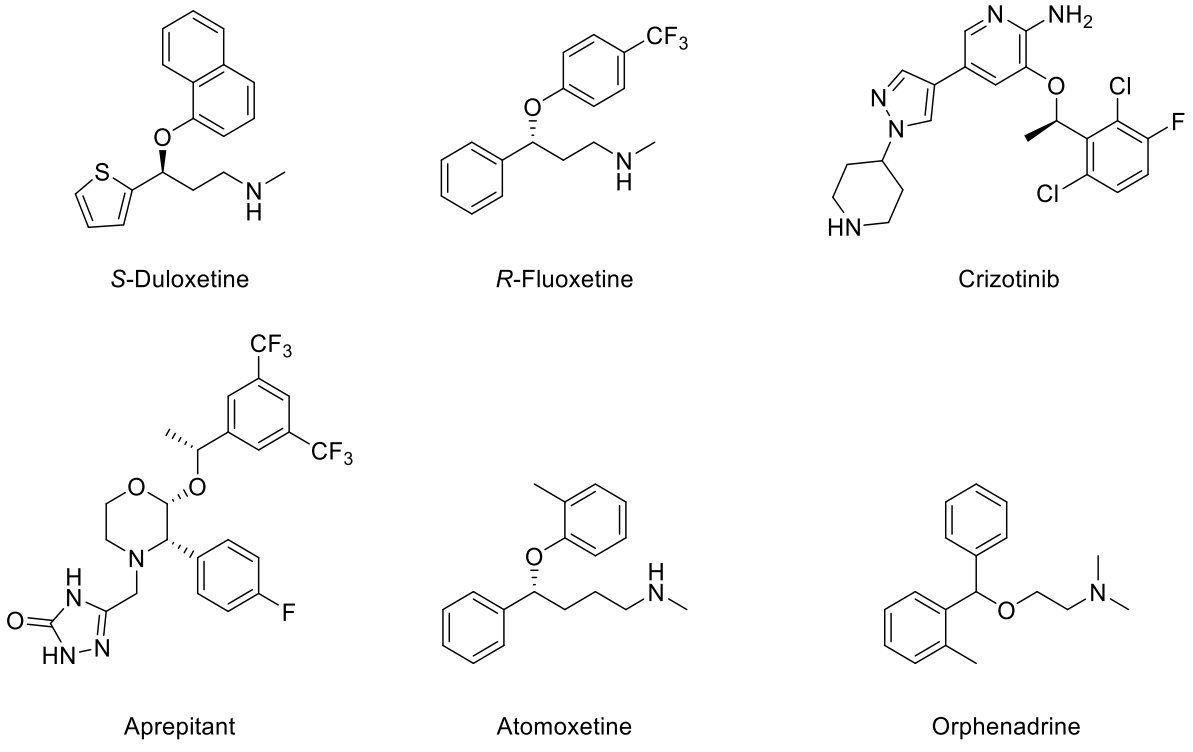

Figure 6.1 Representative examples of biologically active compounds from chiral alcohols [1]

In the 1970s, the first AHS of ketones was reported employing the rhodium-phosphine catalytic system. [5] Over the past four decades, many different transition metals, including expensive metals such as ruthenium, [6] iridium, [7] platinum, [8] and cheap metals such as titanium, [9] zinc, [10] tin,

[11] manganese, [12] chromium, [13] copper, [14] iron, [15] cobalt [16] and nickel, [17] have been exploited and developed in the field of homogeneous AHS of prochiral ketones. Among these metals, copper complexes are particularly attractive compounds due to their high activity, efficiency, low cost and environmental benignancy. The first AHS of ketones using Cu-DIOP catalyst was proposed by Brunner in 1984. [18] Lipshutz and co-workers developed a breakthrough approach by replacing DIOP with expensive ligands MeO-BIPHEP or DTBM-SEGPHOS for AHS reaction in 2003. [19] Bellemin-Laponnaz applied the CuCl-*R*-BINAP catalytic system to AHS of prochiral ketones under mild reaction conditions in 2010 (Scheme 6.1, a). [14a] Later, Liu et al. employed $Cu(OAc)_2$ with *R*-BINAP as the catalytic system using cheap silane-PMHS for AHS at room temperature (Scheme 6.1, b). [14b]

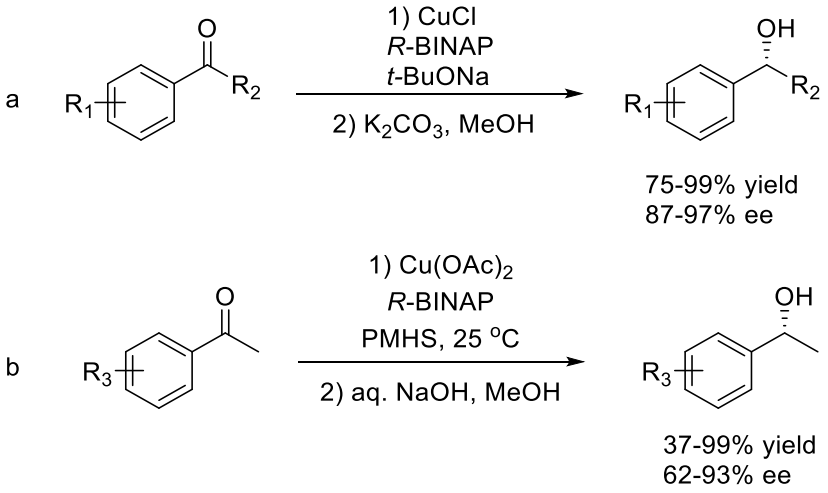

Scheme 6.1 AHS of ketones using Cu-BINAP catalytic systems [14a-b]

Most of these AHS copper-catalyzed systems are composed of copper salts and chiral bisphophine ligands. Except for (*R*)-BINAP, other chiral ligands based on (*R*)-MeO-BIPHEP, (*R*)-SEGPHOS and (*S*)-Xyl-P-Phos, other P-containing ligands were also applied in AHS of ketones (Scheme 6.2). [20, 14c] Compared with other two methods, this AHS economical catalytic system could display high efficiency and enantioselectivity.

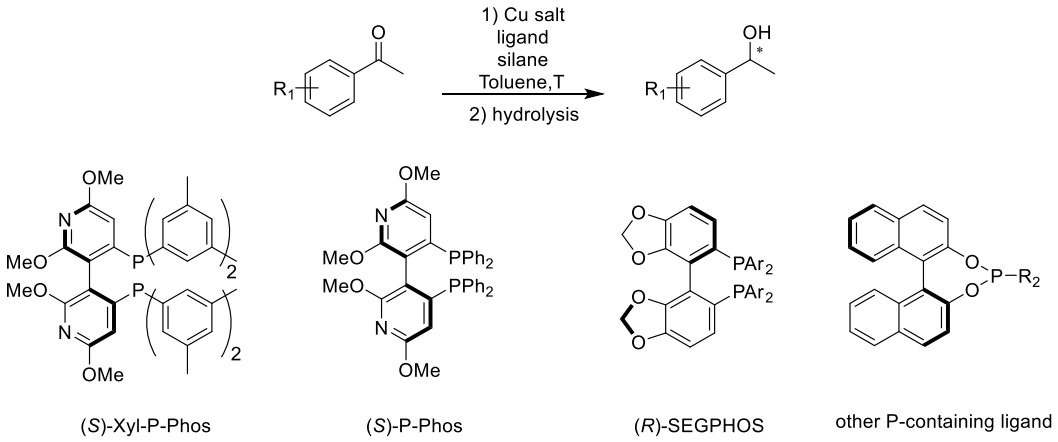

Scheme 6.2 Copper-catalyzed AHS of ketones using various ligands [14, 20, 22]

Despite significant advance in homogeneous AHS of ketones with high enantioselectivity and efficiency, these catalysts are rarely ued in industrial production due to the high cost of chiral ligands and difficulty in catalyst separation. Researchers have never stopped developing a recyclable and economical catalyst that can have same results as homogeneous AHS. Heterogeneous catalysts (such as NPs, POP, MOF and COF), which is based on homogeneous Cu-chiral ligand system, are good alternative to achieve same catalytic efficiency.

Lipshutz and co-workers developed a copper-in-charcoal formation with (*R*)-DTBM-SEGPHOS for AHS of ketones in 2006 (Scheme 6.3, a). [21] In 2007, Choudary combined nanocrystalline copper oxide with (*S*)-BINAP to achieve AHS of ketones with good yields and excellent enantioselectivity in 2007 (Scheme 6.3, b). [22] Shi et al. also demonstrated AHS of ketones in air using mesoporous silica KIT-6 supported superparamagnetic $CuFe_2O_4$ nanoparticles with (*S*)-Xyl-P-Phos (Scheme 6.3, c). [23] Although these three different immobilized copper complexes with homogeneous chiral ligands may produce high yields and enantioselectivity, the cost remains exorbitant when compared to the price of chiral ligands.

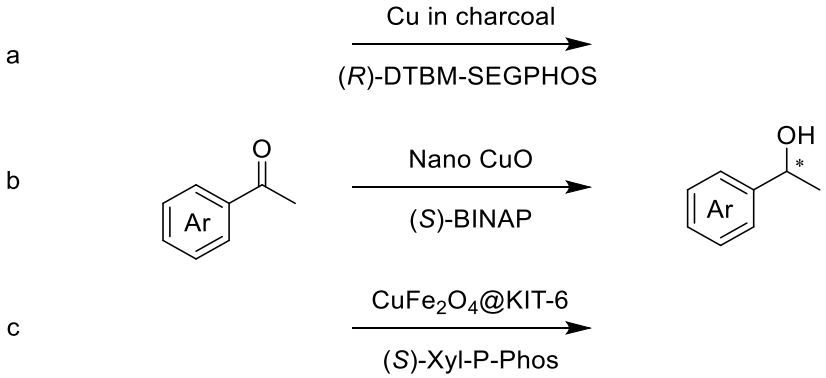

Scheme 6.3 Reusable copper-ligand catalyzed asymmetric hydrosilylation of ketones [21-23]

Converting the ligands into reusable materials is more cost effective. Gade and co-workers devised two methods to immobilize chiral BINAP on dendrimers to generate reusable materials, which could merge with copper salt to achieve AHS of ketones for several times without observable loss of enantioselectivity and activity. [24] However, higher steric requirements must be met for the supporting dendrimers in order to make the reusable materials completely soluble.

Given the strong swelling property of chiral BINAP-POP, there is a good chance that Cu-BINAP-POP SACs can achieve AHS of ketones with high efficiency and enantioselectivity, and can be recyclable.

6.2 Optimization of the reaction conditions

Initially, AHS of acetophenone using Cu-BINAP-POP SACs was chosen as a model reaction. $[Cu(CH_3CN)_4]PF_6$, $[(PPh_3)CuH]_6$, $CuSO_4$, CuO, and CuCl were found to be completely inactive (Table 6.1, entries 1-4 and 7), although $CuCl_2$ produced a low yield (12%) of chiral product with moderate ee (60%) (Table 6.1, entry 6). According to the Cu-BINAP-Base catalytic system

described in the literature, [14a] CuCl had a 26% yield and 79% ee in the presence of NaO^{t}Bu (Table 6.1, entry 5). It showed strong base NaO^{t}Bu could benefit for CuCl-BINAP-POP AHS. $Cu(OAc)_2$ formed the chiral second alcohol with an excellent yield 96% and a good ee 78% (Table 6.1, entry 8). $Cu(OAc)_2$ was chosen as the copper salt since it had the same level ee value and excellent yield without any additives. Another chiral BINAP-POP-7 provided a lower yield (81%) and similar ee (Table 6.1, entry 9). Strong base NaO^{t}Bu did not have a big change for $Cu(OAc)_2$-BINAP-POP AHS (Table 6.1, entry 10). Replacing the solvent from toluene to THF made no difference (Table 6.1, entry 11). Various silanes were also investigated in order to improve the performance of $Cu(OAc)_2$-BINAP-POP AHS (Table 6.1, entries 12-14). DEMS showed no substantial improvement, whereas PTMS totally inhibited catalytic activity. When $PhSiH_3$ was used as the silane source, the yield and ee increased slightly. With the decreasing of the temperature, the ee value increased remarkably (Table 6.1, entries 15-16). High ee (92%) was obtained as homogeneous AHS at -78°C. Although a slightly drop of yield, it was still on the homogeneous level. There was no catalytic activity when $PhSiH_3$ was replaced by PMHS at -78°C (Table 6.1, entry 17). Considering the low temperature affects the catalytic activity and the swelling property of BINAP-POP, 10 h reaction time was acceptable. The optimized conditions were shown as Table 6.1 entry16.

Table 6.1 Optimization of reaction conditions for asymmetric hydrosilylation of ketones

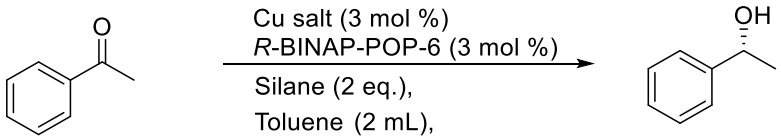

0.25 mmol

Entry	Cu salt	Base(3 mol%)	Silane	Yield[%][a]	ee[%][b]
1	$[Cu(CH_3CN)_4]PF_6$	-	PMHS	0	-
2	$[(PPh_3)CuH]_6$	-	PMHS	0	-
3	$CuSO_4$	-	PMHS	0	-
4	CuCl	-	PMHS	0	-
5	CuCl	NaO^{t}Bu	PMHS	26	79
6	$CuCl_2$	-	PMHS	12	60
7	CuO	-	PMHS	0	-
8	$Cu(OAc)_2$	-	PMHS	96	78
9[c]	$Cu(OAc)_2$	-	PMHS	81	77
10	$Cu(OAc)_2$	NaO^{t}Bu	PMHS	93	77
11[d]	$Cu(OAc)_2$	-	PMHS	91	75
12	$Cu(OAc)_2$	-	DEMS	95	77
13	$Cu(OAc)_2$	-	PTMS	0	-
14	$Cu(OAc)_2$	-	$PhSiH_3$	97	79
15[e]	$Cu(OAc)_2$	-	$PhSiH_3$	96	85
16[f]	$Cu(OAc)_2$	-	$PhSiH_3$	93	92
17[f]	$Cu(OAc)_2$	-	PMHS	1	-

[a] Yield quantified by ^{1}H-NMR. [b] Enantiomeric exces determined by chiral HPLC. [c] POP-7. [d] THF as solvent. [e] -20 °C,10 h. [f] -78 °C,10 h.

6.3 Substrate scope

The substrate scope and generality of AHS of ketones were investigated using the optimized conditions with a series of derivatives of acetophenone, and the corresponding chiral secondary alcohols were obtained in excellent yields and good ee (Table 6.2). A wide range of both electron-withdrawing groups and electron-donating groups *para*-substituted acetophenone derivatives demonstrated very high yields ranging from 90% to 100%, and high ee values ranging from 79% to 99% (entries 2-10). When compared to *para*-chloroacetophenone, the yield and ee value of 3′-chloroacetophenone droped slightly from 97% to 94% and 91% to 82%, respectively (entry 11). 2-Acetonaphthone had a 100% yield and 79% ee, which was same level ee as homogeneous AHS (entry 12). Disubstituted acetophenone (4-methyl-3-nitroacetophenone) was also evaluated with 92% yield and 86% ee, which was higher than ee of 2-acetonaphthone (entry 13). Overall, the scope indicated that this Cu-BINAP-POP catalytic system was highly tolerant to a wide range of acetophenone derivatives.

Table 6.2 Substrate scope

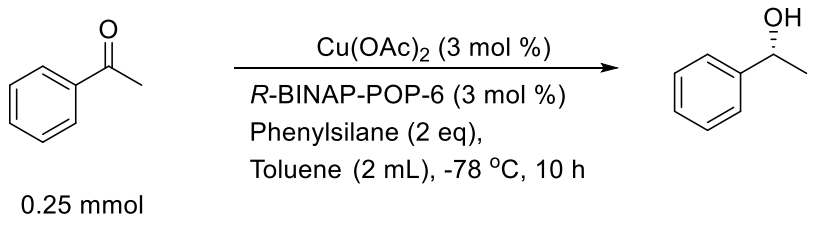

0.25 mmol

Entry	ketone	Yield[%][a]	ee[%][b]
1	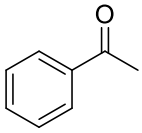	93	92
2	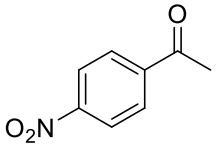	92	96
3	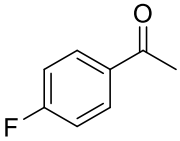	90	99
4	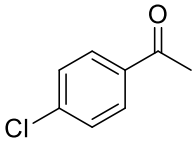	97	91

[a] Yield quantified by ^{1}H-NMR.

[b] Enantiomeric excess determined by chiral HPLC.

Table 6.2 (Continued)

Entry	ketone	Yield[%][a]	ee[%][b]
5	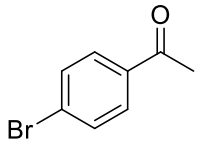	98	91
6	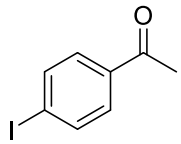	96	83
7	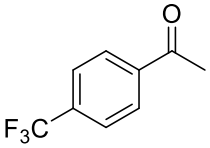	99	90
8	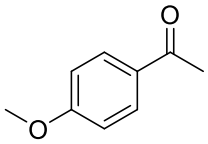	100	79
9	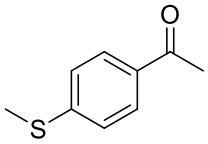	98	91
10	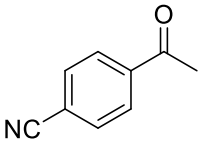	96	89
11	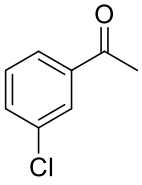	94	82
12	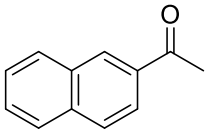	100	79
13	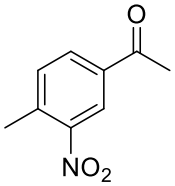	92	86

[a] Yield quantified by ^{1}H-NMR.

[b] Enantiomeric excess determined by chiral HPLC.

6.4 Recycling

Recyclability is the essential property of POP as a heterogeneous catalyst. In order to test whether the BINAP-POP could perform recycling reactions, two standard reactions were run under the optimized conditions (Table 6.2, entries 1 and 3). BINAP-POP is easy to collect after washing with ethyl acetate and drying in the oven. Unfortunately, the low yield (12%) demonstrated that the first recycle run did not work without the addition of fresh $Cu(OAc)_2$ (Table 6.3, entry 2). The reason may be the Cu-BINAP-POP catalyst decomposed in the hydrolysis step. However, the BINAP-POP remained its original size and ^{31}P NMR revealed it did not change. The Cu-BINAP-POP catalytic system could be recovered by adding fresh $Cu(OAc)_2$ (Table 6.3, entries 4-6). To our delight, the enantioselectivity was the same as the first run (92%), and the yield was still at a high level (83%). It was acceptable that the yield had a slight drop after three recycle reactions. Therefore, BINAP-POP demonstrated high recyclability. Maintaining consistent enantioselectivity and high reaction activity, and ease of separation of POP may have a great potential in the future.

Table 6.3 Recycling experiments

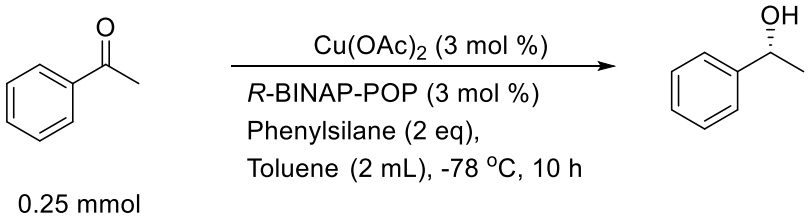

0.25 mmol

Entry	Run times	Modifications	Yield[%][a]	ee[%][b]
1	1	-	93	92
2	2	-	12	-
3	1	-	93	92
4	2	$Cu(OAc)_2$ (3 mol%)	89	92
5	3	$Cu(OAc)_2$ (3 mol%)	87	92
6	4	$Cu(OAc)_2$ (3 mol%)	83	92

[a] Yield quantified by ^1H-NMR.

[b] Enantiomeric excess determined by chiral HPLC.

6.5 Summary

The first Cu-BINAP-POP SACs was investigated for AHS of acetophenone and a series of derivatives. The catalytic system showed excellent activity (90-100%), high enantioselectivity (79-99%), and good functional groups tolerance. The Cu-BINAP-POP SACs performance was comparable to homogeneous catalysis. Ease separation of BINAP-POP is a highly appealing property. The BINAP-POP can be recycled three times; meanwhile, the catalytic system can maintain excellent enantioselectivity and high activity. BINAP-POPs have great potential as stable SACs in future catalysis applications.

6.6 Characterization of chiral (*R*)-BINAP-POP-6

6.6.1 Thermal Gravimetric Analysis (TGA)

There is no loss weight of POP-6 from 0 ˚C to 135 ˚C, which has a higher decompose temperature than POP-5 (100˚C in asymmetric α-arylation of ketones). A 5% of weight loss was recorded by TGA accompanied by an endothermic DTA in a temperature range of 100-250 ˚C. It is a smaller percentage than POP-5 (10%). The reason for these two differences may be that POP-6 has a higher component content of Arabic acacia gum. Here an 80 % weight loss of POP-6 from 300 ˚C to 400 ˚C is the same as POP-5. The decomposition of the organic block from POP-6 has an exothermic DTA peak, which was shown by the weight decrease from 20% to 10% at 400 ˚C. In the asymmetric hydrosilylation of ketones project, the catalytic reaction temperature is below 0 ˚C, and POP-6 can maintain stablility without loss of weight.

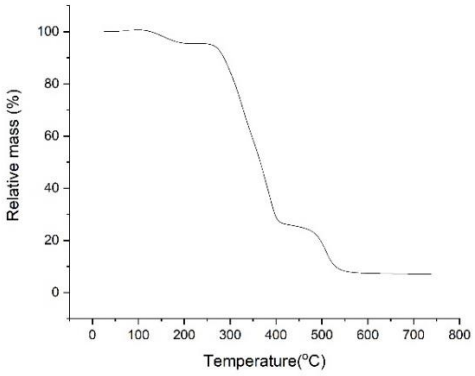

Figure 6.2 TGA of **POP-6**

6.6.2 Scanning Electron Microscopy (SEM)

SEM shows that the diameter of POP-6 is around 400 μm which much bigger than POP-5. The surface of POP-6 is irregular. There are some protruding clusters on the surface. It also has tiny holes to form the SACs catalyst.

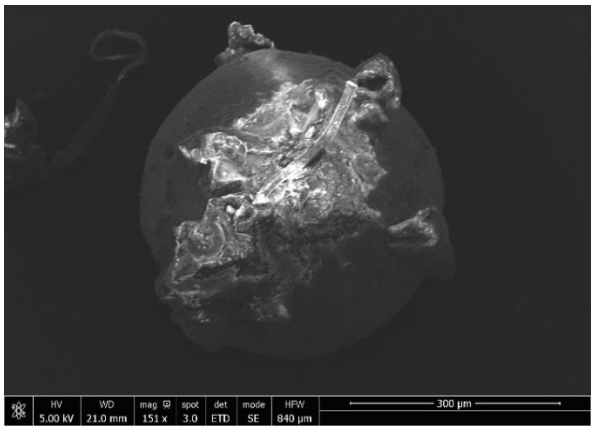

Figure 6.3 SEM image of **POP-6**

6.6.3 N_2-physisorption

The surface area of POP-6 (102.3192 m^2/g) is twice that of POP-5 (53.8268 m^2/g), and the pore volume of POP-6 (0.187223 cm^3/g) is 2.6 times that of POP-5 (0.071535 cm^3/g). These data are in line with the fact that the amount of acacia gum in POP-6 is twice as much as in POP-5.

6.7 Experimental

Chemicals

All chemicals were reagent grade and used as received without further purification. CuCl, $CuCl_2$, $Cu(OAc)_2$, $CuSO_4$, CuO, $[Cu(CH_3CN)_4]PF_6$, $[(PPh_3)CuH]_6$, sodium *tert*-butoxide, dibenzyl ether, NH_4F, $PhSiH_3$, methyldiethoxysilane, phenyltrimethylsilane, polymethylhydrosiloxane, are acquired from Sigma Aldrich.

Equipments

Anhydrous solvents were from Puresolv MD-7 (a solvent purification system). Quanta 200 ESEM FEG microscope (FEI) was used for SEM images. Micrometrics 3Flex instrument measured the BET and surface area and pore volume of POPs. Mettler Toledo TGA/DSC 1 STARe System test the TGA of POPs. ^{1}H-NMR, ^{13}C-NMR, and ^{31}P-NMR spectra were measured on a Bruker Ascend 400 (400 MHz) spectrometer. The deuterated solvents were $CDCl_3$ and d_8-Toluene. Silica gel 60 was used for column chromatography. MS was carried out on either GC-MS/FID analysis on an Agilent 7890A GC equipped with an HP-5 column and a 5975C VLMSD with triple-axis detector (EI) or Waters AQUITY UPLC system equipped with PDA and SQD2 electrospray (ESI) MS detector. The enantiomeric excess was measured by a chiral HPLC with stationary phases.

General procedure for the hydrosilylation reaction

$Cu(OAc)_2$ (1.4 mg, 0.0075 mmol, 3 mol%), R-BINAP-POP-6 (56.4 mg, 0.0075 mmol, 3 mol%) were weighed out under air and placed in a 4-mLscrew-capped vial equipped with a magnetic stirring bar. The vial was made inert by 3 vacuum/nitrogen cycles with Schlenk techniques. Dry toluene (1 mL) was added under nitrogen and the mixture was stirred for 1 h at room temperature. After cooling to -78 °C (dry ice in acetone), the silane was added by a Hamilton syringe and the vial was stirred for another 1 h. A solution of ketone (0.25 mmol) and internal standard (dibenzyl ether, 0.0625 mmol) in toluene (1 mL) was injected into the vial. The mixture solution was stirred at -78 °C for 10 h. Upon completion, the reaction mixture was treated with 1 mL of NH_4F in methanol and the resulting solution was stirred for 1 h at room temperature. The mixture was filtered with a glass funnel, washed with ethyl acetate, and concentrated by rotation. The NMR yield was analyzed by 400 MHz NMR. The enantiomeric excess was measured by chiral HPLC after purification of the crude mixture by silica gel chromatography.

Recycling Experiment

An experiment was started as a Standard Catalytic Reaction with acetophenone (0.25 mmol) and internal standard (dibenzyl ether, 0.0625 mmol). After 10 h, the reaction mixture was treated with 1 mL of NH_4F in methanol and the resulting solution was stirred for 1 h at room temperature. The POP was collected by a glass funnel and washed with ethyl acetate (10 mL x3). Then POP was dried in a vacuum oven overnight for next time use. The crude mixture was concentrated under vacuum. NMR analyzed the yield and the enantiomeric excess was quantified by chiral HPLC. The recycling experiment was repeated as Standard Catalytic Reaction with $Cu(OAc)_2$, recycled POP, silane, acetophenone, and internal standard.

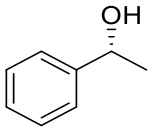

(*R*)-1-phenylethan-1-ol

The title product was synthesized according to Standard Catalytic Reaction. The crude product was purified by silica gel chromatography (EtOAc/hexane) affording the title product as a colorless oil in 93% (92% ee). The enantiomeric excess was determined by Chiralpack OJ-H column with hexane/isopropanol = 95:5, 1.0 mL/min; retention times = 9.12 min for minor isomer and 9.85 min for major isomer.

^{1}H NMR (400 MHz, Chloroform-*d*) δ 7.42 – 7.35 (m, 4H), 7.33 – 7.28 (m, 1H), 4.91 (q, *J* = 6.4 Hz, 1H), 2.09 (s, 1H), 1.52 (d, *J* = 6.5 Hz, 3H). ^{13}C NMR (101 MHz, Chloroform-*d*) δ 145.8, 128.5, 127.5, 125.4, 70.4, 25.2. MS (EI) m/z ($M^{\cdot+}$) calcd for $C_8H_{10}O$: 122, found 122. NMR data are in accordance with literature values. [14c]

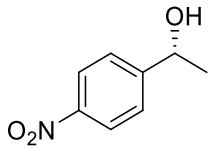

(*R*)-1-(4-nitrophenyl)ethan-1-ol

The title product was synthesized according to Standard Catalytic Reaction. The crude product was purified by silica gel chromatography (EtOAc/hexane) affording the title product as a colorless oil in 92% (96% ee). The enantiomeric excess was determined by Chiralpack OJ-H column with hexane/isopropanol = 95:5, 0.7 mL/min; retention times = 43.17 min for minor isomer and 44.18 min for major isomer.

^{1}H NMR (400 MHz, Chloroform-*d*) δ 8.25 – 8.20 (m, 2H), 7.60 – 7.53 (m, 2H), 5.05 (q, *J* = 6.5 Hz, 1H), 1.96 (s, 1H), 1.54 (d, *J* = 6.5 Hz, 3H). ^{13}C NMR (101 MHz, Chloroform-d) δ 153.0, 126.1, 123.8, 69.5, 25.5. MS (EI) m/z ($M^{\cdot+}$) calcd for $C_8H_9NO_3$: 167, found 167. NMR data are in accordance with literature values. [14c]

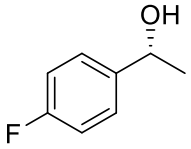

(*R*)-1-(4-fluorophenyl)ethan-1-ol

The title product was synthesized according to Standard Catalytic Reaction. The crude product was purified by silica gel chromatography (EtOAc/hexane) affording the title product as a colorless oil in 90% (99% ee). The enantiomeric excess was determined by Chiralpack OJ-H column with hexane/isopropanol = 97:3, 1.0 mL/min; retention times = 28.03 min for major isomer and 29.98 min for minor isomer.

^{1}H NMR (400 MHz, Chloroform-d) δ 7.36 – 7.31 (m, 2H), 7.06 – 7.00 (m, 2H), 4.89 (q, *J* = 6.5 Hz, 1H), 1.86 (s, 1H), 1.48 (d, J = 6.4 Hz, 3H). ^{13}C NMR (101 MHz, Chloroform-d) δ 163.3, 160.9, 141.5, 141.5, 127.1, 127.0, 115.4, 115.2, 69.8, 25.3. MS (EI) m/z ($M^{\cdot+}$) calcd for C_8H_9FO : 140, found 140. NMR data are in accordance with literature values. [14c]

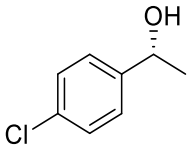

(*R*)-1-(4-chlorophenyl)ethan-1-ol

The title product was synthesized according to Standard Catalytic Reaction. The crude product was purified by silica gel chromatography (EtOAc/hexane) affording the title product as a colorless oil in 97% (91% ee). The enantiomeric excess was determined by Chiralpack OD-H column with hexane/isopropanol = 97:3, 1.0 mL/min; retention times = 12.27 min for minor isomer and 13.72 min for major isomer.

^{1}H NMR (400 MHz, Chloroform-d) δ 7.31 (s, 4H), 4.89 (q, *J* = 6.5 Hz, 1H), 1.78 (s, 1H), 1.48 (d, *J* = 6.5 Hz, 3H). ^{13}C NMR (101 MHz, Chloroform-d) δ 144.2, 133.1, 128.6, 126.8, 69.8, 25.3. MS (EI) m/z ($M^{\cdot+}$) calcd for C_8H_9ClO : 156, found 156. NMR data are in accordance with literature values. [14c]

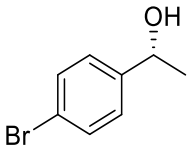

(*R*)-1-(4-bromophenyl)ethan-1-ol

The title product was synthesized according to Standard Catalytic Reaction. The crude product was purified by silica gel chromatography (EtOAc/hexane) affording the title product as a colorless oil in 98% (91% ee). The enantiomeric excess was determined by Chiralpack OD-H column with hexane/isopropanol = 97:3, 1.0 mL/min; retention times = 13.33 min for major isomer and 14.87 min for minor isomer.

^{1}H NMR (400 MHz, Chloroform-d) δ 7.49 – 7.45 (dt, *J* = 6.6, 1.5 Hz, 2H), 7.25 (dt, *J* = 6.6, 1.5 Hz, 2H), 4.87 (q, *J* = 6.5 Hz, 1H), 1.75 (s, 1H), 1.47 (d, *J* = 6.4 Hz, 3H). ^{13}C NMR (101 MHz, Chloroform-d) δ 144.8, 131.6, 127.1, 121.2, 69.8, 25.3. MS (EI) m/z ($M^{\cdot+}$) calcd for C_8H_9BrO : 200, found 200. NMR data are in accordance with literature values. [14c]

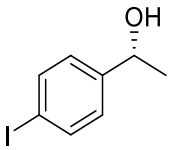

(*R*)-1-(4-iodophenyl)ethan-1-ol

The title product was synthesized according to Standard Catalytic Reaction. The crude product was purified by silica gel chromatography (EtOAc/hexane) affording the title product as a colorless oil in 96% (83% ee). The enantiomeric excess was determined by Chiralpack OJ-H column with hexane/isopropanol = 97:3, 1.0 mL/min; retention times = 19.28 min for minor isomer and 20.03 min for minor isomer.

^{1}H NMR (400 MHz, Chloroform-*d*) δ 7.67 (d, *J* = 8.3 Hz, 2H), 7.13 (d, *J* = 8.3 Hz, 2H), 4.85 (q, *J* = 6.4 Hz, 1H), 1.76 (s, 1H), 1.47 (d, *J* = 6.4 Hz, 3H). ^{13}C NMR (101 MHz, Chloroform-*d*) δ 145.5, 137.5, 127.4, 92.7, 69.9, 25.2. MS (EI) m/z ($M^{\cdot+}$) calcd for C_8H_9IO : 248, found 248. NMR data are in accordance with literature values. [25]

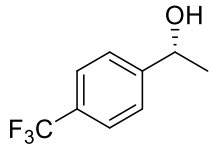

(*R*)-1-(4-(trifluoromethyl)phenyl)ethan-1-ol

The title product was synthesized according to Standard Catalytic Reaction. The crude product was purified by silica gel chromatography (EtOAc/hexane) affording the title product as a colorless oil in 99% (90% ee). The enantiomeric excess was determined by Chiralpack OJ-H column with

hexane/isopropanol = 99:1, 1.0 mL/min; retention times = 28.17 min for minor isomer and 31.07 min for major isomer.

^{1}H NMR (400 MHz, Chloroform-*d*) δ 7.62 (d, *J* = 7.8 Hz, 2H), 7.49 (d, *J* = 8.8 Hz, 2H), 4.95 (q, *J* = 6.5 Hz, 1H), 2.29 (bs, 1H), 1.51 (d, *J* = 6.5 Hz, 3H). ^{13}C NMR (101 MHz, Chloroform-*d*) δ 149.7, 130.1, 129.8, 129.4, 129.1, 125.6, 125.5, 125.4, 125.4, 125.4, 69.8, 25.3. MS (EI) m/z ($M^{\cdot+}$) calcd for $C_9H_9F_3O$: 190, found 190. NMR data are in accordance with literature values. [14c]

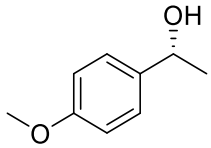

(*R*)-1-(4-methoxyphenyl)ethan-1-ol

The title product was synthesized according to Standard Catalytic Reaction. The crude product was purified by silica gel chromatography (EtOAc/hexane) affording the title product as a colorless oil in 99% (79% ee). The enantiomeric excess was determined by Chiralpack OD-H column with hexane/isopropanol = 97:3, 1.0 mL/min; retention times = 13.67 min for minor isomer and 18.00 min for major isomer.

^{1}H NMR (400 MHz, Chloroform-*d*) δ 7.30 (dt, *J* = 8.0, 1.3 Hz, 2H), 6.89 (dt, *J* = 8.0, 2.6 Hz, 2H), 4.86 (q, *J* = 6.4 Hz, 1H), 3.81 (s, 3H), 1.72 (s, 1H), 1.48 (d, *J* = 6.4 Hz, 3H). ^{13}C NMR (101 MHz, Chloroform-*d*) δ 159.0, 138.0, 126.7, 113.9, 70.0, 55.3, 25.0. MS (EI) m/z ($M^{\cdot+}$) calcd for $C_9H_{12}O_2$: 152, found 152. NMR data are in accordance with literature values. [14b]

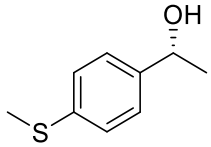

(*R*)-1-(4-(methylthio)phenyl)ethan-1-ol

The title product was synthesized according to Standard Catalytic Reaction. The crude product was purified by silica gel chromatography (EtOAc/hexane) affording the title product as a colorless oil in 98% (91% ee). The enantiomeric excess was determined by Chiralpack OJ-H column with hexane/isopropanol = 99:1, 1.0 mL/min; retention times = 92.15 min for major isomer and 108.85 min for minor isomer.

^{1}H NMR (400 MHz, Chloroform-*d*) δ 7.30 (d, *J* = 8.2 Hz, 2H), 7.27 – 7.24 (m, 2H), 4.87 (q, *J* = 6.4 Hz, 1H), 2.49 (s, 3H), 1.78 (br, 1H), 1.48 (d, *J* = 6.5 Hz, 3H). ^{13}C NMR (101 MHz, Chloroform-*d*) δ 142.8, 137.5, 126.8, 126.0, 70.0, 25.1, 16.0. MS (EI) m/z ($M^{\cdot+}$) calcd for $C_9H_{12}OS$: 168, found 168. NMR data are in accordance with literature values. [26]

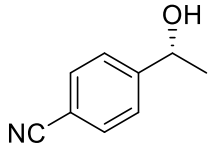

(*R*)-4-(1-hydroxyethyl)benzonitrile

The title product was synthesized according to Standard Catalytic Reaction. The crude product was purified by silica gel chromatography (EtOAc/hexane) affording the title product as a colorless

oil in 96% (89% ee). The enantiomeric excess was determined by Chiralpack OJ-H column with hexane/isopropanol = 90:10, 1.0 mL/min; retention times = 15.25 min for minor isomer and 16.38 min for major isomer.

^{1}H NMR (400 MHz, Chloroform-*d*) δ 7.66 – 7.61 (m, 2H), 7.49 (d, *J* = 8.0 Hz, 2H), 4.96 (q, *J* = 6.5 Hz, 1H), 1.94 (s, 1H), 1.50 (d, *J* = 6.5 Hz, 3H). ^{13}C NMR (101 MHz, Chloroform-*d*) δ 151.0, 132.4, 126.1, 118.9, 111.1, 69.7, 25.4. MS (EI) m/z ($M^{\cdot+}$) calcd for C_9H_9NO : 147, found 147. NMR data are in accordance with literature values. [20a]

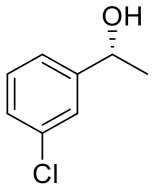

(*R*)-1-(3-chlorophenyl)ethan-1-ol

The title product was synthesized according to Standard Catalytic Reaction. The crude product was purified by silica gel chromatography (EtOAc/hexane) affording the title product as a colorless oil in 94% (82% ee). The enantiomeric excess was determined by Chiralpack OJ-H column with hexane/isopropanol = 95:5, 1.0 mL/min; retention times = 9.67 min for minor isomer and 10.70 min for major isomer.

^{1}H NMR (400 MHz, Chloroform-*d*) δ 7.40 (t, *J* = 1.8 Hz, 1H), 7.32 – 7.24 (m, 3H), 4.90 (q, *J* = 6.5 Hz, 1H), 1.90 (s, 1H), 1.51 (d, *J* = 6.5 Hz, 3H). ^{13}C NMR (101 MHz, Chloroform-*d*) δ 147.8, 134.4, 129.8, 127.5, 125.6, 123.5, 69.8, 25.3. MS (EI) m/z ($M^{\cdot+}$) calcd for C_8H_9ClO : 156, found 156. NMR data are in accordance with literature values. [13c]

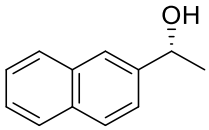

(*R*)-1-(naphthalen-2-yl)ethan-1-ol

The title product was synthesized according to Standard Catalytic Reaction. The crude product was purified by silica gel chromatography (EtOAc/hexane) affording the title product as a colorless oil in 99% (79% ee). The enantiomeric excess was determined by Chiralpack OJ-H column with hexane/isopropanol = 95:5, 1.0 mL/min; retention times = 25.23 min for minor isomer and 31.55 min for major isomer.

^{1}H NMR (400 MHz, Chloroform-*d*) δ 7.89 – 7.82 (m, 4H), 7.56 – 7.48 (m, 3H), 5.15 – 5.06 (m, 1H), 1.92 (d, *J* = 3.6 Hz, 1H), 1.61 (d, *J* = 6.5 Hz, 3H). ^{13}C NMR (101 MHz, Chloroform-*d*) δ 143.2, 133.3, 132.9, 128.3, 128.0, 127.7, 126.2, 125.8, 124.1, 123.8, 70.5, 25.1. MS (EI) m/z ($M^{\cdot+}$) calcd for $C_{12}H_{12}O$: 172, found 172. NMR data are in accordance with literature values. [20a]

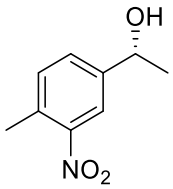

(*R*)-1-(4-methyl-3-nitrophenyl)ethan-1-ol

The title product was synthesized according to Standard Catalytic Reaction. The crude product was purified by silica gel chromatography (EtOAc/hexane) affording the title product as a colorless oil in 92% (86% ee). The enantiomeric excess was determined by Chiralpack OJ-H column with hexane/isopropanol = 95:5, 1.0 mL/min; retention times = 22.03 min for minor isomer and 22.88 min for major isomer.

^{1}H NMR (400 MHz, Chloroform-*d*) δ 7.98 (d, *J* = 1.8 Hz, 1H), 7.51 (dd, *J* = 7.9, 1.9 Hz, 1H), 7.32 (d, *J* = 7.9 Hz, 1H), 4.96 (q, *J* = 6.5 Hz, 1H), 2.58 (s, 3H), 1.89 (br, 1H), 1.51 (d, *J* = 6.5 Hz, 3H). ^{13}C NMR (101 MHz, Chloroform-*d*) δ 149.2, 145.2, 132.9, 132.4, 130.0, 121.6, 69.2, 25.3, 20.1. MS (EI) m/z ($M^{\cdot+}$) calcd for $C_9H_{11}NO_3$: 181, found 181. NMR data are in accordance with literature values. [27]

6.8 References

[1] a) Breuer, M., Ditrich, K., Habicher, T., Hauer, B., Keßeler, M., Stürmer, R. and Zelinski, T., *Angew. Chem. Int. Ed*. **2004**, *43*, 788-824. b) Astelford, B.A. and Weigel, L.O., in *Chirality in Industry II*, (Ed.: A. N. Collins), Wiley, New York, **1997**, 99. c) Farina, V., Reeves, J.T., Senanayake, C.H. and Song, J.J., *Chem. Rev*., **2006**, *106*, 2734–2793. d) Robertson, D.W., Krushinski, J.H., Fuller, R.W. and Leander, J.D., *J. Med. Chem.*, **1988**, *31*, 1412–1417. e) Kamal, A., Malik, M.S., Shaik, A.A. and Azeeza, S., *J. Mol. Catal. B: Enzym.*, **2009**, *58*, 132–137. f) Nishii, H., Chiba, T., Morikami, K., Fukami, T.A., Sakamoto, H., Ko, K. and Koyano, H., *Bioorg. Med. Chem. Lett.* **2010**, *20*, 1405-1409. g) Wan, W.L., He, Y., Guan, M., Li, X.L., Cheng, X. and Wu, Y., *Chin. Chem. Lett*. **2013**, *24*, 1118-1122. h) Klingler, F.D. *Acc. Chem. Res*. **2007**, *40*, 1367-1376. i) Van der Stelt, C., Heus, W.J. and Nauta, W.T., *Arzneim. Forsch.* **1969**, *19*, 2010-2012.

[2] a) Krabbe, S.W., Hatcher, M.A., Bowman, R.K., Mitchell, M.B., McClure, M.S. and Johnson, J.S., *Org. Lett.* **2013**, *15*, 4560-4563. b) Cui, Y.M., Wang, L.L., Kwong, F.Y. and Sun, W., *Chin. Chem. Lett*. **2010**, *21*, 1403-1406.

[3] a) Cetin, A. and Dayan, O., *Chin. J. Chem*. **2009**, *27*, 978-982. b) Liu, G., Yao, M., Zhang, F., Gao, Y., Li, H., *Chem. Commun*. **2008**, *3*, 347-349.

[4] a) Seliger, J. and Oestreich, *Chemistry-A European Journal*, **2019**, *25*, 9358-9365. b) Sartori, G., Ballini, R., Bigi, F., Bosica, G., Maggi, R. and Righi, P., *Chem. Rev*. **2004**, *104*, 199-250. c) Arena, C.G., *MiniRev. Org. Chem*. **2009**, *6*, 159 –167. d) Riant, O., Mostefai, N. and Courmarcel, J., *Synthesis* **2004**, *18*, 2943 – 2958.

[5] a) Ojima, I., Nihonyanagi, M. and Nagai, Y., *J. Chem. Soc., Chem. Commun*. **1972**, 938-938. b) Ojima, I., Kogure, T., Nihonyanagi, M. and Nagai, Y., *Bull. Chem. Soc. Jpn*. **1972**, *45*, 3506-3506. c) Ojima, I., Kogure, T., Nihonyanagi, M. and Nagai, Y., *Bull. Chem. Soc. Jpn.* **1972**, *45*, 3722-3722. d) Corriu, R.J.P. and Moreau, J.J.E., *J. Chem. Soc., Chem. Commun*. **1973**, 38-39. e) Dumont, W., Poulin, J.C., Phat, D.T. and Kagan, H.B., *J. Am. Chem. Soc*. **1973**, *95*, 8295-8299.

[6] a) Zhu, G., Terry, M. and Zhang, X., *J. Organomet. Chem*. **1997**, *547*, 97-101. b) Nishibayashi, Y., Takei, I., Uemura, S. and Hidai, M., *Organometallics* **1998**, *17*, 3420-3422. c) Song, C., Ma, C., Ma, Y., Feng, W., Ma, S., Chai, Q. and Andrus, M.B., *Tetrahedron Lett*., **2005**, *46*, 3241-3244.

[7] a) Chen, L., Liu, Y., Hou, G., Song, H. and Zi, G., *Inorg. Chem. Commun*. **2013**, *29*, 141-144. b) Kawabata, S., Tokura, H., Chiyojima, H., Okamoto, M. and Sakaguchi, S., *Adv. Synth. Catal*. **2012**, *354*, 807-812. c) Shinohara, K., Kawabata, S., Nakamura, H., Manabe, Y. and Sakaguchi, S., *Eur. J. Org Chem*. **2014**, *25*, 5532-5539. d) Szewczyk, M., Bezłada, A. and Mlynarski, J., *ChemCatChem*, **2016**, *8*, 3575-3579. e) Teramoto, H. and Sakaguchi, S., *J. Organomet. Chem*,**2018**, *875*, 52-58.

[8] a) Brunner, H. and Riepl, G., *Angew. Chem. Int. Ed.* **1982,** *21*, 377-379. b) De Vekki, D.A., Uvarov, V.M., Reznikov, A.N. and Skvortsov, N.K., *Rus. Chem. Bull. Int. Ed.* **2008**, *57*, 349-357.

[9] a) Rahimian, K. and Harrod, J.F., *Inorg. Chim. Acta* **1998**, *270*, 330 –336. b) Yun, J. and Buchwald, S.L., *J. Am. Chem. Soc.* **1999,** *121*, 5640-5644. c) Beagley, P., Davies, P.J., Blacker, A.J. and White, C., *Organometallics* **2002**, *21*, 5852 – 5858. d) Bandini, M., Bernardi, F., Bottoni, A., Cozzi, P.G., Miscione, G.P. and Umani-Ronchi, A., *Eur. J. Org. Chem*. **2003**, *15*, 2972-2984. e) Gan, L. and Brook, M.A., *Can. J. Chem*. **2006**, *84*, 1416.

[10] a) Mastranzo, V.M., Quintero, L., de Parrodi, C.A., Juaristi, E. and Walsh, P.J., *Tetrahedron*, **2004**, *60*, 1781–1789. b) Bette, V., Mortreux, A., Savoia, D. and Carpentier, J.F., *Tetrahedron*, **2004**, *60*, 2837–

2842. c) Bette, V., Mortreux, A., Savoia, D. and Carpentier, J.F., *Adv. Synth. Catal*., **2005**, *347*, 289–302. d) Bandini, M., Melucci, M., Piccinelli, F., Sinisi, R., Tommasi, S. and Umani-Ronchi, A., *Chem. Commun*., **2007**, *43*, 4519–4521. e) Gajewy, J., Kwit, M. and Gawroński, J., *Adv. Synth. Catal*., **2009**, *351*, 1055–1063. f) Inagaki, T., Yamada, Y., Furuta, A., Ito, J.I. and Nishiyama, H., *Synlett*, **2009**, 2, 253–256. g) Marinos, N.A., Enthaler, S. and Driess, M., *ChemCatChem*, **2010**, *2*, 846–853.

[11] Lawrence, N.J. and Bushell, S.M., *Tetrahedron Lett*., **2000**, *41*, 4507–4512.

[12] a) Wenz, J., Vasilenko, V., Kochan, A., Wadepohl, H. and Gade, L.H., *Eur. J. Inorg. Chem*. **2017**, 47, 5545-5556. b) Ma, X., Zuo, Z., Liu, G. and Huang, Z., *ACS Omega* **2017,** *2*, 4688-4692. c) Zhang, L., Zuo, Z., Wan, X. and Huang, Z., *J. Am. Chem. Soc* **2014**, *136*, 15501-15504. d) Chen, J., Xi, T. and Lu, Z., *Org. Lett*. **2014,** *16*, 6452-6455. e) Mukhopadhyay, T.K., Rock, C.L., Hong, M., Ashley, D.C., Groy, T.L., Baik, M.H. and Trovitch, R.J., *J. Am. Chem. Soc*. **2017,** *139*, 4901-4915.

[13] a) Schiwek, C.H., Vasilenko, V., Wadepohl, H. and Gade, L.H., *Chem. Commun*. **2018,** *54*, 9139-9142. b) Wenz, J., Kochan, A., Wadepohl, H. and Gade, L.H., *Inorg. Chem.* **2017,** *56*, 3631-3643. c) Wenz, J., Vasilenko, V., Kochan, A., Wadepohl, H. and Gade, L.H., *Eur. J. Inorg. Chem*. **2017, 47,** 5545-5556.

[14] a) Issenhuth, J.T., Dagorne, S. and Bellemin-Laponnaz, S., *C.R. Chimie* **2010,** *13*, 353-357. b) Liang, M., Xia, X., Liu X. and Li, H., *Chin. J. Chem*. **2015,** *33*,578-582. c) Zhang, X.C., Wu, F.F., Li, S., Zhou, J.N., Wu, J., Li, N., Fang, W., Lam, K.H. and Chan, A.S., *Adv. Synth. Catal*. **2011,** *353*, 1457-1462. d) Albright, A. and Gawley, R.E., *J. Am. Chem. Soc* **2011,** *133*, 19680-19683. e) Zeng, W., Tan, X., Yu, Y., Chen, G.Q. and Zhang, X., *Org. Lett.* **2020,** *22*, 858-862.

[15] a) Bleith, T. and Gade, L.H., *J. Am. Chem. Soc.* **2016,** *138*, 4972-4983. b) Enthaler, S., Junge, K. and Beller, M., *Angew. Chem*. **2008,** *120*, 2531-2535. c) Addis, D., Shaikh, N., Zhou, S., Das, S., Junge, K. and Beller, M., *Chem. Asian J.* **2010,** *5*, 1687-1691. d) Satyanarayana, T., Abraham, S. and Kagan, H.B., *Angew. Chem. Int. Ed.* **2009,** *48*, 456-494. e) Inagaki, T., Ito, A., Ito, J.I. and Nishiyama, H., *Angew. Chem.* **2010**, *49*, 9384-9387. f) Deng, Q.H., Melen, R.L. and Gade, L.H., *Acc. Chem. Res.* **2014**, *47*, 3162-3173.

[16] a) Wu, F.F., Zhou, J.N., Fang, Q., Hu, Y.H., Li, S., Zhang, X.C., Chan, A.S. and Wu, J., *Chem. Asian J*. **2012,** *7*, 2527-2530. b) Qi, S.B., Li, M., Li, S., Zhou, J.N., Wu, J.W., Yu, F., Zhang, X.C., Chan, A.S. and Wu, J., *Org. Biomol. Chem*. **2013,** *11*, 929-937. c) Sauer, D.C., Wadepohl, H. and Gade, L.H., *Inorg. Chem*. **2012,** *51*, 12948-12958. d) Langlotz, B., Wadepohl, H. and Gade, L.H., *Angew. Chem.* **2008**, *47*, 4670-4674. e) Chen, X. and Lu, Z., *Org. Lett.* **2016,** *18*, 4658-4661.

[17] a) Gudun, K.A., Segizbayev, M., Adamov, A., Plessow, P.N., Lyssenko, K.A., Balanay, M.P. and Khalimon, A.Y., *Dalton Trans.* **2019**,*48*, 1732-1746. b) Tafazolian, H., Yoxtheimer, R., Thakuri, R.S. and Schmidt, J.A., *Dalton Trans.* **2017,** *46*, 5431-5440.

[18] Brunner, H. and Miehling, W., *J. Organomet. Chem.* **1984**, *275*, C17-C21.

[19] Lipshutz, B.H., Noson, K., Chrisman, W. and Lower, A., *J. Am. Chem. Soc*. **2003**, *125*, 8779-8789.

[20] a) Junge, K., Wendt, B., Addis, D., Zhou, S., Das, S. and Beller, M., *Chem. Eur J*. **2010,** *16*, 68-73. b) Sui, Y.Z., Zhang, X.C., Wu, J.W., Li, S., Zhou, J.N., Li, M., Fang, W., Chan, A.S. and Wu, J., *Chem. Eur J.* **2012**, *18*, 7486-7492. c) Zhou, J.N., Fang, Q., Hu, Y.H., Yang, L.Y., Wu, F.F., Xie, L.J., Wu, J. and Li, S., *Org Biomol. Chem.* **2014**, *12*, 1009-1017.

[21] Lipshutz, B.H., Frieman, B.A. and Tomaso Jr, A.E., *Angew. Chem. Int. Ed*. **2006**, *45*, 1259-1264.

[22] Kantam, M.L., Laha, S., Yadav, J., Likhar, P.R., Sreedhar, B. and Choudary, B.E., *Adv. Synth. Catal*. **2007**, *349*, 1797-1802.

[23] Li, M., Li, B., Xia, H.F., Ye, D., Wu, J. and Shi, Y., *Green Chemistry*, **2014**, *16*, 2680-2688.

[24] a) Kassube, J.K., Wadepohl, H. and Gade, L.H., *Adv. Synth. Catal*. **2008**, *350*, 1155-1162. b) Kassube, J.K., Wadepohl, H. and Gade, L.H., *Adv. Synth. Catal*. **2009**, *351*, 607-616.

[25] Benítez-Mateos, A.I., San Sebastian, E., Ríos-Lombardía, N., Morís, F., González-Sabín, J. and López-Gallego, F., *Chemistry–A European Journal*, **2017**, *23*, 16843-16852.

[26] Yu, J., Long, J., Yang, Y., Wu, W., Xue, P., Chung, L.W., Dong, X.Q. and Zhang, X., *Org. Lett.* **2017**, *19*, 690-693.

[27] Sappino, C., Primitivo, L., De Angelis, M., Domenici, M.O., Mastrodonato, A., Romdan, I.B., Tatangelo, C., Suber, L., Pilloni, L., Ricelli, A. and Righi, G., *ACS omega*, **2009**, *4*, 21809-21817.

7. Conclusions

Chapter 1 introduced the various applications of catalysis and heterogenized homogeneous catalysts, including mesoporous silica, polymers, MOFs, COFs, and POPs. Chapter 2 introduced SACs and summarized the different strategies to synthesize POPs.

As mentioned in Chapters 1 and 2, heterogeneous SAC plays a vital role in catalytic reactions, and the development of the heterogenization of homogeneous catalysts and their catalytic application has been very topical in recent years. POPs have potential applications in catalysis owing to their good stability, high surface area and swelling, robustness, and high flexibility.

Chapter 3 introduced the nine different types of POP that were synthesized using the general strategy. These POPs were based on three types of ligands: 2,2′-bipyridine, (*R*)-BINAP, and (*R*)-MeO-BIPHEP (Figure 7.1). POP-1, 5, and 6 were used in the following three chapters. POP 2-4 and 7-9 will be applied in other catalysis reactions in the future.

Chapter 4 described the *in-situ* Ir-bpy-POP-1 catalytic system in the direct C(sp^2)-H borylation of arenes. The Ir-bpy-POP-1 active sites exhibited excellent activity and good tolerance. B_2pin_2 could borylate twice the quantity of arenes and release hydrogen gas. This procedure has a high atomic economy and hydrogen can replenish the energy of the earth. The system could be recycled three times with a quantitative yield.

In Chapter 5, the merger of Ni with chiral (*R*)-BINAP-POP-5 was the first example of a catalyst used for the asymmetric α-arylation of ketones with chloroarenes, discussed. This catalytic system exhibited excellent activity and enantioselectivity over a wide substrate scope. Chiral (*R*)-BINAP-POP-5 was easily recovered and could run three times without any loss of enantioselectivity. The gram-scale reaction indicated the high efficiency and promising application of the Ni-BINAP-POP catalytic system for the generation of chiral products in the future.

Chapter 6 demonstrated a formation of $Cu(OAc)_2$ with chiral (*R*)-BINAP-POP-6 for the asymmetric hydrosilylation of ketones with excellent yields and high enantioselectivities. The Cu-BINAP-POP-6 catalytic system could be recycled three times while maintaining consistent enantioselectivity and high activity. The corresponding chiral alcohols could be precursors in the synthesis of many pharmaceuticals.

Overall, POPs exhibited high activity and excellent selectivity in catalytic reactions owing to the formation of heterogeneous SACs. Although there are still challenges in reusing POP-based SACs, POPs have the potential in the catalysis industry.

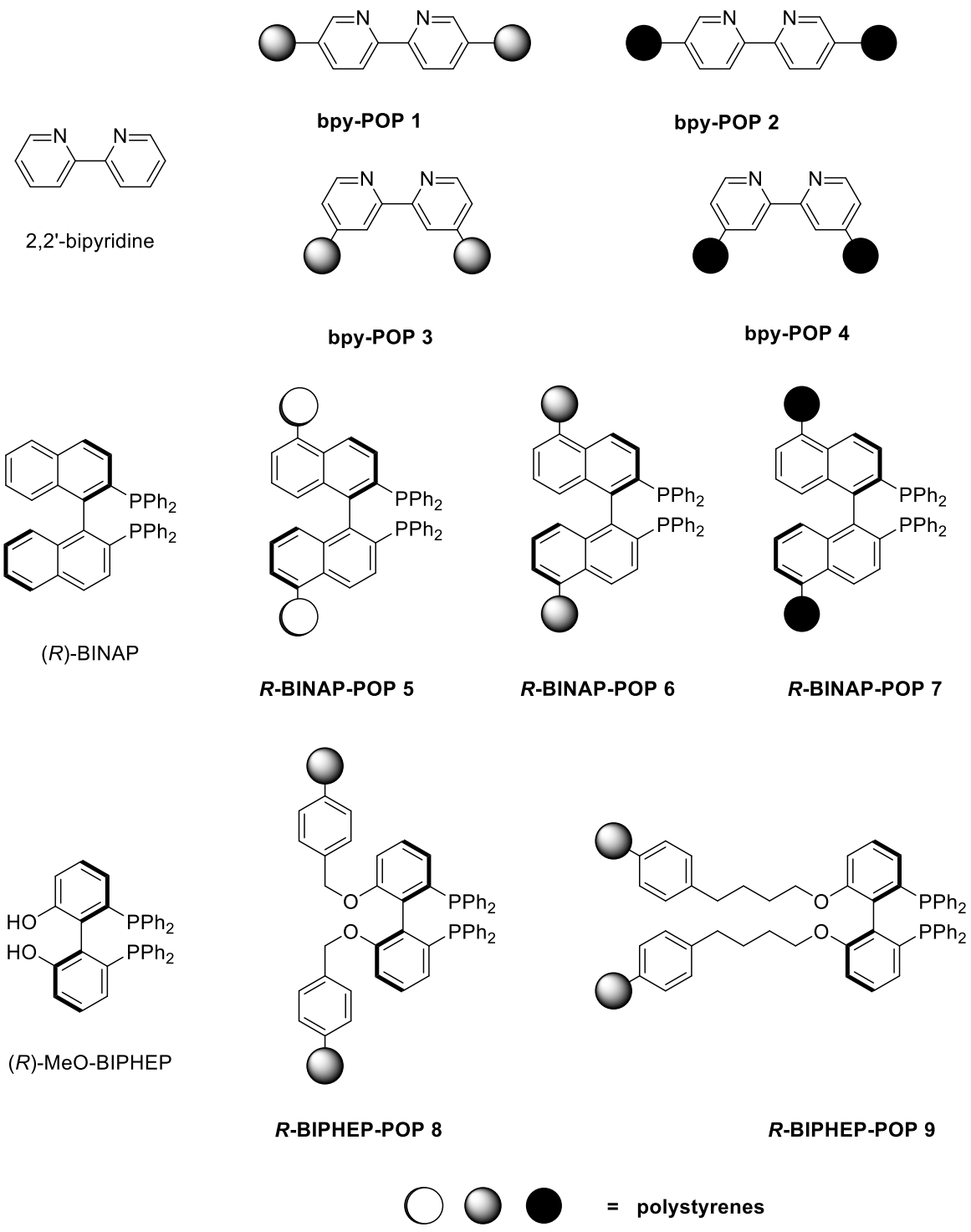

Figure 7.1 Structures of ligands and all POPs

8. Appendix: co-author statements

Declaration of co-authorship at DTU

If a PhD thesis contains articles (i.e. published journal and conference articles, unpublished manuscripts, chapters, etc.) written in collaboration with other researchers, a co-author statement verifying the PhD student's contribution to each article should be made.

If an article is written in collaboration with three or less researchers (including the PhD student), all researchers must sign the statement. However, if an article has more than three authors the statement may be signed by a representative sample, cf. article 12, section 4 and 5 of the Ministerial Order No. 1039, 27 August 2013. A representative sample consists of minimum three authors, which is comprised of the first author, the corresponding author, the senior author, and 1-2 authors (preferably international/non-supervisor authors).

DTU has implemented the Danish Code of Conduct for Research Integrity, which states the following regarding attribution of authorship:

"Attribution of authorship should in general be based on criteria a-d adopted from the Vancouver guidelines[1], and all individuals who meet these criteria should be recognized as authors:

a. Substantial contributions to the conception or design of the work, or the acquisition, analysis, or interpretation of data for the work, *and*
b. drafting the work or revising it critically for important intellectual content, *and*
c. final approval of the version to be published, *and*
d. agreement to be accountable for all aspects of the work in ensuring that questions related to the accuracy or integrity of any part of the work are appropriately investigated and resolved."[2]

For more information regarding definition of co-authorship and examples of authorship conflicts, we refer to DTU Code of Conduct for Research Integrity (pp. 19-22).

By signing this declaration, co-authors permit the PhD student to reuse whole or parts of co-authored articles in their PhD thesis, under the condition that co-authors are acknowledged in connection with the reused text or figure.

It is **important** to note that it is the responsibility of the PhD student to obtain permission from the publisher to use the article in the PhD thesis[3]

[1] International Committee of Medical Journal Editors – Recommendations for the Conduct, Reporting, Editing, and Publication of Scholarly Work in Medical Journals, updated December 2016
[2] DTU Code of Conduct for Research Integrity (E-book p. 19)
[3] Many journals will allow you to use only the post-print version of your article, meaning the accepted version of the article, without the publisher's final formatting. In the event that your article is submitted, but still under review, you should of course use the latest submitted version of your article in your thesis. Always remember to check your publisher's guidelines on reuse of published articles. Most journals, unless open access, have an embargo period on published articles, meaning that within this period you cannot freely use the article. Check your publisher's rules on this issue.

Title of article
Nickel-Catalyzed Asymmetric α-Arylation of ketones by POP
Journal/conference
Journal
Author(s)
Faliu Yang, Søren Kramer & Søren Kegnæs
Name (capital letters) and signature of PhD student
FALIU YANG
PhD student's date of birth
19/08/91
Declaration of the PhD student's contribution
For each category in the table below, please specify the PhD student's contribution to the article as appropriate (please do not fill in with names or x's)

Category	**Minor contribution to the work** *(please specify the nature of the PhD student's contribution)*	**Substantial contribution to the work** *(please specify the nature of the PhD student's contribution)*
Formulation of the conceptual framework and/or planning of the design of the study including scientific questions		Literature study, selected reaction conditions, prepared paper outline and discussed the direction of the project with the other authors.
Carrying out of experiments/data collection and analysis/interpretation of results		Carried out the synthesis of all catalysts, collect catalysis reaction data and analysis work.
Writing of the article/revising the manuscript for intellectual content		Wrote the initial draft of the manuscript, applied the comments and corrections from the co-authors and revising it continuously.

Signatures

Faliu Yang

Title of article
Nickel-Catalyzed Asymmetric α-Arylation of ketones by POP
Journal/conference
Journal
Author(s)
Faliu Yang, Søren Kramer & Søren Kegnæs
Name (capital letters) and signature of PhD student
FALIU YANG
PhD student's date of birth
19/08/91

Date	Name	Title	Signature
28/4 -2022	Faliu Yang	PhD Student	Faliu Yang
28/4 -2022	Søren Kramer	Associate Professor	
18/5-2022	Søren Kegnæs	Professor	

Please note that by signing this declaration, co-authors permit the PhD student to reuse whole or parts of co-authored articles in their PhD thesis, under the condition that co-authors are acknowledged in connection with the reused text or figure.

Declaration of co-authorship at DTU

If a PhD thesis contains articles (i.e. published journal and conference articles, unpublished manuscripts, chapters, etc.) written in collaboration with other researchers, a co-author statement verifying the PhD student's contribution to each article should be made.

If an article is written in collaboration with three or less researchers (including the PhD student), all researchers must sign the statement. However, if an article has more than three authors the statement may be signed by a representative sample, cf. article 12, section 4 and 5 of the Ministerial Order No. 1039, 27 August 2013. A representative sample consists of minimum three authors, which is comprised of the first author, the corresponding author, the senior author, and 1-2 authors (preferably international/non-supervisor authors).

DTU has implemented the Danish Code of Conduct for Research Integrity, which states the following regarding attribution of authorship:

"Attribution of authorship should in general be based on criteria a-d adopted from the Vancouver guidelines[1], and all individuals who meet these criteria should be recognized as authors:

a. Substantial contributions to the conception or design of the work, or the acquisition, analysis, or interpretation of data for the work, *and*
b. drafting the work or revising it critically for important intellectual content, *and*
c. final approval of the version to be published, *and*
d. agreement to be accountable for all aspects of the work in ensuring that questions related to the accuracy or integrity of any part of the work are appropriately investigated and resolved."[2]

For more information regarding definition of co-authorship and examples of authorship conflicts, we refer to DTU Code of Conduct for Research Integrity (pp. 19-22).

By signing this declaration, co-authors permit the PhD student to reuse whole or parts of co-authored articles in their PhD thesis, under the condition that co-authors are acknowledged in connection with the reused text or figure.

It is **important** to note that it is the responsibility of the PhD student to obtain permission from the publisher to use the article in the PhD thesis[3]

---

[1] International Committee of Medical Journal Editors – Recommendations for the Conduct, Reporting, Editing, and Publication of Scholarly Work in Medical Journals, updated December 2016
[2] DTU Code of Conduct for Research Integrity (E-book p. 19)
[3] Many journals will allow you to use only the post-print version of your article, meaning the accepted version of the article, without the publisher's final formatting. In the event that your article is submitted, but still under review, you should of course use the latest submitted version of your article in your thesis. Always remember to check your publisher's guidelines on reuse of published articles. Most journals, unless open access, have an embargo period on published articles, meaning that within this period you cannot freely use the article. Check your publisher's rules on this issue.

Title of article
Asymmetric Hydrosilylation of ketones by Cu-POP
Journal/conference
Journal
Author(s)
Faliu Yang, Søren Kramer & Søren Kegnæs
Name (capital letters) and signature of PhD student
FALIU YANG
PhD student's date of birth
19/08/91
Declaration of the PhD student's contribution
For each category in the table below, please specify the PhD student's contribution to the article as appropriate (please do not fill in with names or x's)

Category	**Minor contribution to the work** *(please specify the nature of the PhD student's contribution)*	**Substantial contribution to the work** *(please specify the nature of the PhD student's contribution)*
Formulation of the conceptual framework and/or planning of the design of the study including scientific questions		Planned the direction of the project, optimized reaction conditions, prepared paper outline.
Carrying out of experiments/data collection and analysis/interpretation of results		Carried out the synthesis of all POPs catalysts, collect catalysis reaction data and analysis work.
Writing of the article/revising the manuscript for intellectual content		Made the initial draft of the manuscript and a majority of the Fig. Schemes,etc. Applied the comments and corrections from the co-authors and revising it continuously.

Signatures

Faliu Yang

Title of article
Asymmetric Hydrosilylation of ketones by Cu-POP
Journal/conference
Journal
Author(s)
Faliu Yang, Søren Kramer & Søren Kegnæs
Name (capital letters) and signature of PhD student
FALIU YANG
PhD student's date of birth
19/08/91

Date	Name	Title	Signature
18/5-2022	Faliu Yang	PhD Student	Faliu Yang
2022-22	Søren Kramer	Associate Professor	
20/5-2022	Søren Kegnæs	Professor	Søren Kegnæs

Please note that by signing this declaration, co-authors permit the PhD student to reuse whole or parts of co-authored articles in their PhD thesis, under the condition that co-authors are acknowledged in connection with the reused text or figure.